



**Harper Adams
University**

A Thesis Submitted for the Degree of Doctor of Philosophy at
Harper Adams University

Copyright and moral rights for this thesis and, where applicable, any accompanying data are retained by the author and/or other copyright owners. A copy can be downloaded for personal non-commercial research or study, without prior permission or charge.

This thesis and the accompanying data cannot be reproduced or quoted extensively from without first obtaining permission in writing from the copyright holder/s. The content of the thesis and accompanying research data (where applicable) must not be changed in any way or sold commercially in any format or medium without the formal permission of the copyright holder/s.

When referring to this thesis and any accompanying data, full bibliographic details including the author, title, awarding institution and date of the thesis must be given.

Investigating Fusarium resistance in UK winter oats

Joseph Richard Cottrell Blackshaw-Crosby

A thesis submitted in partial fulfilment of the requirements of
Harper Adams University for the degree of Doctor of
Philosophy

September 2021

Harper Adams University

Newport, Shropshire TF10 8NB

Abstract

The European Union is currently drafting legislation for maximum limits of the mycotoxins HT2 and T2 in cereals and cereal products intended for human consumption. *Fusarium langsethiae* has been identified as the main HT2+T2 mycotoxin producer in UK oats. Until the discovery of high concentrations of HT2+T2 in UK oats, oats were considered largely resistant to *Fusarium* infection. Strong evidence of the epidemiology of the pathogen is still lacking, the infection is symptomless and as yet no sexual stage has been observed.

Cultivars have been demonstrated to have varying resistances to the accumulation of HT2+T2 with ranking remaining relatively consistent across years. This work sought to further clarify the resistance imparted on oat plants by the parental origin of four quantitative trait loci (QTL) identified previously as being associated with *F. langsethiae* DNA and HT2 +T2 concentration in harvested oat grains. The QTL are designated Mrg04, Mrg20, Mrg21 and Mrg11 and were examined using near isogenic lines (NIL) developed from a mapping population derived from crossing Tardis (a taller earlier cultivar) and Buffalo (a semi-dwarf later cultivar).

Introgression of the Buffalo derived Mrg04 QTL into the Tardis background resulted in a shorter plant with only panicles only partially emerged from the flag leaf boot. The opposite introgression lead to plant taller than either parent line.

Introgression of the Tardis Mrg21 into the Buffalo background resulted in a later plant when sown in autumn, the effect was close to tenfold when sown in spring. The introgression of the Buffalo Mrg21 into the Tardis background caused the resultant plant to be earlier in autumn sown plots and four times as much so in spring sown plots.

Buffalo is the more susceptible of the two cultivars to *F. langsethiae*. Through comparison of the NIL with original parent lines reductions in HT2+T2 concentrations were seen when Tardis Mrg04 and Mrg21 alleles were introgressed into the Buffalo background genome. The impact of Mrg04 was consistent across all experiments whilst the impact of Mrg21 was dependant on sowing season. The Mrg21 QTL had a weaker effect compared to Mrg04 but introgression of the Buffalo alleles into the Tardis background resulted in a reduction of HT2+T2 in autumn sown plots. Introgression of Tardis derived Mrg20 into Buffalo had no impact on the HT2+T2 concentration, and introgression of Buffalo derived Mrg20 into Tardis had inconsistent effects across years.

Successful artificial inoculation of the NIL was achieved under glass, but the ranking of the NIL did not match that of the naturally infected field grown plots. Artificial inoculation attempted in field experiments failed to achieve higher infection levels than uninoculated plots.

Plant height and panicle extrusion were correlated to one another, and evidence is presented that either or both could be influencing plant susceptibility to *F. langsethiae* infection. Dissection of naturally infected panicles and quantification of *F. langsethiae* DNA concentration at the spikelet level demonstrated the independent nature of the infection in each spikelet reinforcing previous work that oats have high type II resistance to *Fusarium* infection. Window-pane analysis of summarised environmental variables utilising the NIL field experiments over four years demonstrated that the warm

dry conditions post panicle emergence are conducive to higher HT2+T2 concentrations in harvested oats.

Acknowledgements

I would like to acknowledge my director of studies Professor Simon Edwards (Harper Adams University) for his time and advice. I would also like to thank Catherine Howarth (Aberystwyth University) my second supervisor for the use of the near isogenic lines as well as her ideas that shaped the thesis. Thanks too to Dr Sandy Cowen for his time and resource.

Special thanks to Professor Xiangming Xu (NIAB EMR) for the Window-pane analysis he conducted on my behalf in the project.

I would also like to acknowledge my funders: The Perry Foundation, The Felix Cobbold Trust, and The Agriculture and Horticulture Development Board (AHDB) for their support.

Thanks too to Grace, Gary, Sarah, Hadi, Kasia, Alex, Emily and Esti from CERC for their assistance with the field and glasshouse experiments during those difficult bottlenecks when friendly help makes the work not only possible but pleasant.

Special thanks to Danielle Henderson-Holding for stepping in and finishing lab work that I was unable to complete due to work commitments.

Lastly, I thank my wife Elsie for her average support in field assessments but mostly for taking care of me during the write up and for taking care of the write up with her exceptional editing skills.

Contents Table

Abstract	i
Acknowledgements.....	iii
List of Tables	ix
List of Figures	xii
1. Chapter 1: Literature review.....	1
1.1. Oats.....	1
1.1.1. History, distribution and consumption	1
1.1.2. Biology	4
1.1.3. Oat production in the UK	6
1.2. Oat genome.....	8
1.2.1. Dwarfing genes.....	9
1.3. Fusarium of small grain cereals	12
1.3.1. History of Fusarium within small grain cereals	12
1.3.2. Range of species and typical hosts.....	13
1.3.3. Sporotrichiella section.....	16
1.4. Current knowledge on <i>F. langsethiae</i> epidemiology.....	21
1.4.1. <i>HT2+T2 distribution in the panicle</i>	28
1.4.2. <i>Arthropod vectoring of F. langsethiae</i>	29
1.4.3. <i>Measuring F. langsethiae infection</i>	31
1.5. Mycotoxins	32
1.5.1. Metabolic variants of HT2 and T2	34
1.5.2. Mycotoxin production.....	34
1.6. Current successes and failures of artificial inoculation of <i>Fusarium langsethiae</i> onto oat plants.....	37
1.6.1. In field artificial inoculations	39
1.7. Management through fungicide application.....	40
1.8. Resistance of oats among current varieties	41
1.8.1. Types of resistance to Fusarium.....	42
1.8.2. Physiological traits of oats with potential to influence Fusarium resistance:	

1.8.3.	Breeding methods	47
1.9.	Aims of the project.....	48
2.	Chapter 2: Artificial Inoculation of Oats with <i>Fusarium Langsethiae</i>	50
2.1.	Introduction.....	50
2.2.	2016 Outdoor inoculation.....	53
2.2.1.	Objectives.....	53
2.2.2.	Null-hypotheses.....	53
2.2.3.	Method	53
2.3.	2019 Field inoculation.....	59
2.3.1.	Objectives.....	59
2.3.2.	Null hypothesis	59
2.3.3.	Method	59
2.3.4.	Preparation and application of Inoculum.....	61
2.3.1.	Spore harvest for inoculation suspensions.....	62
2.4.	Gerald glasshouse inoculation 2017	63
2.4.1.	Objectives.....	63
2.4.2.	Null hypothesis	63
2.4.3.	Method	64
2.5.	Balado glasshouse inoculation 2018.....	65
2.5.1.	Objectives.....	65
2.5.2.	Null Hypothesis.....	66
2.5.3.	Method	66
2.6.	NIL Glasshouse Inoculation 2019	67
2.6.1.	Objectives.....	67
2.6.2.	Null Hypotheses	67
2.6.3.	Method	68
2.7.	Results	70
2.7.1.	2016 Field Inoculation.....	70
2.7.1.	2019 field inoculation	71
2.7.2.	2017 Glasshouse Gerald Inoculation	72

2.7.3.	2018 Glasshouse Balado Inoculation.....	73
2.7.4.	2019 Glasshouse inoculation.....	75
2.8.	Discussion	76
3.	Chapter 3: Quantitative traits in Buffalo and Tardis NIL as impacted by sowing date	86
3.1.	Introduction.....	86
3.2.	Method	89
3.2.1.	Statistical analysis	90
3.3.	Results	91
3.3.1.	Height.....	91
3.3.2.	Panicle length related to height.....	100
3.3.3.	Panicle Extrusion.....	101
3.3.4.	Flowering time	101
3.4.	Discussion	110
3.4.1.	Pearson correlations.....	110
3.4.2.	Height model	111
3.4.3.	Height Mrg04.....	111
3.4.4.	Panicle length and panicle extrusion.....	111
3.4.5.	Mrg04	112
3.4.6.	Mrg21	114
3.4.7.	Mrg20	115
3.4.8.	Mrg11	115
3.4.9.	Conclusions.....	115
4.	Chapter 4: Examination of genetic basis for resistance or susceptibility of winter oats (<i>Avena sativa</i>) to <i>Fusarium langsethiae</i>	117
4.1.	Introduction.....	117
4.2.	Methodology.....	120
4.2.1.	Experimental Design and Environment.....	120
4.2.2.	Harvest and Sampling	120
4.2.3.	Statistical analysis	120
4.3.	Results	121

4.3.1.	Summary results for the field experiments	121
4.3.2.	Plant height	122
4.3.3.	Panicle Extrusion.....	123
4.3.4.	Earliness.....	126
4.3.5.	Mrg04	143
4.3.6.	Mrg21	147
4.3.7.	Mrg20	150
4.3.8.	Mrg11	154
4.4.	Discussion	156
4.4.1.	Height.....	157
4.4.2.	Days to panicle emergence	160
4.4.3.	Contrasts	162
4.4.4.	Across flowering time and height	164
4.4.5.	Mrg011	164
4.5.	Conclusions.....	165
5.	Chapter 5: Correlating weather conditions relative to panicle emergence with HT2+T2 concentration in harvested grain	166
5.1.	Introduction.....	166
5.2.	Method	168
5.3.	Results	169
5.4.	Discussion	174
6.	Chapter 6: Spatial distribution.....	177
6.1.	Introduction.....	177
6.2.	Methods.....	178
6.2.1.	Panicle dissection.....	178
6.2.1.	Single grain DNA extraction.....	178
6.2.2.	Grid	180
6.3.	Statistical analysis	180
6.4.	Results	181
6.4.1.	Panicle dissection.....	181

6.4.2.	Small Grids.....	189
6.4.3.	Large Grids.....	191
6.5.	Discussion	194
6.5.1.	Distribution within a panicle	194
6.5.2.	Distribution within a field	196
7.	Chapter 7: General Discussion	199
7.1.	Conclusions.....	204
7.2.	Future work	205
	References	207
1.	Appendix 1	230
2.	Appendix 2	231
3.	Appendix 3	239
4.	Appendix 4	242
5.	Appendix 5	246

List of Tables

Table 1.1: Description of the most common <i>Fusarium</i> disease causing pathogens (Hanson and Hill, 2004; Hanson, 2006; Thrane et al., 2004; Parry et al., 1995; Leonard and Bushnell, 2003 14	
Table 2.1: Growth stages according to Zadok's decimal code (Zadok et al., 1974).....	54
Table 2.2: <i>Fusarium langsethiae</i> isolates and source	55
Table 2.3: Treatment list for 2016 field inoculation.	56
Table 2.4: Conditions on the day of inoculation.....	56
Table 2.5: Name and description of the <i>F. langsethiae</i> isolates used in all inoculation experiments excluding the 2016 outdoor inoculation experiment.	61
Table 2.6: Near isogenic lines (NIL) grown to harvest and treatments applied. The Code column refers to the code of the NIL. The Name column refers to the name applied in this thesis to identify the parent genome and the introgressed QTL (Appendix 1). The Treatment column refers to whether or not the plants were fully extruded and/or the boot damaged.....	69
Table 3.1: Key NILs used within this study. QTL name refers to the Mrg designations for linkage groups described in Chaffin et al. (2016). The Allele column describes from which parent the QTL is originally derived (B denoting Buffalo and T denoting Tardis). In some instances, multiple genotypes have been grouped together when they consist of near identical genetic compositions.	89
Table 3.2: Sowing and harvest dates of each NIL experiment.	90
Table 3.3: Pearson correlation coefficients for height, degree days to panicle emergence (GS51) in the harvested grain from autumn sown plots.	91
Table 3.4: Pearson correlation coefficients for height, degree days to panicle emergence (GS51) in the harvested grain from spring sown plots.	91
Table 3.5: Output from the model examining the impact year, sowing season, and genotype on plant height.....	91
Table 3.6: Contrast analysis comparing height of the parent line Buffalo with Buffalo+T Mrg04. Cohen's D is included as a measure of effect size, N is the sample number.....	92
Table 3.7: Contrast analysis comparing the heights of the parent line Tardis with Tardis+B Mrg04. Cohen's D is included as a measure of effect size, N is the sample number.....	93
Table 3.8: Contrast analysis comparing the heights of the parent line Buffalo with Buffalo+T Mrg21. Cohen's D is included as a measure of effect size, N is the sample number.....	95
Table 3.9: Contrast analysis comparing the heights of the parent line Tardis against Tardis + B Mrg21. Cohen's D is included as a measure of effect size, N is the sample number.....	95
Table 3.10: Contrast analysis comparing the heights of the parent line Buffalo against Buffalo + T Mrg20. Cohen's D is included as a measure of effect size, N is the sample number.	97
Table 3.11: Contrast analysis comparing the heights of the parent line Tardis against Tardis + B Mrg20. Cohen's D is included as a measure of effect size, N is the sample number.....	98
Table 3.12: Contrast analysis comparing the heights of the parent line Buffalo against Buffalo + T Mrg11. Cohen's D is included as a measure of effect size, N is the sample number.	99
Table 3.13: Output from the plant degree days linear model. Percentage variance is calculated based on the sums of square values for each factor and each combination of factors.....	102
Table 3.14: Contrast analysis comparing degree days and Julian days of the parent line Buffalo with Buffalo + T Mrg04. Results are reported in accumulated degree days to panicle emergence and Julian days to panicle emergence. Cohen's D is included as a measure of effect size, N is the number of samples.....	103
Table 3.15: Contrast analysis comparing degree days and Julian days of the parent line Tardis and the Tardis + B Mrg04 NIL. Results are reported in accumulated degree days to panicle emergence and Julian days to panicle emergence. Cohen's D is included as a measure of effect size, N is the number of samples.....	104
Table 3.16: Contrast analysis comparing degree days and Julian days of the parent line Buffalo to Buffalo+T Mrg21. Results are reported in accumulated degree days to panicle emergence and Julian days to panicle emergence. Cohen's D is included as a measure of effect size, N is the number of samples.....	105
Table 3.17: Contrast analysis comparing degree days and Julian days of the parent line Tardis with Tardis+B Mrg21. Results are reported in accumulated degree days to panicle emergence and Julian days to panicle emergence. Cohen's D is included as a measure of effect size. ..	106

Table 3.18: Contrast analysis comparing degree days and Julian days of the parent line Buffalo to Buffalo + T Mrg20. Results are reported in accumulated degree days to panicle emergence and Julian days to panicle emergence.....	108
Table 3.19: Contrast analysis comparing degree days and Julian days of the parent line Tardis with Tardis+B Mrg20. Results are reported in accumulated degree days to panicle emergence and Julian days to panicle emergence. Cohen's D is included as a measure of effect size. ..	109
Table 3.20: Contrast analysis comparing degree days and Julian days of the parent line Buffalo to Buffalo + T Mrg11. Results are reported in accumulated degree days to panicle emergence and Julian days to panicle emergence. Cohen's D is included as a measure of effect size. ..	110
Table 4.1: Output from the plant height model showing the significance and the percentage variance accounted for by each factor in the model as well as their interactions.....	123
Table 4.2: Output from multiple linear model based on panicle extrusion of the panicle showing the F value, statistical significance and percentage variance, accounted for by selected factors and interactions entered into the model.....	124
Table 4.3: Output from multiple linear model based on days from sowing to panicle emergence, year and the parental origin of Mrg04 showing the F value, P value and percentage variance accounted for by selected factors and interactions entered into the model. Percentage variation was not calculated for non-significant results.	132
Table 4.4: Output from multiple linear model based on days from sowing to panicle emergence, year and the parental origin of Mrg21 showing the F value, P value and percentage variance accounted for by selected factors and interactions entered into the model. Percentage variation was not calculated for non-significant results.	133
Table 4.5: Output from multiple linear model based on degree days from sowing to panicle emergence, year and the parental origin of the Mrg04 QTL showing the F value, statistical significance and percentage variance accounted for by selected factors and interactions entered into the model. Percentage variation was not calculated for non-significant results.	136
Table 4.6: Output from multiple linear model based on degree days from sowing to panicle emergence, year and the parental origin of Mrg21 showing the F value, statistical significance and percentage variance accounted for by selected factors and interactions entered into the model. Percentage variation was not calculated for non-significant results.	137
Table 4.7: Output from multiple linear model based on Julian day of panicle emergence, year, and the parental origin of Mrg04 showing the F value, statistical significance and percentage variance accounted for by selected factors and interactions entered into the model. Percentage variation was not calculated for non-significant results.	140
Table 4.8: Output from multiple linear model based on Julian day of panicle emergence, year, and the parental origin of Mrg21 showing the F value, statistical significance and percentage variance accounted for by selected factors and interactions entered into the model. Percentage variation was not calculated for non-significant results.	141
Table 4.9: Contrast analysis comparing average log transformed HT2+T2 concentrations of the parent line Buffalo with Buffalo + T Mrg04. Percentage differences were calculated from the differences between back transformed values.....	144
Table 4.10: Contrast analysis comparing average Log10 transformed HT2+T2 concentrations of the parent line Tardis with the NIL Tardis + B Mrg04. Percentage differences were calculated from the differences between back transformed values.	146
Table 4.11: Contrast analysis comparing average Log transformed HT2+T2 concentrations of the parent line Buffalo with the NIL Buffalo + T Mrg21.	147
Table 4.12: Contrast analysis comparing average Log transformed HT2+T2 concentrations of the parent line Tardis with the NIL Tardis + B Mrg21. Percentage differences were calculated from the differences between back transformed values.	149
Table 4.13: Contrast analysis comparing average Log transformed HT2+T2 concentrations of the parent line Buffalo with the NIL Buffalo + T Mrg20. Percentage differences were calculated from the differences between back transformed values.	151
Table 4.14: Contrast analysis comparing average Log transformed HT2+T2 concentrations of the parent line Tardis with the NIL Tardis + B Mrg20. The estimate is the difference between the logged values of the Parent and NIL. Percentage differences were calculated from the differences between back transformed values.	153
Table 4.15: Contrast analysis comparing average Log transformed HT2+T2 concentrations of the parent line Buffalo with the NIL Buffalo + T Mrg11. The estimate is the difference between the	

<i>logged values of the parent and NIL. Percentage differences were calculated from the differences between back transformed values.</i>	<i>155</i>
<i>Table 6.1: The composition of the master mix used in the single grain DNA quantification.</i>	<i>179</i>
<i>Table 6.2: Details for grid dimensions, variety and whether or not GPS locations were stored for each year.</i>	<i>180</i>
<i>Table 7.1: Cultivar ranking from field to glasshouse experiments conducted in Norway (Adapted from Aamot, 2017).</i>	<i>200</i>
<i>Table A1 1 :Selection of the main NIL grown as part of the NIL population examined. Genotype refers to the original unique breeders code, the background column details from which parent the majority of the plants genome comes from, Mrg columns detail the source of the QTL Mrg11, 20, 21 and 04, and the NIL name column details the generic name given to each NIL to describe their genomic composition.</i>	<i>230</i>
<i>Table A3.1: Mean LOD scores from experiments conducted by Stancic (2016) relating traits to marker positions identifying QTL.</i>	<i>239</i>
<i>Table A5.1: Fungicide programme applied each year across the NIL experiments for autumn and spring sown experiments. Growth stages are described using according to Zadoks et al. (1974). Variations in rate were made according to disease pressure, no crown rust was seen in the field across all four seasons and as such no sprays were made to specifically tackle it.</i>	<i>246</i>

List of Figures

Figure 1.1: World annual production of oats by country for 2018 (Source: data from FAO, 2020). Greyed out countries were not represented in the FAO data set.	1
Figure 1.2: Area of barley, oats, OSR and wheat grown in the UK over the past 125 years (Source: data from pers comm: Ian Knapper,; Survey Manager, Analysis and Evidence Team, Department of Environment Food and Rural Affairs (DEFRA), 2020).....	3
Figure 1.3: Anatomy of an oat panicle (Source: Author).....	4
Figure 1.4: (a) A primary and (b) secondary floret within an oat spikelet. (Source: Author)	5
Figure 1.5: On farm yield (t/ha) of barley, oats, OSR and wheat in the UK over the past 125 years (Source: data from per comm: Ian Knapper Survey Manager, Analysis and Evidence Team Department of Environment and Rural Affairs (DEFRA) (2020)).....	6
Figure 1.6: Avena sativa karyotype, a: A genome chromosomes, b: C genome chromosomes, c: D genome chromosomes. Adapted from Sanz et al. (2010), Chaffin et al. (2016), Zhao et al. (2018), and Canales et al. (2021).	9
Figure 1.7: Proposed <i>F. langsethiae</i> life cycle based on the current literature.....	24
Figure 1.8: Effect of cultivation and previous crop on HT2+T2 concentration in harvested oat grain. Error bars represent 95% confidence limits for predictions. Adapted from Edwards (2017). The previous crop history is described on the x axis; Year – 1 and Year -2 refer to the year before the sampled oat crop and the crop two years before the sampled oat crop respectively. Previous crops are described as either cereal or non cereal.....	26
Figure 1.9: Skeletal structure of type A trichothecenes, HT2 (R group is H) and T2 (R group is an acetyl). Adapted from: Sigma Aldrich (No Date) and Li et al. (2011).....	33
Figure 1.10: Skeletal formula of HT2-3-glucoside. Adapted from: Li et al. (2011).....	36
Figure 1.11: The skeletal structure of the phase II metabolite T2-Sulphate (Knutsen et al., 2017). A sulphate group is attached via an Oxygen bridge to Carbon 3.	37
Figure 1.12: Skeletal formula of the 3-Acetyl-T2 phase II metabolite (Knutsen et al., 2017). An additional acetyl group is present on Carbon 3.	37
Figure 2.1: Oat plants with spore suspension applied to the flag leaf (a) at late booting/sheath split (GS49) with no spore suspension applied (b) and at fully emerged panicle after spore suspension applied (c).....	57
Figure 2.2: An example standard curve using the standard solutions provided in the Radiscreen® T-2/HT-2 ELISA assay kit. The y axis is absorbance at 450 nm, and the x axis the known concentrations of the standard solutions.	58
Figure 2.3: Misting running on two blocks of the 2019 outdoor field inoculation experiment.	60
Figure 2.4: a: naturally extruded plant; b: mechanically extruded plant prior to inoculation; c: panicle immediately after inoculum applied, small droplets are visible on the spikes; d: bagged plant post inoculation.	70
Figure 2.5: HT2+T2 concentration in harvested oat grain (cultivar Gerald) in the 2016 field experiment after <i>F. langsethiae</i> inoculations a: by growth stage of inoculation; b: for plots either inoculated or not with and without simulated rain; c: for plots inoculated with different spore concentrations. Control not inoculated or irrigated and 0 treatment inoculated with water only. Error bars represent one standard error of the mean.	71
Figure 2.6: Buffalo and Tardis HT2+T2 mycotoxin concentration in harvested grain from <i>F. langsethiae</i> inoculated field plots in 2019. Error bars represent the standard error of the mean calculated for individual means.....	72
Figure 2.7: Back-transformed concentration of HT+T2 (µg/kg) in panicles of oat (var. Gerald) in the 2017 glasshouse experiment for the Control, GS 59, and GS65-9 <i>F. langsethiae</i> inoculated treatments. Different bar colours represent different concentrations of potato dextrose broth detailed in the legend. Error bars represent one standard error of the mean. Columns headed with the same letter were not statistically different (Tukey, $P < 0.05$).....	73
Figure 2.8: Balado growing in the glasshouse in 2018 simultaneously at early panicle emergence (GS51) and early anthesis (GS61).....	74
Figure 2.9: Back-transformed concentration of HT+T2 (µg/kg) in panicles of oats (var. Balado) for the 2018 glasshouse experiment inoculated with <i>F. langsethiae</i> . The x axis describes the growth stage at which inoculant or control water sprays were applied. The legend describes the treatments that included PDA amendment at 2.4 g/L. Error bars represent one standard error of the mean. Columns with the same letter are not significantly different (Tukey, $P > 0.05$).....	75

Figure 2.10: Back-transformed concentration of HT+T2 ($\mu\text{g/kg}$) in panicles of oat for 2019 glasshouse experiment for the variety Buffalo with and without inoculation, the Buffalo NIL (B NIL) undamaged and unextruded, damaged and unextruded, damaged and extruded, Buffalo + T Mrg04 damaged and undamaged. The Legend describes the expected heights of the plants predicted from their growth habits in the field. Error bars represent one standard error of the mean. Columns headed with the same letter are not significantly different (Tukey; $P>0.05$)....	76
Figure 2.11: Flow diagram illustrating the development of the glasshouse experiments investigating artificial inoculation.....	80
Figure 3.1: Plant height of Buffalo+T Mrg04, Buffalo and Tardis sown in autumn and spring. Results from four years of autumn and spring sown field experiments (2017-2020). The error bars represent the standard error of the mean.	92
Figure 3.2: Plant height of Tardis+B Mrg04, Buffalo and Tardis grown in autumn and spring. Results from four years of autumn and spring sown field experiments (2017-2020). The error bars represent one standard error of the mean.	93
Figure 3.3: Plant heights of Buffalo+T Mrg21, Buffalo and Tardis grown in autumn and spring. Results from four years of autumn and spring sown field experiments (2017-2020). The error bars represent one standard error of the mean.	94
Figure 3.4: Plant heights of Tardis + B Mrg21, Buffalo, and Tardis grown in autumn and spring. Results from four years of autumn and spring sown field experiments (2017-2020). The error bars represent one standard error of the mean.	95
Figure 3.5: Plant height of Buffalo, Buffalo+T Mrg20 and Tardis grown in autumn and spring. Results from four years of autumn and spring sown field experiments (2017-2020). The error bars represent one standard error of the mean.	97
Figure 3.6: Plant height of Buffalo, Tardis + B Mrg20 and Tardis grown in autumn and spring. Results from four years of autumn and spring sown field experiments (2017-2020). The error bars represent one standard error of the mean.	98
Figure 3.7: Plant height of Buffalo, Buffalo + T Mrg11 and Tardis grown in autumn and spring. Results from three years of autumn and spring sown field experiments (2018-2020). The error bars represent one standard error of the mean.	99
Figure 3.8: Panicle length plotted against plant height for genotypes that were present in 2018-2020. The lines represent the linear relationship between plant height and panicle length for plants with either Mrg04 from Buffalo (B) or Tardis (T). Equations and R^2 values are shown on the figure.	101
Figure 3.9: Panicle extrusion plotted against plant height for genotypes that were present in 2018-2020. The lines represent the linear relationship between plant height and panicle extrusion for plants with either Mrg04 from Buffalo (B) or Tardis (T). Equations and R^2 values are shown on the figure.	101
Figure 3.10: Degree days (5°C baseline) from sowing to panicle emergence for Buffalo+ T Mrg04, Buffalo, and Tardis. Results from four years of autumn and spring sown field experiments (2017-2020). Error bars represent the standard error of the mean.	103
Figure 3.11: Degree days (5°C baseline) for Tardis + B Mrg04, Buffalo, and Tardis. Results from four years of autumn and spring sown field experiments (2017-2020). Error bars represent the standard error of the mean.	103
Figure 3.12: Degree days (5°C baseline) for Buffalo+ T Mrg21, Buffalo, and Tardis. Results from four years of autumn and spring sown field experiments (2017-2020). Error bars represent the standard error of the mean.	105
Figure 3.13: Degree days (5°C baseline) for Buffalo, Tardis+ B Mrg21. Results from four years of autumn and spring sown field experiments (2017-2020). Error bars represent the standard error of the mean.	106
Figure 3.14: Degree days (5°C baseline) for Buffalo+ T Mrg20, Buffalo, and Tardis. Results from four years of autumn and spring sown field experiments (2017-2020). Error bars represent the standard error of the mean. Cohen's D is included as a measure of effect size and N is the number of samples.	107
Figure 3.15: Degree days (5°C baseline) for Buffalo, Tardis + B Mrg20, and Tardis. Results from four years of autumn and spring sown field experiments (2017-2020). Error bars represent the standard error of the mean.	108

Figure 3.16: Degree days (5°C baseline for Buffalo, Buffalo + T Mrg11, and Tardis. Results from three years of autumn and spring sown field experiments (2018-2020). Error bars represent the standard error of the mean.....	110
Figure 4.1: a Crop debris from the previous wheat crop visible amongst young oat plants. b Wheat straw distributed in between plants after sowing.	120
Figure 4.2: HT2+T2 average concentrations in the harvested oat grain from the NIL experiments for each sowing season in each harvest year. Error bars represent the standard error of the mean.	122
Figure 4.3: A graphical representation of the model presented in Table 5.1, plotting HT2+T2 concentration against plant height. The shape of the data points indicates the parental origin of the Mrg04 QTL, the colours indicate the different years described in the legend. Differently textured lines represent the fitted values according to year from the model described in Table 5.1.	123
Figure 4.4: A graphical representation of the model presented in Table 5.2, plotting log ₁₀ transformed HT2+T2 concentration against panicle extrusion. The shape of the data points indicates the parental origin of the Mrg04 QTL, the colours indicate the different years described in the legend. Differently textured lines represent the fitted values according to year from the model described in Table 5.2.	125
Figure 4.5: Boxplot comparing plants with fully extruded panicles against those with only partially extruded panicles. The y axis displays log ₁₀ transformed HT2+T2 values, the mean values for each the fully extruded and partially extruded plant's are represented by the grey boxes and labelled with the back transformed HT2+T2 concentrations.....	126
Figure 4.6: A graphical representation of the model presented in Table 4.4, plotting log ₁₀ transformed HT2+T2 concentration against days from sowing to panicle emergence of the autumn sown plots. The shape of the data points indicates the parental origin of the Mrg21 QTL, the colours indicate the different years described in the legend. Differently textured and coloured lines represent the fitted values according to year from the model described in Table 5.4.....	134
Figure 4.7: A graphical representation of the model presented in Table 4.4, plotting log ₁₀ transformed HT2+T2 concentration against days from sowing to panicle emergence of spring sown plots. The shape of the data points indicates the parental origin of the Mrg21 QTL, the colours indicate the different years described in the legend. Differently textured and coloured lines represent the fitted values according to year from the model described in Table 5.4.....	135
Figure 4.8: A graphical representation of the model presented in Table 4.6, plotting log ₁₀ transformed HT2+T2 concentration against degree days from sowing to panicle emergence for autumn sown plots. The shape of the data points indicates the parental origin of the Mrg21 QTL, the colours indicate the different years described in the legend. Differently textured and coloured lines represent the fitted values from the model described in Table 5.6.	138
Figure 4.9: A graphical representation of the model presented in Table 4.6, plotting log ₁₀ transformed HT2+T2 concentration against degree days from sowing to panicle emergence for spring sown plots. The shape of the data points indicates the parental origin of the Mrg21 QTL, the colours indicate the different years described in the legend. Differently textured and coloured lines represent the fitted values from the model described in Table 5.6.	139
Figure 4.10: A graphical representation of the model presented in Table 5.8, plotting log ₁₀ transformed HT2+T2 concentration against Julian day of panicle emergence for autumn sown plots. The shape of the data points indicates the parental origin of the Mrg21 QTL, the colours indicate the different years described in the legend. Differently textured and coloured lines represent the fitted values according to year from the model described in Table 5.8.	142
Figure 4.11: A graphical representation of the model presented in Table 5.8, plotting log ₁₀ transformed HT2+T2 concentration against Julian day of panicle emergence for spring sown plots. The shape of the data points indicates the parental origin of the Mrg21 QTL, the colours indicate the different years described in the legend. Differently textured and coloured lines represent the fitted values according to year from the model described in Table 5.8.	143
Figure 4.12: Back transformed concentrations of HT2+T2 from Buffalo + T Mrg04, Buffalo and Tardis sown in autumn and spring. Results from four years of autumn and spring sown field experiments (2017-2020). The error bars represent the back transformed standard error of the means.....	145
Figure 4.13: Back transformed concentrations of HT2+T2 from Tardis + B Mrg04, Buffalo and Tardis sown in autumn and spring. Results from four years of autumn and spring sown field	

experiments (2017-2020). The error bars represent the back transformed standard error of the means.....	146
Figure 4.14: Back transformed HT2+T2 concentrations for Buffalo + T Mrg21, Buffalo and Tardis for all years and both sowing seasons. Error bars represent one standard error of the mean.	148
Figure 4.15: Back transformed HT2+T2 concentrations for Tardis + B Mrg21, Buffalo and Tardis for all years and both sowing seasons. Error bars represents one standard error of the mean.	150
Figure 4.16: Back transformed concentrations of HT2+T2 from Buffalo + T Mrg20, Buffalo and Tardis sown in autumn and spring. Results from four years of autumn and spring sown field experiments (2017-2020). The error bars represent the back transformed standard error of the means.....	152
Figure 4.17: Back transformed concentrations of HT2+T2 from Tardis+B Mrg20, Buffalo and Tardis sown in autumn and spring. Results from four years of autumn and spring sown field experiments (2017-2020). The error bars represent the back transformed standard error of the means.....	154
Figure 4.18: Back transformed concentrations of HT2+T2 from Buffalo + T Mrg11, Buffalo and Tardis sown in autumn and spring. Results from three years of autumn and spring sown field experiments (2018-2020). The error bars represent the back transformed standard error of the means.....	156
Figure 5.1: Density plots describing the variation in the durations of panicle emergence for each year in spring and winter from 2017 to 2020. Only genotypes that appeared in every year are included. The x axis uses Julian days to panicle emergence, measured in days.	170
Figure 5.2: Pearson correlation coefficients plotted for average rainfall, average relative humidity, and average air temperature against each window-pane length for pre- and post-panicle emergence.	171
Figure 5.3: Pearson correlation coefficients for growing degree hours categories: <15°C (L15DH), >=15°C (G15DH), <20°C (L20DH) and >=20°C (G20DH) with HT2+T2 average concentrations plotted against each window-pane length for pre- and post-panicle emergence.	172
Figure 5.4: Pearson correlation coefficients plotted for rain, relative humidity, and temperature against each window-pane length for pre- and post-panicle emergence. Different panels represent the individual years in which the plots were grown as labelled on the right-hand side of the figure.	173
Figure 5.5: Pearson correlation coefficients plotted for the growing degree hours categories: <15°C (L15DH), >=15°C (G15DH), <20°C (L20DH) and >=20°C (G20DH) plotted against each window-pane length for pre- and post-panicle emergence. Different panels represent the individual years in which the plots were grown as labelled on the right-hand side of the figure	174
Figure 6.1: Mapped panicle of Buffalo + T Mrg04. Red spikelets showed detectable <i>F. langsethiae</i> DNA at 5 pg/ng or above; yellow spikelets showed detectable <i>F. langsethiae</i> DNA at 4.9 pg/ng and below; and black spikelets had no detectable <i>F. langsethiae</i> DNA. The panicle has been drawn so that no branches overlap for clarity, the original panicle was not orientated as depicted but instead as shown in Figure 7.2. A scale is present in the bottom left of the diagram. Whorls were counted from the bottom up and are labelled on the right of the panicle.....	182
Figure 6.2: a: Buffalo + T Mrg04 panicle before it was mapped and dissected (plant 1). b: Tardis + B Mrg04 panicle before it was dissected (plant 2). c: Tardis + B Mrg04 panicle before it was dissected (plant 3). d: Tardis + B Mrg04 panicle before it was dissected (plant 4). Panicles were selected from a larger sample of panicles collected on the day of harvest.	183
Figure 6.3: Mapped panicle of Tardis + B Mrg04 (plant 2). Red spikelets showed detectable <i>F. langsethiae</i> DNA at 5 pg/ng or above; yellow spikelets showed detectable <i>F. langsethiae</i> DNA at 4.9 pg/ng and below; and black spikelets had not detectable <i>F. langsethiae</i> DNA. The panicle has been drawn so that no branches overlap for clarity, the original panicle was not orientated as depicted but instead as shown in Figure 7.2 b. A scale is present in the bottom left of the diagram. Whorls were counted from the bottom up and are labelled on the right of the diagram.	184
Figure 6.4: Mapped panicle of Tardis + B Mrg04 (plant 3). Red spikelets showed detectable <i>F. langsethiae</i> DNA at 5 pg/ng or above; yellow spikelets showed detectable <i>F. langsethiae</i> DNA at 4.9 pg/ng and below; and black spikelets had no detectable <i>F. langsethiae</i> DNA. The panicle has been drawn so that no branches overlap for clarity; the original panicle was not orientated as	

depicted but instead as shown in Figure 7.2 c. A scale is present in the bottom left of the diagram. Whorls were counted from the bottom up and are labelled on the right of the panicle.	185
Figure 6.5: Mapped panicle of Tardis + B Mrg04 (plant 4). Red spikelets showed detectable <i>F. langsethiae</i> DNA at 5 pg/ng or above; yellow spikelets showed detectable <i>F. langsethiae</i> DNA at 4.9 pg/ng and below; and black spikelets had no detectable <i>F. langsethiae</i> DNA. The panicle has been drawn so that no branches overlap for clarity; the original panicle was not orientated as depicted but instead as shown in Figure 7.2 d. A scale is present in the bottom left of the diagram. Whorls were counted from the bottom up and are labelled on the right of the panicle.	186
Figure 6.6: Scatter plot showing the difference between individual spikelets from plants 2 and 3 and 4 in terms of <i>F. langsethiae</i> DNA concentration (pg/ng) against their respective branch distances from one another (mm).	187
Figure 6.7: Boxplot of <i>F. langsethiae</i> DNA of spikelets by whorl for Tardis + B Mrg04 (plants 2, 3 and 4). The +, x, and Δ symbols represent DNA concentrations for individual spikelets, grey squares represent the mean of whorl, values of which in pg/ng are labelled directly above each boxplot.	188
Figure 6.8: Density plot of <i>F. langsethiae</i> DNA concentration (pg/ng) of individual spikelets from three Tardis + B Mrg04 (plant 2, 3, and 4) panicles.	189
Figure 6.9: A heat map of the HT2+T2 concentrations of grain samples taken in 2017 from the experimental field. Colours on the chart represent linear interpolations of the HT2+T2 concentrations of each sampled location and can be interpreted using the scale in the legend. The relative position of each location is marked by a black x, labelled with the HT2+T2 value for each location.	190
Figure 6.10: A heat map of the HT2+T2 concentrations of grain samples taken in 2019 from the experimental field. Colours on the chart represent linear interpolations of the HT2+T2 concentrations of each sampled location and can be interpreted using the scale in the legend. The relative position of each location is marked by a black x, labelled with the HT2+T2 value for each location.	190
Figure 6.11: A heat map of the HT2+T2 concentrations of grain samples taken in 2016 from the experimental field. Colours on the chart represent linear interpolations of the HT2+T2 concentrations of each sampled location and can be interpreted using the scale in the legend. The relative position of each location is marked by a black x, labelled with the HT2+T2 value for each location.	192
Figure 6.12: A heat map of the HT2+T2 concentrations of grain samples taken in 2018 from the experimental field. Colours on the chart represent linear interpolations of the HT2+T2 concentrations of each sampled location and can be interpreted using the scale in the legend. The relative position of each location is marked by a black x, labelled with the HT2+T2 value for each location.	193
Figure 6.13: A heat map of the HT2+T2 concentrations of grain samples taken in 2020 from the experimental field. Colours on the chart represent linear interpolations of the HT2+T2 concentrations of each sampled location and can be interpreted using the scale in the legend. The relative position of each location is marked by a black x, labelled with the HT2+T2 value for each location.	194
Figure A2.1 Bar chart showing the autumn and spring plant height for all field grown genotypes in 2017, 2018, 2019, and 2020. Breeder's names according to table A1 are displayed on the x axis with the NIL name below. Error bars represent the standard error of the mean.	231
Figure A2.2: Bar chart showing the autumn and spring days to panicle emergence for all field grown genotypes in 2017, 2018, 2019, and 2020. Breeder's names according to table A1 are displayed on the x axis with the NIL name below. Error bars represent the standard error of the mean.	232
Figure A2.3: Bar chart showing the autumn and spring degree days for all field grown genotypes in 2017, 2018, 2019, and 2020. Breeder's names according to table A1 are displayed on the x axis with the NIL name below. Error bars represent the standard error of the mean.	233
Figure A2.4: Bar chart showing the autumn and spring Julian days to panicle emergence for all field grown genotypes in 2017, 2018, 2019, and 2020. Breeder's names according to table A1 are displayed on the x axis with the NIL name below. Error bars represent the standard error of the mean.	234

Figure A2.5: Bar chart showing the autumn and spring backtransformed HT2+T2 concentrations for all field grown genotypes in 2017. Breeder's names according to table A1 are displayed on the x axis with the NIL name below. Error bars represent the standard error of the mean.	235
Figure A2.6: Bar chart showing the autumn and spring backtransformed HT2+T2 concentrations for all field grown genotypes in 2018. Breeder's names according to table A1 are displayed on the x axis with the NIL name below. Error bars represent the standard error of the mean.	236
Figure A2.7: Bar chart showing the autumn and spring backtransformed HT2+T2 concentrations for all field grown genotypes in 2019. Breeder's names according to table A1 are displayed on the x axis with the NIL name below. Error bars represent the standard error of the mean.	237
Figure A2.8: Bar chart showing the autumn and spring backtransformed HT2+T2 concentrations for all field grown genotypes in 2020. Breeder's names according to table A1 are displayed on the x axis with the NIL name below. Error bars represent the standard error of the mean.	238
Figure A4.1: Weather data for the Harper Adams weather station from the 1 st April 2017 to the beginning of August 2017. Graph details the total daily rainfall in blue (ml) the temperature in yellow (°C, primary y axis) and the relative humidity in red (% , secondary y axis).....	242
Figure A4.2: Weather data for the Harper Adams weather station from the 1 st April 2018 to the beginning of August 2018. Graph details the total daily rainfall in blue (ml) the temperature in yellow (°C, primary y axis) and the relative humidity in red (% , secondary y axis).....	243
Figure A4.3: Weather data for the Harper Adams weather station from the 1 st April 2019 to the beginning of August 2019. Graph details the total daily rainfall in blue (ml) the temperature in yellow (°C, primary y axis) and the relative humidity in red (% , secondary y axis).....	244
Figure A4.4: Weather data for the Harper Adams weather station from the 1 st April 2020 to the beginning of August 2020. Graph details the total daily rainfall in blue (ml) the temperature in yellow (°C, primary y axis) and the relative humidity in red (% , secondary y axis).....	245

1. Chapter 1: Literature review

1.1. Oats

1.1.1. History, distribution and consumption

Oats are members of the Poaceae family and the genus *Avena*; the commonly cultivated oat plant species name is *Avena sativa*. Modern hexaploid oats are commonly believed to be derived from *Avena sterilis*, and to have first been cultivated in Southwest Asia (Iran, Iraq, and Turkey) (Zhou *et al.*, 1999). It is believed that this likely happened four to five thousand years ago and that oats came to the attention of early farmers as weeds in previously domesticated cereals. This common belief is perhaps thrown into question by more recent evidence from Lippi *et al.* (2015) with the discovery of oat traces on grinding tools used to mill grains nearly 33,000 years ago in Southern Italy, although no evidence of farming the grain was suggested.

Oats are still popular in temperate latitudes as spring crops but are rarely grown as winter crops in these climates due to their lack of winter hardiness (Rines *et al.*, 2006). More northerly countries such as Russia and Canada grow oats on a large scale as spring crops and in 2018 produced 4,719,324 and 3,436,000 t respectively.

Figure 1.1 shows the production of oats in 2018 by country.

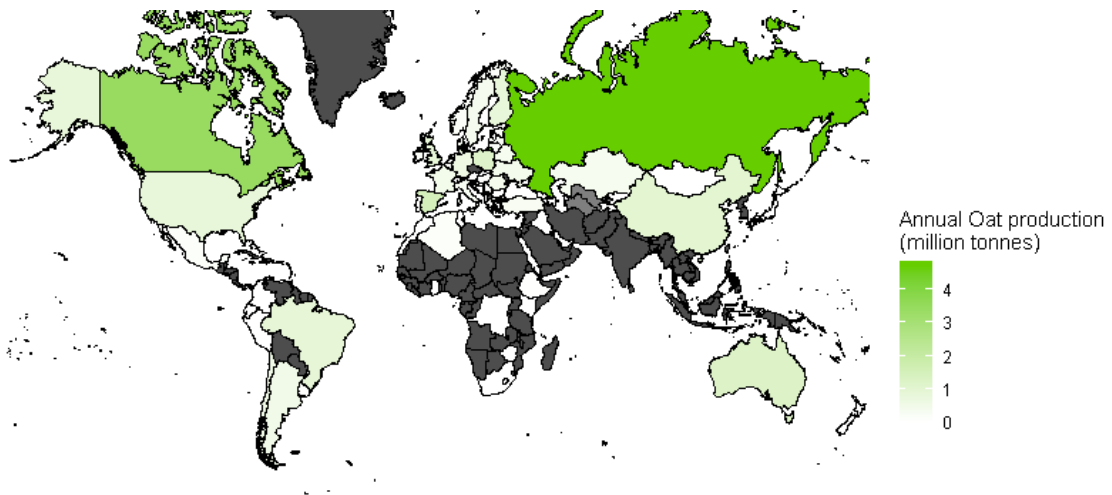


Figure 1.1: World annual production of oats by country for 2018 (Source: data from FAO, 2020). Greyed out countries were not represented in the FAO data set.

Oats are currently the seventh largest cereal crop in Europe after wheat (soft and durum), barley, maize, rye and triticale in terms of production, but third in the UK after wheat and barley (European Commission, 2021). Prior to the mechanisation of transport and agriculture, oats were an important component of horse feed. Since the Second World War there has been a decline in the area of oats grown until ~1985,

from which date the level of production has been relatively stable, with a recent upturn in production initially driven by perceived health benefits and latterly by a reduction in oilseed rape (OSR) area (Figure 1.2). This decline was driven by competition from other more profitable cereals as well as the replacement of oats as break crops from those cereals by crops such as oilseed rape. Even so oats have many characteristics that keep the crop relevant in modern agriculture. In terms of a human food, oats provide a source of oat beta-glucan, for which a causal relationship has been accepted by European Food Safety Agency (EFSA) between oat beta-glucan consumption and the lowering of low-density lipoprotein cholesterol. Low density lipoprotein cholesterol, colloquially referred to as “bad cholesterol”, is associated with coronary heart disease and it’s lowering is regarded as beneficial (EFSA, 2018). Oats also contain avenanthramides, tocopherols, sterols, phytic acid and avenacosides, all of which have been shown to reduce cardiovascular disease, type two diabetes, gastrointestinal disorders, and even cancer through the inhibition of tumour cell growth and the stimulation of apoptosis (Martinez-Villaluenga and Peñas, 2017). Avenanthramides are polyphenols of which 20 unique types have been identified in oats. As a group they have been attributed antioxidant activity, as well as having been associated with anti-inflammatory and antiproliferative (reduction in the spread of cells, specifically malignant cells) activity (Meydani, 2009). In addition, oats contain high levels of protein, essential fatty acids and fibre (Marshall *et al.*, 2013). More recently milk substitutes have been made from oats by companies such as Oatly®, which are marketed as dairy-free and having lower carbon footprints than dairy milk. Oats have also been shown not to evoke the symptoms of celiac disease, typically caused by intolerance to gluten, when eaten in typical quantities over long-term feeding trials (Hardy *et al.*, 2015). This opened a market in oats grown and processed in isolation from wheat to be sold to people suffering from celiac disease, although cross contamination from wheat must be controlled.

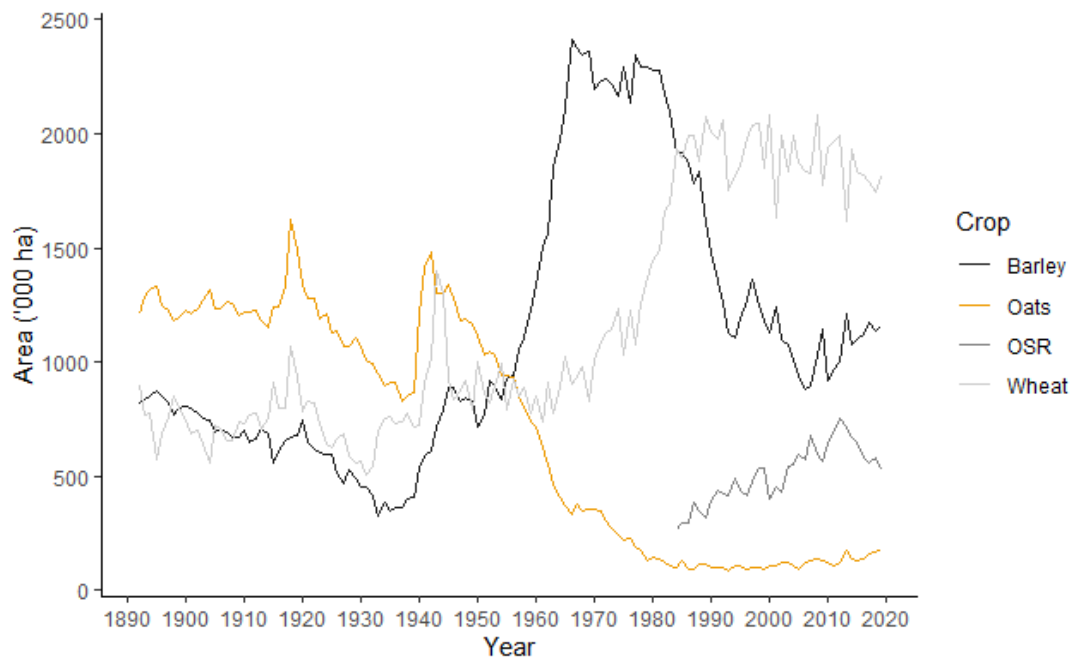


Figure 1.2: Area of barley, oats, OSR and wheat grown in the UK over the past 125 years (Source: data from pers comm: Ian Knapper, : Survey Manager, Analysis and Evidence Team, Department of Environment Food and Rural Affairs (DEFRA), 2020).

In addition to human consumption, oat grain is also used for animal feed. Oats are commonly grown for forage for livestock and this is achieved either through grazing, whole cropping for silage or hay making, or mechanised zero grazing. It has been estimated that in the UK 200 000 t of silage dry matter from oats is produced annually (Wilkins and Kirilov, 2003). Naked oats are of special interest for feeding monogastrics as their lack of husk increases the available energy. Naked oats also have greater protein and fat contents than husked varieties but with lower fibre. However, the lower yield of naked oat varieties reduces the incentive for farmers to grow them.

1.1.2. Biology

Similar to other small grain cereals, oats are monocarpic annuals. The flowers of oats are organised as panicles as shown in Figure 1.3. The anthesis period across an individual panicle is between 10-11 days in oats (Rajala and Peltonen, 2011) as opposed to 4-5 days for a wheat ear, although the latter can be much longer should temperature conditions be cool. Figure 1.3 shows four clear nodes with the lowest labelled as the first node, multiple branches grow from each node forming whorls. Figure 1.3 shows an entire panicle of an oat plant with four whorls, far fewer than typical for simplicity. The branches divide into smaller branches, those ending in spikelets are called pedicels.

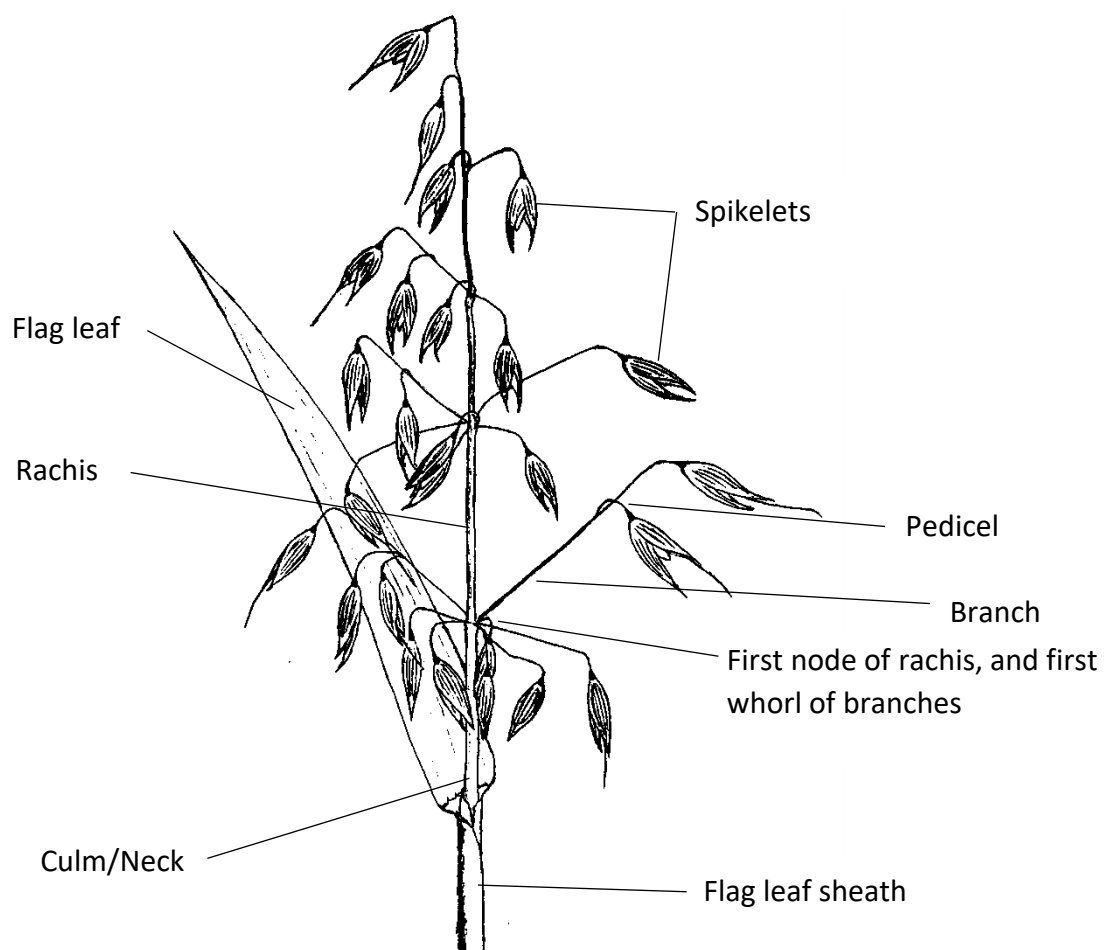


Figure 1.3: Anatomy of an oat panicle (Source: Author).

Each oat spikelet can contain up to four florets although in the UK no more than three grain per spikelet usually develop. *Figure 1.4* shows the structure of a spikelet containing two florets with the glumes removed and the lemma and palea pulled apart to reveal the flowering parts prior to fertilisation.

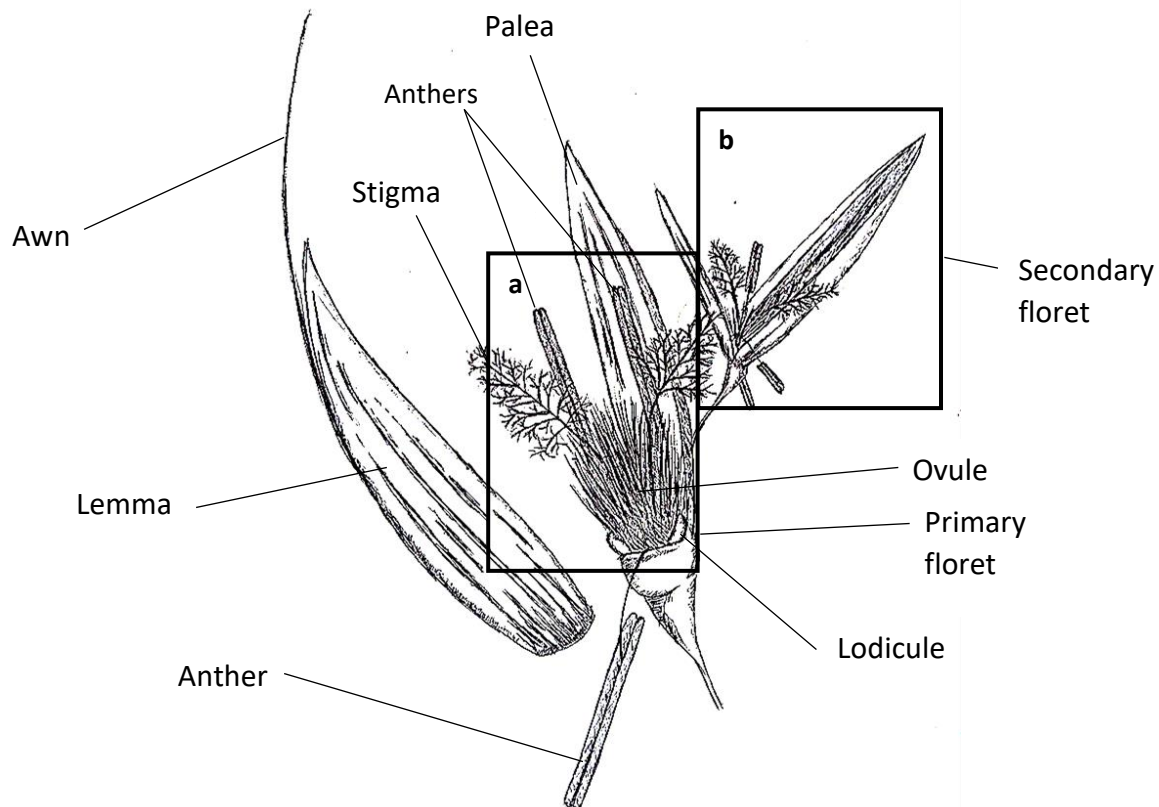


Figure 1.4: (a) A primary and (b) secondary floret within an oat spikelet. (Source: Author)

When the spikelet is intact the lemma encases the flowering parts and wraps partially around the palea. Oats are self-fertile and the anthers are not always visible outside of the floret. Anthers are attached to the base of the ovary by a filament and may be extruded (chasmogamous) or retained (cleistogamous) within the lemma and palea after anthesis. During flowering in chasmogamous oats the lemma and palea separate when the two lodicules expand; the stigma are exposed at the same time the filaments elongate the anthers outside of the spikelet. Figure 1.4 shows for two anthers in the primary floret how the anthers are arranged in line with the palea prior to flowering (the third anther is shown below the floret for clarity). The ovary is largely obscured by trichomes; it is positioned at the base of the floret and the stigma are attached to its apex. Misonoo (1936) observed the panicles of two oat plants and recorded the manner in which they flowered. Spikelets at the top of the panicle flower first and flowering progresses down the panicle. Flowering on branches starts from the branch end and proceeds towards the rachis. Within a spikelet when more than one floret exists (Figure 1.4), the primary floret flowers before secondary. It requires about eight days for flowering to complete across the entire panicle (cultivar: Clydesdale) or approximately 100 degree-days (Rajala and Peltonen-Sainio, 2011). The main stem also flowers earlier than tillers which can cause flowering to go on for over two weeks. Furthermore, Misonoo (1936) noted the oats bloomed in the late afternoon, florets were

open for between 60-80 minutes, and spikelets were more likely to be sterile if derived from the lowest whorls.

Once the oat spike has developed the lemma and palea adhere to the groat to form the husk (often referred to as the hull) which encases the groat (also known as the kernel). During harvesting of husked oats, the husks remain in place and are removed during the primary stages of processing for human consumption (de-hulling). For naked oat varieties, the lemma and palea are less tightly bound and the husks are removed during harvesting.

1.1.3. Oat production in the UK

Typically, winter oats are viewed as a low input crop with the UK nutrient management guide (RB209) recommendation stating a maximum of 140 kg N/ha, such inputs allowing a yield for winter oats to be as high as 9.3 t/ha (AHDB, 2021). However, research suggests that winter oats are responsive to greater quantities of nitrogen, with yields reaching 12 t/ha in one experiment in which 200 kg N/ha was applied (Clarke, 2015). However, in practice lodging becomes a bigger problem at such yields and the value of the crop must justify the cost of inputs.

Similarly, to barley and wheat, oat yields increased dramatically from 1950 through to 1970 during the Green Revolution highlighted in Figure 1.5.

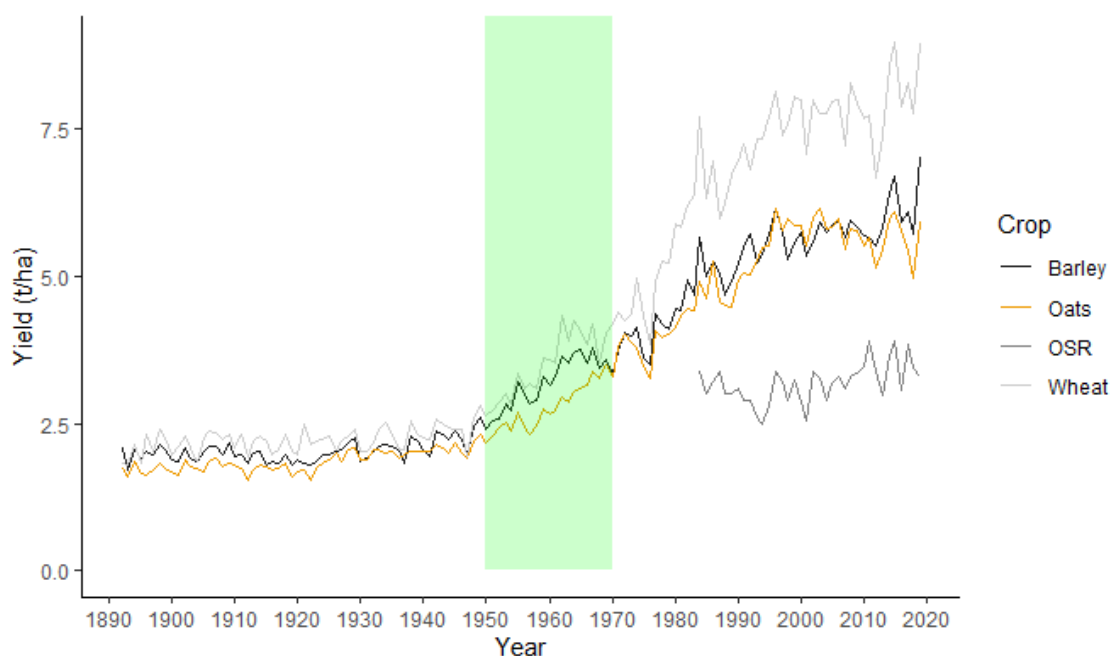


Figure 1.5: On farm yield (t/ha) of barley, oats, OSR and wheat in the UK over the past 125 years (Source: data from per comm: Ian Knapper Survey Manager, Analysis and Evidence Team Department of Environment and Rural Affairs (DEFRA) (2020)). The period often referred to as the green revolution is highlighted in green.

Oats have some advantages within an arable rotation; oats are resistant to take-all of wheat and barley (*Gaeumannomyces graminis* var. *graminis*), a yield reducing pathogen that builds up inoculum in the soil in the first three to five years of continuous wheat/barley production. Placing oats in the rotation can increase the following wheat yield by 1-3 t/ha (Marshall *et al.*, 2015). However, there are few herbicide options to control grass weeds in oats meaning that a broadleaf break crop can be more economic.

Oats generally receive fewer fungicide inputs than either wheat or barley, likely because yield penalties associated with disease are lower in oats. Comparing the five-year averages of differences in the AHDB Recommended Lists (RL) between the fungicide treated (designed to keep disease below 5%) yields and untreated yields, husked varieties of oats lost between 1 and 8% of yield compared with 8 to 23% for winter wheat (Marshall *et al.*, 2015).

Winter oats offer up to 2.5 t/ha more yield in milder climates compared to spring oats. This is reflected in UK growing habits, with the southern UK growing predominantly winter oats, while Scotland grows predominantly spring oats as winter oats are not sufficiently winter hardy to grow in Scotland over winter. The average yield for oats achieved on farms across the UK has remained between 5–6 t/ha in recent decades (Figure 1.5). DEFRA do not distinguish between winter and spring sown crops in their yield statistics so a comparison of yields in commercial crops is not available. However, RL variety trials conducted by the AHDB do allow a comparison. In 2019 plot yields of winter oats ranged between 8.5 and 9.3 t/ha for husked varieties and 6.4 to 6.9 t/ha for naked varieties; and spring yields ranged between 7.1 and 7.9 t/ha for husked varieties and 4.8 and 5.6 t/ha for naked varieties (AHDB, 2021). Naked varieties have a yield penalty due to the lack of the husk which is removed during harvesting.

Oats require a degree of processing before they can be consumed by people even in their most basic form which is rolled porridge oats. First the oats are cleaned using a 2 mm sieve, the loss from which is measured as the percentage screenings; then they are dehulled and polished to remove trichomes from the groat; and finally cleaned again before further sorting by size and kilning. The kernel content (proportion of the weight of the grain comprising the kernel) is an important attribute of the oat in terms of the mill extract yield, as such varieties with higher kernel contents are desirable (Marshall *et al.*, 2015).

1.2. Oat genome

The genome of the common oat, *Avena sativa*, is hexaploid consisting of three sets of seven chromosome pairs (Marshall *et al.*, 2015) as a result of interspecific hybridisation in the same manner as other cereals such as wheat, this polyploidisation that brought together three diploid genomes. The chromosome pairs are labelled as AA, CC and DD (O'Donoghue *et al.*, 1995); AA and CC diploid oat species exist in isolation but no DD genome diploid oats have yet been identified. It is possible, given its close similarity to the AA genome, that the DD genome is a recent duplication of that chromosome pair (Rines *et al.*, 2006). There is one domesticated AA diploid oat species, *Avena strigosa*, popular as a winter crop in Brazil, where it is grown as a forage crop and often referred to as black oats.

Producing a consensus genetic map for oats has not been straight forward. The reasons for this include the genome's repetitive nature and its estimated length, 12.5 Gbp (Chaffin *et al.*, 2016). Another complication is the tendency for nonhomologous pairings resulting in reciprocal translocations within or between any of the three constituent genomes A, C or D. Translocations between the chromosome pairs such as the translocation of genetic material from chromosome 7C and 17A (Jellen *et al.*, 1994) can make mapping of those chromosomes difficult when using a mapping population with one parent that possesses the translocation and one parent that does not (Chaffin *et al.*, 2016).

In 2021 the International Oat Nomenclature Committee (IONC) met to approve a new chromosome nomenclature for oat replacing the Mrg prefix (Chaffin *et al.*, 2016) and the alpha numeric system used in Sanz *et al.* (2010) with "Chr" prefix using the Pepsico OT3089 reference genome (Pepsico, 2021). Figure 1.6 shows the *A. sativa* karyotype with the consensus chromosome labels for those chromosomes that were assigned by three authors: Sanz *et al.*, 2010; Chafin *et al.*, 2016; Chong, Howarth (Institute of Biological, Environmental and Rural Sciences), Tinker (Agriculture and Agri-Food Centre), Blake (Montana State University, Herrmann (Julius Kühn-Institut), Huang (National Taiwan University), Jellen (Brigham Young University), Katsiotis (Cyprus University of Technology), Langdon (Institute of Biological, Environmental and Rural Sciences), Li (Murdoch University), Mascher (Helmholtz Center Munich), Park (University of Sydney), Sen (USDA/Agricultural Research Service), and Wight (Agriculture and Agri-Food Centre), 2021. Information taken from IONC meeting minutes.

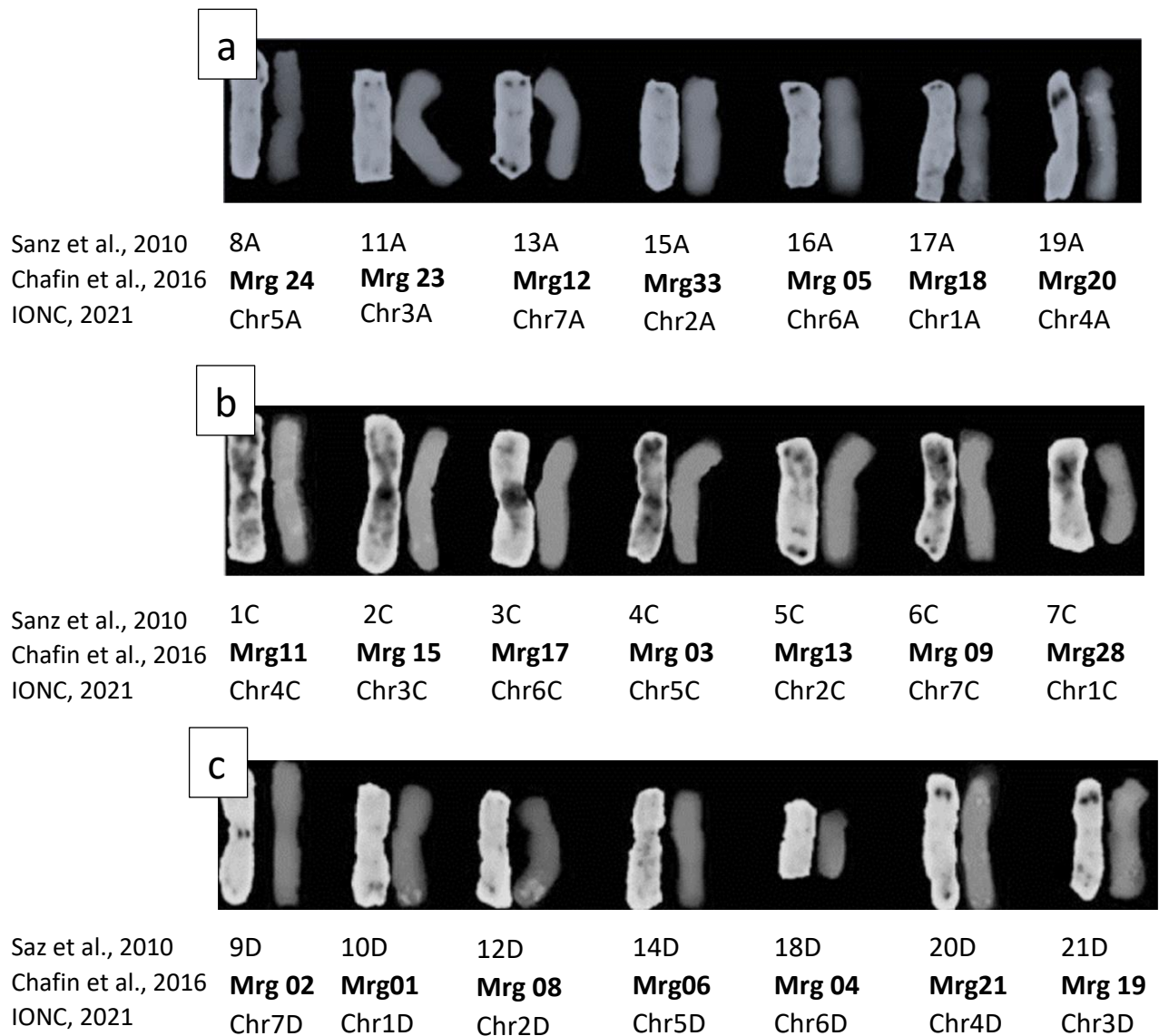


Figure 1.6: *Avena sativa* karyotype, **a**: A genome chromosomes, **b**: C genome chromosomes, **c**: D genome chromosomes. Adapted from Sanz et al. (2010), Chaffin et al. (2016), Zhao et al. (2018), and Canales et al. (2021).

1.2.1. Dwarfing genes

Wheat is a more valuable crop globally than oats and as a result there has been more research and breeding conducted to improve its agronomy and disease resistance. A large aspect of that research has focused on reducing the height of the wheat crop. In agriculture it is advantageous to reduce the height of plants such as cereals and increase the straw stiffness to lower the likelihood that they will lodge prior to harvest and support greater weights of the harvestable part. Such attributes allow higher applications of nitrogenous fertilisers to increase yield. Increased height has been speculated to be a resistance factor in wheat against fusarium head blight (FHB) (Buerstmayr *et al.*, 2000). Most wheat varieties in containing *Rht8* Europe inherited their dwarfing or reduced height gene *Rht8* from the Japanese wheat variety Akakomagi (Borojevic and Borojevik, 2005) which was crossed with Italian varieties by

Nazareno Strampelli in the early twentieth century from where it spread through southern and central Europe. The Green Revolution in Mexico, India and Pakistan in cereals was driven in part by successful introgressions of the dwarfing genes *Rht1* and *Rht2* from the Japanese variety Norin 10 acquired by US scientists after the Second World War and crossed into stem rust resistant Mexican and US wheats by Dr Norman Borlaug before being distributed in the late 1960s around the world (Hessor, 2006). Shorter stiffer strawed varieties allowed more fertiliser to be applied to crops that were then less likely to lodge before they could be harvested (Borojevic and Borojevic, 2005), resulting in large increases in the global yield of wheat. The first dwarf wheat was introduced into the UK market in 1976 and was developed by the breeder Francis Lupton by crossing Norin 10 with native varieties to generate, amongst others, the variety Hobbit. At the time Hobbit out-yielded other commercial varieties by 10% (Gale, 1975). Prior to the introduction of Hobbit, wheats had been reducing in height in the UK since the Second World War and varieties such as Cappelle-Desprez were approximately 100 cm tall, much shorter than the 130 cm typical of wheat in the UK at the start of the twentieth century (Gale, 1975). Wheat yields in the UK began to increase during the 1950s, a trend which continued until the 1990s (Figure 1.5), in part driven by short, lodging-resistant wheat. The most common dwarfing gene within UK wheat is currently *Rht1*.

Dwarfing genes are also present in oats, and although eight dwarfing genes have been identified, only three have ever been successfully used in breeding programmes (Milach *et al.*, 1998; Milach and Federizzi, 2001; Molnar *et al.*, 2012). The *Dw6* gene is dominant and reduces the length of the upper three internodes; lines possessing *Dw6* can have their upper two internodes reduced in length by as much as 50% compared to their progenitor lines (Milach *et al.*, 2002). This gene can cause the panicle to not fully emerge from the boot/flag leaf sheath and the overall length of the panicle can be reduced. Farnham *et al.* (1990) experimented with the heritability of panicle extrusion from *Avena fatua* and *A. sterilis* sources and found increased panicle extrusion was highly correlated to peduncle length, the parameter being reduced by the dwarfing gene.

The *Dw7* gene (present in the oat cultivar Curt) is semi-dominant and shortens the first and last internodes more than the internodes between; it also causes a decrease in the number of internodes (Milach *et al.*, 1998). Milach *et al.* (2002) examined the *Dw7* gene in the dwarfed line NC2469-3 derived from a spontaneous mutation of the non-dwarf line NC2469 and observed a 46% reduction in height mostly achieved from the reduced internode length of the lower internode lengths as opposed to the loss of one internode. The panicle length was also reduced compared to the non-dwarfed line;

however, that was caused by an additional gene present in the NC2469-3 genotype rather than it being an additional effect of the *Dw7* gene. In the same experiment it was observed that the panicle extrusion was greater in the *Dw7* carrying genotype compared to the *Dw6* genotype. The *Dw8* dwarfing gene was isolated in accessions of *A. fatua* in Japan and introgressed into the variety Kanota (Milach *et al.*, 1998). The gene is dominant and shortens all internodes reducing the plant height by up to 50%. Much like *Dw6* this often results in the panicle not fully extruding from the flag leaf sheath (Yan *et al.*, 2021). It has been seen that the gene can be used in the background of taller varieties to generate plants of intermediate height more in the region of 80 cm which are likely to be more commercially appealing, although in the UK at least, this has not happened.

Dwarfing genes in oats have not been as successful as they have been in wheat as they have not delivered the yield benefits that came with the wheat dwarfing genes. Balado was released in 2010, containing the *Dw6* dwarfing gene and giving rise to an 8% yield increase over the control varieties. However, it has since been removed from the AHDB RL due to its low specific weight, kernel content and low disease resistance. In 2020, Fusion, developed by IBERS, was the only dwarf variety currently on the AHDB RL, but it failed to be included in the 2021 RL.

All three discussed oat dwarfing genes are classed as gibberellic acid (GA) sensitive, in contrast to the wheat dwarfing genes which are classed as GA insensitive. Dose response tests carried out by Milach *et al.* (2002) to GA₂₀ and GA₁ showed similar responses from dwarf plants carrying the *Dw6*, 7, and 8 genes and their respective non dwarfed progenitor lines. This suggests that the dwarf plants are still able to metabolise GA₂₀ to GA₁ and utilise GA₁ to manipulate plant height and suggests that they are deficient in GA. Given that the genes in question are dominant the authors suggested that the dwarfing genes are involved in down regulating the expression of other genes involved in GA metabolism rather than being defective genes themselves within the GA metabolism pathway. Being associated with GA pathways can cause the dwarfing genes in question to have multiple pleiotropic effects.

1.3. Fusarium of small grain cereals

1.3.1. History of *Fusarium* within small grain cereals

Certain species of fungi within the *Fusarium* genus are of economic importance within food supply chains: the most commonly researched are those that infect wheat crops such as *F. graminearum* and *F. culmorum*. These species can reduce crop yield, displaying visible symptoms within the field, and contaminate the grain with the harmful mycotoxins, deoxynivalenol and zearalenone. However, within the UK the species of *Fusarium* leading to fusarium head blight (FHB) rarely cause commercial damage to

oat crops and oats are regarded as being *Fusarium* resistant. This is in contrast to more northerly growing areas, where oats are a popular cereal crop and can be severely impacted by FHB, such as Norway (Hofgaard *et al.*, 2016a; Tekle *et al.*, 2018), Finland (Hautsalo *et al.*, 2020), Denmark, Sweden, Russia, parts of the USA, and Canada (He *et al.*, 2013).

Fusarium head blight was brought to people's attention after two large outbreaks in wheat in 1917 and 1919 in the Mid-Western and Mid-Atlantic USA, causing grain losses of a quarter of a million tons and two million tons respectively. Gradual progress was made understanding the nature of the disease: Bolley (1913), as cited in Leonard and Bushnell (2003), suggested that it was important to have seed initially clean of the fungus prior to drilling. This was supported by Dickson's observations published in 1923 that following severe blight infections cereal crop stands were diminished by up to 30% (Dickson, 1923, as cited in Leonard and Bushnell, 2003). Perhaps some of the severity of these initial outbreaks can be attributed to the wide-spread growing of a susceptible cultivar of wheat called Marquis that became popular in the 1920s in the American Mid-West. It was H.K. Hayes who first began to cross wheat germplasms at the University of Minnesota to develop head blight resistant wheat in 1915 (Leonard and Bushnell, 2003). At this time, various *Fusarium* species were being identified and no strong host preferences had been observed between the typical cereals grown at the time; wheat, barley, oats, rye and grasses. Around the turn of the twentieth century *Fusarium* in some form had been identified in Russia, Germany, Siberia, Denmark, The Netherlands, Australia, the UK and the USA (Leonard and Bushnell, 2003).

One of the most conspicuous events in *Fusarium*'s history was the discovery of alimentary toxic aleukia in Russia in the first half of the twentieth century. Outbreaks recorded as early as the 1920s, were mostly in poor rural communities and tended to occur after a mild winter with an early snowfall. Such outbreaks were exacerbated by hunger during the Stalinist genocides of the 1930s and again from 1942-44 during the Second World War when over 10% of the population of Orenburg became affected (Joffe, 1960; Torp and Langseth, 1999). It was later identified by Abraham Joffé and published in 1950 that the alimentary toxic aleukia was caused by eating overwintered grain infected with either *Fusarium poae* or *Fusarium sporotrichioides* producing the mycotoxin T2 (Torp and Langseth, 1999; Yagan and Joffe, 1976). In times of food shortages, grain which was buried under early snow was collected once the snow had thawed, causing people to ingest potentially lethal doses of T2.

1.3.2. Range of species and typical hosts

Several *Fusarium* species are causal agents of FHB (or referred to fusarium panicle blight in oats) and mycotoxin contamination in cereals. Several species have been

identified and undergone extensive study such as *F. graminearum* and *F. culmorum*, producers of deoxynivalenol (DON) and zearalenone (ZON) mycotoxins in wheat. Legislative limits were introduced in the EU in 2006 (Commission Regulation (EC) No 1881/2006) for both DON and ZON. The maximum limits for DON and ZON in unprocessed oats are 1750 and 100 µg kg⁻¹ respectively with lower limits for intermediate and finished food products. Table 1.1 details a selection of *Fusarium* species along with their conidia morphology, mycotoxin profile and typical hosts.

Table 1.1: Description of the most common *Fusarium* disease causing pathogens (Hanson and Hill, 2004; Hanson, 2006; Thrane et al., 2004; Parry et al., 1995; Leonard and Bushnell, 2003)

Pathogen	Microconidia shape	Macroconidia shape	Mycotoxin profile	Reported hosts
<i>Fusarium graminearum</i>	None	Fusiform	Deoxynivalenol (DON), zearalenone (ZON)	Grasses including wheat, barley, oats and triticale, sugar beet
<i>Fusarium culmorum</i>	None	Fusiform	Deoxynivalenol (DON), nivalenol (NIV)	Grasses including wheat, barley, oats and triticale, sugar beet
<i>Fusarium poae</i>	Globose to limoniform	Fusiform	15-monoacetoxyscirpenol (15-MAS), diacetoxyscirpenol (DAS), nivalenol (NIV), triacetoxyscirpenol (TAS), neosolaniol (NEO), and scirpentiol (SCR), fusarenon-X (FX), aurofusarin (AUF), and enniatin (EN)	Wheat, barley and oats
<i>Fusarium avenacium</i>	None	Thin elongated fusiform	Diacetoxyscirpenol (DAS), zearalenone (ZON), T2,	Wheat, barley, oats and triticale, and sugar beet
<i>Fusarium sporotrichioides</i>	Ovate, pyriform to spindle shaped	Fusiform	HT2, T2, Diacetoxyscirpenol, 15-monoacetoxyscirpenol (15-MAS), neosolaniol (NEO), aurofusarin (AUF), and enniatin (EN)	Wheat, barley and oats
<i>Fusarium langsethiae</i>	Globose to napiform	None	Chrysogine (CHRYG), aurofusarin (AUF), and enniatin (EN), diacetoxyscirpenol (DAS), HT2, T2, neosolaniol (NEO)	Oats, wheat, and barley
<i>Microdochium nivale</i>	None	None	None	Grasses including wheat, barley, oats and triticale

1.3.2.1. *Fusarium graminearum*

Fusarium graminearum is the most important causal agent of FHB worldwide. This species predominantly produces the type B trichothecene, DON, but some isolates are nivalenol (NIV) producers. It is pathogenic to wheat, barley, maize, rye and in certain regions oats (Miller *et al.*, 1983; Parry *et al.*, 1995; Munkvold, 2003; Hofgaard *et al.*, 2016a), amongst other minor cereal crops. In wheat and barley, the pathogen causes the diseases; seedling blight, foot rot and FHB. These are a result of infection at anthesis for head blight, and a combination of infected seed and/or infection from crop debris for seedling blight and foot rot. Infection studies have shown that *F. graminearum* infects after germinating within the spikelet of wheat and subsequently forming infection hyphae that invade the ovary and inner surfaces of the lemma and palea (Wanjiru *et al.*, 2002). After this initial infection the pathogen continues to grow inter and intracellularly using enzymes to degrade the cell wall components cellulose, pectin and xylan (Wanjiru *et al.*, 2002). *Fusarium graminearum* is a facultative saprophyte and can overwinter in crop debris to infect the following crop (Parry *et al.*, 1995) as such previous crop and tillage method can influence subsequent *F. graminearum* infection risks (Dill-Macky and Jones, 2000). It is possible to partially control *F. graminearum* infection through the application of fungicides such as prothioconazole immediately before anthesis (Edwards and Godley, 2010).

In Norway, varieties of oats have been removed from the market due to their susceptibility to *F. graminearum* and resultant DON contamination (Bjørnstad and Skinnnes, 2008).

1.3.2.2. *Fusarium culmorum*

Fusarium culmorum along with *F. graminearum* is one of the main causal pathogens of FHB (Edwards, 2004). *Fusarium culmorum* is a DON or NIV producer depending on the isolate; its epidemiology and host preference is very similar to that of *F. graminearum*. It differs in its preferential conditions: *F. culmorum* prefers a cool maritime climate (Parry *et al.*, 1995). In 1926 and 1927, northern areas of the UK were affected by what was termed as “deaf ears” which was shown to be *F. culmorum* by F.T. Bennett (Parry *et al.*, 1995).

1.3.2.3. *Microdochium* Species

Although not within the genus *Fusarium*, *Microdochium nivale* and *Microdochium majus* are both causal agents of FHB, seedling blight and foot rot in cereals (Walker *et al.*, 2009; Simpson *et al.*, 2000; Hare, 1997), and was at one stage named *Fusarium nivale* (Abdelhalim *et al.*, 2020). However, neither *M. nivale* nor *M. majus* produce any

mycotoxins and because they tend to exist in complexes with *Fusarium* species, although control of *Microdochium* species can lead to greater accumulation of mycotoxins by reducing competition with mycotoxin producing species such as *F. graminearum* and *F. culmorum*. In terms of biological behaviour, *M. nivale* and *M. majus* can be considered as broadly equivalent as there are very few differences in host range, growth rate or fungicide sensitivity, although differences in host virulence do exist (Simpson *et al.*, 2000). *Microdochium nivale* and *M. majus* are pathogenic on perennial grasses including rye, as well as annual cereals such as wheat, barley and oats. Both species can be largely controlled through various fungicidal seed treatments (Glynn *et al.*, 2008).

1.3.3. *Sporotrichiella* section

Within the *Fusarium* genus, *F. langsethiae* sits within the *Sporotrichiella* section (Schmidt *et al.*, 2004). Two further significant mycotoxin producing species of the same section are *F. poae* and *F. sporotrichioides* (Thrane *et al.*, 2004).

1.3.3.1. *Fusarium poae*

Fusarium poae is a species of *Fusarium* with very similar morphology to *F. langsethiae*, to the extent that it has been speculated that the two have been mis-identified for one another in the past (Torp and Langseth, 1999). When cultured on potato dextrose agar *F. poae* produces aerial mycelium and appears pale pink to white and it also has a fruity smell in culture. The lack of a fruity smell and reduced aerial mycelium are two important characteristics that differentiate *F. langsethiae* from *F. poae*. *Fusarium poae* is pathogenic to wheat and barley as well as several other plants including maize, oats, soybean and alfalfa (Stenglein, 2009). What is unusual for this species is that it produces both type A and type B trichothecenes. The pathogen has been demonstrated to produce HT2 and T2 but only at low concentrations in a minority of isolates (Thrane *et al.*, 2004). More commonly *F. poae* produces monoacetoxyscirpenol (MAS), diacetoxyscirpenol (DAS), nivalenol (NIV), triacetoxyscirpenol (TAS), neosolaniol (NEO), and scirpentiol (SCR) (Stenglein, 2009). Thrane *et al.* (2004) did not record *F. poae* as producing DON, however previous work has reported DON production by *F. poae* in liquid media (Abramson *et al.*, 1993), and low concentrations of DON being produced in *F. poae* inoculated barley (Salas *et al.*, 1999). Salas *et al.* (1999) observed DON production in five of ten *F. poae* isolates but advised caution in the interpretation of those results as plated grain latterly showed *F. graminearum* growth.

Fusarium poae DNA was found in 90% of 240 oat samples examined by Edwards *et al.* (2012a) collected from across the UK between 2002 to 2005. The quantity of *F. poae*

DNA in those samples did not correlate with the concentration of HT2 and T2 in the grain suggesting that that *F. poae* did not produce the mycotoxins.

1.3.3.2. *Fusarium sporotrichioides*

Fusarium sporotrichioides is another species within the *Sporotrichiella* section of *Fusarium*; it has some similar morphological characteristics to *F. langsethiae* although differs in that it produces macroconidia and chlamydospores; does not have a powdery appearance in culture; is faster growing; and has more aerial mycelia on PDA (Schmidt *et al.*, 2004). However, *F. sporotrichioides* does produce a very similar secondary metabolite profile to *F. langsethiae*: most notably it is a producer of HT2 and T2, as well as NEO and DAS (Thrane *et al.*, 2004). Edwards *et al.* (2012a) were unable to amplify any *F. sporotrichioides* DNA within their 260 samples of oats selected from harvest samples between 2002-2005 collected from across the UK, suggesting that the pathogen is not present or at least not a significant pathogen of oats within the UK.

1.3.3.3. *Fusarium langsethiae*

In 1999 a new type of *Fusarium* was identified as “powdery poae” (Torp and Langseth, 1999). It was seen that this “powdery poae” produced large amounts of HT2 and T2 trichothecenes which was at odds with the typical mycotoxin profile of *F. poae*, which produces very little T2 or HT2. Torp and Langseth (1999) compared 18 isolates of the “powdery poae” (from three countries) with 12 isolates of *F. poae* and found that none of the *F. poae* produced T2 whereas all the “powdery poae” isolates produced large amounts of T2. Seventy three percent of Norwegian cereal samples from 1996-1998 (n=89) contained HT2 and T2 above the limit of quantification (LoQ = 20 µg/kg) with a maximum of 880 µg/kg (Torp and Langseth, 1999). The only other *Fusarium* species at that time known to produce high levels of HT2 and T2 was *F. sporotrichioides* which was rarely seen in Norway. Torp and Langseth (1999) therefore suggested that “powdery poae” was present and being mis-identified as *F. poae*, the pair went one step further and suggested that “powdery poae” has been mis-identified as *F. poae* in cases where high levels of T2 and HT2 have been recorded. An example highlighted by the authors was Joffe, who had identified HT2 and T2 as being the causal agents of ATA outbreaks in Russia in the 1940s, suggesting that Joffe had in fact isolated strains of “powdery poae” from the over wintered cereals and not *F. poae* as he had reported, as all his 25 isolates produced T2. Later work has supported this in demonstrating repeatedly that *F. poae* rarely produces T2 in appreciable quantities. For example, Thrane *et al.* (2004) found that out of 49 isolates of *F. poae*, only three and four isolates produced HT2 and T2 respectively. In 2004, *F. langsethiae* was officially described as a distinct species by Torp and Nirenberg and named after their late colleague Dr Wenche Langseth (Torp *et al.*, 2004). In the same year Schmidt *et al.*

(2004) published a paper detailing an integrated taxonomic study of *F. langsethiae*, *F. poae* and *F. sporotrichioides* using morphological, chromatographic and molecular DNA data to build a composite data set which they were able to use to distinguish each *Fusarium* species from each other.

Morphologically *F. langsethiae* is most similar to *F. poae*: *F. langsethiae* has globose and pyriform microconidia born on monophialides and lacks chlamydospores. However, *F. langsethiae* completely lacks macroconidia, something that both *F. poae* and *F. sporotrichioides* can produce (Torp and Nirenberg, 2004). *Fusarium langsethiae* further distinguishes itself by its slow growth rate on both potato dextrose agar (PDA) and potato sucrose agar (PSA), growing at almost half the rate as compared to *F. poae* and *F. sporotrichioides*. Without a microscope *F. langsethiae* and *F. poae* look similar, both with peach/grey colouration. *Fusarium langsethiae* can be differentiated because it has a powdery appearance caused by it having little aerial mycelium and profuse microconidia, and *F. langsethiae* lacks a fruity odour present with *F. poae*. In terms of each species mycotoxin profile *F. langsethiae* has been described as being more similar to *F. sporotrichioides* (Torp and Langseth, 1999). The most important aspect of this is the species' ability to produce large amounts of HT2 and T2, a characteristic it shares with *F. sporotrichioides* and not *F. poae* (Thrane *et al.*, 2004).

1.3.3.4. Evidence gathered through field research on *F. langsethiae* and HT2 +T2 production

From 2002 to 2005 a survey was carried out on the effects of agronomic practices on the mycotoxin content and profile of UK oat and barley crops (Edwards, 2009a). The survey revealed that although barley had low incidence and concentrations of HT2 and T2 mycotoxins on a par with wheat, quantifiable concentrations (greater than 10 µg/kg) of the HT2 and T2 were found in 92% and 84% of oat samples respectively. Across all years the combined mean concentration was 570 µg/kg for oats as compared to the highest concentration in barley of 138 µg/kg. The maximum combined concentration of HT2 and T2 (HT2+T2) found in oats was 9990 µg/kg (Edwards, 2009a).

Fusarium langsethiae is now known to be the chief producer of HT2 and T2 mycotoxins in UK oats. In a study conducted at Harper Adams University (Edwards *et al.*, 2012a), oat samples of known mycotoxin concentration from a previous study (Edwards, 2009a) were assayed using real time PCR to quantify the concentration of *F. langsethiae*, *F. poae*, and *F. sporotrichioides* DNA. *Fusarium langsethiae* was found in almost all the samples, and *F. poae* in 90%, whereas *F. sporotrichioides* was absent from all samples. A regression analysis showed no correlation between *F. poae* DNA concentrations and HT2+T2 mycotoxins, however *F. langsethiae* strongly correlated

($P < 0.001$, $r^2 = 0.60$). Although there are other species of *Fusarium* that can synthesise HT2 and T2 mycotoxins (*F. poae*, *F. sibiricum*, *F. sporotrichioides* and *F. armeniacum* (T2 only)), Edwards *et al.* (2012a) presents strong evidence from this correlation that the previously seen high levels of HT2+T2 mycotoxins found in oats were a result of *F. langsethiae* infection. When multiple regression was carried out with *F. langsethiae* and *F. poae* with DNA concentrations grouped by year, both fungi were shown to be significantly correlated, however *F. poae* was negatively correlated to HT2+T2 concentration. It is therefore possible that the two fungi co-exist on the same host but as Kokkonen *et al.* (2010) showed, *F. poae* did not produce HT2 or T2 when grown on a cereal based medium, meaning that the *F. poae* was potentially competing with the *F. langsethiae* to cause the negative correlation. Year was shown not to be significant, suggesting that the relationship between *F. langsethiae* infection level and mycotoxin production will be stable regardless of climatic variations across years (Edwards *et al.*, 2012a). A similar study was conducted in Norway (Hofgaard *et al.*, 2016b) where *F. graminearum*, *F. culmorum*, *F. langsethiae*, *F. poae*, and *Fusarium avenaceum* DNA were quantified in 289 samples of oat over six years along with 18 mycotoxins including HT2 and T2. *Fusarium graminearum* was identified as the main producer of DON in oats and binary logistic regression showed a positive relationship between *F. langsethiae* DNA concentration and HT2+T2 concentration in oats (accounting for 51% of the variation).

Schöneberg *et al.* (2018) reported similar findings from a survey of oats in Switzerland conducted over the three years 2013-2015. The survey collected 325 samples of unprocessed oat grain directly from the field with associated agronomic data. *Fusarium langsethiae* DNA was present in all three years at an incidence of between 5% and 9.2%, far less than *F. poae* which was present between 6.9% and 44.5%. Regression analysis again showed a strong correlation between DNA concentrations of *F. langsethiae* and the concentration of HT2+T2. *Fusarium langsethiae* has also been reported in Poland (Lukanowski *et al.*, 2008), Belgium (Dedeurwaerder *et al.*, 2014) and Italy (Infantino *et al.*, 2007), in addition to Switzerland (Schöneberg *et al.*, 2018) and the Nordic states (Pettersson *et al.*, 2008; Sundheim *et al.*, 2013).

Opoku *et al.* (2013) surveyed wheat, barley, oat and triticale crops over three years (2009-2011) in Shropshire and Staffordshire under commercial conditions, quantifying *F. langsethiae* DNA in plant organs at various growth stages. Concentrations of *F. langsethiae* DNA were lower and less consistent in terms of the plant organs infected in wheat, barley (spring and winter) and triticale than in oats. This survey relied on natural infection of the crops with the fungus and therefore only highlighted the preference of the fungus for oats in the environment tested. However, a separate piece

of *in vitro* work by Imathiu *et al.* (2009) showed that under the same conditions *F. langsethiae* was more pathogenic to oats than wheat. In this study, the authors inoculated detached oat and wheat leaves and found that *F. langsethiae* was only able to infect wheat when the detached leaf was wounded but was able to infect unwounded detached oat leaves. Opoku (2012) conducted field experiments to investigate the pathogenicity of *F. langsethiae* towards wheat, barley and oats cultivated together with identical agronomy. For both spring and winter cereals DNA and HT2+T2 concentrations were statistically higher in oats than in wheat or barley, with the exception of *F. langsethiae* DNA between spring oats and wheat. Interestingly HT2 + T2 accumulated in significantly higher concentrations in the oats per unit *F. langsethiae* DNA than in either wheat or barley suggesting that not only are oats more susceptible to *F. langsethiae* infection but that they are also more susceptible to the accumulation of HT2+T2. There was a significant difference between the oat grain and the rest of the head, being rachis, rachis branches and the glumes. Opoku (2012) did not find an interaction between cereal part and the variety of cereal in the winter cereal lines, however only three varieties of oat (Gerald, Dalguise, and Mascani) were examined. Cultivar differences in accumulation in the rest of the head and the varying quantities of non-grain material in harvested plot samples caused by the different threshing requirements and maturity times of cultivars harvested on the same date could be a contributing factor to varietal differences in HT2+T2 accumulation. In artificial inoculation work performed by Divon *et al.* (2019) on wheat and oats it was shown that *F. langsethiae* infected both wheat and oats in the same manner in terms of where the hyphae infected the developing grain but that in wheat the infection progressed more slowly and resulted in less hyphal mass and increased sporulation relative to the growth on oat.

Evidence from these previous studies suggests that *F. langsethiae* is the major producer of potentially harmful concentrations of HT2 and T2 trichothecenes in UK oats, but also that the problem is restricted to oats due the preference of *F. langsethiae* for oats and its weak pathogenicity for other cereals.

The difficulty thus far in the study of *F. langsethiae* has been two-fold; firstly, the fungus elicits few if no visible symptoms in any host crop (Opoku *et al.*, 2013), and secondly the inability to inoculate any field crop reliably with the pathogen to levels of infection that would allow comparative studies to be conducted examining methods of control (Schöneberg *et al.*, 2019), as can currently be performed for other *Fusarium* species on cereals.

1.4. Current knowledge on *F. langsethiae* epidemiology

So far, the epidemiology of *F. langsethiae* is unknown. Opoku *et al.* (2013) suggested a lifecycle for the fungus, the crucial aspect of which was the increased growth of the fungus on the emerged heads of the plants with the pathogen DNA almost undetectable prior to anthesis. In two of the three years surveyed Opoku *et al.* (2013) had data showing the low-level presence of the pathogen at panicle emergence and from this it was postulated that the infection occurred at panicle emergence with the subsequent fungal growth happening in the spikes of the crop.

Wheat plants are most susceptible to FHB at anthesis; infection is believed to take place when ascospores and or macroconidia are deposited within or close to the florets. Initial germination likely takes place on the anther, a hypothesis which is supported by work showing that differences in anther retention between genotypes has an impact on host susceptibility (Buerstmayr and Buerstmayr, 2015) and that hyphal growth then infects the ovary and subsequently the entire spike. Drying events after rainfall stimulates the ballistic release of ascospores from perithecia and rain splash moves conidia up the plant profile to reach the ears (Parry *et al.*, 1995). As such rain at anthesis encourages *Fusarium* infection leading to head blight. FHB in oats received relatively little attention in the UK until recently (Edwards, 2007a), however in the Nordic countries FHB in oats is more prevalent (Hofgaard *et al.*, 2016a).

Seedling blight is yet to be observed for *F. langsethiae* (Imathiu *et al.*, 2010; Divon *et al.*, 2012; Opoku *et al.*, 2013), only low concentrations of *F. langsethiae* DNA have been found before panicle emergence (Opoku *et al.*, 2013) suggesting that the pathogen prefers florets and grain as a substrate and is therefore more pathogenic in the later stages of the crop's growth. Opoku *et al.* (2013) observed a dramatic increase in *F. langsethiae* DNA by growth stage 92 (late/hard dough) (Tottman *et al.*, 1979), as well as small increases in the concentration of fungal DNA in the leaves and stems of plants; from this it was postulated that the fungus produces spores upon senescence of the plant. In similar survey work conducted in the same region of the UK Imathiu *et al.* (2013) found relatively low *F. langsethiae* DNA concentrations at anthesis (GS 59) and typically higher concentrations at late milk to soft dough (GS77-85).

Microscopy work conducted by Divon *et al.* (2019) on artificially infected oat plants demonstrated that the fungal hyphae of *F. langsethiae* entered the grain by the apex or via the overlap between the lemma and palea and then grew toward the base of the grain developing penetration structures on internal surfaces. The pathogen grew on the caryopsis of the developing grain below the lemma and palea in much the same way *F. graminearum* has been observed to in wheat with hyphae entering through natural openings at the apex of the kernel via the overlap between the lemma and

palea. *Fusarium langsethiae* was also seen to exude a viscous liquid that was speculated to have helped the hyphae to adhere to the plant surfaces (Divon *et al.*, 2019). The fungus forms infection cushions on the pericarp surface in much the same way *F. graminearum* does in wheat and grows branching hyphae around the brush hairs between the pericarp and the lemma and palea. The fungus was observed to directly penetrate the pericarp from runner hyphae growing across the pericarp surface (Divon *et al.*, 2019).

Anthesis as the timing for infection is supported by Divon *et al.* (2019), who observed that the microconidia used in the spore suspension to inoculate the plants had not germinated three days after inoculation unless they were in the presence of pollen. In the referenced experiment, anthers were retained within the oat spikelet clenched between the lemma and palea at the apex and these areas were typically overgrown with hyphae. Figure 1.7 shows a proposed life cycle of *F. langsethiae* incorporating proposals from both Opoku and Divon as well as evidence from survey studies on crop rotation, debris management and cereal intensity (Edwards, 2017; Hofgaard *et al.*, 2016a; Schöneberg *et al.*, 2018). Three potential infection timings are illustrated in Figure 1.7, each of which have been suggested in the literature either for *F. langsethiae* or are common to *Fusarium* species: - panicle emergence (GS59) (Opoku *et al.*, 2013), anthesis for most *Fusarium* species (GS61-69) (Parry *et al.*, 1995) and late anthesis/early milk (GS69-71) (Divon *et al.*, 2019).

Edwards (2007a) found a significant interaction ($P < 0.001$) between region and year when HT2+T2 concentrations in oats were analysed between the years of 2002-2005. The full model (including year, region, practice, previous crop, plough and variety) accounted for 46% of the variation in the examined data set with year and region accounting for 17% of the variance. Given that such a large proportion of the explained variance is accounted for by the year and region is indicative of weather being influential. Weather has also been implicated as an influential factor in the epidemiology of other *Fusarium* species (Kriss *et al.*, 2010; Parry *et al.*, 1995). In a similar study on wheat during the same period a model for DON in wheat showed an even greater association, with year and region accounting for 35% of the variance in a model that accounted for 41% of the observed variance (Edwards, 2007b).

Several studies have attempted to associate weather conditions such as humidity, rainfall and temperature with HT2+T2 concentration in commercially grown oat crops. Xu *et al.* (2014) used 300 samples from UK oats with agronomic data and environmental data to identify conditions at key periods within the growing season. The study identified warm humid conditions in early and mid-May and dry conditions thereafter as inductive to high HT2+T2 concentrations in the harvested grain. Hjelkrem

et al. (2017) estimated phenological windows in 188 fields of oats in Norway along with weather variables recorded at weather stations within 20 km of the farm addresses which were then used to correlate weather variables with HT2+T2 concentration in the harvested grain. The study found that in the lead up to flowering (booting) cool (<12 °C) or moderate (10-20°C) temperatures coupled with humid conditions correlated with higher HT2+T2 concentrations. High temperature and high humidity were seen to be negatively correlated to HT2+T2 concentration. Conditions during flowering were not found to correlate to HT2+T2 concentrations, but high humidity and high temperatures during the early milk stage (GS70-75) were found to correlate to higher HT2+T2 concentrations at harvest. The analysis also identified that high temperatures and low humidity could negatively impact the concentration of HT2+T2 if they occurred during dough development. Kaukoranta *et al.* (2019) also examined the relationship between weather and growth stage in terms of HT2+T2 concentration in 804 spring oat crops in Norway, estimating the date of mid-flowering (GS65). They determined that warm weather from four weeks preceding mid anthesis up until harvest, and humid conditions in the two weeks leading up to mid anthesis, were the most important climatic factors in terms of *F. langsethiae* infection.

Some of the above studies report conflicting results: Kaukoranta *et al.* (2019) identified anthesis as a key growth stage whereas Hjelkrem *et al.* (2017) did not identify anthesis itself as important rather the growth stages surrounding it. Both Xu *et al.* (2014) and Kaukoranta *et al.* (2019) found that warm dry conditions after flowering through until harvest led to higher HT2+T2 concentrations, but Hjelkrim *et al.* (2017) stated the opposite, instead suggesting that such conditions reduced HT2+T2 concentrations when they occurred during dough development (GS80-90).

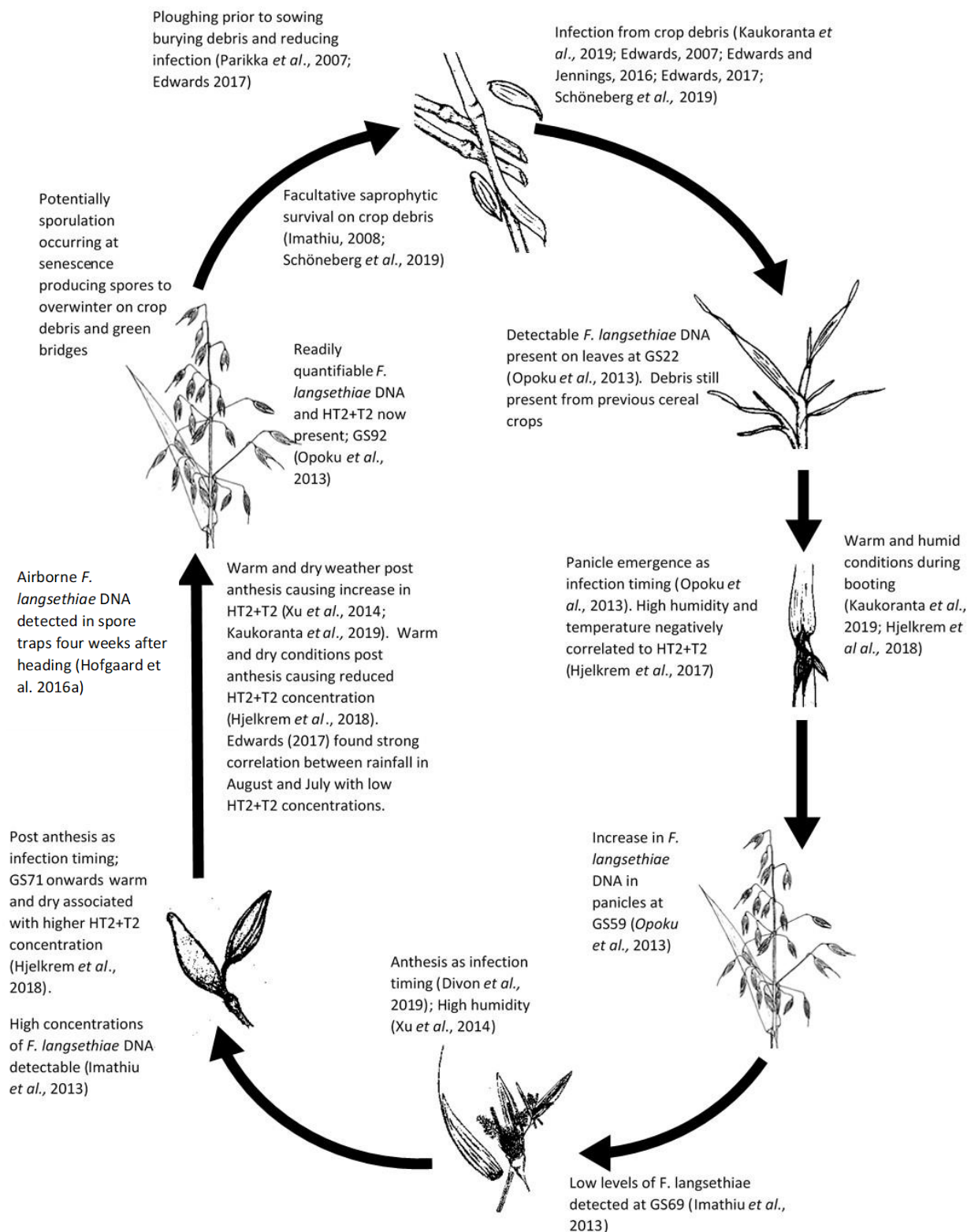


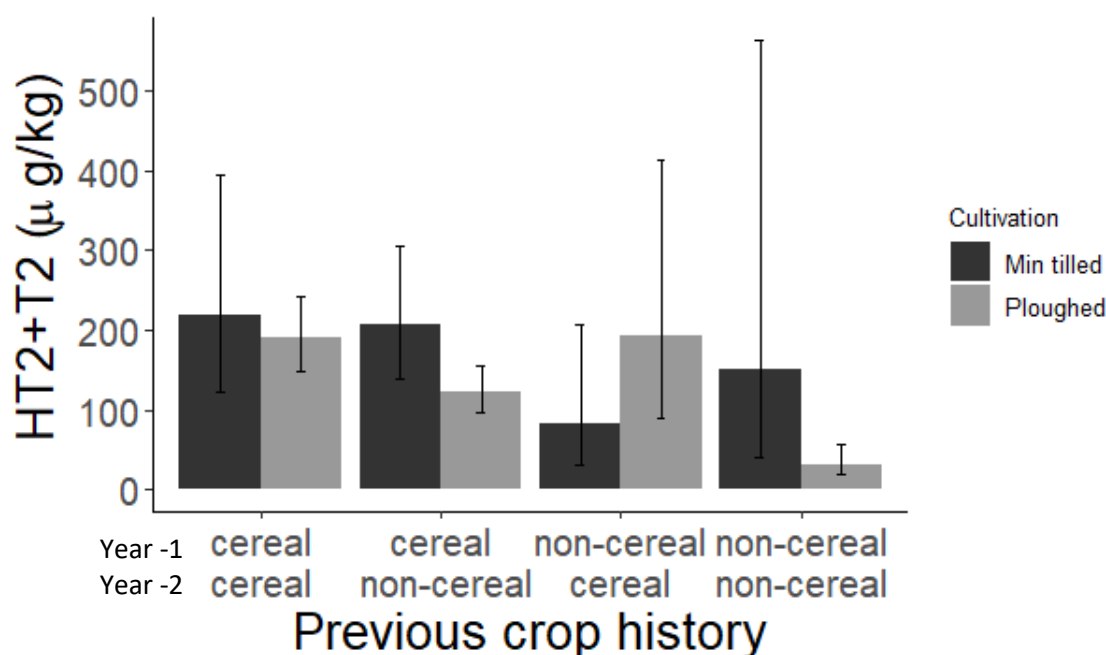
Figure 1.7: Proposed *F. langsethiae* life cycle based on the current literature

The life cycle proposed in Figure 1.7 is not proven and presents minimal evidence on how the pathogen overwinters. Crop debris has been suggested as a source of inoculum and various authors (Schöneberg *et al.*, 2019; Imathiu, 2008) have managed to inoculate oat straw with *F. langsethiae* and isolate the pathogen from the straw afterwards. No observations have been published on winter hardy spores produced by *F. langsethiae* that would enable the pathogen to overwinter without a host plant. Hofgaard *et al.* (2016a) collected cereal crop debris left after harvest and subsequent groundwork and drilling to measure the proportion of residues infested with *Fusarium* species. Among the species identified as present, *F. langsethiae* was the least common in the straw, only being present at one of the two examined sites and then only at less than 1% of the crop debris examined. In terms of a life cycle finding, any *F. langsethiae* present in crop debris after drilling of the following crop presents the possibility of crop debris being the source of inoculum in the field, although the levels reported by Hofgaard *et al.* (2016a) are not sufficient evidence on their own to reach this conclusion. Sturz and Johnston (1983) isolated a *Fusarium* species and identified it as *F. poae* from surface sterilised un-emerged barley ears at mid-booting (GS45). The description of the most prevalent isolate in that study matches what we now recognise as *F. langsethiae*. Given that the pathogen could be isolated from the un-emerged ear suggests that the pathogen was able to penetrate the leaf sheath protecting the ear.

Edwards (2007a) identified that *F. langsethiae* incidence was greater in conventional growing systems as opposed to organic systems. This was attributed to more cereal intense crop rotations in the conventional systems as well as more resistant oat varieties in the organic systems. Edwards (2007a) identified that there were equivalent concentrations of HT2+T2 in oat crops following the cereals barley, wheat and oats regardless of ploughing whereas HT2+T2 in oat crops following non-cereals were in comparison significantly lower after ploughing compared cereal crops either ploughed or min tilled. This survey did not ask for rotation details prior to the crop preceding the examined oat. Edwards (2017) repeated the same survey from 2006-2008 and collected additional agronomic data including previous cropping for the preceding four years. Crops in the rotation three and four years prior did not significantly influence HT2+T2 accumulation, and debris management (baled or chopped) was also not significant, regardless of previous crop. However, the interaction of the previous crop, one and two years prior to the examined oat crop, was significantly with cultivation ($P < 0.05$). Figure 1.8 below shows the past two years crops as either cereal or non-cereal as well as whether or not the field was ploughed prior to drilling. The error bars are large and prevent confident conclusions from being drawn. If one were to imagine

that the act of ploughing brought up crop debris from the Year -2 then each column on the graph could be said to have either cereal or non-cereal debris on the soil surface. There is a trend for cereal debris on the surface leading to higher HT2+T2 concentrations. However, Figure 1.8 shows that the only significant difference was between sites ploughed after two years of non-cereal and all other ploughed samples; and sites ploughed after two years of non-cereal and the sites min-tilled after cereals.

Figure 1.8: Effect of cultivation and previous crop on HT2+T2 concentration in harvested oat grain.



Error bars represent 95% confidence limits for predictions. Adapted from Edwards (2017). The previous crop history is described on the x axis; Year – 1 and Year -2 refer to the year before the sampled oat crop and the crop two years before the sampled oat crop respectively. Previous crops are described as either cereal or non-cereal.

Within the lowest concentration above (two years of non-cereal) most of the contributing samples were grass lays of four years or more. Grass as a preceding crop has been shown to reduce the concentration of HT2+T2 in the following oat crop (Edwards, 2007a); grass is often grown for longer than one year giving the site a longer break from potential host crops such as wheat. *Fusarium langsethiae* has been shown to be capable of growing on barley, wheat and triticale, albeit as a weak pathogen likely to be out competed by other *Fusarium* species (Opoku *et al.*, 2013). Therefore, in this study, the removal of any such crop through a grass lay, which changes the annual cycle of drilling and harvesting typical of winter arable crops, could have removed a large proportion of potential inoculum sources.

In another study, based solely on 2014 oat samples, previous crop data was used to identify a relationship between the number of cereal crops in the previous four years to

oats being sowed and the concentration of HT2+T2 in the oat crop. It was found that HT2+T2 concentration increased with increasing numbers of cereal crops in the previous four years (Edwards and Jennings, 2016). This, along with evidence from Edwards (2007a) and Edwards (2017), would suggest that cereals in addition to solely oats have a large role in the life cycle of *F. langsethiae*. Crop debris can act as a nutrient source for *Fusarium* species allowing them to survive in the field until suitable hosts are present again. *Fusarium langsethiae* however does not infect seedlings (Imathiu, 2010) or the stem of more mature plants (Divon *et al.*, 2012) so the pathogen would have to survive until panicle emergence, the most likely time of infection. Imathiu (2008) was able to culture *F. langsethiae* on straw and prove that it could act as a saprophyte. Results from Nordic experiments on tillage (Hofgaard *et al.*, 2016a; Kaukoranta *et al.*, 2019; Parikka *et al.*, 2007) also suggested that removing the previous crop debris through ploughing reduced the inoculum in the field available to the following crop.

Schöneberg *et al.* (2018) conducted a survey in Switzerland collecting 325 oat samples from fields with agronomic details from 2013 to 2015. Statistical analysis of the mycotoxin and DNA levels across all three years showed that the previous crop and the preceding crop to that were significant factors in terms of the HT2+T2 accumulation in a crop of oats. Whether the field had been min tilled or ploughed was another significant factor according to the data examined over the full three years. For other *Fusarium* species in wheat, preceding maize can increase the severity of infection and Schöneberg *et al.* (2018) did survey fields that had had maize in the rotation with oats. However, as the previous crop to oats, maize resulted in less HT2+T2 in all three years compared to a preceding small grain cereal, with the difference being statistically different in 2014 and 2015 ($P < 0.05$). Opoku *et al.* (2013) examined Italian rye grass from fields within his survey and found no *F. langsethiae* DNA to suggest they were acting as a source within the field. This is further supported by Edwards *et al.* (2009a) who found that HT2+T2 concentrations in oat crops following grass were very low.

Thus far no studies have successfully identified the source of inoculum within the field, however cultivation and debris management as well as previous crop are consistently found to be significant factors. From that evidence and demonstrations that *F. langsethiae* can act as a saprophyte (Imathiu, 2008; Hofgaard *et al.*, 2016a; Schöneberg *et al.*, 2019), overwintering of the pathogen on crop debris, as shown in Figure 1.8, is currently the best working theory. Divon *et al.* (2012) attempted a soil inoculation without success, although there is currently no published work examining the presence or absence of *F. langsethiae* in soil.

1.4.1. HT2+T2 distribution in the panicle

Opoku (2012) quantified the distribution of *F. langsethiae* DNA and HT2+T2 between the husked grain and the rest of the panicle in three varieties of winter oats and three varieties of spring oats. It was seen that the panicle without the grain accumulated five times the quantity of DNA across all three winter varieties ($P < 0.001$) and 17 times the concentration across the spring varieties ($P < 0.05$). These patterns were mirrored in the distribution of HT2+T2 across the rest of the panicle and the grain, but with only double the concentration of the mycotoxins in the panicle compared to the grain. The rest of the head was described as rachis, rachis branches and the glumes. Divon *et al.* (2019) observed the infection mechanism of *F. langsethiae* in oats after artificial inoculation in the glasshouse and rarely observed growth of the fungus reaching the basal end of the grain. In the instances where such growth was observed, there was no indication that the fungus spread into the rachis. It was observed that the fungus grew on the glumes of the plant in the presence of pollen grains. Potentially the DNA and mycotoxins detected by Opoku (2012) was derived from the glumes. In terms of examining differences in the mycotoxin accumulation between cultivars or treatments it would be wise to ensure that grain is equally if not entirely clean of any other debris. This is particularly relevant to cultivar trials where a plot combine harvester might not thresh samples of cultivars at different maturity to the same extent.

Scudamore *et al.* (2007) showed that the HT2 concentration in grain samples submitted to commercial processing was reduced by 90-95% from initial unprocessed husked oats to oat flakes. The husk is the main constituent of the pelleted by-product which in all the examined samples had a greater concentration of HT2+T2 than the original unprocessed oats. The key stage within the processing for reducing HT2 concentration was therefore highlighted as shelling/removing the husk. The study did not manage to account for all the mycotoxins lost from the original unprocessed sample; potentially some of the initial mycotoxin concentration in the grain delivered to mill could have been present within panicle straw/chaff that would have been removed during the cleaning process before the shelling process. Scudamore *et al.* (2007) did not sample the grain after the cleaning stage and therefore could not differentiate any mycotoxin reduction between cleaning and shelling. Brodal *et al.* (2020) showed that a large fraction of HT2+T2 in uncleaned oats delivered to the mill resided in the below 2.2 mm fraction of grain, and that removal of that fraction reduced the HT2+T2 concentration in the grain by 32-56%. Edwards (2007a) used four naturally infected samples of oats to examine the impact of de-hulling on the mycotoxin concentration. Removing the husk reduced the mycotoxin concentration by over 90% and the concentration in the residual husk was ca. 300% higher compared to the unprocessed

husked oat in all four samples. Van der Fels-Klerx and Stratakou, (2010) reported high HT2+T2 contamination of the by products from oat milling used for animal feed.

The reduction of mycotoxins during milling and the reductions seen by removing small kernels is evidence that *F. langsethiae* deposits a high proportion of the HT2+T2 within the husk or between the husk and the caryopsis.

Edwards *et al.* (2012a) measured the HT2+T2 and *F. langsethiae* DNA concentration of 122 individual grains from one oat sample with an HT2+T2 concentration of 8399 µg/kg. The range of HT2+T2 mycotoxins was 53 to 491,712 µg/kg, and the range of *F. langsethiae* DNA concentrations was from 0.0002 to 13.85 pg/ng. These ranges are high but as the grains would have come from different plants as they were samples taken from the combine, the variation can only be attributed to the field. Examining the variation and distribution in a single panicle would give some indication of whether the pathogen infects multiple florets without movement between florets in the manner described by Brown *et al.* (2010) for *F. graminearum* on wheat or whether it infects one floret and spreads no further.

Without the visual symptoms of other *Fusarium* diseases, less is known about the infection mechanism of *F. langsethiae*. Divon *et al.* (2019) demonstrated some similarities between the *F. langsethiae* infection pathway of an oat floret with the infection pathway described by Walter *et al.* (2010), Pritsch *et al.* (2000) and, Jansen *et al.* (2005) for *F. graminearum* in wheat, the major difference being *F. graminearum* tends to infect wheat glumes via the stomata rather than the caryopsis.

1.4.2. Arthropod vectoring of *F. langsethiae*

There are several ways in which arthropods can either vector a pathogen or increase the detrimental effects a pathogen infection might have upon the host. Kemp *et al.* (1996) investigated the ability of *Siteroptes avenae* to carry and infect wheat with *F. poae* under glasshouse conditions and found that mites fed exclusively for three generations on *F. poae* cultures were able to infect plants when released from the containers in which they were fed. Drakulic *et al.* (2016a) noted that this was not sufficient evidence that the mite was vectoring the disease as it had acquired the pathogen from a synthetic media rather than an infected host. Although field observations by Kemp *et al.* (1996) do record the mite appearing alongside the fungus, this does not prove the mite infected the crop as it was clearly a fungivore having lived on *F. poae* for three generations, suggesting it could have been there to feed on the pathogen. Kemp *et al.* (1996) provided further evidence by photographing sporothecae on the mites containing microconidia and showing these structures

containing four microconidia. Such a small number could feasibly be picked up by passing over a sporulating patch of fungus on an infected host.

Sturz and Johnston (1983) reported *F. poae* as infecting barley and spring wheat ears. The paper described two morphotypes of *F. poae*, one of which was described as being slow growing and having “suppressed aerial mycelium”, lacking characteristic *F. poae* colour, and lacking in the fruity odour associated with *F. poae*. It has been suggested by Torp and Langseth (1999) that Sturz and Johnston (1983) mis-identified *F. langsethiae* as *F. poae* prior to *F. langsethiae* being identified as a new species in 2004 (Torp and Nirenberg, 2004). The description given by Sturz and Johnston (1983) matches that of *F. langsethiae* rather than *F. poae*. Both morphotypes were isolated from ears of barley and spring wheat at mid-booting (GS45) seven days before the emergence of the ears from the boot. Both morphotypes were more prevalent in barley than wheat, and the slow growing one was more prevalent than the faster growing one in both hosts. Vectoring by arthropods could be one explanation as to how the two pathogens were able to access the interior of the boot. That barley had a greater level of infection compared to wheat could reflect the access granted to a vectoring arthropod mediated by the awns of barley protruding from the top of the boot before the boot is split. Drakulic *et al.* (2016b) investigated the possibility *F. langsethiae* being vectored by grain aphids (*Sitobion avenae*) between wheat plants. No transmission was detected between an infected plant and a neighbouring healthy plant by alate or apterous aphids above the background level of infection. Transmission was seen when apterous aphids were manually transferred between plants, and microscopy showed that it was possible for hyphae to become entangled around aphids as well as spores washed from an aphid’s body. However, the lack of infection in experiments where aphids moved un-aided between plants perhaps suggested that such movement dislodged the potential inoculum. Previous work by Drakulic *et al.* (2015) examining *F. graminearum* and grain aphid interactions also showed the aphid to be a poor vector of *Fusarium* pathogens, after aphids were unable to vector *F. graminearum* between wheat plants infected with *F. graminearum* and un-infected wheat plants.

In the case of wheat plants that had been infected with *F. langsethiae* using spray inoculations prior to receiving aphids or already infected with aphids at inoculation, the magnitude of the infection was increased, potentially as a result of wounding (Drakulic *et al.*, 2016b). Imathiu *et al.* (2009) showed wounding was required for *F. langsethiae* infection on detached wheat leaves. The increase in HT2+T2 was from 15.2 to 52.2 µg/kg. Although this was statistically significant ($P < 0.001$), such small differences could easily occur due to small changes in the pathogens’ ability to produce either mycotoxin. When similar experiments were performed using *F. graminearum* examining the timing

of the introduction of the aphids compared to the inoculation of the plants, the results showed that the longer the aphids were present on the plant, the greater the level of disease. One explanation for this would be that with greater time on the plant, more aphids would be generated and more wounding caused, giving greater opportunity for those wounded sites to be used by the pathogen. Other explanations could include effectors impacting plant defence systems being delivered by the aphids feeding (De Zutter *et al.*, 2016); honey dew providing nutrients on which *F. graminearum* spores can germinate; and aphids moving inoculum around the ear of the plant (Drakulic *et al.*, 2015). Bagga (2008) showed that timely reduction in the aphid population at booting or heading could reduce the severity of FHB infection in bread and durum wheat, but that insecticide applications 15 days after heading would reduce aphid populations but have no impact on FHB infection.

Oats did not require wounding in the Imathiu *et al.* (2009) detached leaf assay to be susceptible to lesion development. Wounding did increase the length of lesions but whether or not aphid wounding would cause similar increases in infection as was seen in Drakulic's work with wheat requires investigation. Using a more susceptible host from which the aphids can acquire and transfer the pathogen might potentially lead to more dramatic increases than seen in Drakulic's work. This work does, however, suggest that *F. langsethiae* could be aided by arthropod wounding to advance an infection already present or facilitate a new infection.

1.4.3. Measuring *F. langsethiae* infection

Oats generally show few visible symptoms of any *Fusarium* infection, and visible symptoms are not considered reliable (Hautsalo *et al.*, 2018). This contrasts with wheat where bleaching of spikes and partial bleaching of ears are a reliable measure of infection for several *Fusarium* species. It is possible to see symptoms of *F. graminearum* in oats between anthesis and ripening; however as yet no visible symptoms have ever been observed from natural infection of oats with *F. langsethiae*. Estimating the proportion of infected kernels by surface sterilising and incubating on a growth medium is also problematic as shown by Edwards *et al.* (2012a) in an experiment where *F. langsethiae* DNA was detectable from all individual grains by real time PCR but incubation on PDA only showed 8% of grains to be infected with *F. langsethiae*.

Yield and thousand grain weight reductions have been used in the past as a measure of infection of *Fusarium* species (Hautsalo *et al.*, 2018) but again no yield reduction has been reported with *F. langsethiae*, although the yield impact may not have been fully assessed (Bjørnstad and Skinnnes, 2008) given the difficulty in comparing infected and uninfected plots of the same variety within the same experiment. It is possible to

measure a plant's resistance to a pathogen in the non-reproductive organs, such as leaves. This is achieved through measuring lesion size over successive days in wounded or unwounded detached leaves (Opoku *et al.*, 2011). Other measures might be useful in explaining the presence or absence of infected material in the harvested grain. For example, floret sterility was used by Bjørnstad *et al.* (2017) to correct DON values as florets suffering heavy infection failed to develop into grain and were lost in the threshing process.

Given the correlation between *F. langsethiae* DNA as measured by quantitative PCR and HT2+T2 in oat grain samples, there is a strong argument for using the HT2+T2 concentration in oat flour as a proxy measure for the level of *F. langsethiae* infection (Edwards *et al.*, 2012a). Given the primary issue surrounding *F. langsethiae* infection is the accumulation of HT2+T2, and that resistance to the accumulation of mycotoxins is as valuable a trait as resistance to the pathogen itself, measuring the mycotoxins is an efficient method to phenotype oat lines for resistance. Enzyme linked immunosorbent assays (ELISA) are a quick method of measuring mycotoxins concurrently in multiple samples and have been shown to be comparable with GC/MS (Edwards *et al.*, 2012a).

1.5. Mycotoxins

Mycotoxins are secondary metabolites of fungi; the most common are aflatoxins, ochratoxin A, patulin, fumonisins, zearalenone and DON (WHO, 2021). Mycotoxins can appear in food available to the public through fungal infection before and after harvest, and from livestock fed with contaminated feed. Aflatoxins are amongst the most poisonous mycotoxins, they are produced by *Aspergillus* spp. and can contaminate cereals, oilseeds, spices and tree nuts (WHO, 2021).

Fusarium species are capable of producing a range of mycotoxins including trichothecenes, zearalenone and fumonisins. Different *Fusarium* species have different mycotoxin profiles and host preferences causing certain mycotoxins to be more prevalent on certain crops. As described above, *F. langsethiae* is the major producer of trichothecenes in UK oats.

Trichothecenes are a large family of structurally similar chemicals produced by taxonomically unrelated fungi (Li *et al.*, 2011), they include deoxynivalenol, nivalenol, HT2 and T2. Figure 1.9 shows a skeletal diagram of HT2 and T2 with selected carbon atoms labelled. Trichothecenes are classified by their core structure consisting of a six membered cyclic component in the centre containing an ether flanked by cyclic carbon rings on both sides, one of which contains a double bond between carbon 9 and 10 and the other, an epoxide involving carbon 12 and 13 (Figure 1.9) (Li *et al.*, 2011)

essential for toxicity (Desjardins *et al.*, 1993). This central structure is common to all trichothecenes and further classification into types A, B, C, and D is based on the different functional groups at various carbon positions in the central structure. In particular, type A trichothecenes have hydroxyl, or ester functional groups bound to the central cyclic structure at the carbon 8 position. All type B trichothecenes such as deoxynivalenol and nivalenol have a keto group at the carbon 8 position. Boxes a and b in Figure 1.9 encompass ester groups unique to type A trichothecenes.

The only difference between HT2 and T2 is the functional group labelled R in Figure 1.9, for HT2 it is a hydrogen atom and for T2 it is an acetyl group. T2 is quickly metabolised to HT2 after ingestion and therefore the two compounds can be considered to have equivalent toxicity (Schuhmacher-Wolz *et al.*, 2010).

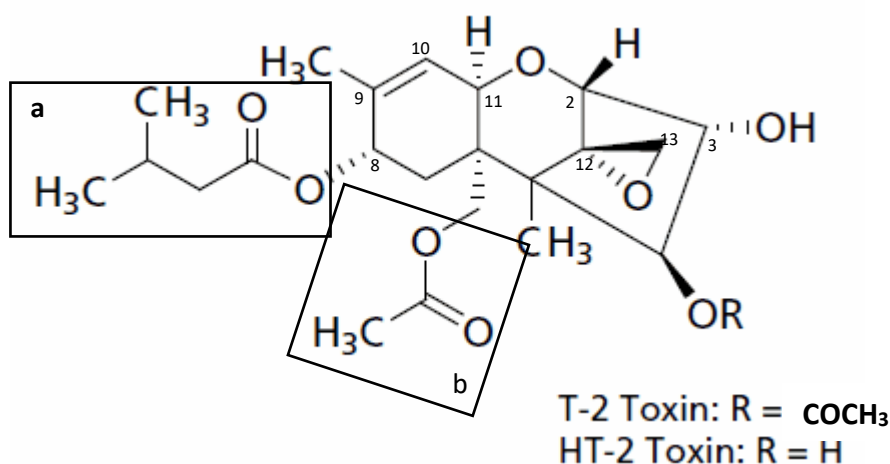


Figure 1.9: Skeletal structure of type A trichothecenes, HT2 (R group is H) and T2 (R group is an acetyl). Adapted from: Sigma Aldrich (No Date) and Li *et al.* (2011).

The mycotoxins HT2 and T2 are absorbed orally and by inhalation; dermal absorption is far slower. Within a mammalian body, they can cross the blood brain barrier as well as the placenta and even be transmitted to milk and eggs. Metabolites have been recorded as being more toxic than T2 (Schuhmacher-Wolz *et al.*, 2010). The cellular toxicity of T2 is a result of inhibiting protein synthesis and at high doses, DNA synthesis. Actively dividing tissues such as bone marrow, lymph nodes and intestinal mucosa are most severely affected. The mycotoxins are also dermal irritants with an irritation threshold of $0.5 \mu\text{g}/\text{cm}^2$ in rats (Schuhmacher-Wolz *et al.*, 2010).

So far, the most relevant toxicological study to assess safe limits of HT2 and T2 mycotoxins for humans was conducted by Rafai *et al.* (1995) on pigs, although work has also been conducted on rats and rhesus monkeys (Rukmini *et al.*, 1980). The study was based on a T2 feeding trial and lasted three weeks delivering a lowest observed adverse effect level of $0.029 \text{ mg/kg bw/day}$. Using a safety factor of 500

generated a temporary tolerable daily intake of 60 ng/kg bw/day which was accepted by the Scientific Committee on Food in 2001 as a combined value for HT2 and T2 (HT2+T2) (The European Food Standards Agency (EFSA), 2017). The EFSA Panel on Contaminants in the Food Chain (CONTAM) subsequently set a tolerable daily intake (TDI) of 20 ng/kg bw/day and acute reference dose of 0.3 µg (Knutsen *et al.*, 2017).

1.5.1. Metabolic variants of HT2 and T2

Phase I and II metabolites of HT2 and T2 have been identified as being present in grain: phase I metabolites are products of the fungus' own metabolism and a result of cleavage of one or more of the ester groups; phase II metabolites are products of the host plant metabolism and include conjugated forms of the mycotoxins with glucose, sulphate, feruloyl or acetyl groups (Knutsen *et al.*, 2017). These metabolites have been found in grain although their concentration relative to the original compounds varies. There is no data on the absorption of the phase I or II metabolites and an assumption has been made that they will be absorbed at the same rate as T2. The TDI for HT2+T2 has been extended to a group TDI to include their respective modified forms (EFSA, 2017). Potency factors, between 1 and 0 have been set relative to T2 to calculate the combined toxicity of phase I metabolites. Phase II metabolites were assigned the same potency factor as their respective phase I metabolites even though phase II metabolites are less toxic as it is assumed they are cleaved to release their aglycones once ingested (Knutsen *et al.*, 2017).

1.5.2. Mycotoxin production

The first unique step in the biosynthesis of trichothecenes is widely accepted as the cyclisation of farnesyl pyrophosphate to trichodiene, catalysed by trichodiene synthase (Desjardins *et al.*, 1993). The *Tri5* gene encodes for trichodiene synthase (Doohan *et al.*, 1999). During the synthesis of T2 toxin trichodiene is manipulated through a series of oxygenations, isomerizations, cyclizations, and esterifications, the process is 15 steps including the synthesis of trichodiene. Subsequently the gene cluster found to encode parts of the biosynthesis of trichothecenes was named the *Tri5* cluster (Kimura *et al.*, 2003; Kimura *et al.*, 2007). The *Tri5* gene cluster is conserved between *F. graminearum* and *F. sporotrichioides* (Kimura *et al.*, 2007), in addition to the *Tri5* gene there are 11 other *Tri* genes: *Tri4*, *Tri6*, *Tri3*, *Tri11*, *Tri12*, *Tri7*, *Tri10*, *Tri13*, *Tr8*, *Tri9*, and *Tri14* within the cluster (Kimura *et al.*, 2007). Three further genes have been identified outside of the gene cluster: *Tri1*, *Tri16* and *Tri101*. The *Tri1* and *Tri16* genes exist on the two gene cluster (*Tri1-Tri16*) (Meek *et al.*, 2003), and *Tri101* exists on its own (Kimura *et al.*, 2007). Lysøe *et al.* (2016) found the *Tri5* cluster in *F. langsethiae* to be highly syntenic to the *Tri5* cluster in *F. sporotrichioides*, the *Tri1-Tri16* cluster and *Tr101* gene to also be present in *F. langsethiae*. Specifically, the presence of the TR7

and Tri13 genes within the Tri5 cluster code for enzymes specifically involved in the synthesis of T2 (Lysøe *et al.*, 2016). Medina and Magan (2010 and 2011) found that the ideal water activity for fungal growth of *Fusarium langsethiae* and mycotoxin production was 0.98-0.995 a_w , equating to ~28-30% moisture in the grain. Observations by Opoku *et al.* (2013) throughout the growth of commercial oats recorded an increase from panicle emergence (GS 59) (Zadoks *et al.*, 1974) through to ripened grain (GS 92) in *F. langsethiae* DNA; such timing would pass through the ideal moisture content for growth and mycotoxin production conditions. When Kokkonen *et al.* (2010) examined *F. langsethiae* under similar circumstances, but on a mixture of wheat, barley and oat grains, *F. langsethiae* was able to produce its typical mycotoxin profile as low as 0.94 a_w (water activity). Medina and Megan (2010 and 2011) grew *F. langsethiae* on oat-based media as did Mateo *et al.* (2011). In both cases this appeared to alter the mycotoxin profile relative to what has been observed in the field (Edwards, 2009a) where HT2 has been in a consistent ratio with T2 of approximately 3:1. The highest ratio found by Medina and Magan (2011) was 1:2.85, HT2:T2; Mateo *et al.* (2011) also found higher concentrations of T2 compared to HT2, whereas Edwards (2009a) found that HT2 was more abundant in UK oat crops. The lab grown samples used by Medina and Magan (2011) and Mateo *et al.* (2011) were grown for 10 days whereas the field crop studied by Edwards (2009a) could be accumulating mycotoxins on the scale of months which could have an impact on the final HT2 to T2 ratio.

Mycotoxins are secondary metabolites that endow advantages to the fungi through enhanced competition for habitat and nutrients or increased virulence towards plants (Knutsen *et al.*, 2017). Isolates of *Fusarium graminearum* incapable of producing deoxynivalenol (DON) have been shown to be pathogenic to wheat, rye and triticales seedlings (Adams and Hart, 1989; Proctor *et al.*, 1995). Snijders and Krechting (1992) suggested that during the infection of wheat by *Fusarium culmorum*, DON was first transported from the chaff to the developing kernel before colonisation of the kernel, a process which was inhibited by resistant lines of wheat. Proctor *et al.* (1995) observed an inconsistent reduction in virulence of *F. graminearum* when the *Tri5* gene involved in the production of trichothecenes was disabled. McDonald *et al.* (2005) and Langevin *et al.* (2004) were able to suppress mycotoxin production in *F. graminearum*, the physical characteristics of the fungus were unchanged but the mycotoxin suppressed fungi was less virulent on wheat than the wild type. No such studies have been conducted on *F. langsethiae*.

HT2 and T2 have several metabolites that have been seen in oat grain: these include glucosides of both T2 and HT2 (Lattanzio *et al.*, 2012; Li *et al.*, 2011) (Figure 1.10).

Secondary or phase II metabolites are those produced by the host plant from the parent mycotoxin. There is concern that metabolites of HT2 and T2 mask their measurement in analysis (Lattanzio *et al.*, 2012). Glucosylation of type A trichothecenes has been observed in naturally contaminated oats and wheat (Lattanzio *et al.*, 2012). Similarly, reductions in mycotoxins during the growth season in other plants has led to the suggestion that they have been metabolised by the plant (Miller and Young, 1985). Nathanail *et al.* (2015) injected spring wheat at mid-flowering (GS 65) with solutions of HT2 or T2 and used ultra-high performance liquid chromatography coupled with a quadrupole time-of-flight mass spectrometer system to identify the metabolites present at maturity. In total, 11 HT2 and 12 T2 secondary metabolites were identified in the harvested grain. The epoxy group is an important determinant of toxicity, all of the metabolites recovered had intact epoxy groups at Carbon12-13 (Figure 1.9). The dominant transformation for both HT2 and T2 was to HT2-3-Glucoside (Figure 1.10). In this molecule the hydroxyl group at Carbon 3 has been converted to an oxygen bridge to a glucose molecule.

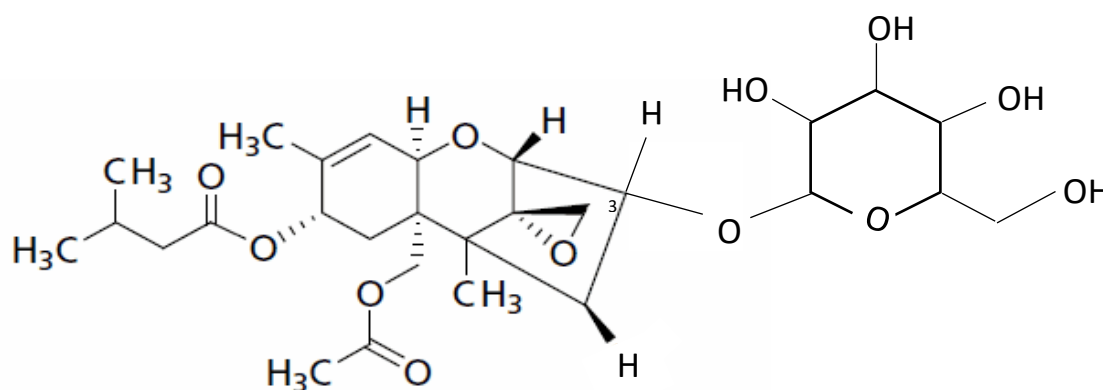


Figure 1.10: Skeletal formula of HT2-3-glucoside. Adapted from: Li *et al.* (2011).

Glucosylation of T2 and HT2 has been reported as more likely in wheat than oats (Lattanzio *et al.*, 2012), and is most likely used as a detoxification process in *planta* potentially removing a virulence factor of the pathogen. Glucosylated mycotoxins are not detected by standard analytical methods but once ingested the glucose is removed through hydrolysis leaving the original mycotoxin in the body (Lattanzio *et al.*, 2012). Meng-Reiterer *et al.* (2016) found that 74% and 48% respectively of exogenously applied HT2 and T2 to oats were metabolised to HT2-3-Glucoside within one day of application. The HT2-3-Glucoside was also found to be fractionally more mobile in the

plant than either HT2 or T2, potentially allowing the plant to store the toxin in vacuoles or move them away from the point of infection to help mitigate against further infection induced from their presence. Further phase II metabolites are illustrated in Figure 1.11 and Figure 1.12.

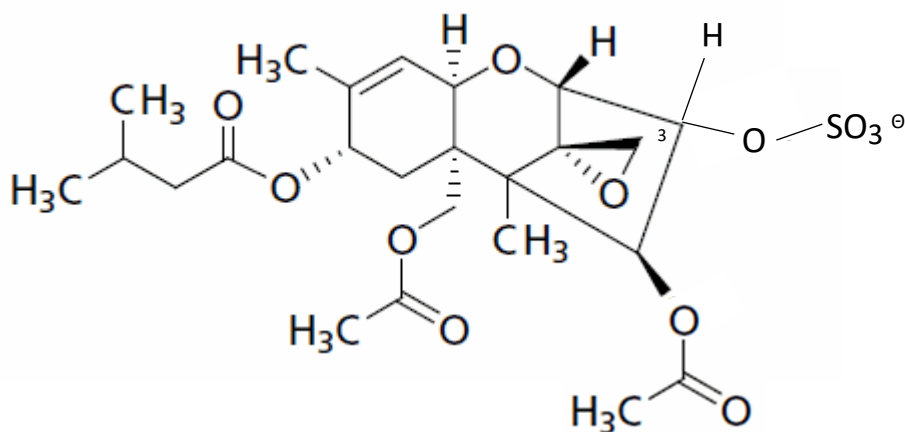


Figure 1.11: The skeletal structure of the phase II metabolite T2-Sulphate (Knutsen et al., 2017). A sulphate group is attached via an Oxygen bridge to Carbon 3.

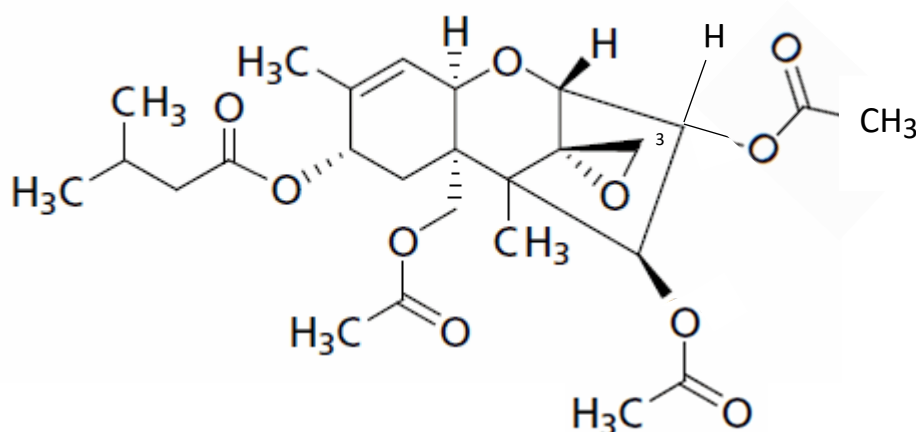


Figure 1.12: Skeletal formula of the 3-Acetyl-T2 phase II metabolite (Knutsen et al., 2017). An additional acetyl group is present on Carbon 3.

1.6. Current successes and failures of artificial inoculation of *Fusarium langsethiae* onto oat plants

Previous studies on *F. langsethiae* have focused on the development of artificial means of inoculation which would ideally reflect the natural epidemiology of the pathogen. Often success of the inoculation is based on its ability to produce FHB symptoms. However, such symptoms have not been conclusively observed in the field, therefore a better measure of success is the accumulation of DNA of *F. langsethiae* or HT2+T2 mycotoxins in harvested oat grains.

Booting as the point of infection under glasshouse conditions was studied by Divon et al. (2012), Mousavi (2016) and Opoku (2012) by injecting and spraying microconidial

suspensions into the swollen flag leaf sheaths or just open flag leaf sheaths (GS45, 47 and 49). Although this was found to be a reliable method of infecting the plant, the method caused stunting of the culm and of emerged panicles, as well as flag leaf wilting and stem yellowing, not typically seen with natural *F. langsethiae* infections. Mousavi (2016) failed to induce any *F. langsethiae* DNA or associated mycotoxin accumulation with applications at booting (GS40-45) but spray inoculation at mid-head emergence (GS55) and mid-anthesis (GS65) followed by bagging for six days did result in high levels of *F. langsethiae* DNA and HT2+T2 mycotoxins. These DNA and mycotoxin accumulations were accompanied however by high proportions of symptoms described as necrosis, discolouration, or spots around panicles and flag leaf sheaths.

Opoku (2012) also recorded a dose response in terms of the spore concentration applied by injection to the plants relative to the DNA measured at maturity. However, no relationship between DNA recovered and the growth stage at which the plants were inoculated was recorded, although the growth stages examined were close together (between GS 45, 47, and 49). In a separate experiment (Opoku, 2012), plants were bagged with perforated and non-perforated clear plastic bags after being sprayed with 5 ml of spore suspension directly to the panicle at panicle emergence (GS59). Bleaching and mycelium growth was observed after plants had been bagged. Given that *F. langsethiae* has been repeatedly observed as symptomless, such symptoms from the boot infection suggest an atypical infection of the plant. Plants were left bagged for between 7 and 56 days the highest DNA and HT2+T2 concentrations (3 pg/ng and 9078 µg/kg respectively) were in panicles kept within bags for 56 days after inoculation.

Divon *et al.* (2012) were able to infect the oat plants with sprays of microconidial suspensions at anthesis and early dough with subsequent bagging for six days, both of which produced greater quantities of *F. langsethiae* DNA at harvest than the boot injection and with less conspicuous symptoms that could be easily overlooked in the field.

Schöneberg *et al.* (2019) compared inoculation using spore suspensions of three isolates at four growth stages: beginning of panicle emergence (GS51); mid-panicle emergence (GS55); beginning of flowering (GS61); and mid-flowering (GS65), all followed by varying periods of 99% relative humidity. The inoculations made during flowering all resulted in higher concentrations of *F. langsethiae* DNA and HT2+T2 than the panicle emergence growth stages. Different temperatures and duration of time spent at 99% humidity were applied and found to have some effect on DNA and HT2+T2 respectively. Lower temperatures at inoculation promoted *F. langsethiae* DNA concentration although variation was sufficiently high that statistical difference was only

detected between 10 and 20°C within one growth stage (early anthesis, GS61) of the four tested (early panicle emergence: GS51, mid panicle emergence: GS55, early anthesis: GS61, and mid-anthesis: GS65). No statistical differences between different durations of 99% relative humidity were seen in the HT2+T2 concentration within the growth stages at which plants were inoculated. The highest concentration of HT2+T was recorded as 699 µg/kg from the mid-anthesis (GS65) 10°C and 12 h 99% relative humidity treatment, the lowest value was not reported but came from the mid-anthesis (GS55) inoculated plants at 20°C with 4 h of 99% relative humidity.

Later work by Divon *et al.* (2019) in which plants were bagged to induce high humidity, introduced inoculum shortly after anthesis and the infection tracked using microscopy up until 14 days after infection. Scanning electron micrographs were taken of the fungus as it colonised the panicles of the plant and through these it was observed that the fungus preferentially grew in the immediate presence of pollen. These results suggest that anthesis may be more successful in artificial inoculations in part because of the presence of pollen. Such a relationship could have implications for the natural physiological timing of infection in the field.

It might be possible to create a more severe and prolific infection in the crop if the crop were to be artificially stressed as well as being inoculated although this could cause genotype stress interaction factors leading to false results in terms of resistance seen by any given genotype (Miedenaar, 1997).

1.6.1. *In field artificial inoculations*

There are two main forms of inoculum commonly used in inoculating *Fusarium* species to cereals: spore suspension and grain spawn. Spore suspension has the advantage of being generated quickly and cheaply, being easy to work with and capable of application over a large area of crop (Imathiu *et al.*, 2014; Lacey *et al.*, 1999). Grain spawn refers to growing a pathogen on grain and then distributing that grain over the ground. Attempts in the field have been made to artificially inoculate *F. langsethiae* onto oats using the same methods described above for *F. graminearum* and *F. culmorum*. Grain spawn and mist irrigating the heads of the plants mid-anthesis (GS 65) is a successful means by which one can inoculate wheat with *F. graminearum* particularly to wheat. This method is based on the epidemiology of *F. graminearum*: ascospores of *F. graminearum* are ejected from the perithecia after rainfall (Parry *et al.*, 1995) or after relative humidity has exceeded 80%, allowing ascospores to be released during drying events (Osborne and Stein, 2007). *Fusarium* Head Blight symptoms caused by *F. graminearum* are often worse after wet periods during anthesis when rain splash moves spores around the crop canopy (Parry *et al.*, 1995). Imathiu (2008) attempted to use *F. langsethiae* inoculated oat grains applied at early stem extension

(GS 32) to oats in combination with misting for two weeks from mid-flowering (GS65) but saw no significant effect of *F. langsethiae* DNA concentration with either inoculation or misting or both. *Fusarium langsethiae* was isolated from the original inoculated grain again at the end of the growing season showing that the pathogen was present in the field throughout the experiment. In terms of spore morphology and host preference the two pathogens are different; it is also likely that their epidemiology and entire life cycles are also distinct and therefore the same artificial inoculation method may not work for both. In this instance the lack of perithecia in *F. langsethiae* is a disadvantage compared to *F. graminearum* as spores are potentially not ejected into the canopy of the crop in the same way. Imathiu (2008) also attempted to inoculate a field crop of oats using inoculated straw applied at flag leaf (GS39) and using a spore suspension (10^5 spores/ml) sprayed at mid anthesis (GS65) in combination with misting but again found that misting (spore suspension only) had no impact or a negative impact and that neither inoculation was effective at increasing the DNA concentration of *F. langsethiae*. Schöneberg *et al.* (2019) attempted to inoculate plots of spring oats in Switzerland with *F. langsethiae* inoculated straw. Control plots were grown adjacent to inoculated plots to detect any progression of the pathogen outside of the inoculated plot and spore traps using *Fusarium* selective agar were placed amongst plots at the oat panicle height. The HT2+T2 and *F. langsethiae* DNA concentrations from control and inoculated plots were not statistically distinct and no *F. langsethiae* colonies were isolated from the spore traps.

1.7. Management through fungicide application

The application of fungicides at flowering can control FHB causing pathogens in wheat and barley (Haidukowski *et al.*, 2012; Edwards and Godley, 2010). Mateo *et al.* (2011) conducted a study looking at the effectiveness of three fungicides (fenpropimorph, procloraz, and tebuconazole) on the reduction of *F. langsethiae* growth and mycotoxin production on an oat-based agar. All the fungicides were able to control growth of the fungus and reduce the production of HT2 and T2 *in vitro*, with the best control seen at the lowest temperature used within the test (15°C). Another study conducted by Edwards and Anderson (2011) in the field over two years (2007/8 and 2008/9) in Fife examined 13 fungicide regimes involving sprays at stem extension, flag leaf and early flowering (GS 31-32, 39, and 59-61) timings. This experiment made use of epoxiconazole, azoxystrobin, fluoxastrobin, prothioconazole, metrafenone, tebuconazole and pyraclostrobin at the GS 59-61 timing. None of the fungicides had a significant effect in reducing the mycotoxin contents of the oats at harvest.

In the later of the two studies tebuconazole was ineffective whereas in the first it had been effective in reducing fungal growth and mycotoxin production. However, conditions are vastly different between an *in vitro* study and a field experiment.

1.8. Resistance of oats among current varieties

In surveys of mycotoxins of UK oats (Edwards, 2007a; Edwards, 2009a; Edwards, 2017) cultivars of oats were seen to vary in the quantity of HT2+T2 in their grain. These studies are, however, limited by the highly unbalanced nature of the varieties used commercially. Analysis of HT2+T2 in oat samples from AHDB RL trials conducted from 2012 to 2014 harvests (Edwards, 2015) showed statistically significant differences between varieties. These differences appeared in every year and varieties were consistent in their relative positions. Balado was the highest accumulator of HT2+T2 in every year and Gerald the second highest. Balado possesses the dwarfing gene *Dw6* which reduces the length of the upper internodes and its straw length reported in the AHDB RL was 87 cm (AHDB, 2013). Furthermore, it was identified that spring oats were less susceptible to the production of HT2+T2, with the most susceptible spring variety (Firth) averaging a lower concentration in the period from 2012-2014 than the least susceptible winter oat in the same period (Edwards, 2015). Although a solution might be to simply plant spring oats, this would have a severe impact on productivity of oats considering the reduction in yield that would be incurred. Stančić (2016) demonstrated that the difference in susceptibility between winter and spring oats is genetic rather than being dependant on planting date by sowing winter and spring varieties in both autumn and spring and comparing their HT2+T2 accumulations. For both drilling dates, the winter varieties used still accumulated the most HT2+T2 and their relative positions to one another were also retained when sown in spring. Winter oats were also found to accumulate more HT2+T2 per unit of *F. langsethiae* DNA than spring oats (Opoku, 2012).

Given that the issue of mycotoxin accumulation in oats was only recorded in the literature in 2007 (Edwards, 2007a) and *F. langsethiae* found to be the producer of these high levels of HT2+T2 in 2012 (Edwards *et al.*, 2012a), it is unsurprising that resistance to the pathogen is as yet relatively unexplored and efforts have instead been given by breeders to more economic traits such as yield, winter hardiness, grain quality and resistances to more widely known diseases such as crown rust (Marshall *et al.*, 2013; Montilla-Bascón *et al.*, 2015). Work completed by Loskutov *et al.* (2017) suggested, however, that resistance to crown rust, Barley Yellow Dwarf virus and Drechslera leaf spot could also impart some resistance to *Fusarium* diseases.

In wheat, resistance to FHB has been shown to be quantitative (Buerstmayr and Buerstamayr, 2015) meaning it is controlled by many genes coding for multiple traits.

Resistance to *Fusarium* can be broken down into five forms: the first two are resistance against initial infection and resistance against the spread of the pathogen after initial infection (Parry *et al.*, 1995). Furthermore, a specific resistance can be classified as being passive or active: a passive example would be the height of the plant allowing it to avoid infection from inoculum on the ground, and an active resistance would be some form of immune response from the plant such as the recognition of the pathogen and activation of a defence (Jones and Dangl, 2006). The remaining three types of resistance are resistance to kernel infection; resistance to the symptoms of FHB; and resistance to mycotoxin accumulation.

1.8.1. *Types of resistance to Fusarium*

Below is a brief description of five the different recognised resistance types to *Fusarium* species.

Type I: Resistance against initial infection, these are mechanisms that reduce the likelihood and severity by which a plant initially becomes infected with any pathogen. An example is the retention or not of anthers after flowering, or cleistogamous (closed florets) and chasmogamous (open florets) traits in oats.

Type II: Resistance against the spread of the pathogen after initial infection (Spanic *et al.*, 2013). A plant with high type two resistance will resist the spread of the infection through the plant.

Type III: Resistance to the colonisation of the kernel or caryopsis during infection. This can be assessed by the germination capacity of the resultant grain (Tekle *et al.*, 2013).

Type IV: the ability of the plant to continue to follow its growth cycle in the presence of an infection (tolerance). An example would be the resistance to further bleaching or spikelet death above the initial point of infection in wheat (Hautsolo, 2018).

Type V: Resistance to mycotoxin formation can be divided into two categories: the resistance to the initial formation of mycotoxins, and the metabolisation of mycotoxins into less toxic forms such as HT2-3-glucoside (Li *et al.*, 2011), T2-sulphate, and 3-acetyl-T2 (Knutsen *et al.*, 2017) or DON into DON –3-O-glucoside in wheat (Lemmens *et al* 2005).

1.8.2. *Physiological traits of oats with potential to influence Fusarium resistance:*

1.8.2.1. *Plant height*

Height has previously been put forward as a passive quantitative resistance mechanism for wheat against FHB. Taller plants are at a lower risk of infection from rain splash (Jenkinson and Parry, 1994) and the ears exist in a less conducive microclimate for the infection compared to shorter plants where humidity may be higher.

Shortness as a risk factor has previously been investigated in oats. Stančić (2016) conducted field experiments relying on natural infection over two years on *F. langsethiae* susceptible cultivars Gerald and Balado, in which six regimes of varying intensity of plant growth regulators were used to manipulate the height of plants. This experiment had the advantage of plants within their cultivar being genetically identical, removing any possibility of genetic linkage confounding results. It also used the two varieties previously identified as being most susceptible to *F. langsethiae* (Edwards, 2015). Stančić (2016) was able to account for 55% of the variation in HT2+T2 accumulation in the first year of the experiment by height and cultivar but only 17% in the second year. Height as an explanatory factor for *Fusarium* infections has been explored in wheat; Yan *et al.* (2011) used NIL pairs artificially inoculated with *F. graminearum* to differentiate the physical attribute of height from genetic linkage in type I resistance (ability to resist initial infection), by comparing the NIL pairs at their naturally different heights as well as by raising the dwarf plants to the same height as the non-dwarf. When the wheat heads were at the same level, the increased resistance to initial infection in the taller plants was no longer present. The work was conducted in a controlled environment cabinet and inoculation was achieved by spraying the heads with a macroconidial suspension, with the heads being placed in plastic bags and then paper bags for the entire time between initial infection and symptom assessment. This means that it was not the difference in distance between the head and the source of inoculum on the ground that was the cause of resistance in the tall wheat in the experiment, as the natural height difference and the differences in microclimates would be much reduced by the bagging. The raised height and natural height data sets came from two separate experiments conducted consecutively, with the raised height experiments having a replication of two and the natural heights four. There was no detail of decontamination between experiments and so there is a risk that inoculum could have built up in the controlled environment cabinet causing a more uniform infection in the later work. As a trait scored in the AHDB RL, lodging is an important breeding target. Lodging is a complex trait and is dependent on straw length

and stiffness. Resistance to lodging has been shown to reduce *Fusarium* infection in cereals (Loskutov *et al.*, 2017; Bjørnstad *et al.*, 2017). Dwarfing genes have been used to achieve good lodging resistance in some varieties such as Balado and Buffalo, however these two varieties are susceptible to *F. langsethiae* (Edwards, 2015; Stančić, 2016).

1.8.2.2. Panicle architecture

One important question with regards to oat resistance to *F. langsethiae* is 'Does the fungus grow through the pedicels of the panicle?' Stančić (2016) recorded high mycotoxin concentrations of the entire panicles, and Opoku (2012) also recorded high concentrations of HT2+T2 in panicle structures. Langevin *et al.* (2004) suggests that *F. graminearum* infection is unlikely to move from one spikelet to another within the oat panicle. Brown (2015) showed that *F. graminearum* moves from one spikelet down the peduncle into the rachis and up into other spikelets by hyphal growth in wheat. For the same to be true in oats, the hyphae would need to grow much further to reach the rachis. It has been speculated that longer branches on oat panicles will increase Type II resistance to *Fusarium* (Bjørnstad and Skinnes, 2008). Loskutov *et al.* (2017), using principle component analysis of genotypes from four species of oat, suggested that an increase in panicle length along with lateness, a decrease in plant height, resistance to lodging and resistance to other plant diseases, is detrimental to *Fusarium* resistance in oats. The *Fusarium* species was not defined, only that the pathogen should produce DON or T2 and be observed on PDA. Loskutov *et al.* (2016) also found through the same analysis that plants with equilateral (branches on all sides) rather than unilateral panicle shapes (branches only occurring on one side of the panicle) were less likely to be susceptible to *Fusarium* infection. Langevin *et al.* (2004) compared six cereal crops in terms of their Type II resistance by using point inoculations of *F. graminearum* on single spikelets and found that in the oat accessions, the infection never spread beyond the first floret.

1.8.2.3. Flowering period

Hexaploid oats are long day plants (Holland *et al.*, 2002) and winter oats have either a vernalisation requirement or at least a tolerance for cold that allows crops to be drilled in autumn and early winter (Nava *et al.*, 2012). Vernalisation has been described as a quantitative trait with multiple loci contributing to the response of the plant to cold periods (Nava *et al.*, 2012). The anthesis period across an individual panicle is between 10-11 days in oats (Rajala and Peltonen, 2011) as opposed to 5-6 days in wheat, although the latter can be much longer should conditions be cold and overcast.

Flowering time has been suggested as a mechanism by which winter oat varieties are more susceptible to *F. langsethiae* than spring ones (Opoku, 2012), as in the winter

varieties the panicles are extruded for longer and have a higher chance of becoming infected with *F. langsethiae*. Such differences between winter and spring varieties were, however, not observed in wheat or barley (Opoku, 2012). Bjørnstad *et al.* (2017) found negative correlations between days to flowering and days to maturity with FHB in oats in Norway over two years of data. However, when correlating days to flowering and days to maturity to DON concentration at harvest, the correlation coefficients were much reduced although they were still significant in most cases.

Using *F. graminearum* studies in oats as a proxy for the infection mechanism of oats by *F. langsethiae*, a likely infection point on the plant is the apical part of florets and the first plant organ to be colonised is likely to be the anthers (Tekle *et al.*, 2012). During oat flowering the lemma and palea separate entirely exposing all the flowering parts of the oat. This, however, is only brief: once the floret has closed up again the anther may be retained within the floret, partially exposed or completely exposed providing a favourable initial colonisation site. If the pathogen infects via the floret apex, as has been observed for *F. graminearum* by Tekle *et al.* (2012), the susceptibility of a variety would be tied to flowering. Tekle suggested that the stage at which a plant was infected relative to flowering had an impact on the DON concentration in grain, the germination capacity of resultant grain and the percentage of infected kernels. However, Divon *et al.* (2012) spray inoculated oat plants in glasshouse conditions with spore suspensions of *F. langsethiae* at anthesis (GS65) as well as later (early dough (GS71)) and recorded equivalent quantities of the pathogens' DNA in both, showing later infection of the kernel is possible. Opoku *et al.* (2013) suggested an epidemiology for *F. langsethiae* that involved infection of the panicle shortly after panicle emergence and then colonisation of the panicle. Infection at anthesis agrees with previous studies which modelled weather parameters to HT2+T2 concentrations and showed wet weather just prior to or during anthesis increased HT2+T2 concentration in the grain (Xu *et al.*, 2014; Kaukoranta *et al.*, 2019; Hjelkrem *et al.*, 2017).

1.8.2.4. Presence of anthers after pollination

In wheat, the ability to extrude or retain anthers during flowering is an important resistance trait against *Fusarium* and mycotoxin accumulation (Tekle *et al.*, 2012; Kubo *et al.*, 2013b; Buerstmayr and Buerstmayr, 2015). The anther, once degraded, are a potential route into the flower for the pathogen (Skinnes *et al.*, 2010). This mechanism proved by Strange and Smith (1971) when wheat florets had their anthers mechanically removed, and as a result accumulated significantly less DON than those with their anthers left intact. *Fusarium graminearum* has been shown to positively respond to betaine and choline as growth stimulants, being chemicals that have been found in greater concentrations in anthers than in other floral parts of wheat (Tekle *et al.*, 2012;

Strange and Smith, 1978). In oats, Tekle *et al.* (2012) observed that varieties characterised as having strong anther extrusion presented a lower percentage infection of *F. graminearum* (by floret) than those plants characterised as having low anther extrusion in an inoculated glasshouse experiment. Divon *et al.* (2019) captured images of hyphal masses of *F. langsethiae* growing around pollen grains and at the apex of oat spikelets where anthers had been retained between the lemma and palea. These images recorded that the microconidia germinated faster in the presence of pollen. In the same experiment *F. langsethiae* was observed to only germinate on wheat in the presence of pollen, which was less available due to the anthers being extruded and not retained.

1.8.2.5. *Cleistogamy*

The degree to which the lemma and palea open during flowering to allow anthers to extrude could be another trait related to resistance. If the plant pathogen interface is the floret and within the floret the anthers or ovary, florets remaining entirely closed during flowering could protect these structures from infection during their most vulnerable period. Cleistogamous wheat and barley have been observed as more resistant to DON accumulation than their chasmogamous equivalents (Hautsalo *et al.*, 2018; Pugh *et al.*, 1933; Kubo *et al.*, 2013a).

1.8.2.6. *Nakedness*

Husk is the retained lemma and palea on the groat of oats (Rines *et al.*, 2006). Typically, oats have a husk which is removed as part of the milling process and it has been demonstrated that after the de-hulling process the mycotoxin content of the groat is 90-95% lower than before processing (Scudamore *et al.*, 2007). Naked varieties of oat have a loose husk that is lost during harvest and immediately after harvesting these oats have far lower concentrations of mycotoxins, due to most of the mycotoxins being on the husk (Edwards, 2007a). Stančić (2016) measured the HT2+T2 accumulation in entire panicles of naked and husked oat varieties sown in winter and spring from experiments across three locations and two years. The naked varieties accumulated the highest concentrations of HT2+T2 in their panicles in the winter sown experiments and among the highest in the spring sown ones. Cleaned grain from the same experimental plots was also examined and seen to be in line with previous researchers' results (Gagkaeva *et al.*, 2011), showing lower levels of mycotoxins in the naked compared to conventional hulled oats. Stančić (2016) concluded that naked varieties had no extra genetic resistance over husked varieties and found that they are in fact more susceptible, but the mycotoxins were simply accumulating in plant parts that were lost during harvest. Therefore, from a breeding perspective, the naked oat is not a source of resistance for hulled varieties.

1.8.2.7. Chemical composition of the cuticle

Loskutov *et al.* (2016) proved a difference in resistance to *F. sporotrichioides* in different hull colours, with darker hulls being more resistant. This could be caused by various compounds in the darker hulls such as phenolic acids, flavonoids and lignin. Furrez *et al.* (2016) showed that phenolic acids inhibited the growth of *F. langsethiae*.

1.8.3. Breeding methods

Phenotypic selection and conventional breeding have been used to improve crop traits since the inception of agriculture. The basis is to select a parent for a cross based on heritable beneficial traits, such selection being achieved by observing the phenotype in the parent first. If the phenotypic trait in question is disease resistance, it will likely only be observable in the presence of disease. In the example of *F. langsethiae*, which is as yet poorly understood and therefore unpredictable, to observe the phenotypic trait of resistance would be difficult if it were required throughout a breeding programme. In this example it would only be possible to assess the phenotype after the opportunity to make a cross that season has passed as the harvested grain must be examined for its mycotoxin content.

A qualitative trait is one dictated by one or very few genes (oligogene); they show discrete variation and are not influenced by environment, eye colour in people being an example. A quantitative trait locus (QTL) is the genomic region that is in part responsible for coding of a quantitative trait. The effect size of the QTL is a measure of the trait's heritability; the higher the effect size, the more impact the QTL will have on the trait. Selecting plants for breeding purposes based on traits coded for by a few high effect size QTL is generally successful, however when a trait is coded for by a large number of QTL with small effect sizes, it becomes difficult to select for that trait.

In terms of finding new variation to incorporate into a breeding programme potentially time-consuming trade-offs must be made. Harlan and De Wet (1971) defined sources of variation into three pools, the first being genotypes from the same species that could be crossed to generate fertile hybrids. Examples in oats would be other cultivars of domestic oats or even hexaploid wild oats. The second gene pool is formed by genotypes more distantly related to the genotype looking to be improved and these sources might only generate very few fertile hybrids. The third pool contains genotypes sufficiently distantly related that they would likely require some form of additional manipulation to generate fertile hybrids. The more divergent the new source of variation from the original genotype, the more backcrosses will be required to obtain a plant suitable for commercial use.

Genetic markers can be morphological markers, protein markers or DNA markers. A morphological marker is one that can be observed by the naked eye in the phenotype of the plant, an example being flower or seed colour. These traits can potentially be associated to QTL in a similar manner to a molecular marker and used in Marker Assisted Selection (MAS). Limitations of morphological markers are their scarcity and potential to be scorable only at specific growth stages of the plant or that they could have specific environmental requirements to express them. A protein marker works in much the same way as morphological markers except that the presence of a specific protein is associated with a QTL. The drawbacks are similar.

DNA markers work in the same manner as the above-described markers, they are based on base pair sequence variations between genomes that can be observed. A genetic or DNA marker can be a very short sequence such as a single nucleotide polymorphism (SNP) which relies on differences of one single nucleotide or a longer sequence such as an SSR microsatellite polymorphism (simple sequence repeat) which can be up to 50 repetitions of ten up to nucleotide long DNA motifs. Such DNA markers can be associated with traits of interest, it might be that the marker is located close to the gene or genes that code for the trait or is part of a gene itself coding for the trait.

1.8.3.1. *Wild oats as a source of variation*

Wild oats in the UK are mainly *A. fatua*, a predominantly spring germinating variety, and *A. sterilis*, a less common autumn germinator. The two species are not possible to distinguish from one another at the vegetative stage, however once panicles have emerged the presence of an awn on the third seed in the spikelet denotes *A. fatua*. Wild oats are typically taller than domestic oats, possess awns on the majority of their seeds, have a hairier husk, shed their seed easily, and are earlier flowering than most domestic oats. *Avena sterilis* and *A. fatua* are commonly termed wild oats and are considered a weed within modern agricultural systems (Marshall *et al.*, 2013; Rines *et al.*, 2006). They are hexaploid and can be successfully crossed with conventional domestic hexaploid oats. Disease resistance is a heritable trait that can be utilised in wild oats to introgress resistant genes into domestic oats. An example of this was the production of Barley Yellow Dwarf Virus resistant hybrids from crosses between *A. sterilis* and a domestic oat variety Lamar (Landry *et al.*, 1984). He *et al.* (2013) generated a mapping population using *A. sterilis* and a Norwegian variety called Hurdal (spring) to look for resistance QTL to DON accumulation in spawn inoculated field experiments but found the largest effect size QTL within the Hurdal genome. Landraces are another source of variation to draw upon (Montilla-Bascón *et al.*, 2013); a landrace is defined as a cultivated and genetically heterogeneous variety that has

evolved within a particular ecogeographical area to which it is uniquely adapted (Casanas *et al.*, 2017).

1.9. Aims of the project

The criteria recorded on the AHDB oat RL for agronomic traits are resistance to lodging, straw length/height, ripening days, winter hardiness, mildew resistance and crown rust resistance. As yet, *Fusarium* resistance is not recorded in the RL and as such growers cannot make informed decisions on cultivar to reduce their *F. langsethiae* infection risk. Given the inconsistent nature of infection, the current inability to inoculate in the field, and the expense of measuring mycotoxin concentrations, it would be difficult to include *F. langsethiae* assessments in oats within large scale variety trials such as the RL. Were it possible to understand the impact physical traits such as height and flowering time had on *F. langsethiae* resistance, those traits could be used to estimate the resistance of any cultivar to the pathogen. Similarly, if QTL were identified that infer resistance, then those could be stacked by breeders into new cultivars to give resistance. Some QTL have been identified by Stančić (2016), but more work is required to understand their impact in isolation, and the mechanism by which they infer resistance. Identifying resistance based on artificial inoculation has the advantage of reliable infection and therefore higher throughput of genotypes to phenotype in the presence of the pathogen. However, methods used to introduce the pathogen may bypass mechanisms of resistance possessed by the plant such as tall plants avoiding infection from the ground; entire panicles being inoculated at once rather than individual spikes requiring the pathogen to move through the plant limbs; or the timing of flowering avoiding a flush of *F. langsethiae* spores.

The aims of this project were to: -

- Further research and understand the impact and mechanisms of the QTL previously identified by Stančić (2016) on *F. langsethiae* resistance in oats.
- Further develop methods for artificial inoculation of oats in the glasshouse and field.
- Gain insight into the epidemiology of *F. langsethiae* through dissection of infected plant materials and analysis of weather data occurring in and around flowering in naturally infected plots of oats.

2. Chapter 2: Artificial Inoculation of Oats with *Fusarium Langsethiae*

2.1. Introduction

Artificially inoculating agricultural plants with economically important pathogens is a common tactic to understand mechanisms of infection, measure susceptibility and examine control methods such as fungicides. Inoculation typically involves introducing the pathogen to the crop at an appropriate growth stage of the crop and during environmental conditions conducive to infection (Imathiu *et al.*, 2014). Previous studies on *F. langsethiae* have focused on the development of artificial means of inoculation within some form of controlled environment to better understand ideal growth stages and conditions (Imathiu, 2008; Divon *et al.*, 2012; Opoku, 2012; Mousavi, 2016; Divon *et al.*, 2019; Schöneberg *et al.*, 2019). Often success of inoculating a plant with a *Fusarium* pathogen is based on the observation of FHB symptoms, however such symptoms are rarely, if almost never, observed in the field for *F. langsethiae*. Therefore, a better measure of success is often the concentration of HT2+T2 mycotoxins or *F. langsethiae* DNA in the oat grains or panicles.

Booting as the point of infection was studied by Divon *et al.* (2012) and Opoku (2012) by injecting and spraying microconidial suspensions into the swollen flag leaf sheaths or just open flag leaf sheaths at mid and late booting (GS45 to 49). This was found to be a reliable method of infecting the plant although the method did cause stunting of the culm, browning, lesions and fungal growth not typically seen with natural *F. langsethiae* infections, as well as flag leaf wilting and stem yellowing.

Opoku (2012) also recorded a dose response between spore concentration applied by injection to the plants and the *F. langsethiae* DNA measured at maturity. But no relationship was found between the DNA recovered and the growth stage at which the plants were inoculated, although the growth stages examined were close together; mid booting (GS45), boot swollen (GS47), and flag leaf sheath split (GS49).

In a separate piece of work (Opoku, 2012), plants were bagged with perforated or non-perforated clear plastic after being sprayed with 5 ml of spore suspension directly to the boot at panicle fully emerged (GS 59). Bleaching and mycelial growth was observed after plants had been bagged. Given that *F. langsethiae* has been repeatedly observed to be symptomless, such symptoms from the artificial infection suggest an atypical infection of the plant. Plants were left bagged for between 7 and 56 days; the highest DNA and HT2+T2 concentrations (3.025 ng/pg and 9078 µg/kg respectively) were in panicles kept within bags for 56 days after inoculation.

Mousavi (2016) attempted to inoculate plants during the booting stage by spray and point inoculation using a spore suspension comprising of two isolates at 10⁵ spores per

ml and bagging for six days. Spray and injection failed to induce any *F. langsethiae* DNA or associated mycotoxin accumulation; however, spray inoculation at mid panicle emergence (GS55) and mid anthesis (GS65) followed by bagging for six days did result in high levels of *F. langsethiae* DNA and HT2 + T2 concentrations greater than 900 µg/kg. These DNA and mycotoxin accumulations were accompanied, however, by high proportions of symptoms described as necrosis, discolouration, or spots around panicles and flag leaf sheaths.

Divon *et al.* (2012) were able to infect the oat plants with sprays of microconidial suspensions at anthesis and early dough with subsequent bagging for six days, both of which produced greater quantities of *F. langsethiae* DNA at harvest than the boot injection, and with symptoms more closely matching those described in the field (Opoku *et al.*, 2013; Imathiu *et al.*, 2008).

Schöneberg *et al.* (2019) compared inoculation using spore suspensions of three isolates at four growth stages; beginning of panicle emergence (51), mid panicle emergence (55), beginning of flowering (61) and mid flowering (65) all followed by varying periods of 99% relative humidity (RH). The inoculations made during flowering all had significantly ($P < 0.001$ - 0.029) higher concentrations of *F. langsethiae* DNA and HT2+T2 than those made during the panicle emergence growth stages. Different levels of temperature and duration of time spent at 99% humidity were applied and found to have some effect on DNA and HT2+T2; 10°C held at 99% RH for 12 h had the highest HT2+T2 concentration (~300 µg/kg). Schöneberg *et al.* (2019) did not report any symptoms on infected plants, although the HT2+T2 concentrations were low.

Work by Divon *et al.* (2019) introduced inoculum shortly after anthesis, plants were then bagged to induce high humidity and infection tracked using microscopy up until 14 days after infection. Scanning electron micrographs were taken of the fungus as it colonised the panicles of the plant; through these, it was observed that the fungus preferentially grew in the immediate presence of pollen. These results suggest that anthesis may be optimal in artificial inoculations in part because of the presence of pollen. Such a relationship could have implications for the natural physiological timing of infection in the field.

Attempts in the field have been made to artificially inoculate *F. langsethiae* onto oats using methods similar to those used for *F. graminearum* on oats (Tekle *et al.*, 2018). An example of such a method is incubating the fungus on a sterile growth media until it sporulates, growing the fungus further in a broth and then using that broth to inoculate sterile grain which after another incubation period is distributed within a crop. Irrigating the heads of the plants at mid anthesis (GS 65) promotes the release of ascospores

and is a successful means by which one can inoculate cereals with *F. graminearum* (Imathiu *et al.*, 2014; Tekle *et al.*, 2018). This method is based on the epidemiology of *F. graminearum*; ascospores are more abundant after rainfall (Parry *et al.*, 1995) or after relative humidity has exceeded 80%, allowing ascospores to be released from perithecia (Osborne and Stein, 2007). Fusarium Head Blight symptoms caused by *F. graminearum* are often worse after wet periods during anthesis when rain splash moves spores around the canopy, with some landing on the ears and infecting florets (Parry *et al.*, 1995). Imathiu (2008) attempted to use *F. langsethiae*-inoculated oat grains applied at second node detectable (GS32) to Gerald oats in combination with misting for two weeks at mid-anthesis (GS65) but saw no significant effect of *F. langsethiae* DNA concentration due to either inoculation or misting or both. *Fusarium langsethiae* was isolated from the original inoculated grain again at the end of the growing season showing that the pathogen was present in the field throughout the experiment.

In terms of spore morphology and host preference there is evidence that the two pathogens (*F. langsethiae* and *F. graminearum*) are different (Torp and Nirenberg, 2004; Parry *et al.*, 1995). It is likely that their epidemiology and entire life cycles are also distinct and therefore the same artificial inoculation method may not work for both. Perithecia have yet to be observed for *F. langsethiae* which are an important component in the *F. graminearum* life cycle, ejecting ascospores into the canopy. Imathiu (2008) also attempted to inoculate a field crop of oats using inoculated straw applied at flag leaf fully emerged (GS 39) and separately using a spore suspension (10^5 spores per ml) sprayed at mid-anthesis GS65 in combination with misting, but again found that misting (spore suspension only) had no impact or a negative impact, and that neither inoculation was effective at increasing the DNA concentration of *F. langsethiae*. Isidro-Sánchez *et al.* (2020) used artificial inoculation in the field to infect a collection of oat genotypes. The resultant concentrations of HT2+T2 were reported as either above or below 1000 µg/kg; 89.5% of genotypes had HT2+T2 concentrations below 1000 µg/kg.

This chapter details the investigation into inoculation methods of oat genotypes with *F. langsethiae* under controlled conditions (2017, 2018, and 2019) as well as in the field (2016, and 2019). The aim was to further refine a method for inoculation in the glasshouse identifying important aspects of successful inoculation techniques leading to successful inoculation in the field. The HT2+T2 concentration in the harvested part has been used as the measure of infection in the following experiments. Although the HT2+T2 concentration is not a direct measure of the degree to which the *F. langsethiae* has infected the plant it has been shown that there is a consistent

relationship between HT2+T2 concentration and *F. langsethiae* DNA (Edwards et al., 2012a).

2.2. 2016 Outdoor inoculation

2.2.1. Objectives

Understand the optimum timing and conditions for introducing a *F. langsethiae* spore suspension inoculate to oat plants in the field.

2.2.2. Null-hypotheses

Applying *F. langsethiae* spores suspended in water to oat plants does not result in higher concentrations of HT2+T2 in the harvested grain.

The growth stage at which spore suspensions are applied to field grown oats does not influence the concentration of HT2+T2 in the harvested grain.

Irrigation applied after the introduction of spore suspension does not result in higher concentrations of HT2+T2 in the harvested grain.

A higher concentration of spore in suspension does not lead to a greater accumulation of HT2 + T2 mycotoxins in the harvested grain.

2.2.3. Method

2.2.3.1. Crop

Oats cv. Gerald was drilled on the 30th September 2016 at 250 seeds m⁻² after minimum tillage to the preceding wheat crop in Black Britch (experimental field) on the Harper Adams University farm. Standard agronomy was practiced except that fungicide T3 head sprays were omitted over the trial area. Prior to 2016 the Black Britch field has been maintained in constant cereal production (wheat/oat rotation) for over six years to encourage the build-up of *F. langsethiae* inoculum.

2.2.3.1. Determination of oat growth stages

Growth stages of oat plants in field and glasshouse experiments were defined according to Zadok's decimal growth stage (Zadok, 1974) as detailed in Table 2.1.

Table 2.1: Growth stages according to Zadok's decimal code (Zadok et al., 1974)

Zadoks	Description for oat
GS47	Boot swelling but not yet separating to reveal any of the panicle
GS49	Boot swollen and the flag leaf sheath split showing the un-emerged panicle
GS51	The first spike has emerged above the flag leaf ligule
GS59	The panicle has completely left the flag leaf sheath with no whorls remaining below the flag leaf ligule
GS61	Beginning of anthesis, 10% of spikes are flowering or have flowered
GS65	50% of spikelets have flowered or are flowering

2.2.3.2. Preparation of inoculum

Isolates were provided by Tijana Stančić of Harper Adams University. All isolates were originally isolated from Gerald oats harvested in the UK in 2012 (Stančić, 2016), and are detailed in Table 2.2.

Table 2.2: *Fusarium langsethiae* isolates and source

Isolate name	Source location	Host Oat Variety
D5	Devon	Gerald
R2	Rosemaund	Gerald
B1	Balgonie	Gerald
G1	Glenrothes	Gerald

Spores were harvested from plates prepared according to Chapter 2. A stock solution was then made from all four isolates represented evenly with the concentration 10^7 spores per ml; this was diluted ten-fold again to make the second inoculum concentration of 10^6 spores per ml. This suspension was either used the same day or refrigerated overnight and used the following day.

2.2.3.3. Experimental design

The experiment was designed as a randomised block three-way factorial design with treatment factors: growth stage (4), spore concentration (2), and with or without simulated rain (2). There were 21 treatments in total detailed in Table 2.3. Each treatment had three replicates, the experiment included one untreated control that received no inoculant or irrigation, each growth stage had two spore concentrations treatments both with and without irrigation. Plots were 0.5 x 2 m with of 7.5 m between each inoculated plot.

Table 2.3: Treatment list for 2016 field inoculation.

Treatment number	GS	Inoculation concentration	Inoculated	Irrigated
1	Control	0	N	No
2	GS43	10 ⁷ spores per ml	Y	No
3	GS43	10 ⁶ spores per ml	Y	No
4	GS47	10 ⁷ spores per ml	Y	No
5	GS47	10 ⁶ spores per ml	Y	No
6	GS72	10 ⁷ spores per ml	Y	No
7	GS72	10 ⁶ spores per ml	Y	No
8	GS59	10 ⁷ spores per ml	Y	No
9	GS59	10 ⁶ spores per ml	Y	No
10	GS43	10 ⁷ spores per ml	Y	Yes
11	GS43	10 ⁶ spores per ml	Y	Yes
12	GS47	10 ⁷ spores per ml	Y	Yes
13	GS47	10 ⁶ spores per ml	Y	Yes
14	GS72	10 ⁷ spores per ml	Y	Yes
15	GS72	10 ⁶ spores per ml	Y	Yes
16	GS59	10 ⁷ spores per ml	Y	Yes
17	GS59	10 ⁶ spores per ml	Y	Yes
18	GS43	None	N	Yes
19	GS47	None	N	Yes
20	GS72	None	N	Yes
21	GS59	None	N	Yes

2.2.3.4. Conditions at spraying

Inoculum was sprayed in the evening close to dusk to minimise damage to the spores from UV light. After inoculum was sprayed onto the plots the irrigation was applied; in most cases this was two hours later apart from the last application at early milk (GS72) when irrigation was applied twenty minutes after the inoculum. Conditions on the day of inoculation are recorded in Table 2.4.

Table 2.4: Conditions on the day of inoculation

Date	Crop growth stage	Volume of irrigation (ml) prior to inoculation	Average RH % on day	Rain within 2 hrs of inoculation
25/05/16	GS43	0.609	72	Yes
04/06/16	GS47-51	0	76	No
17/06/16	GS59	1.827	81	No
29/06/16	GS72	6.496	94	No

Spraying was done using a lunch box plot sprayer (Trials Equipment UK Ltd): flat fan 03 110 nozzles were used, the spray pressure was 2 bar and the spray volume was 20

ml/m². Irrigation was applied using the same equipment after it had been triple rinsed, irrigation was applied to the inoculated 0.5 x 2 m area in the centre of the plot until run-off. Figure 2.1 shows a flag leaf from a plant at mid to early booting (GS 43) after the application of the spore suspension, a panicle from a plant at late booting/sheath split (GS49) without spore suspension applied, as well as a plant at panicle fully emerged (GS 59) after the application of the spore suspension.

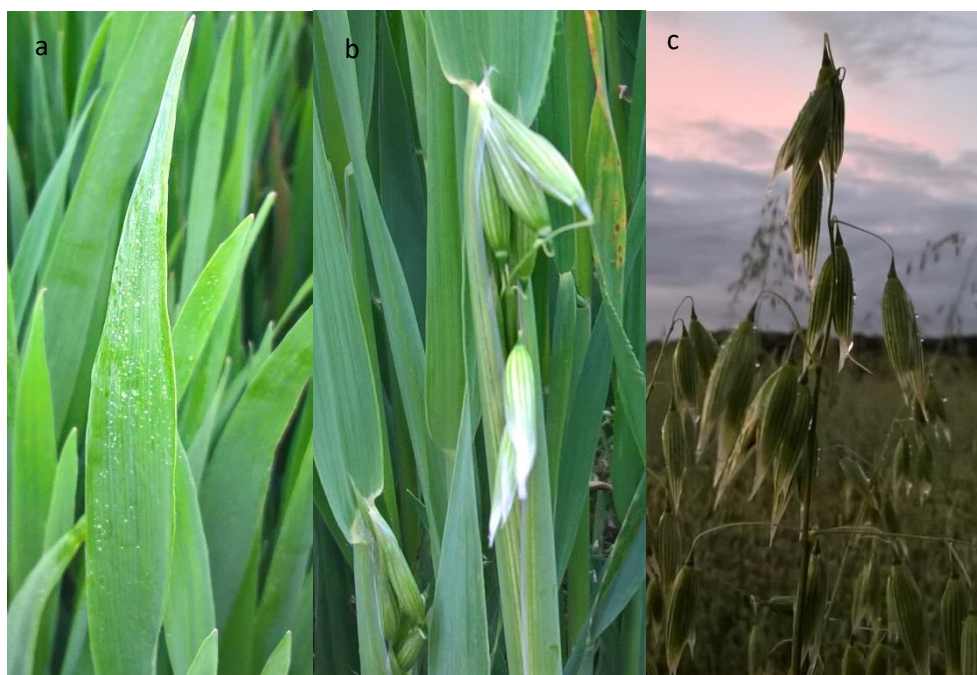


Figure 2.1: Oat plants with spore suspension applied to the flag leaf **(a)** at late booting/sheath split (GS49) with no spore suspension applied **(b)** and at fully emerged panicle after spore suspension applied **(c)**.

2.2.3.5. Sampling and HT2+T2 analysis

Entire plants were hand harvested from plots at maturity: a minimum of fifty plants were collected into a paper bag in the field from each plot and then dried at 30°C to 10% moisture, before being threshed with a standalone F. Walter & H. Wintersteiger FG thresher and milled with a ZM200 centrifugal laboratory mill (Retsch, Leeds, England).

Many of the experiments in this thesis use the HT2+T2 concentration of the unprocessed oat grain as the sole parameter for measuring the infection of the *F. langsethiae* pathogen. The contamination of grain with HT2+T2 mycotoxins is the exclusive reason for *F. langsethiae* being worthy of investigation in the food chain. Mycotoxin quantification also represents an inexpensive and efficient proxy measure for the pathogen. Edwards *et al.* (2012a) demonstrated the strong relationship between HT2+T2 concentrations determined by GC/MS (the other popular method) and ELISA. Edwards *et al.* (2012a) performed a regression between HT2+T2 concentrations determined by GC/MS and HT2+T2 concentrations obtained from ELISA, the resulting

R^2 value was 0.9 and the equation for the line was $y = 1.03x$ indicating an almost 1:1 ratio.

2.2.3.6. Quantifying HT2+T2 in oat samples

Ridascreen® T-2/HT-2 Toxin ELISA kits (R-Biopharm, AG, Germany) were used to measure the combined concentration of HT2 and T2 in field and glasshouse experiment samples. A 5 g sample of milled oat grains was weighed into 50 ml centrifuge tubes to which were also added 25 ml of Ridascreen T-2/HT-2 extraction buffer. The suspension was then mechanically shaken at 300 ms^{-1} for 10 minutes (HS 501, JK IKA Labortechnik, Germany) before being centrifuged at 3000 G for a further 10 minutes. One millilitre of supernatant was then added to 1 ml of 70% methanol before being vortexed. If further dilutions were required to reduce the concentration of the extract to within the range of the ELISA standards, 35% methanol was used. Samples were then added to the ELISA wells and the procedure was carried out according to the instructions of the Ridascreen® T-2/HT-2 ELISA assay. Once the stop solution was added, the plate was read within 30 minutes at 450 nm on a V BioTek Plate reader (ELx800, BioTek Instruments Limited, USA), and the concentrations of the samples determined from the standard curve (Figure 2.2). Original concentrations were calculated after accounting for dilutions involved in the extraction process.

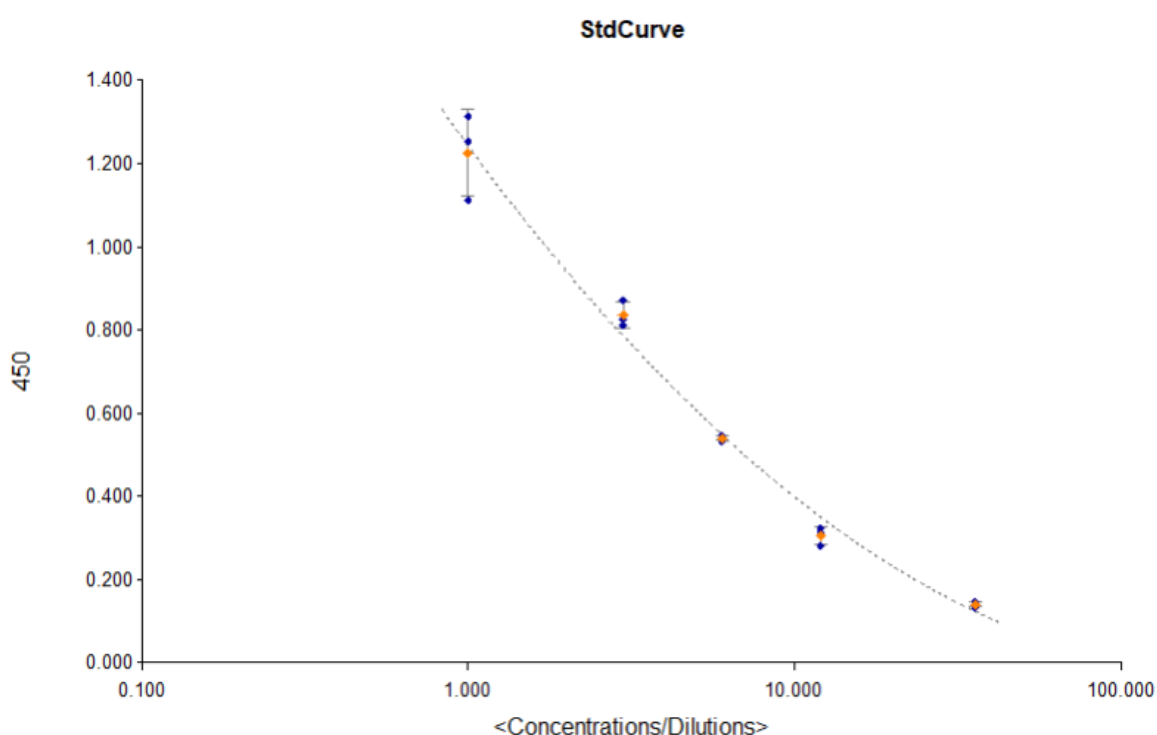


Figure 2.2: An example standard curve using the standard solutions provided in the Ridascreen® T-2/HT-2 ELISA assay kit. The y axis is absorbance at 450 nm , and the x axis the known concentrations of the standard solutions.

The lower limit of detection and quantification was 0.836 µg/kg, any values below this threshold were recorded as half of the limit of detection: 0.418 µg/kg.

2.2.3.7. *Statistical Analysis*

All statistical analysis was performed in R version 4.0.4 (R Core team, 2020). Linear models were produced in the `lm()` function and expressed in ANOVA tables using the `anova()` function. To allow for the untreated control irrigation, spore concentration and timing were all nested with inoculation. The Shapiro test was applied to the residuals generated from the linear model to test for a sufficiently Gaussian distribution. If required either log base 10 or square root transformations were performed until the residuals from the model rejected the null hypothesis of the Shapiro test, that the data is normally distributed, could be accepted. The Tukey's post hoc test was performed using the `agricolae` package in R, alpha level was set to 0.05.

2.3. 2019 Field inoculation

2.3.1. *Objectives*

To investigate field inoculating oats under irrigation.

To compare the relative HT2+T2 concentrations of field inoculated near isogenic lines (NIL) to naturally infected NIL (results from experiments reported in Chapter 5).

2.3.2. *Null hypothesis*

Applying *F. langsethiae* spores (10^6 spores per ml) suspended in a water to oat plants does not affect the concentration of HT2+T2 in the harvested oat grains.

The parental origin of the Mrg04 chromosome in the plant genome does not influence the plants' susceptibility to *F. langsethiae* inoculation by application of spore suspension.

The height of a plant does not influence its susceptibility to *F. langsethiae* after application of spore suspension.

2.3.3. *Method*

2.3.3.1. *Crop*

A further field inoculation was conducted in 2019: NILs from six of the NIL groups defined in Chapter 3 (Table 3.1) from the Buffalo Tardis mapping population were selected on the basis of their variation in panicle emergence times, height and possession of certain QTL of interest. Plants were sown to 300 plants/m² into a sandy loam after inversion tillage and power harrowing to achieve a fine seed bed. Standard agronomy was applied to control weeds and other fungal diseases (no applications beyond flag leaf emergence) and no plant growth regulators were applied. A fine seed bed was produced by first ploughing to bury the previous crop debris (lucerne) then

power harrowing to reduce aggregate size. Plots were drilled using a Winterstieger self-propelled plot drill with Suffolk coulters (12/10/2018).

2.3.3.2. *Design*

The experiment was in four blocks with each block consisting of 12 different genotype plots of 10 m length. The experiment was a split plot design, one half of the 10 m plot was equipped with three misting heads spaced 1.5 m apart, for logistical reasons misting irrigation was not randomised but applied systematically. Within the 5 m of misted plot one meter had inoculum applied and the remainder was left as misted control. Figure 2.3 shows the experiment with the irrigation misting running on two of the blocks. The misting was applied during the day in the early afternoon on days the plots were inoculated, but misting was stopped several hours before the inoculant was applied. The misting was then left off until the morning after inoculation when it was switched on from 9 am to 7pm at one minute of misting every four minutes for the following day.



Figure 2.3: Misting running on two blocks of the 2019 outdoor field inoculation experiment.

2.3.4. Preparation and application of Inoculum

2.3.4.1. Isolation of *F. langsethiae* from cereal grain

Six isolates were isolated from oat grains and are detailed in Table 2.5 these were used in all inoculation experiments excluding the 2016 field inoculation.

Table 2.5: Name and description of the *F. langsethiae* isolates used in all inoculation experiments excluding the 2016 outdoor inoculation experiment.

Isolate code	Origin location	Region	HT2+T2 concentration of sampled grain ($\mu\text{g kg}^{-1}$)	Appearance in culture on PDA
16M1765 1c	Birmingham	Central West England	721.6	White
16M1767 17	Wiltshire	Central South England	718.7	Peach
46971 13b	Brotherstone	Southeast Scotland	451.7	Violet
46971 1c	Brotherstone	Southeast Scotland	451.7	Peach
46971 12a	Brotherstone	Southeast Scotland	451.7	Peach/pink
46984	Kelso	Southeast Scotland	666.9	Light Pink

To isolate *F. langsethiae* from grains they were first surface sterilised by being placed within a sterile 50 ml centrifuge tube and immersed in a solution of sodium hypochlorite (1% available chlorine) for one minute while being shaken. The sodium hypochlorite was then drained off and the grains were triple rinsed with sterile deionised water (SDW). The grains were then allowed to dry in a Petri dish in the presence of a Bunsen flame within a NordicSafe Class II Biological Safety Cabinet. Once dry, one hundred grains were plated onto sterilised potato dextrose agar (PDA) amended with streptomycin 70 mg/ml, at five grains per plate. Plates were incubated at room temperature. Once sufficient time passed for fungal colonies to develop characteristic traits (5-10 days), fungal isolates were screened first by eye on macro-morphology and then under the microscope at four, 20, and when necessary 40 times magnification for micromorphology. Streak plates were made from identified *F. langsethiae* colonies, from which single germinating spores were identified, removed and placed on a new un-amended PDA plate to grow single spore derived colonies.

For identification of isolates as *F. langsethiae* conventional PCR was used. For extraction samples were taken from single spore colonies grown on PDA and placed in snap lock Eppendorf tubes. Samples were then crushed using a sterile micro-pestle in a 250 μl of freshly agitated Chelex carbon buffer (2.5 g activated charcoal and 5 g Chelex in 50 ml SDW) after which samples were heated to 56°C for 20 minutes and vortexed. The samples were further heated to 99°C for 10 minutes and again vortexed

before being centrifuged at 12000 G for 15 minutes. Fifty micro litres of supernatant were removed and vortexed with another 50 µl of TE buffer (10 mM Tris-Cl pH 7.5, 1 mM EDTA) and stored at 4°C for PCR. After extraction a preliminary PCR was run using the internal transcriber spacer primers 4 and 5 (TCC TCC GCT TAT TGA GC and GGA AGT AAA AGT CGT AAC AAG G respectively) for amplification to confirm the presence of amplifiable DNA (Opoku *et al.*, 2013). The *F. langsethiae* primers: FlangF3 (5'-CAAAGTTCAGGGCGAAAAC) and LanspoR1 (5'-TACAAGAAGACGTGGCGATAT) reported by Wilson *et al.* (2004) were used for the *F. langsethiae* identifying PCR and were sourced from Eurofins MWG Operon. The PCR buffer used was prepared according to Edwards *et al.* (2012a) and SDW was used as a negative control. The PCR programme ran on a Bio-Rad T100™ Thermal Cycler (UK) and had 40 cycles: the annealing temperature was 66°C for the first five cycles, 64°C for the following five cycles and 62°C for the last 30 cycles. The cycles started with denaturation at 95 °C for 30 seconds then annealing for 20 s and extension for 45 s at 75°C. The first denaturation step was held for 90 seconds and the final extension step was maintained for 5 minutes until cooling to 4°C. After amplification, gel electrophoresis was performed on the samples using a Kodak BioMax HR 2025 running a 2% agarose gel (Electran®, BDH, UK) stained with GelRed™ (Gel Stain 10 000 x in water, Biotium, USA). Once the gel had run it was viewed using a GelLogic 212 PRO (Carestream, UK).

2.3.1. Spore harvest for inoculation suspensions

Sporulating plates, obtained by placing plugs from the PDA slopes and allowing them to grow at room temperature for up to ten days, of the desired isolates were flooded with 5 ml of sterile water. The plate was gently agitated using a sterile plate spreader to release the spores from the plate surface and the resulting suspension was withdrawn from the plate using a 5 ml pipette tip. Once enough suspension had been collected or all the plates of each isolate were harvested, the spores were counted using a Neubauer haemocytometer and the spore concentration calculated. When blending isolate suspensions to make inoculum, each isolate suspension was diluted to the same spore concentration prior to blending, either 10⁶ or 10⁷ spores per ml.

Three isolates originated from the same grain batch but were isolated from different grains from the 46971 sample. The isolates showed the typical morphological characteristics of *F. langsethiae*, but they all varied in their colour sufficiently that they were treated as distinct isolates. Several more isolates were originally isolated and characterised by morphology and species identity was confirmed by species-specific PCR but the six in Table 2.5 grew and sporulated the most consistently in culture.

After the spore suspension inoculum was applied, the remaining suspension was returned to the laboratory where the number of viable CFU was determined by plating out a 10-fold serial dilution on Rose Bengal Chloramphenicol Agar plates. After five to ten days the fungal colonies were counted as a means of assessing the spore viability.

Three applications of inoculum were made on 30th May 2019, 3rd June 2019 and 13th June 2019, and these dates were used as the target of the sprays was anthesis. On the first date most, plants had surpassed early panicle emergence (GS51) with the most advanced at mid panicle emergence (GS55); by the second date all plants had passed mid panicle emergence (GS55); and by the third and last application date all panicles were at their fullest extension but some of the lower spikes had yet to flower. Applications of inoculum were made in the evenings to prevent degradation of the spores by UV light and retain moisture through the night. Spores were sprayed onto the canopy using a pump action killa spray bottle, the application was approximately 40 ml/m², the inoculum did not saturate the canopy to the point of run-off. By applying over three days the aim was to make at least one application at full panicle emergence (GS59) for each NIL. Heights of plants in the misted and unmisted plots were measured at mid to late flowering (GS59/65) once they were no longer likely to grow further. Once plants had ripened, samples (40 plants) were collected by hand from the relevant areas of the plot, dried to 10% moisture and threshed using a threshing machine (standalone F. Walter & H. Wintersteiger FG thresher). HT2+T2 was extracted from a 5 g sample and quantified by ELISA as described in Chapter 2.

2.4. Gerald glasshouse inoculation 2017

2.4.1. Objectives

To determine the impact of introducing inoculum at earlier or later growth stages on the final concentration of HT2+T2 in the harvested panicle.

To determine the impact of a potato dextrose broth nutrient addition to the spore suspension applied to plants on the final concentration of HT2+T2 in the harvested panicle.

2.4.2. Null hypothesis

The application of *F. langsethiae* spore suspension to oat plants does not affect the concentration of HT2+T2 in harvested panicles.

Spore suspension application at full panicle emergence (GS59) is equivalent to late anthesis (GS65-9) in terms of the concentration of HT2+T2 concentration in harvested panicles.

The application of potato dextrose broth alongside *F. langsethiae* spore suspension does not affect the concentration of HT2+T2 in the harvested panicles.

2.4.3. Method

2.4.3.1. Experimental Design

The experiment was design as a fully randomised design with no blocking structure with seven treatments (including the untreated control and 15 replications. A complete randomised design was used to increase the degrees of freedom and increase the statistical power. Each pot contained three plants and constituted one replication.

2.4.3.2. Spore harvest for inoculation suspensions

Six isolates were grown from spore suspensions derived from single spore isolates on PDA as described in Chapter 2, from which spores were harvested and suspended in sterile water. Spore numbers per ml were counted using a Neubauer haemocytometer and each harvested spore suspension was diluted to the same concentration, 10^7 spores per ml. A blend of spore suspension was made by adding equal quantities of each individual suspension. Potato dextrose broth (PDB) (26.64 g/l) was made using deionised water and sterilised in an autoclave at 121°C for 30 minutes to give a sterile 11.11% stock solution. The 11.11% PDB was then used to dilute the 10^7 spores per ml blended suspension ten-fold to give a 10% solution of PDB and 10^6 spores per ml. To achieve a 1% PDB solution the 11.11% solution was diluted a further ten-fold before using it to dilute the 10^7 spores per ml suspension. The spore suspension with no PDB was diluted using SDW. This resulted in three spore suspension all at 10^6 spores per ml with one in SDW and two amended with 1 and 10% PDB.

2.4.3.3. Plants

This experiment was run in the glasshouse at Harper Adams University using Gerald oats dressed with a Kento seed treatment. Seed was sown into 20 cm square pots, in John Innes No. 2 compost on the 10th February 2017. The glasshouse had lighting and heating provided a daylength of 16 h and day and night minimum temperature of 15°C and 5°C respectively. Five plants were sown per pot and thinned to three plants once at the initiation of stem extension (GS30). Plants were vernalised in a polytunnel for 14 days one week after sowing. Minimum temperatures per day ranged between 0.37 and 6.3°C. Plants were given two applications of Nitram, the first 46 days after emergence and the second 91 days after emergence.

Due to powdery mildew infection in the plants in early April (10th April 2017) plants were sprayed with Vegas at 0.35 L/ha (cyflufenamid). Aphids continued to be an issue and the plants were treated with Hallmark (Lambda-cyhalothrin) at a rate of 50 ml/ha and Gazell (acetamiprid) at 250 g/ha. In May, 105 pots were selected from the 161

available on the basis of uniformity; these were spaced on the growing table and labelled according to the fully randomised design.

2.4.3.4. Inoculation

Plants were inoculated at two growth stages: full panicle emergence and late anthesis (GS59 and GS65-9), and on the day of inoculation, tillers at the required growth stages were labelled. Each of the 15 pots was removed from the growing table and sprayed with the relevant spore suspension from four angles at an upward incline, so the spray moved up into the downward facing glumes. Once sprayed, clear non-perforated plastic bags were placed over plants supported by canes and the bags were sealed around the base of the pots. Plants were sprayed between 7pm and 9:30pm to avoid UV damage of the spores and bags were left on the plants for 14 days. The control plants were not sprayed or bagged.

2.4.3.5. Harvest and HT2+T2 measurement

Once ripe, entire panicles, cut below the lowest whorl, were collected from the labelled tillers and milled using a laboratory mill (Model M20, IKA, Germany). Where possible 1 g of milled panicle was used for extracting HT2+T2 but for some samples of low weight, 0.5 g was used. The volumes of extraction buffer applied were modified according to the mass of the sample but the 1:5 ratio was always maintained. Otherwise extraction and quantification were performed as described in section 2.2.3.6. Entire panicles were used as greater concentrations from entire panicles have been recorded (Opoku, 2012) and it allowed more harvestable material.

2.5. Balado glasshouse inoculation 2018

A further glasshouse experiment was conducted to investigate similar hypothesis to the 2017 Gerald experiment; the key differences were the use of a dwarf variety with high susceptibility (Balado), applying the inoculum at earlier growth stages and using panicles from the same plant but different growth stages to measure the impact of growth stage.

2.5.1. Objectives

To determine the impact of inoculating an earlier growth stage than panicle emergence on the concentration of HT2+T2 in harvested panicles.

To confirm lack impact of amending the inoculating spore suspension with PDA nutrient on the concentration of HT2+T2 in harvested panicles.

To validate the spore suspension method.

2.5.2. Null Hypothesis

Spore suspension application at mid booting (GS47) is equivalent to panicle emergence/early anthesis (GS5/63) in terms of the concentration of HT2+T2 concentration in harvested panicles.

The application of potato dextrose broth alongside *F. langsethiae* spore suspension does not affect the concentration of HT2+T2 in the harvested panicles for the variety Balado.

The application of *F. langsethiae* spore suspension to oat plants does not affect the concentration of HT2+T2 in harvested panicles of the variety Balado.

2.5.3. Method

2.5.3.1. Experimental Design

The experiment was designed as a two factorial design examining the difference in infection between growth stage of the oat when inoculated and the addition of PDB as a nutrient. The growth stages examined are earlier than in the 2017 Gerald experiment, late booting (GS47) was used and compared to early panicle emergence/early anthesis (GS51/63). The experiment had six treatments, pots were laid out as a fully randomised block design with 10 replicates each: untreated control (water sprayed at GS47 and GS51/63, spore suspension (10^6 spores per ml), and spore suspension (10^6 spores per ml) with PDB at 2.4 g/L, each at late booting (GS47) and early anthesis (GS61).

2.5.3.2. Spore harvest for inoculation suspensions

The same six isolates were used in the 2018 experiment as the 2017 inoculation. All spores and spore suspensions were harvested and prepared in the same manner.

2.5.3.3. Plants

Untreated Balado oats were sown in John Innes No.2 in 20 cm square pots at a rate of five seeds per pot on the 27th November 2017. Plants were moved to a polytunnel on the 6th December 2017 to vernalise, once most plants had emerged. After 14 days plants were returned to the glasshouse and once plants had established, 60 pots were selected on the basis of uniformity and within those pots, plants were thinned to three per pot at stem extension (GS30). Plants received two applications of Nitram prior to panicle emergence.

Gazelle (250 g/ha) and Talius (0.25 l/ha) were applied one week before inoculation to combat aphids and powdery mildew respectively.

2.5.3.4. *Inoculation*

Two panicles on the same plant were selected to be inoculated at the same time but at two growth stages (late booting (GS47) and early panicle emergence/early anthesis (GS51/GS61)). Within the same pots and on the same plants different tillers were at different growth stages so tillers at the designated growth stages were tagged with tape to allow those same tillers to be harvested at the end of the experiment. These growth stages were very close together in terms of time. Anthers were visible in the tillers at early panicle emergence (GS51), meaning that they were concurrently at early panicle emergence (GS51) and early anthesis (GS61). Plants were moved from the bench to be inoculated with the prepared spore suspension in the same manner as the previous inoculation. Inoculated plants were bagged for one week using non-perforated clear plastic bags.

2.5.3.5. *Harvest and HT2+T2 measurement*

Once mature, entire panicles were collected from the labelled tillers, typically three panicles per pot, milled and analysed for HT2+T2 as described previously (section 1.4.3.5).

2.6. NIL Glasshouse Inoculation 2019

The experiment was grown in the glasshouse with the aims of understanding how selected NIL reacted to inoculation in the glasshouse environment and whether or not manually extruding varieties which naturally retain some of the panicle within the flag leaf boot would change their reaction to the inoculation. A potential mechanism inferring resistance to taller plants is different environmental conditions surrounding the panicle in taller versus shorter plants, by bagging the panicles plants varying in height this experiment sought to investigate such a mechanism.

2.6.1. *Objectives*

To understand impact of panicle extrusion on reaction to spore suspension application.

Compare in field resistances to those in the glasshouse.

2.6.2. *Null Hypotheses*

Level of panicle extrusion has no impact on the concentration of HT2+T2 in harvested panicles.

Damaging the flag leaf sheath of plants does not increase the concentration of HT2+T2 in harvested panicles.

Height has no impact on the concentration of HT2+T2 in harvested panicles.

Different NIL have the same concentration of HT2+T2 in harvested panicles.

2.6.3. Method

2.6.3.1. Plants

Selected NIL detailed in Table 2.6 were sown into John Innes No.2 compost in square 25 cm pots, seven plants per pot, on the 21st November 2018 and one week after emerged plants were moved to a polytunnel to vernalise. While in the polytunnel plants were sprayed for powdery mildew with Talus (proquinazid) at 0.25 L/ha. Plants were moved back to the glasshouse after one month. On the 4th February 2019 five plants per pot were selected based on uniformity. Two applications of Nitram (34.5% N) were made to the pots prior to panicle emergence applying an equivalent rate of 150 kg N/ha over both applications. Growth stages of plants were recorded in the lead up to inoculation. Table 2.6 shows the treatment list of the experiment detailing which NILs were included and the treatments imposed on them.

The NILs were derived from a mapping population created from the cultivars Buffalo and Tardis. Buffalo is a dwarfed cultivar and of the two lines is the later developing. Tardis, in contrast, is taller (non-dwarfed) and earlier in terms of its maturity. The two parent lines also differ in their respective susceptibility to *F. langsethiae*; Buffalo is more susceptible than Tardis typically accumulating greater concentrations of HT2+T2 in harvested grain (Edwards, 2007a). Four NILs were used in the experiment two of which had tall alleles on chromosome Mrg04 from Tardis introgressed into a Buffalo background and 1 NIL as a control which had undergone the same backcrossing but was selected to have the Buffalo alleles on Mrg04. Two distinct NIL, possessing the Tardis derived alleles on the Mrg04 QTL introgressed within the Buffalo background genome, were present in the described experiment (Table 3.4) and are referred to as Buffalo + T Mrg04 throughout the remainder of this chapter. The two NIL in question were represented in the experiment equally having the same replication and being exposed to the same treatments.

Table 2.6: Near isogenic lines (NIL) grown to harvest and treatments applied. The Code column refers to the code of the NIL. The Name column refers to the name applied in this thesis to identify the parent genome and the introgressed QTL (Appendix 1). The Treatment column refers to whether or not the plants were fully extruded and/or the boot damaged.

Code	Name	Attributes	Treatment		Inoculation
			Panicle Extrusion	Flag leaf sheath	
Buffalo	Buffalo	Parent line	Unextruded	Undamaged	Control
			Unextruded	Undamaged	Inoculated
2012-125/1/26	BNIL	NIL pair to 2012-125/1/27	Unextruded	Undamaged	Inoculated
2012-125/1/26	B NIL	NIL pair to 2012-125/1/27	Unextruded	Damaged	Inoculated
2012-125/1/26	B NIL	NIL pair to 2012-125/1/27	Extruded	Damaged	Inoculated
2012-125/1/27	Buffalo + T Mrg04	Tall line that demonstrated consistent low HT2+T2 concentrations	Extruded	Undamaged	Inoculated
			Extruded	Damaged	Inoculated
2012-139/6/25	Buffalo + T Mrg04	Tall line that demonstrated consistent low HT2+T2 concentrations	Extruded	Undamaged	Inoculated
			Extruded	Damaged	Inoculated

2.6.3.2. Experimental Design

The experiment was laid out as randomised block design with five replications of each treatment.

2.6.3.3. Inoculation

At inoculation, prior to the application of the spore suspension, the panicles of specific plants were mechanically extruded or flag sheaths damaged without causing extrusion according to the experimental design. Mechanically extruding plants were achieved by peeling back the flag leaf boot and drawing it down the stem of the plant until the panicle was fully exposed. Damage to plants was caused by roughly cutting the flag leaf sheath in a similar manner to the damage caused when mechanically extruding a plant while not exposing the panicle. The inclusion of the damaged treatment was to enable any damage caused by the mechanical extrusion to be differentiated from the mechanical extrusion itself. Unamended spore suspensions from the same six isolates used in the 2017 and 2018 glasshouse inoculations were used at 10^6 spores per ml.

Plants were inoculated according to their growth stages with the target growth stage being panicle fully extruded (GS59). Inoculated tillers at the targeted growth stage were taped so that they could be identified when sampled at harvest. Plants were bagged in clear non-perforated bags for one week. Once ripe labelled panicles were milled and HT2+T2 quantified as detailed previously.

Figure 2.4 shows oat plants at various stages of the inoculation process.



Figure 2.4: a: naturally extruded plant; b: mechanically extruded plant prior to inoculation; c: panicle immediately after inoculum applied, small droplets are visible on the spikes; d: bagged plant post inoculation.

2.7. Results

2.7.1. 2016 Field Inoculation

In terms of HT2+T2 concentration as determined by ELISA, there were no statistically significant ($P < 0.05$) differences across the 2016 field experiment with no impact of the growth stage of the plants inoculated, irrigation after inoculation or the concentration of inoculum (Figure 2.5). An untreated control was included in the experiment which is represented in all the charts within Figure 2.5. The overall mean concentration of the HT2+T2 ($153 \mu\text{g/kg}$) was low compared to other years of field work described within this body of work.

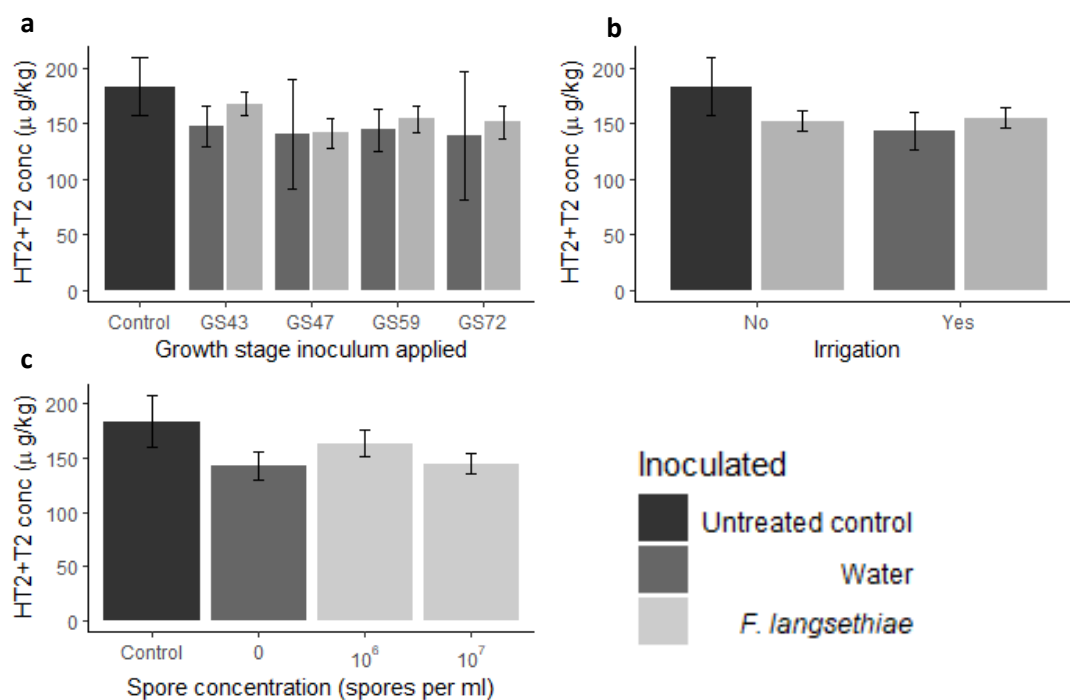


Figure 2.5: HT2+T2 concentration in harvested oat grain (cultivar Gerald) in the 2016 field experiment after *F. langsethiae* inoculations **a**: by growth stage of inoculation; **b**: for plots either inoculated or not with and without simulated rain; **c**: for plots inoculated with different spore concentrations. Control not inoculated or irrigated and 0 treatment inoculated with water only. Error bars represent one standard error of the mean.

2.7.1. 2019 field inoculation

The HT2+T2 concentrations were very low in the inoculated samples. The concentrations from the Buffalo and Tardis parent lines from inoculated and misted plots had an overall mean of 9.76 μg/kg (Figure 2.6). The entire experiment was not analysed as it was unlikely that any differences would be detected with such low concentrations of mycotoxin.

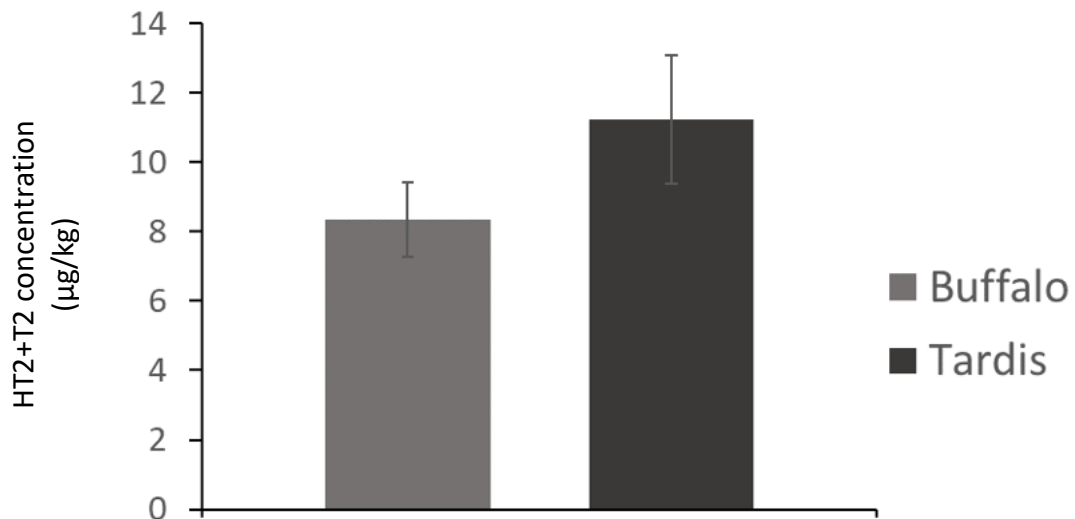


Figure 2.6: Buffalo and Tardis HT2+T2 mycotoxin concentration in harvested grain from *F. langsethiae* inoculated field plots in 2019. Error bars represent the standard error of the mean calculated for individual means.

2.7.2. 2017 Glasshouse Gerald Inoculation

The HT2+T2 concentrations were very high in the inoculated samples as compared to the control (Figure 2.7). To determine the significance of the results, a simple linear model was run using R 4.0.3 using the `lm()` function and a Tukey's post hoc test was performed using the `agricolae` package. This data set required square root transformation to achieve a Gaussian distribution.

An ANOVA was initially conducted on the transformed results; inoculation was significant ($P < 0.001$) as was the growth stage at which inoculation was applied ($P < 0.001$). Visible mycelial growth was seen across the panicles of the inoculated plants, but not on the control plants. The application of inoculum to plants at the earlier growth stage of complete panicle emergence (GS59) resulted in greater concentrations of HT2+T2 in the harvested panicles than spore application at mid to late anthesis (GS65-9). The inclusion of the PDB in the applied spore suspension did not have a statistically significant ($P = 0.488$) effect on the HT2+T2 concentration in harvested panicles. Figure 2.7 shows the back transformed HT2+T2 µg/kg values by treatment.

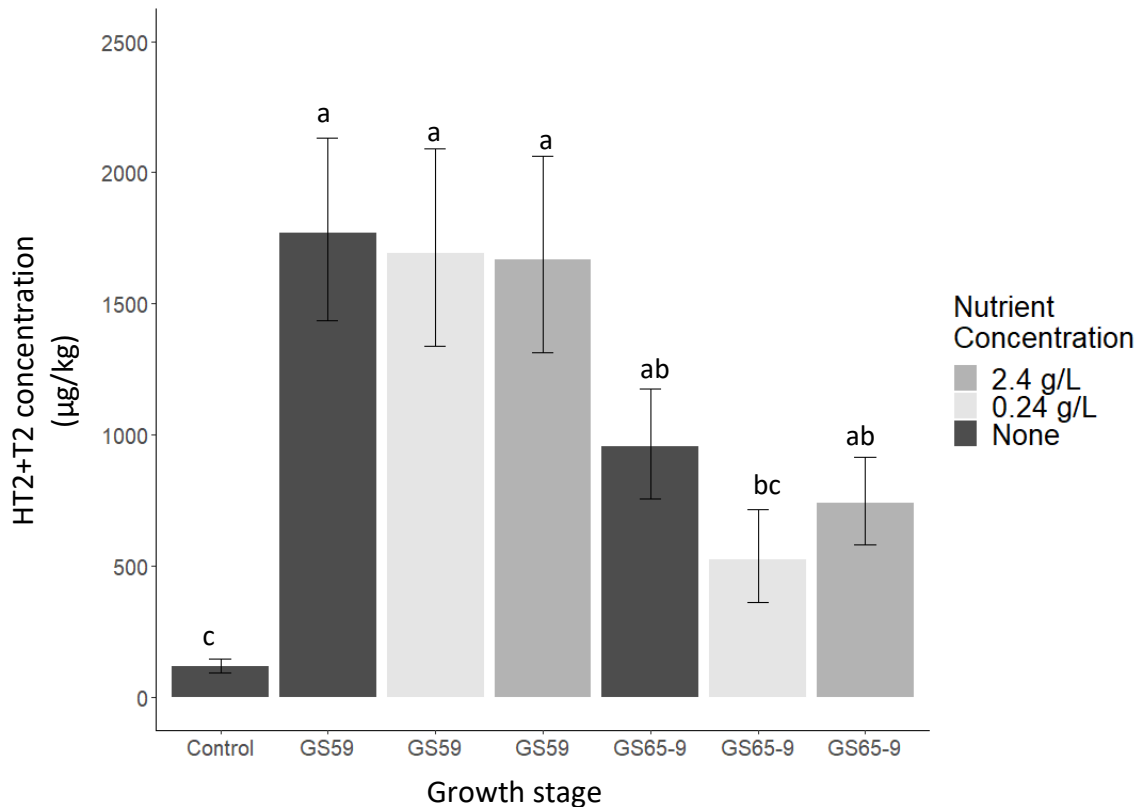


Figure 2.7: Back-transformed concentration of HT+T2 (µg/kg) in panicles of oat (var. Gerald) in the 2017 glasshouse experiment for the Control, GS 59, and GS65-9 *F. langsethiae* inoculated treatments. Different bar colours represent different concentrations of potato dextrose broth detailed in the legend. Error bars represent one standard error of the mean. Columns headed with the same letter were not statistically different (Tukey, $P < 0.05$).

2.7.3. 2018 Glasshouse Balado Inoculation

The HT2+T2 concentrations were high in some of the inoculated samples as compared to the control (Figure 2.9). The results were analysed as in 3.7.2 with Log10 transformation to achieve a Gaussian distribution.

The Balado grew shorter in the glasshouse than in the field and the plants moved quickly through growth stages although tillers were at distinct growth stages. In Figure 2.8 the anthers can be seen protruding from the spikelets while the panicle is still mostly within the flag leaf sheath. The intended growth stage for application was initial panicle emergence (GS51), however Figure 2.8 shows plants at simultaneously early panicle emergence (GS51) and early anthesis (GS61).



Figure 2.8: Balado growing in the glasshouse in 2018 simultaneously at early panicle emergence (GS51) and early anthesis (GS61)

Inoculation was highly significant ($P < 0.001$), proving that the addition of the spore suspension was successful in causing an infection in the inoculated plants. No visible mycelium growth was seen on the panicles in this experiment.

There was no significant interaction between PDB amended inoculum and growth stage at which it was applied ($P = 0.383$). The growth stage at which the inoculum was applied was highly significant ($P < 0.001$); application of inoculum at early panicle emergence/early anthesis (GS51/61) had a large positive impact on the HT2+T2 concentration of the panicle (mean HT2+T2 of 440.5 $\mu\text{g/kg}$) whereas application at GS47 (spikes still within the boot) had no significant effect compared to the uninoculated control (mean HT2+T2 of 58.3 $\mu\text{g/kg}$) (Figure 2.9). The inclusion of PDB had no significant impact on the concentration of HT2+T2 ($P = 0.67$).

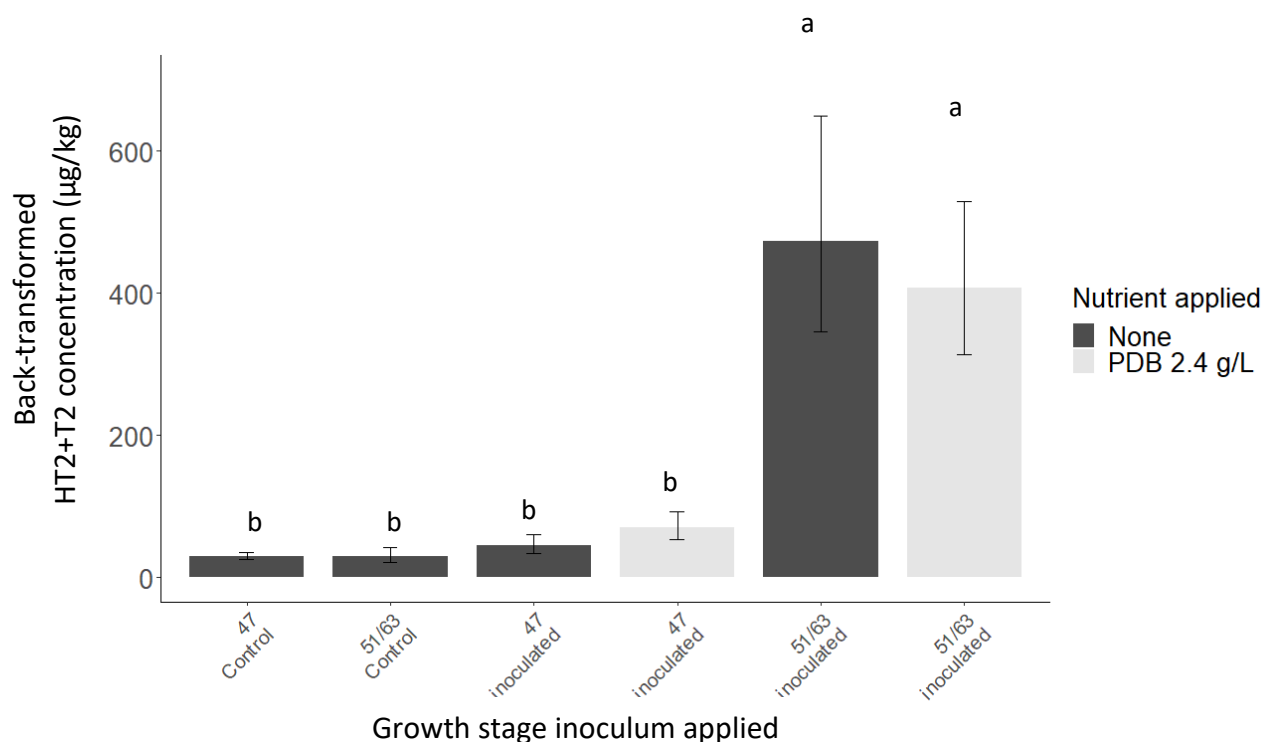


Figure 2.9: Back-transformed concentration of HT+T2 ($\mu\text{g/kg}$) in panicles of oats (var. Balado) for the 2018 glasshouse experiment inoculated with *F. langsethiae*. The x axis describes the growth stage at which inoculant or control water sprays were applied. The legend describes the treatments that included PDA amendment at 2.4 g/L. Error bars represent one standard error of the mean. Columns with the same letter are not significantly different (Tukey, $P>0.05$).

2.7.4. 2019 Glasshouse inoculation

No symptoms were seen on the inoculated panicles when the bags were removed.

Data was Log10 transformed and a one-way ANOVA identified treatment was significant ($P<0.001$). Latterly a Tukey test was applied to the ANOVA model using an alpha level of 0.05 (Figure 2.10). The back transformed concentration of the harvested panicle of the inoculated Buffalo was 226 $\mu\text{g/kg}$ and the untreated control 1.0 $\mu\text{g/kg}$. The two results are statistically distinct from one another (Tukey; $P<0.05$) showing that the inoculation was the source of the infection and that the untreated control was sufficiently protected from the inoculum.

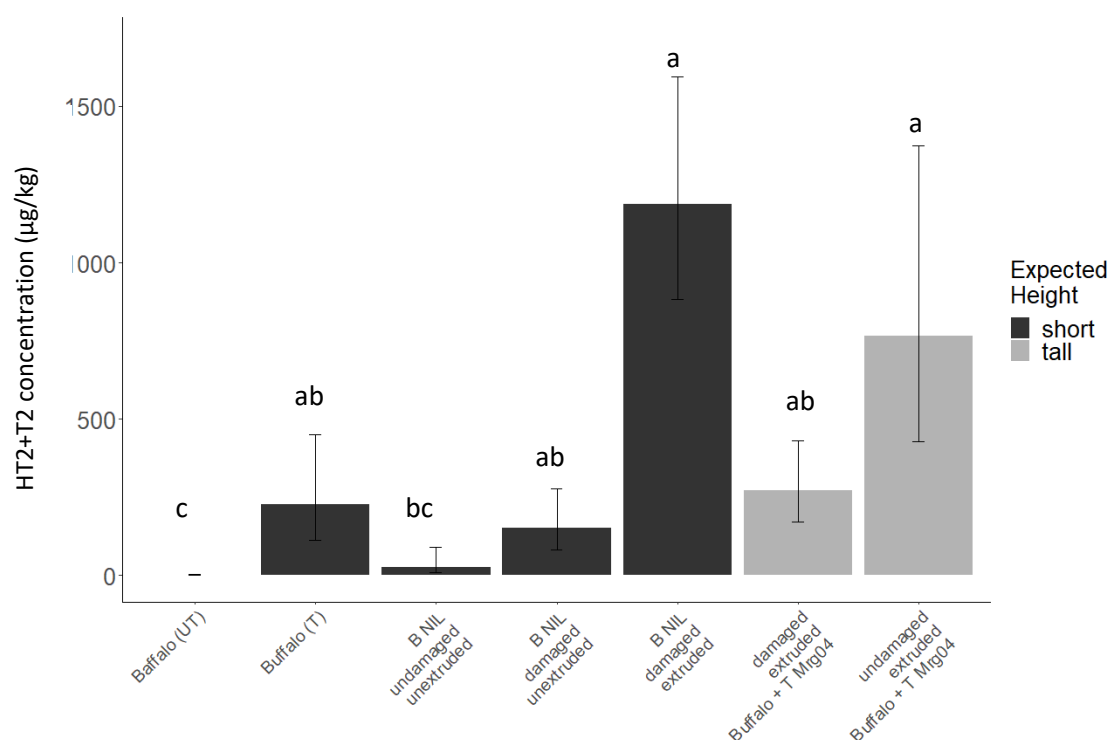


Figure 2.10: Back-transformed concentration of HT+T2 ($\mu\text{g/kg}$) in panicles of oat for 2019 glasshouse experiment for the variety Buffalo with and without inoculation, the Buffalo NIL (B NIL) undamaged and unextruded, damaged and unextruded, damaged and extruded, Buffalo + T Mrg04 damaged and undamaged. The Legend describes the expected heights of the plants predicted from their growth habits in the field. Error bars represent one standard error of the mean. Columns headed with the same letter are not significantly different (Tukey; $P>0.05$).

For the three B NIL inoculated treatments; the unextruded and undamaged treatment did not have a statistically ($P>0.05$) higher concentration of HT+T2 than the Buffalo untreated control whereas the extruded and damaged plants had a statistically ($P<0.05$) higher concentration than both the Buffalo untreated control and the undamaged and unextruded B NIL plants. The damaged but unextruded B NIL plants had a higher concentration than the undamaged and unextruded but not statistically so ($P>0.05$) and they were also not statistically distinct from the damaged and extruded treatment.

The undamaged tall Buffalo + T Mrg04 plants had numerically greater HT2+T2 concentrations than the damaged plants, although differences were not significant ($P>0.05$).

2.8. Discussion

The 2017 Gerald glasshouse inoculation experiment showed mycelial growth on the outside of the panicles similar to that seen by Divon *et al.* (2012), Opoku (2012) and Mousavi (2016). The duration of the bagged time was reduced to seven days in subsequent inoculations and mycelial growth was no longer seen. However, HT2+T2 concentrations were typically lower in the two experiments with shorter bagged periods.

This reduction occurred even in light of Balado and Buffalo previously being seen to be more susceptible to HT2+T2 accumulation than Gerald in commercial crops (Edwards, 2015).

As part of the SafeOats project (Aamot., 2017) 21 isolates of *F. langsethiae* were screened by inoculating a susceptible cultivar of oat under glasshouse conditions. The results showed a range of HT+T2 concentrations in the harvested grain from less than 10 µg/kg to more than 800 ug/kg on a continuous scale showing that the virulence of the pathogen has a normal distribution (Pers. Comm. Dr Heidi Aamot, Postgraduate Researcher, NIBIO, Norway). Miedaner (1997) suggested that isolate by host interactions are not significant and that one sufficiently aggressive isolate or a collection of isolates could be used to identify resistance in the host. This work used six isolates in all inoculations (other than the 2016 field inoculation), all of which were selected on the basis of having been isolated from HT2+T2 contaminated oat grains, as such virulent isolates were likely included in the spore suspensions applied.

Growth stage was examined in the Gerald and Balado experiments, and in both instances was shown to be an important factor in determining the concentration of HT2+T2 in the panicle. The early panicle emergence/and early anthesis (GS51/63) application in the Balado experiment and the late panicle emergence (GS59) application in the Gerald experiment were physiologically close to one another in the growth stage scale, effectively occurring at the beginning of flowering, and each had the highest HT2+T2 concentration in their respective experiments. This is in agreement with other authors who found that applications of inoculum to the plant close to flowering resulted in reliable *F. langsethiae* infections (Schöneberg *et al.*, 2019; Mousavi, 2016; Divon *et al.*, 2012; Opoku, 2012). Divon *et al.* (2019) visualised the infection process after inoculating just after anthesis by microscopic observation; the authors recorded an infection process but did not measure the HT2+T2 concentration in the resultant grain, making it difficult to compare their inoculation timing with those presented above.

In terms of growth stage being important, the Balado result is especially convincing as the tillers were inoculated at different growth stages on the same plants which were then entered into identical conditions within the bag. The first spikes which emerged from the flag leaf boot in the early panicle emergence/early anthesis (GS51/61) tillers had direct contact with the inoculum, whereas the late booting (GS47) tillers could only come into contact with the inoculum if the fungus penetrated the flag leaf boot or if the spores remained viable until the spikes began to emerge later and came into contact with spores as they emerged. The Balado grew uncharacteristically short compared to its habit in the field and as a result had very few spikelets which flowered over a short

period of time potentially meaning that most of the spikelets had pollen present to encourage infection when inoculum was applied (Divon *et al.*, 2019). The large difference in the tillers inoculated at different growth stages provides evidence that the spores need direct contact with the florets. The result also suggests that the pathogen did not cross infect from infected tillers to tillers inoculated at less susceptible growth stages. Divon *et al.*, (2012) attempted early inoculation at the booting stage (GS45) via point inoculation injecting 0.5 or 1 ml of 10^5 and 10^6 spores per ml. Floral abortion, failure of panicle emergence, browning on the stem and plant stunting were all symptoms associated with such early point inoculation, however high *F. langsethiae* DNA concentrations were recovered from harvested plant material. Mousavi (2016) attempted spray application of spore suspension at mid-booting (GS45) and recorded the HT2+T2 concentration in the harvested grain however the concentration was low (19 µg/kg). Earlier inoculations than anthesis might only be putting the inoculant in the immediate environment of the floret ready to infect at the ideal growth stage which would seem to be once pollen becomes present (Divon *et al.*, 2019) similar to the 2018 Balado experiment where the pathogen spores either do not survive on the plant even within the bag or were unable to reach the target plant part. Inoculants applied at earlier growth stages were not able to infect plants once they later passed through more susceptible growth stages. Within the bag there is no mechanism for spores to be mobile around panicles whereas in the field there could be the opportunity for rain splash, wind dispersal or arthropod vectors. In the Balado (2018) experiment, there was sufficient time for the late booting (GS47) tillers to emerge from the boot. Although it was not recorded whether or not the tillers flowered within the bags, the panicles were emerged when the bag was removed. Those panicles had a statistically ($P < 0.05$) lower HT2+T2 concentration than the panicles inoculated at early panicle emergence/early flowering (GS51/63).

This body of work did not examine growth stages later than anthesis but a concurrent study conducted as part of the SafeOats project has shown that the application of a spore suspension as late as early dough (GS81) can result in high (>2000 µg/kg) HT2+T2 concentration in the grain, a higher concentration than when inoculated at earlier growth stages in the same experiment; mid-anthesis (GS65) and early milk (GS73) (Aamot, 2017). Such a late infection would be a large deviation from the main established infection window of other *Fusarium* species known to infect predominantly during anthesis such as *F. graminearum* and *F. culmorum* (Parry *et al.*, 1995; Brown *et al.*, 2010).

In the 2017 Gerald and the 2018 Balado experiments, the addition of the PDB did not have a significant effect on HT2+T2 concentration in the panicles. PDB was picked as

PDA (potato dextrose agar) provides a functional growth medium for *F. langsethiae* in the laboratory and it was hoped that it would encourage the germination of spores on the plants. Divon *et al.* (2019) showed that the pathogen grew preferentially and faster in the presence of pollen. However, if a pollen based or pollen analogues were used, given that inoculants are applied to the entire panicle, they could lead to mycelial growth across the exterior of the panicle and therefore not simulate natural infection.

The 2019 NIL inoculation experiment aimed to understand the impact on different levels of panicle extrusion on HT2+T2 concentration in the harvested panicles. The 2019 NIL experiment used full panicle emergence (GS59) as previous inoculation experiments indicated anthesis as the most susceptible growth stage (Divon *et al.*, 2012; Divon *et al.*, 2019; Drakulic *et al.*, 2016b; Opoku *et al.*, 2012). Full panicle emergence (GS59) was also the earliest opportunity to differentiate plants in terms of panicle extrusion. This study provided evidence that exposing a panicle that would otherwise have been covered by the flag leaf sheath increases the infection level in the harvested panicle. The Buffalo NIL plants with mechanically extruded panicles accumulated significantly higher concentrations of HT2+T2 than the undamaged unextruded control, and the damaged but unextruded panicles' HT2+T2 concentrations were not statistically different to the undamaged and unextruded plants. Potentially extruded panicles have more exposed spikes for spore suspension to land on and infect, whereas unextruded panicles are protected in the boot. Figure 2.11 illustrates how the glasshouse experiments developed on from one another to investigate growth stage, nutrient amendment, and panicle extrusion.

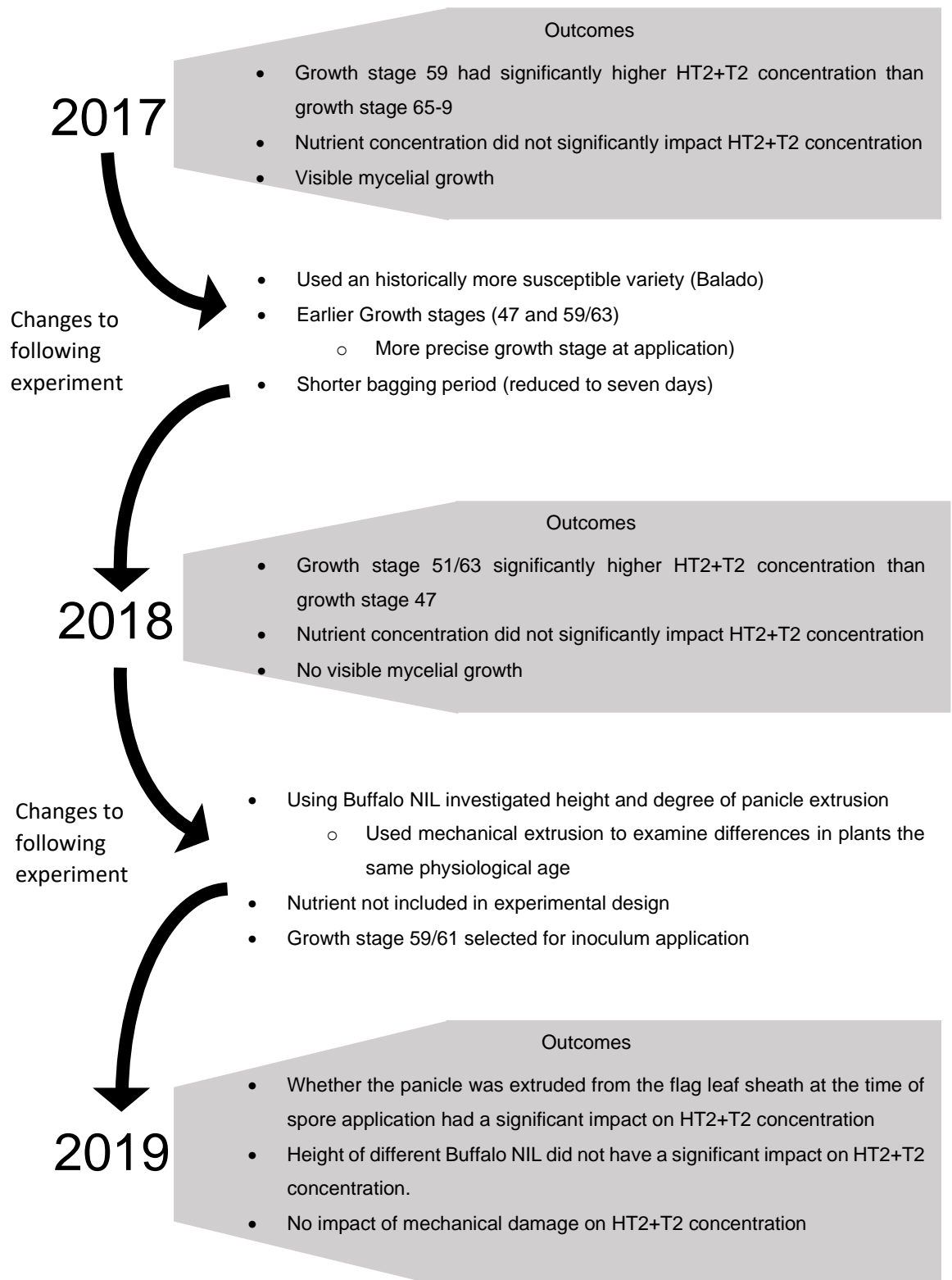


Figure 2.11: Flow diagram illustrating the development of the glasshouse experiments investigating artificial inoculation.

Additional comparisons were planned within the 2019 greenhouse inoculation experiment, however plants grown for those comparisons were lost. Specifically, a taller growing Buffalo NIL was grown as it had shown tall growth in the field while not

extruding fully like other taller genotypes. However, under glasshouse conditions it grew to a similar height to Buffalo and therefore failed to meet the criteria for which it was included. Another NIL originally included was also a close approximation to Buffalo included as it was a sibling line to Buffalo + T Mrg04 (2012-139/6/25) for use in the same treatment regimen as the Buffalo NIL (2012-125/1/26). This genotype was excluded as it failed to grow adequately in the glasshouse. The loss of these samples from the experiment reduced the power of the experiment.

The NIL inoculation experiment also sought to identify whether relative resistances in the field were retained after artificial inoculation. It was not possible to statistically differentiate the NIL in terms of their HT2+T2 concentrations; however, based on the numerical differences the taller Buffalo + T Mrg04 lines accumulated higher HT2+T2 concentrations compared to the shorter Buffalo parent line and the Buffalo NIL, perhaps because they had more exposed spikelets.

There was high variation in the HT2+T2 results obtained from the taller genotypes used in the 2019 experiments, however no significant differences were seen between the damaged and undamaged plants. The same was true for the shorter Buffalo NIL plants where the damaged but unextruded plants could not be statistically differentiated from the undamaged and unextruded plants. These results agree with those of Imathiu *et al.* (2009) who found that oat plants did not require wounding to be susceptible to *F. langsethiae* infection in a detached leaf assay.

Stripping back the flag leaf sheath reduced the plants' ability to grain fill given the importance of the flag leaf in late season growth, potentially leading to smaller grains and higher relative amounts of HT2+T2 per gram of flour. Lower spikelets potentially left in the boot are more likely to be sterile (Misonoo, 1936) causing them to fail to develop any grain and the reduction of HT2+T2 in commercial batches after milling (Scudamore *et al.*, 2007; Edwards, 2007a) is tied to the loss of screenings (empty husks and small grain) and the removal of the husk itself from filled grains. This is supported by Brodal *et al.* (2020) who showed that removal of the smallest size fraction by sieve could reduce HT2+T2 concentration in the batch by over 50%. In this series of experiments all blinds were included in samples collected and in those treatment groups that included mechanical panicle extrusion, those spikelets were also directly sprayed with spore suspensions.

The concentration of the empty husks could be high due to the very low weight relative to the HT2+T2 content. They are not necessarily more susceptible than other grains and may have a similar content of mycotoxins per grain. Potentially this could explain higher HT2+T2 concentrations in panicles that have been mechanically exposed.

Entire panicles were measured due to low grain yields and to add reliability to the experiments yielding concentrations of HT2+T2 that could be used in inferential statistics. Divon *et al.* (2019) demonstrated that the pathogen grew on the inside of the glumes and any accompanying HT2+T2 to that growth would have been picked up by using the entire panicle. Glumes are not typically retained when oats are commercially harvested so their inclusion in this work could be a source of deviation from previous work on varietal differences and glasshouse inoculation work. Field experiments used threshed grain for analysis, perhaps contributing to lower values.

The NIL experiment only had five replications compared with the higher replication of earlier experiments, due to the reduction in NILs used in the experiment and the large variation within treatments large numerical differences were not realised as statistically different. The NIL experiment only showed a small increase from the untreated control in the treated Buffalo plants, much less than either of the two previous experiments conducted in the glasshouse.

All the inoculations took place at dusk to avoid UV damage to the *F. langsethiae* spores which will have meant that the florets of the oats will have likely been closed (Misonoo, 1936). Closed florets preventing access to the pollen as a growth stimulus could have reduced the likelihood of the inoculation being successful.

Successful inoculations appear to include inoculant application close to flowering and an increase in humidity immediately afterwards (Imathiu, 2008; Divon *et al.*, 2012; Mousavi *et al.*, 2016; Aamot, 2017; Divon *et al.*, 2019; Schöneberg *et al.* 2019). Potato dextrose broth as an additional nutrient provided no benefit. It is possible to get a reliable infection in glasshouse experiments but there is no evidence that such an infection is a reliable mimic of natural infection in the field.

There was variation between the glasshouse HT2+T2 concentrations across experiments which can perhaps be mostly explained by the use of different cultivars in each experiment, the comparison of the experiments of susceptible growth stages is likely valid as the pathogen will infect all cultivars of oat in the same manner.

The work presented in this chapter suggests inoculating at growth stages close to flowering provided the highest concentration of HT2+T2. Divon *et al.* (2012) also infected oat plants with sprays of microconidial suspensions at anthesis and early dough with subsequent bagging for six days, both of which produced greater quantities of *F. langsethiae* DNA at harvest and fewer visual symptoms than boot injection. Schöneberg *et al.* (2019) used spore suspension application at panicle emergence or anthesis followed by 99% humidity of varying durations and found that anthesis applications had higher HT2+T2 concentrations. Divon *et al.* (2019) observed

microscopically that pollen encourages the growth of the pathogen indicating that anthesis is the likely optimal infection timing. Successful inoculations achieved through spore application at later growth stages have been achieved (Divon *et al.*, 2012; Aamot, 2017) proving that later infections are possible.

There has yet to be a reliable method of artificial inoculation demonstrated in the field (Imathiu, 2008; Schöneberg *et al.*, 2019; Plăcintă *et al.*, 2015). Inoculum applied as a spore suspension, infected straw and infected grain has been previously attempted (Imathiu, 2008; Schöneberg *et al.*, 2019; Isidro-Sánchez *et al.*, 2020). Spore suspensions applied in the glasshouse have had consistent results (Imathiu, 2008; Opoku, 2012; Mousavi, 2016; Aamot, 2017; Divon *et al.*, 2019; Schöneberg *et al.*, 2019), often using plastic bags covering the freshly inoculated plants to increase humidity. Xu *et al.* (2014) also concluded from weather analysis that wet weather in May coinciding with winter oat flowering correlated with higher HT2+T2 concentration in the harvested grain. The 2016 field inoculation experiment examined the theory that infection occurred by inoculum entering the boot via an opening at the top and rain run-off draining down the flag leaf prior to panicle emergence. Water applied with a plot scale applicator was applied two hours post inoculation after sunset to wet the crop overnight. Results show that there was not a significant increase in HT2+T2 concentration when irrigation was applied. Increasing the spore load from 10^6 spores per ml to 10^7 spores per ml did not have a significant effect on the HT2+T2 concentration in the grain. In the same year and field, some sampling was done on the grid scale presented in Chapter 7 and samples taken from outside of the inoculation experiment had higher concentrations of HT2+T2, showing that natural infection was sufficiently high that year in the Gerald variety to mask any impact of the inoculations. Isidro-Sánchez *et al.* (2020) used application of spore suspension and high-pressure low volume irrigation to inoculate oats, but HT2+T2 concentrations were modest and there was no uninoculated control to compare against (averaged over two years). As demonstrated in this work it is possible for uninoculated plants to have higher HT2+T2 concentrations than inoculated.

Plants in the field were sprayed in the late evening to avoid UV light damaging the spores. However, should it be important for the spore suspension to enter an open floret early afternoon (~3pm) would have been a more ideal timing (Misonoo, 1936; Nishiyama, 1970) as that is when florets have been observed to open.

Although the 2016 field experiment and the 2017 glasshouse experiment used the same variety of oats (and the same seed treatment), the glasshouse inoculation worked in terms of increasing HT2+T2 concentration in harvested panicles whereas the field inoculation failed to produce results above background levels.

Several differences existed between the two experiments beyond being set either within the glasshouse or in the field; the isolates used, growth stage of application, harvested part, and environmental conditions surrounding the panicle immediately after inoculation.

The 2019 field experiment sought to assess selected NIL using artificial inoculation using the method based on successful inoculations performed in the glasshouse. Misting was used to wet the plots in the evening for two hours throughout the flowering period to ensure the humidity would stay high during the night. Three applications were made to two locations in all the plots, the first that received irrigation and the second that did not. From the selection of plots that were initially assessed, HT2+T2 levels were so low that only the parent lines were assessed in the inoculated and misted plots to confirm the lack of HT2+T2 in the experiment. Results shows that there was no difference between Buffalo and Tardis in the misted and inoculated plots. The concentration seen in those parental plots was ~10 µg/kg such a concentration is only just above the level of detection by the ELISA. Natural infection has been recorded at several orders of magnitude higher than such levels and as such it is possible that any small impact from the exogenous application of spore suspensions is masked by modest natural infections. Previous work by Imathiu (2008) showed successful inoculation of Firth in the field, but not Gerald, by the spray application of a spore suspension at mid anthesis (GS65) based on the *F. langsethiae* DNA concentration in the harvested grains, however the additional misting treatment applied had no additional effect on DNA concentration. HT2+T2 was not recorded so it is difficult to make direct comparisons but using Edwards *et al.* (2012a) work, a DNA concentration of 0.0214 pg/ng total DNA equates to a relatively low HT2+T2 concentration (63 µg/kg).

The method used was based on the methodology used in the Norwegian SafeOats project (Pers. comm. Dr Ingerd Hofgaard, Research Scientist, National Institute of Bioeconomy, Norway, 2019). The outdoor inoculation in 2019 used similar techniques to those applied to *F. graminearum*, but the two pathogens rarely occur together (Hofgaard *et al.*, 2016).

Fusarium langsethiae is only known to produce napiform microconidia. Stack (1989) found that in *F. graminearum*, equivalent levels of infection were obtained after point inoculation into spikes from either ascospores or macroconidia. Were there to be a sexual spore of *F. langsethiae* in the field perhaps the same would be true that it would be similarly aggressive as the microconidia available in the lab. The spores were determined to be ~40% viable immediately after collection based on comparison of spore counts and dilution plate counts of colony forming units and are likely to degrade with time. Due to this spore suspensions were prepared on the day or day before

inoculation and kept in a cool dark place prior to application. Assessment of spore viability of remaining spore suspension after application frequently showed a 10-5% viability measured by colony forming units on Rose Bengal Chloramphenicol Agar (results not shown).

Given the disparity between field inoculation and glasshouse inoculation success further work is needed to identify lines of research beyond application of spore suspensions to different growth stages, investigative microscopy work on plants naturally infected in the field would be ideal. The difficulty will be the low incidence of *F. langsethiae* infection in any given year and site. However, insights from such work could support or reject the current understanding of the infection mechanism including the manner and form in which *F. langsethiae* contacts the plant.

3. Chapter 3: Quantitative traits in Buffalo and Tardis NIL as impacted by sowing date

3.1. Introduction

To date the most effective method for controlling or limiting *F. langsethiae* has been the use of resistant cultivars (Edwards, 2007a; Edwards, 2009a; Edwards, 2017). The mechanism through which resistance is attained is as yet unknown, two traits have been suggested in the literature as having been associated with resistance in oats to *Fusarium* infection; earliness (Loskutov *et al.*, 2016; Hautsalo *et al.*, 2020) and height (Hautsalo *et al.*, 2020; Stančić, 2016). This chapter seeks to explore the impact of five QTL on those traits using near isogenic lines (NIL).

Near Isogenic Lines have a near identical genetic background to one parent line but with a single or very few QTL introgressed from another parent. As such NIL can be used for validating the trait originally associated with a QTL and provide further insight into the physiological or genetic mechanism for the trait in question.

Marker assisted selection (MAS) is an indirect selection method for traits of interest: by associating molecular markers such as single nucleotide polymorphisms with those traits, the markers can then be observed rather than the traits. As such MAS removes the need to observe the phenotypic trait every season in the parent if there is already an association of that trait to one or multiple molecular markers. By identifying the molecular markers present in a germplasm and referencing a relevant association map, the selection decision can be made. The marker genotype can be observed at any stage in the plant's development, including before anthesis, and is not influenced by environment. As such observation of the phenotype is now mostly only required in associating QTL with molecular markers and measuring the magnitude of the QTL on the traits.

Buffalo and Tardis are two cultivars of winter oat that differ in height and flowering time: Tardis is a tall earlier flowering cultivar and Buffalo is a dwarf later flowering one. The straw lengths reported by the AHDB Recommended List for Buffalo and Tardis are 97 cm (HGCA, 2005) and 106 cm (HGCA, 2013) respectively, and Tardis is recorded as ripening two days earlier than Buffalo. Buffalo is the more susceptible cultivar to HT2+T2 accumulation (Edwards, 2007a). A genetically annotated mapping population from a Buffalo/Tardis cross was developed and phenotyped at Aberystwyth University (Klos *et al.*, 2016; Chaffin *et al.*, 2016) to examine QTL for agronomic traits including flowering time and height as part of the QUOATS project funded by Defra, BBSRC and industry partners including the AHDB (Marshall *et al.*, 2015). This population comprised 227 F₇ Recombinant Inbred Lines from which leaf material was sampled for DNA extraction and grown in field trials over several seasons (Mellars *et al.*, 2020). In

addition to genotyping with microsatellites and DArT markers (Tinker *et al.*, 2009; Diversity Arrays Technology Pty Ltd, Canberra, Australia), GBS libraries were constructed following the oat protocol developed and described by Huang *et al.* (2014) and processed as reported in Bekele *et al.* (2018) The mapping population was used to generate a genetic map by Dr Catherine Howarth.

Stančić (2016) used these recombinant inbred lines (RIL) and simple interval mapping with an early version of the genetic map (495 loci from a combination of microsatellite, DaRT and SNP markers but no GBS markers) which covered a total of 35 linkage groups. Logarithm of odds (LOD) scores were determined with which to quantify associations between markers and traits, as well as calculating the percentage of variance accounted for by each QTL. The traits used in this quantitative trait analysis (QTL) analysis were height, time to panicle emergence, *F. langsethiae* DNA, and HT2+T2 concentration in the harvested grain.

Over three years Stančić (2016) identified QTL on nine linkage groups associated with *F. langsethiae* DNA concentration and ten associated with HT2+T2 concentration. Those QTL with the highest LOD scores for *F. langsethiae* DNA and HT2+T2 concentrations were in close proximity to QTL for height and flowering time. Some QTL only had associations with *F. langsethiae* DNA or HT2+T2 in single years indicating the effect was not stable across years. The NIL examined in this chapter were identified by Stančić (2016) as being associated with either height or flowering time as well as HT2+T2 and *F. langsethiae* DNA accumulation. The QTL identified on Mrg11 was the only QTL to not be associated with either height or flowering time in Stančić's original work.

Height as a trait has been manipulated over the past century for the purposes of improved agronomy, as described in Chapter One. Earliness of plants is an important agronomic trait under genetic control (Trevaskis *et al.*, 2007) used to adapt germplasm to different environments. One measure of earliness is the time from sowing to panicle emergence. Stančić (2016) measured earliness in this manner and reported it as flowering time. Both traits on their own warrant investigation, and identifying QTL associated with either has value for breeding programmes. Height and earliness are quantitatively inherited, and each show continuous variation coded for by multiple genes. In cereals, specific genes strongly influencing height are labelled dwarfing genes, the Buffalo parent contains the dwarfing gene *Dw6* (Marshall *et al.*, 2015). The molecular mechanism for influencing flowering time in cereals is governed several genes including the *Vrn1*, *Vrn2*, and *Vrn3* genes (Trevaskis *et al.*, 2007; Shrestha *et al.*, 2014; Brambilla *et al.*, 2017) which control the vernalisation requirement.

Vernalisation has been defined as “the acquisition or acceleration of the ability to flower by a chilling treatment” (Chouard, 1960).

The NIL examined in this work were developed from the original population of RIL using several generations of backcrossing of selected RIL to either the Buffalo or Tardis parent and marker assisted selection to identify those plants with desired introgressions in the recipient parent genome. These plants were then selfed to identify lines that were homozygous for those loci. The lines examined in this experiment are a mixture of either Tardis or Buffalo background genomes. The introgressed loci are found on Mrg04 (a QTL containing the dwarfing gene *Dw6* found in Buffalo which causes shortened upper internodes and which is also associated with flowering time); Mrg21 (a QTL strongly associated with flowering time in spring sown Buffalo crops (+14 days) and a smaller effect in autumn sown plants); Mrg20 (a QTL which influences flowering time); and Mrg11 which has no impact on flowering time or height, but decreased *F. langsethiae* DNA concentration and HT2+T2 concentration in harvested grain. Some lines have two or more QTL differing from the parent genotype and are not examined in detail. Key NIL examined in this experiment are described in Table 3.1. In some instances when NIL possessed the same genetic composition (typically sibling lines derived from the same cross), more than one NIL was included under the same name.

Table 3.1: Key NILs used within this study. QTL name refers to the Mrg designations for linkage groups described in Chaffin et al. (2016). The Allele column describes from which parent the QTL is originally derived (B denoting Buffalo and T denoting Tardis). In some instances, multiple genotypes have been grouped together when they consist of near identical genetic compositions.

Breeder's Code	Name	Background genotype	QTL introgressed		
			Allele	QTL name	Trait targeted
2012-137/5/1	Tardis +B Mrg04	Tardis	B	Mrg04	Height (<i>Dw6</i>) and flowering time
2012-137/5/5					
2012-139/6/25	Buffalo +T Mrg04	Buffalo	T		
2012-125/1/27					
2012-134/1/35	Tardis +B Mrg21	Tardis	B	Mrg21	Flowering time (spring sown) (<i>Vrn1</i>)
2012-134/1/36					
2013-214ACnX/4	Buffalo +T Mrg21	Buffalo	T		
2012-130/5/2	Tardis +B Mrg20	Tardis	B	Mrg20	Flowering time
2013-212ACnI/23	Buffalo +T Mrg20	Buffalo	T		
2012-131/429/3	Buffalo + T Mrg11	Buffalo	T	Mrg11	Resistance to HT2+T2 and <i>F. langsethiae</i> DNA accumulation
2012-131/4/29/7					
2012-131/4/4/2					
2012-131/4/4/7					

The work described in this chapter serves to confirm and measure the impact of the selected QTL on height and flowering times measured by time to panicle emergence.

3.2. Method

For each harvest year 2017-2020 a collection of the NIL developed at Aberystwyth University were sown both in autumn and spring in the experimental field. Experiments were sown in 1 m² plots as a randomised block design with four blocks in both autumn and spring. Experiments were treated with a comprehensive programme of fungicides to control foliar pathogens up to flag leaf fully emerged but had no plant growth regulator applied. All experiments were grown in the same field for each of the four years, the field was divided in two, one half growing wheat and the other oats. The crop was drilled using a Winterstieger self-propelled plot drill using Suffolk coulters at a seed rate of 300 seeds/m² the plots were rolled using Cambridge rolls the same day as drilling. For the 2017 and 2018 sown experiments the seed bed was prepared by

discing alone, the rotation within the field caused a build-up of wild oats that were difficult to control. For the 2019 and 2020 experiments, the ground was ploughed to bury the weed bank. Table 3.2 details the sowing and harvest dates of all the experiments discussed in this chapter.

Table 3.2: Sowing and harvest dates of each NIL experiment.

Experiment	Drilling date	Harvest Date
2017 autumn	11/10/2016	16/08/2017
2017 spring	15/03/2017	07/09/2017
2018 autumn	13/10/2017	03/08/2018
2018 spring	20/04/2018	22/08/2018 (hand sampled)
2019 autumn	02/10/2018	27/08/2019
2019 spring	20/03/2019	13/09/2019
2020 autumn	23/10/2019	27/08/2020
2020 spring	25/03/2020	04/09/2020

The date on which the plants reached early panicle emergence (GS 51) for each plot was recorded; a plot was deemed to have reached GS 51 once half the plot was at GS 51. Panicle emergence was used as a proxy for flowering time as it is difficult and time consuming to assess flowering time for oats. Once the plants had stopped increasing in height, the height from the ground to the flag leaf ligule, the first whorl of the panicle (not recorded in 2017) and to the top of the plant was measured to an accuracy of 0.5 cm. Four plants per plot were measured for each height and the average used.

Weather data detailing the maximum and minimum temperature per hour was collected from a MET office weather station located 1 km away from the experimental field and growing degree days were calculated based on the average temperature per day with a base temperature of 5°C. Timing of flowering was calculated as degree days to panicle emergence from sowing date and days from January 1st (Julian days).

3.2.1. Statistical analysis

All statistical analysis was performed in R version 4.0.4 (R Core Team, 2020), linear models were produced in the `lm()` function. Percentage variance accounted for was calculated based on the sum of squares. Contrast analysis was performed using `lsmeans()` and `contrast()` functions in the `lsmeans` package. Cohen's D values were calculated as a measure of effect sizes by dividing the difference between two means of interest by the pooled standard deviation of the two data sets from which those means were derived.

Correlation analysis was performed using the `cor()` function within base R and specifying the Pearson method within the function arguments to give a P value and a correlation coefficient.

3.3. Results

The NIL were consistent in their physiological traits over the four years, Table 3.3 and Table 3.4 show the Pearson correlation coefficients for year to year comparisons of height and degree days to panicle emergence for autumn and spring sown plots. All correlations were significant to $P < 0.001$.

Table 3.3: Pearson correlation coefficients for height, degree days to panicle emergence (GS51) in the harvested grain from autumn sown plots.

Autumn drilled	2017, 2018	2017, 2019	2017, 2020	2018, 2020	2018, 2019	2019, 2020
Height	0.93	0.90	0.91	0.92	0.91	0.89
Degree days to GS51	0.60	0.83	0.70	0.59	0.68	0.75

Table 3.4: Pearson correlation coefficients for height, degree days to panicle emergence (GS51) in the harvested grain from spring sown plots.

Spring sown	2017, 2018	2017, 2019	2017, 2020	2018, 2020	2018, 2019	2019, 2020
Height	0.90	0.96	0.90	0.87	0.90	0.93
Degree days to GS51	0.88	0.90	0.82	0.89	0.93	0.90

3.3.1. Height

The NIL were consistent in their relative heights to one another across all four years, the largest height variation was introduced by Mrg04. A linear model was built using year, genotype and sowing season, the factors were entered in the order listed with year first (Table 3.5).

Table 3.5: Output from the model examining the impact year, sowing season, and genotype on plant height.

Factor	Degrees of freedom	P value	Percentage variation accounted for (%)
Model			82.9
Year	3	<0.001	26.0
Sowing season	1	<0.001	11.4
Genotype	18	<0.001	45.5
Year*sowing season	3	<0.001	11.1
Year*Genotype	54	<0.001	1.6
Sowing season*Genotype	18	<0.001	0.7
Year*sowing season*Genotype	54	<0.001	0.8

3.3.1.1. Mrg04

When the Buffalo derived Mrg04 was introgressed into a Tardis background the resultant plant was short with an unextruded panicle. Tardis+B Mrg04 grew shorter than either parent line in both spring and autumn sown plots. When the Tardis derived Mrg04 QTL was introgressed into the Buffalo background a very tall plant was produced.

Figure 3.1 and Figure 3.2 show the height of the parent lines and the NIL representing introgressions of each parent's Mrg04 into the other cultivar's background genome sown in autumn. A linear model comparing the parent genotype with the NIL comprising of the parent genome with the opposing parent Mrg04 introgressed showed highly significant differences ($P < 0.001$) (Table 3.6 and Table 3.7).

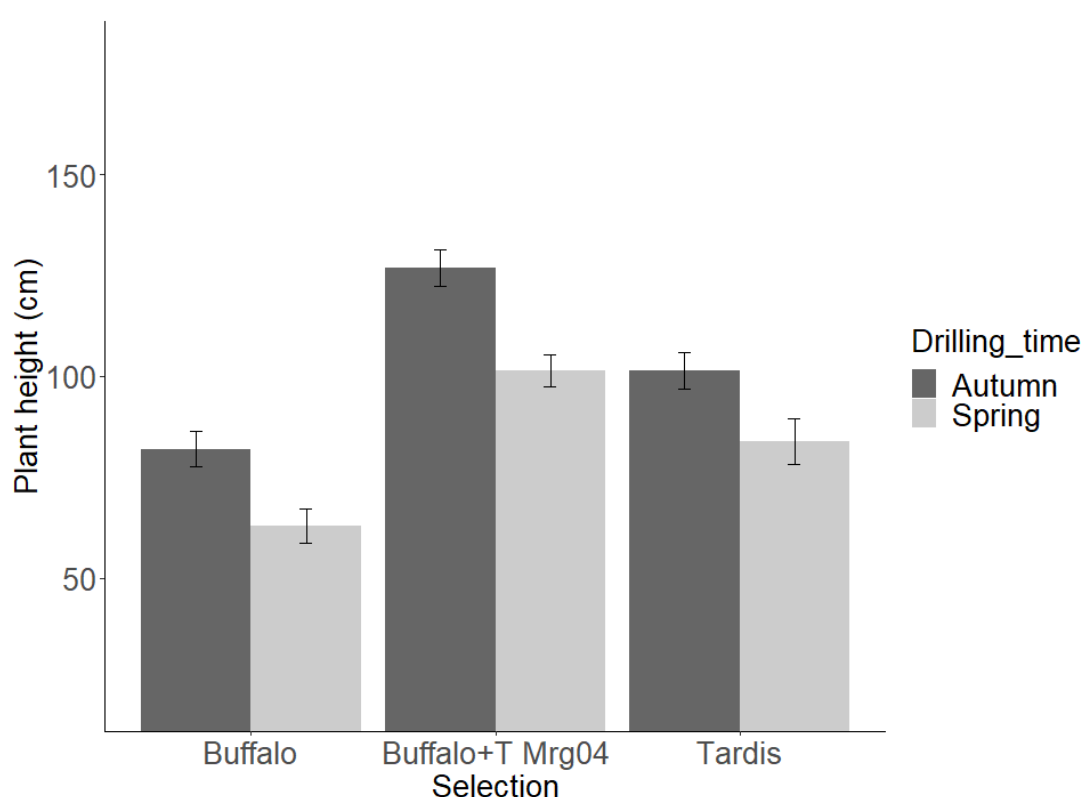


Figure 3.1: Plant height of Buffalo+T Mrg04, Buffalo and Tardis sown in autumn and spring. Results from four years of autumn and spring sown field experiments (2017-2020). The error bars represent the standard error of the mean.

Table 3.6: Contrast analysis comparing height of the parent line Buffalo with Buffalo+T Mrg04. Cohen's D is included as a measure of effect size, N is the sample number.

Contrast	Estimate (cm) (difference between contrasted values)	N	P value	Cohen's D
Autumn: Buffalo vs Buffalo + T Mrg04	44.2	32	<0.001	1.12
Spring: Buffalo vs Buffalo + T Mrg04	38.4	32	<0.001	1.08

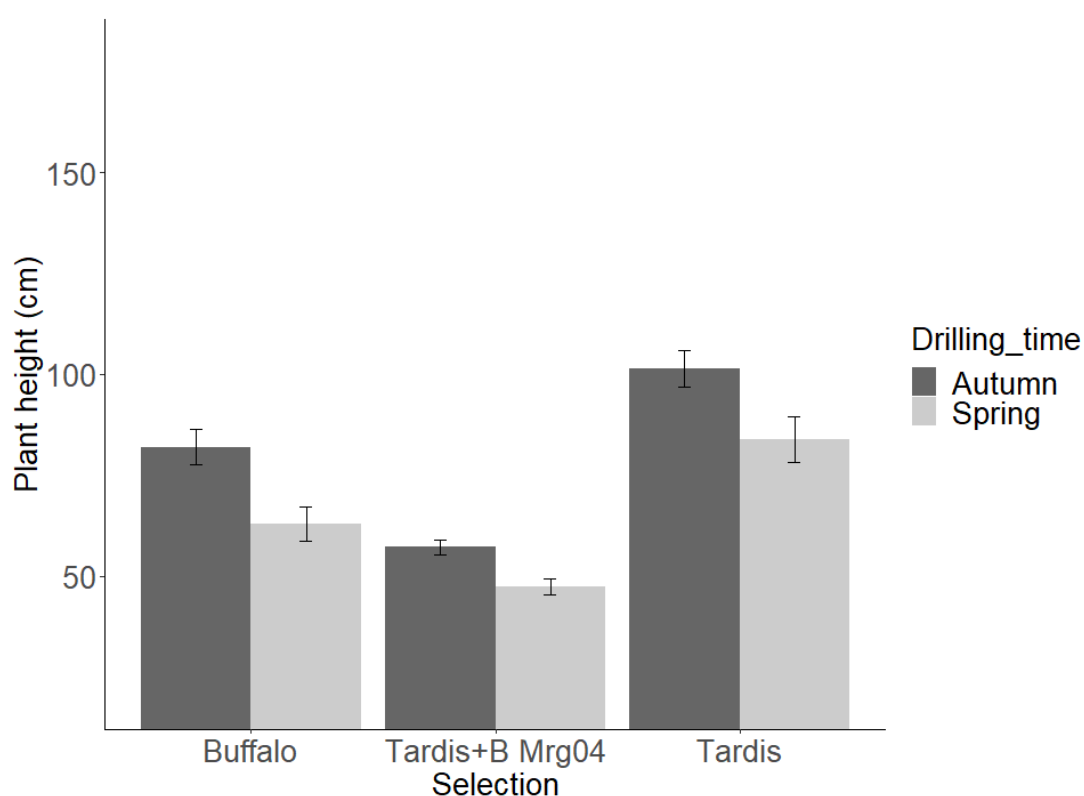


Figure 3.2: Plant height of Tardis+B Mrg04, Buffalo and Tardis grown in autumn and spring. Results from four years of autumn and spring sown field experiments (2017-2020). The error bars represent one standard error of the mean.

Table 3.7: Contrast analysis comparing the heights of the parent line Tardis with Tardis+B Mrg04. Cohen's D is included as a measure of effect size, N is the sample number.

Contrast	Estimate (cm) (difference between contrasted values)	N	P value	Cohen's D
Autumn: Tardis vs Tardis + B Mrg04	-44.2	32	<0.001	1.93
Spring: Tardis vs Tardis + B Mrg04	-36.5	32	<0.001	1.31

3.3.1.2. Mrg21

Figure 3.3 and Figure 3.4 show that there were only very small changes in height after Mrg21 from the opposing parent was introgressed into the background of the Buffalo or Tardis respectively. The changes although small were significant in all contrasts except the autumn sown Buffalo vs Buffalo + T Mrg21. Figure 3.3 and Figure 3.4 show the contrasts of spring and autumn for Buffalo + T Mrg21 and Tardis + B Mrg21 against their respective parent lines, the change in height measured in cm is small in all cases and is reflected by low Cohen's D values (Table 3.8 and Table 3.9).

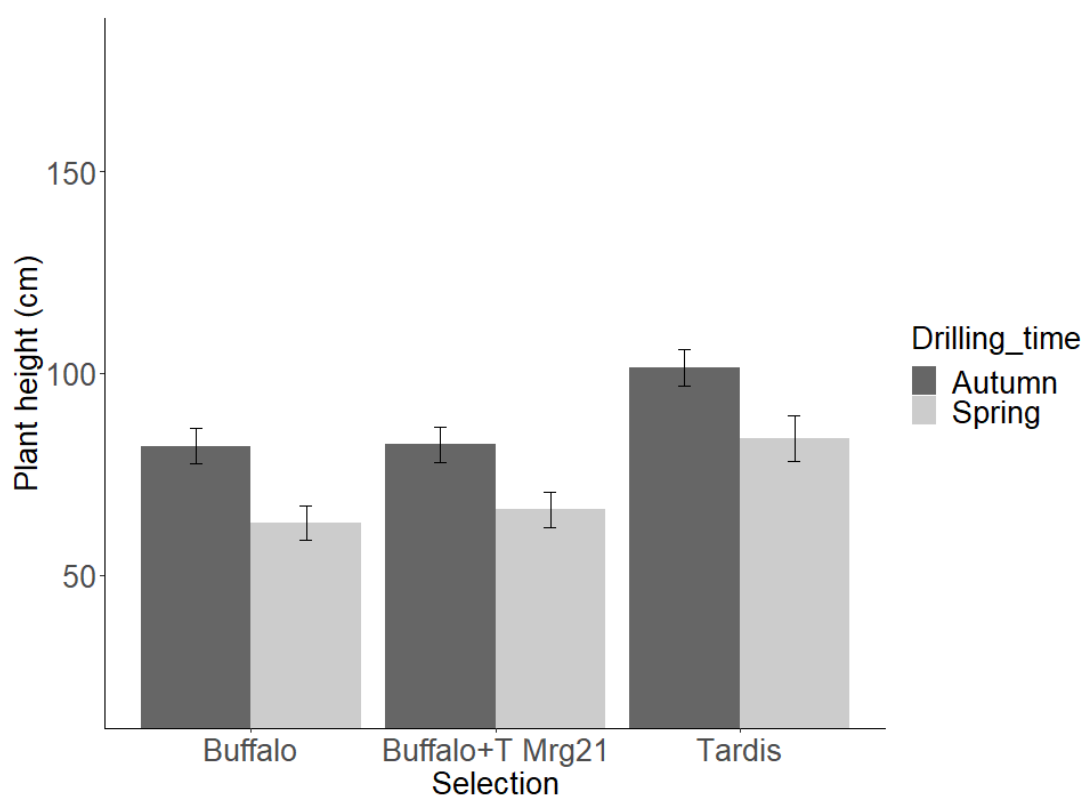


Figure 3.3: Plant heights of Buffalo+T Mrg21, Buffalo and Tardis grown in autumn and spring. Results from four years of autumn and spring sown field experiments (2017-2020). The error bars represent one standard error of the mean.

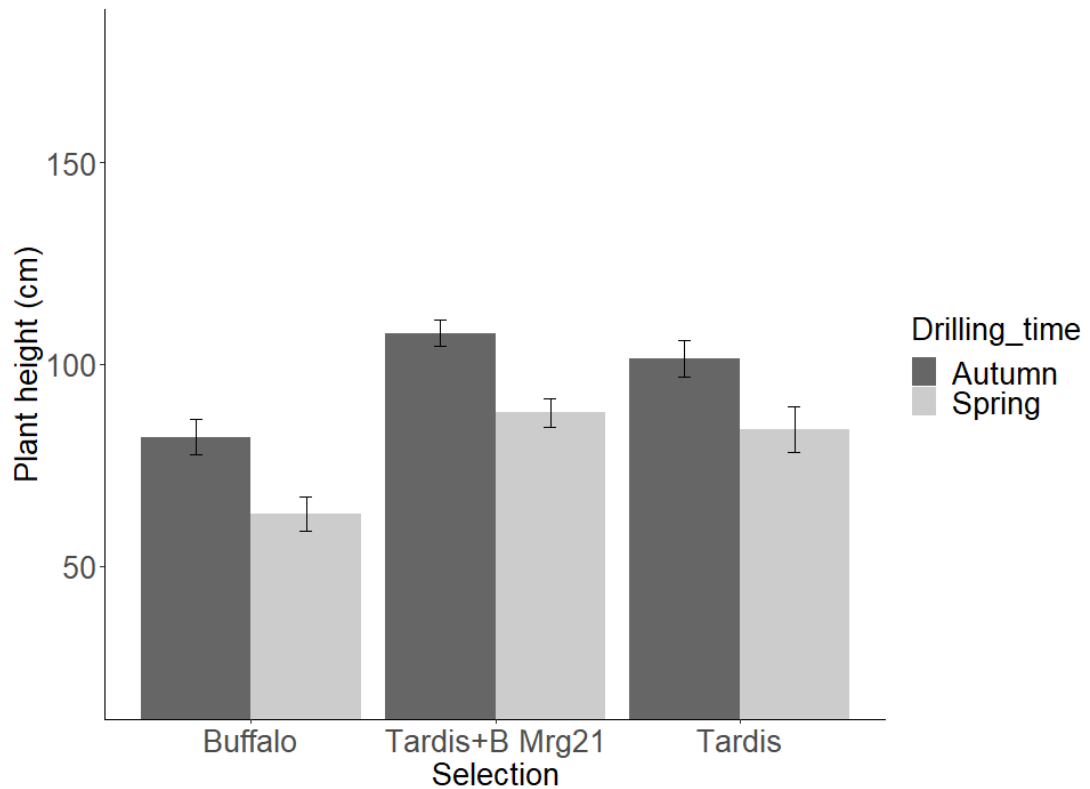


Figure 3.4: Plant heights of Tardis + B Mrg21, Buffalo, and Tardis grown in autumn and spring. Results from four years of autumn and spring sown field experiments (2017-2020). The error bars represent one standard error of the mean.

Table 3.8: Contrast analysis comparing the heights of the parent line Buffalo with Buffalo+T Mrg21. Cohen's D is included as a measure of effect size, N is the sample number.

Contrast	Estimate (difference between contrasted values) (cm)	N	P value	Cohen's D
Autumn: Buffalo vs Buffalo + T Mrg21	0.4	16	0.8409	0.02
Spring: Buffalo vs Buffalo + T Mrg21	3.3	16	0.0386	0.13

Table 3.9: Contrast analysis comparing the heights of the parent line Tardis against Tardis + B Mrg21. Cohen's D is included as a measure of effect size, N is the sample number.

Contrast	Estimate (difference between contrasted values)	N	P value	Cohen's D
Autumn: Tardis vs Tardis + B Mrg21	6.4	32	0.0011	0.20
Spring: Tardis vs Tardis + B Mrg21	4.1	32	0.0028	0.11

3.3.1.3. *Mrg20*

Figures 3.5 and Figure 3.6 show that *Mrg20* introgressions had a low impact on height in either autumn or spring sowings.

Table 3.10 and Table 3.11 show the output from contrasts within a linear model comparing the parent genotype with the NIL comprising of the parent genome with the opposing parent *Mrg20* introgressed. All Tardis + B *Mrg20* vs Tardis contrasts were significant ($P < 0.05$) indicating that the Buffalo alleles on the *Mrg20* QTL did increase the height although only by ~5 cm in either sowing season. Height increases in the Buffalo + T *Mrg20* vs Buffalo contrasts were not significant ($P > 0.05$) and the height increase was less than the Tardis + B *Mrg20* vs Tardis contrast. For all contrasts the Cohen's D value was low, indicating the introgressions had small effect sizes.

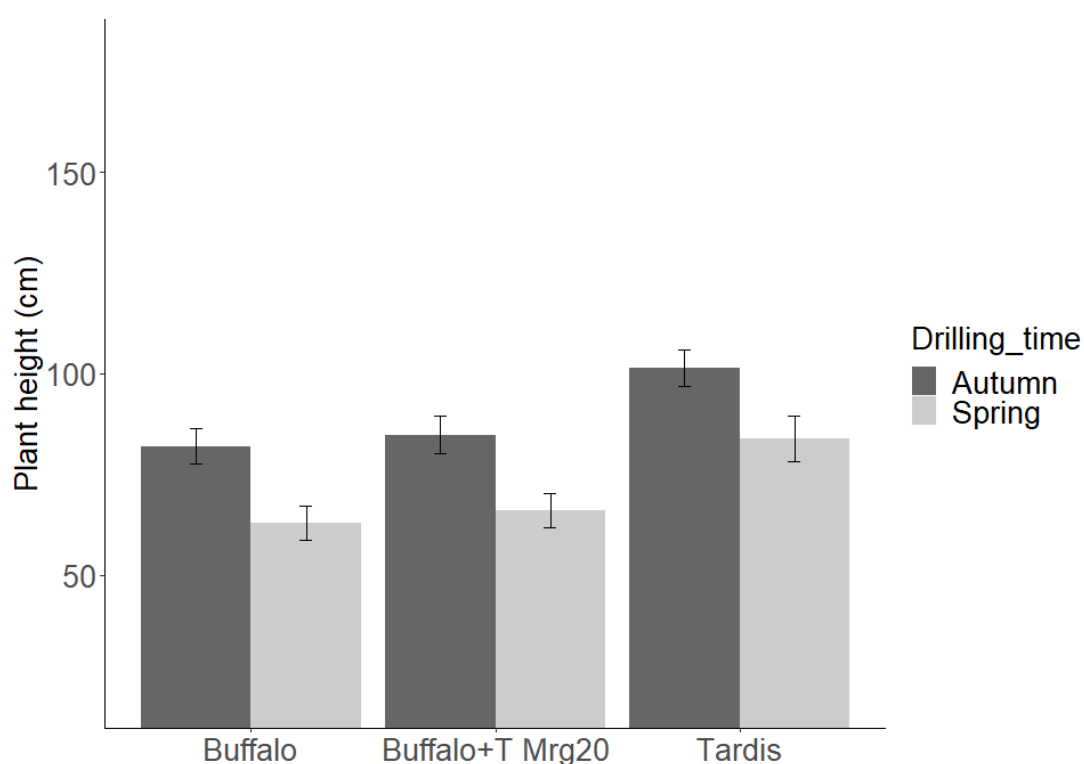


Figure 3.5: Plant height of Buffalo, Buffalo+T *Mrg20* and Tardis grown in autumn and spring. Results from four years of autumn and spring sown field experiments (2017-2020). The error bars represent one standard error of the mean.

Table 3.10: Contrast analysis comparing the heights of the parent line Buffalo against Buffalo + T Mrg20. Cohen's D is included as a measure of effect size, N is the sample number.

Contrast	Estimate (cm) (difference between contrasted values)	N	P value	Cohen's D
Autumn: Buffalo vs Buffalo + T Mrg20	2.8	16	0.2049	0.11
Spring: Buffalo vs Buffalo + T Mrg20	3.0	16	0.0536	0.13

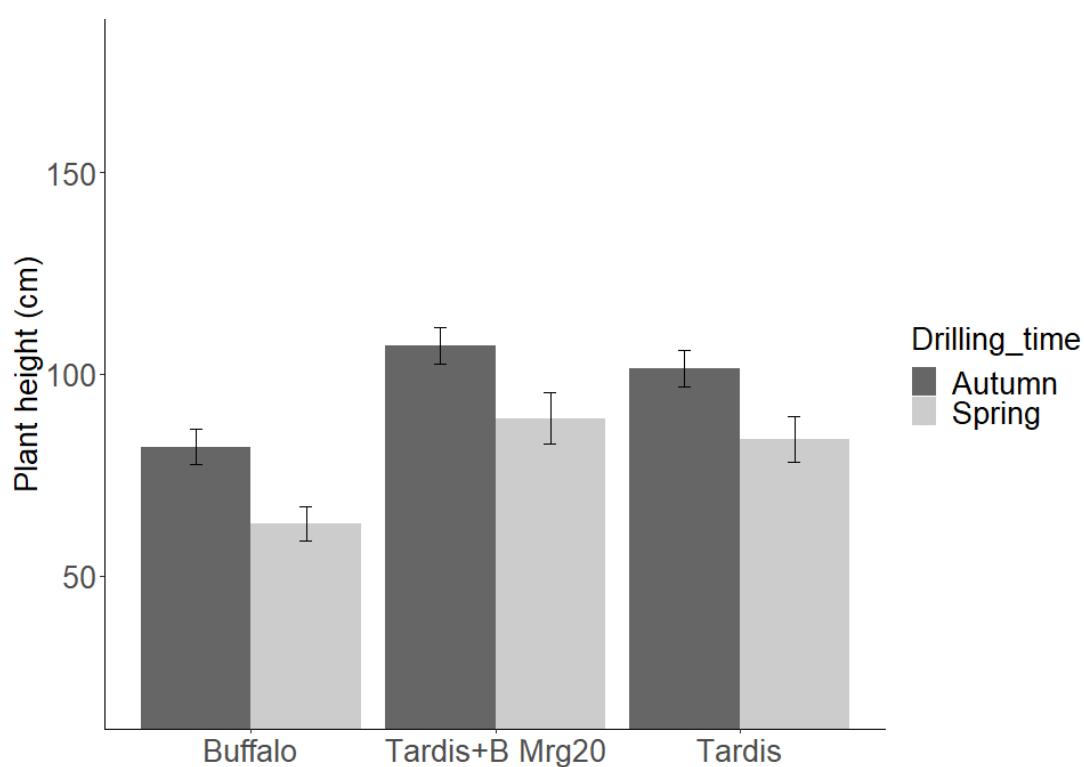


Figure 3.6: Plant height of Buffalo, Tardis + B Mrg20 and Tardis grown in autumn and spring. Results from four years of autumn and spring sown field experiments (2017-2020). The error bars represent one standard error of the mean.

Table 3.11: Contrast analysis comparing the heights of the parent line Tardis against Tardis + B Mrg20. Cohen's D is included as a measure of effect size, N is the sample number.

Contrast	Estimate (cm) (difference between contrasted values)	N	P value	Cohen's D
Autumn: Tardis vs Tardis + B Mrg20	5.6	16	0.0122	0.23
Spring: Tardis vs Tardis + B Mrg20	5.18	16	0.0011	0.16

3.3.1.4. Mrg11

The Mrg11 QTL was identified by Stančić (2016) as inferring resistance to the accumulation of HT2+T2 and F. *langsethiae* DNA without any association with the timing of panicle emergence or plant height. As seen in Table 3.1 four genotypes contributed to the Buffalo + T Mrg11 collection of genotypes giving the large value of N in Table 3.12.

Figure 3.7 and Table 3.12 show that the height of the Buffalo + T Mrg11 lines were not significantly different to the Buffalo parent line; the small error bars for the Buffalo + T Mrg11 columns are a result of the high value of N for the group.

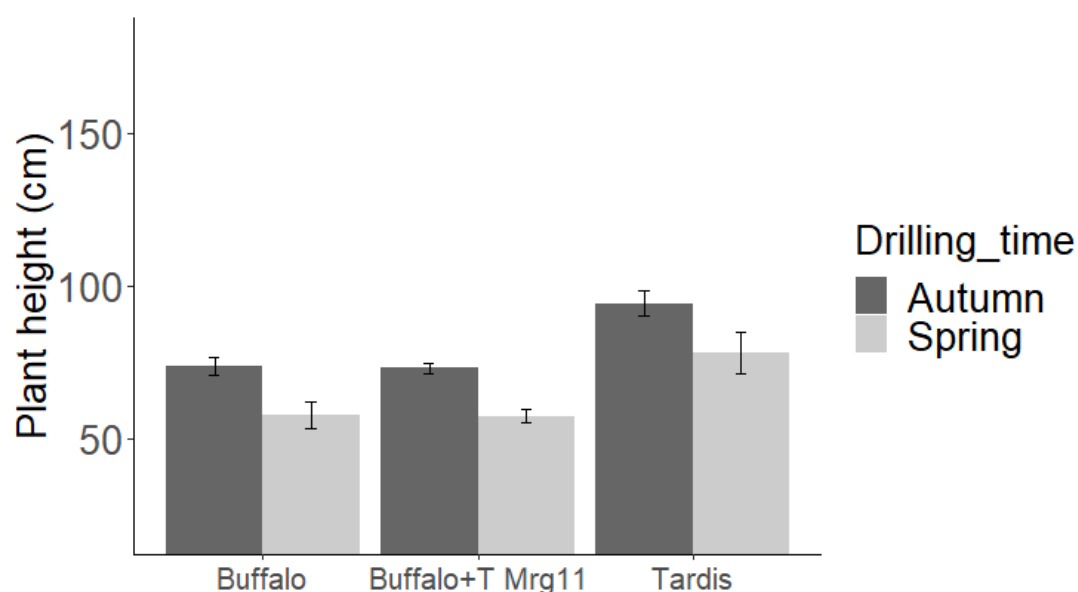


Figure 3.7: Plant height of Buffalo, Buffalo + T Mrg11 and Tardis grown in autumn and spring. Results from three years of autumn and spring sown field experiments (2018-2020). The error bars represent one standard error of the mean.

Table 3.12: Contrast analysis comparing the heights of the parent line Buffalo against Buffalo + T Mrg11. Cohen's D is included as a measure of effect size, N is the sample number.

Contrast	Estimate (cm) (difference between contrasted values)	N	P value	Cohen's D
Autumn: Buffalo vs Buffalo + T Mrg11	-0.59	48	0.8492	0.04
Spring: Buffalo vs Buffalo + T Mrg11	-0.31	48	0.9558	0.02

3.3.2. Panicle length related to height

The length of the panicle was calculated by deducting the height of the lowest whorl from the total plant height. Each data point below (Figure 3.8) represents an average of four values recorded for each plot. The regression of plant height versus panicle length was highly significant ($P < 0.001$) and the simple linear model explained 51% of the variation in panicle length. Once the origin of the Mrg04 QTL was entered into the regression model both the Mrg04 origin and the interaction between Mrg04 origin and plant height were statistically significant ($P < 0.001$). A model with non-parallel lines explained 74.1% of the variance (Figure 3.8). The parental origin of Mrg04 QTL accounted for 21.4% of the variation in panicle length and the interaction between plant height and the Mrg04 origin accounted for 1.2%. One outlier result was removed as the panicle length was calculated as over 50 cm long.

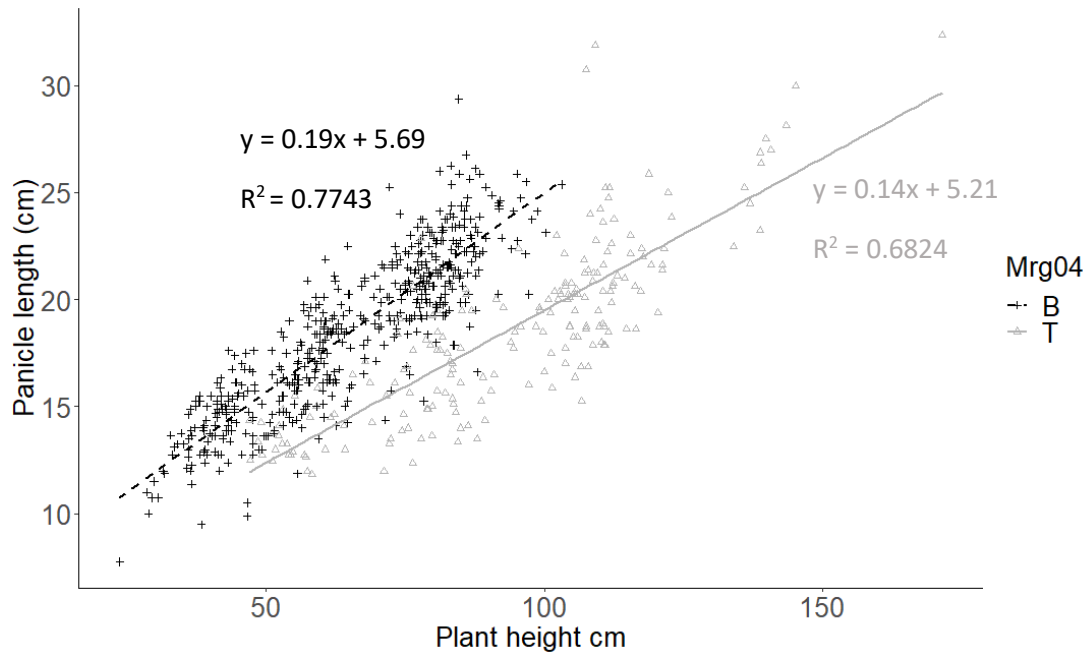


Figure 3.8: Panicle length plotted against plant height for genotypes that were present in 2018-2020. The lines represent the linear relationship between plant height and panicle length for plants with either Mrg04 from Buffalo (B) or Tardis (T). Equations and R^2 values are shown on the figure.

3.3.3. Panicle Extrusion

The degree to which the panicle was extruded was measured by deducting the flag leaf height from the ground from the height of the first whorl from the ground (these measurements were only undertaken in 2018, 2019, and 2020). A negative value indicates that some of the spikelets of the panicle remain within the flag leaf sheath whereas a positive value indicates the entire panicle is extruded free of the flag leaf sheath. A regression of height against the degree of panicle extrusion (length in cm) by the origin of the Mrg04 QTL showed that height accounted for 49.3% of the variation in the degree of panicle extrusion. The origin of the Mrg04 QTL accounted for a further 19.6% of the variation, and the interaction between height and the Mrg04 origin

accounted for a further 2.7%. All three terms were highly significant ($P < 0.001$). Figure 3.9 displays the model and the equations for each line.

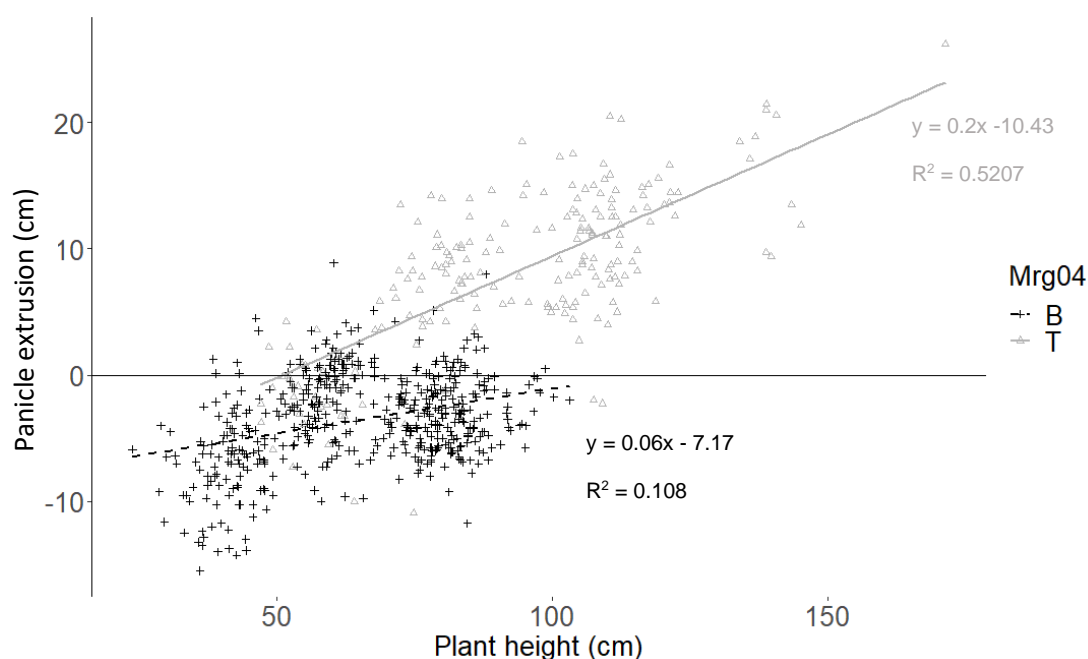


Figure 3.9: Panicle extrusion plotted against plant height for genotypes that were present in 2018-2020. The lines represent the linear relationship between plant height and panicle extrusion for plants with either Mrg04 from Buffalo (B) or Tardis (T). Equations and R^2 values are shown on the figure.

3.3.4. Flowering time

Panicle emergence was used as a proxy for flowering time as flowering in cereals and especially in oats can be difficult to assess in the field. The NIL population contained three QTL that influence flowering time: Mrg04, Mrg20 and Mrg21.

A linear model was generated to examine the impact of year, sowing season and genotype on the degree days to panicle emergence. The resulting model is detailed in Table 3.13. The factors were entered into the model in the order listed with year first. Sowing season had the largest impact on the degree days to panicle emergence followed by year, genotype had the least impact of the three factors.

Table 3.13: Output from the plant degree days linear model. Percentage variance is calculated based on the sums of square values for each factor and each combination of factors.

Factor	Degrees of freedom	P value	Percentage of variance accounted for (%)
Year	3	<0.001	14.4
Sowing season	1	<0.001	53.4
Genotype	18	<0.001	12.6
Year*sowing season	3	<0.001	10.9
Year*genotype	54	<0.001	0.7
Sowing season * Genotype	18	<0.001	5.4
Year*sowing season*genotype	54	0.02128	0.4

3.3.4.1. Mrg04

The Mrg04 QTL had an impact on flowering time as well as height but it was not dependant on sowing season. In Buffalo the flowering time in degree days is reduced when the Tardis Mrg04 QTL was introgressed in autumn and spring by 27.8 and 33.8 degree days respectively (Figure 3.10 and Table 3.14). The autumn change in degree days to panicle emergence was statistically significant ($P < 0.001$), as was the spring reduction ($P < 0.001$). Similar trends are seen when comparing Julian days to panicle emergence: the difference is between 2.5 and 3 days for either spring or autumn sown (Table 3.14).

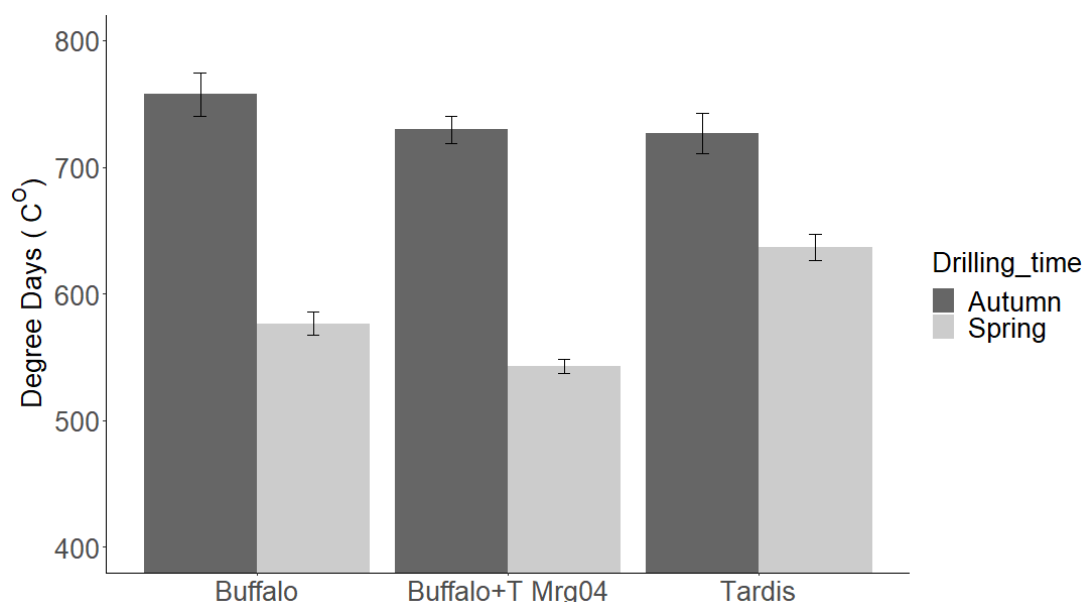


Figure 3.10: Degree days (5°C baseline) from sowing to panicle emergence for Buffalo+ T Mrg04, Buffalo, and Tardis. Results from four years of autumn and spring sown field experiments (2017-2020). Error bars represent the standard error of the mean.

The introgression of the Buffalo derived Mrg04 into the Tardis parent genome caused the resultant NIL to be later than either parent (Figure 3.11). Tardis + BMrg04 was later in spring and autumn sown plots in all years; the difference was particularly clear

in spring sown plots with a difference of 6 days or 79.8 degree days. The contrasts (Table 3.14) show that in autumn and spring sown plots the difference in panicle emergence were highly significant ($P < 0.0001$).

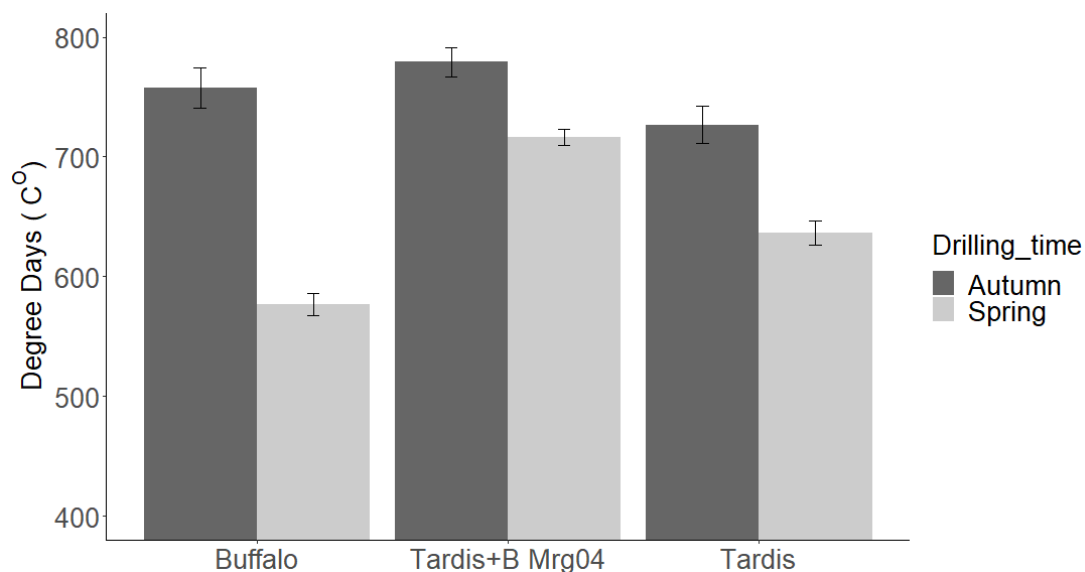


Figure 3.11: Degree days (5°C baseline) for Tardis + B Mrg04, Buffalo, and Tardis. Results from four years of autumn and spring sown field experiments (2017-2020). Error bars represent the standard error of the mean.

Table 3.14: Contrast analysis comparing degree days and Julian days of the parent line Buffalo with Buffalo + T Mrg04. Results are reported in accumulated degree days to panicle emergence and Julian days to panicle emergence. Cohen's D is included as a measure of effect size, N is the number of samples.

Contrast	N	Degree days			Julian Days to panicle emergence		
		Estimate (°C) (difference between contrasted values)	P value	Cohen's D	Estimate (days) (difference between contrasted values)	P value	Cohen's D
Autumn: Buffalo vs Buffalo + T Mrg04	32	-28.58	<0.001	0.26	-2.65	<0.001	0.44
Spring: Buffalo vs Buffalo + T Mrg04	32	-33.79	<0.001	0.58	-2.97	<0.001	0.24

Table 3.15: Contrast analysis comparing degree days and Julian days of the parent line Tardis and the Tardis + B Mrg04 NIL. Results are reported in accumulated degree days to panicle emergence and Julian days to panicle emergence. Cohen's D is included as a measure of effect size, N is the number of samples.

Contrast	N	Degree days			Julian days to panicle emergence		
		Estimate (difference between contrasted values)	P value	Cohen's D	Estimate (difference between contrasted values)	P value	Cohen's D
Autumn: Tardis vs Tardis + B Mrg04	32	52.4	<0.001	0.45	4.72	<0.001	0.77
Spring: Tardis vs Tardis + B Mrg04	32	79.79	<0.001	1.21	6.44	<0.001	0.58

3.3.4.2. Mrg21

Introgression of Tardis Mrg21 in Buffalo had little impact on flowering time in the autumn sown crops causing a non-significant ($P>0.05$) shift of the Buffalo + T Mrg21 line to flower 9.9 degree days or 0.88 days later than Buffalo (Figure 3.12 and Table 3.16). In spring, Buffalo + T Mrg21 is significantly later than Buffalo ($P<0.001$) by 94.5 degree days or 7.3 days. Contrastingly in Tardis the introgression of the Buffalo Mrg21 significantly ($P<0.001$) reduced the time to panicle emergence by 94 degree days or 7.6 days in spring sown plots, but again made only a small difference in autumn sown plots (20 degree days earlier, $P<0.001$) (Table 3.17). The Tardis + B Mrg21 NIL is later than either parent lines in autumn and spring sown plots (Figure 3.13). The Cohen's D values for spring Tardis + B Mrg21 contrasted against Tardis is 0.61, this constitutes a large effect size, whereas the autumn sown Tardis + B Mrg21 is only 0.26, a relatively small effect size.

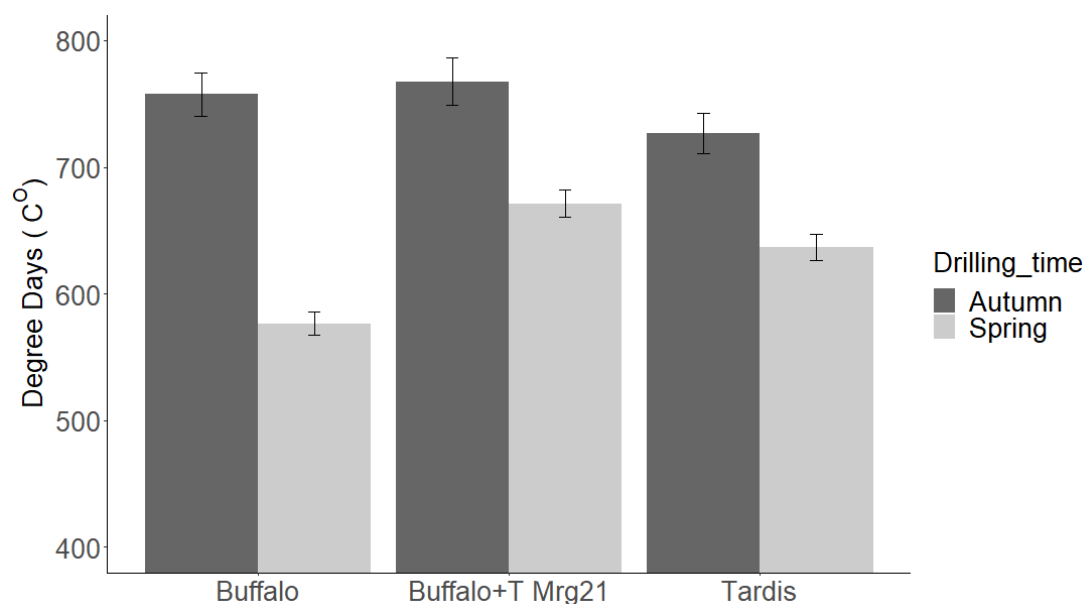


Figure 3.12: Degree days (5°C baseline) for Buffalo+ T Mrg21, Buffalo, and Tardis. Results from four years of autumn and spring sown field experiments (2017-2020). Error bars represent the standard error of the mean.

Table 3.16: Contrast analysis comparing degree days and Julian days of the parent line Buffalo to Buffalo+T Mrg21. Results are reported in accumulated degree days to panicle emergence and Julian days to panicle emergence. Cohen's D is included as a measure of effect size, N is the number of samples.

Contrast	N	Degree days			Julian Days to panicle emergence		
		Estimate (°C) (difference between contrasted values)	P value	Cohen's D	Estimate (days) (difference between contrasted values)	P value	Cohen's D
Autumn: Buffalo vs Buffalo + T Mrg21	16	9.9	0.0313	0.10	0.88	0.0234	0.21
Spring: Buffalo vs Buffalo + T Mrg21	16	94.46	<0.001	1.69	7.31	<0.001	0.75

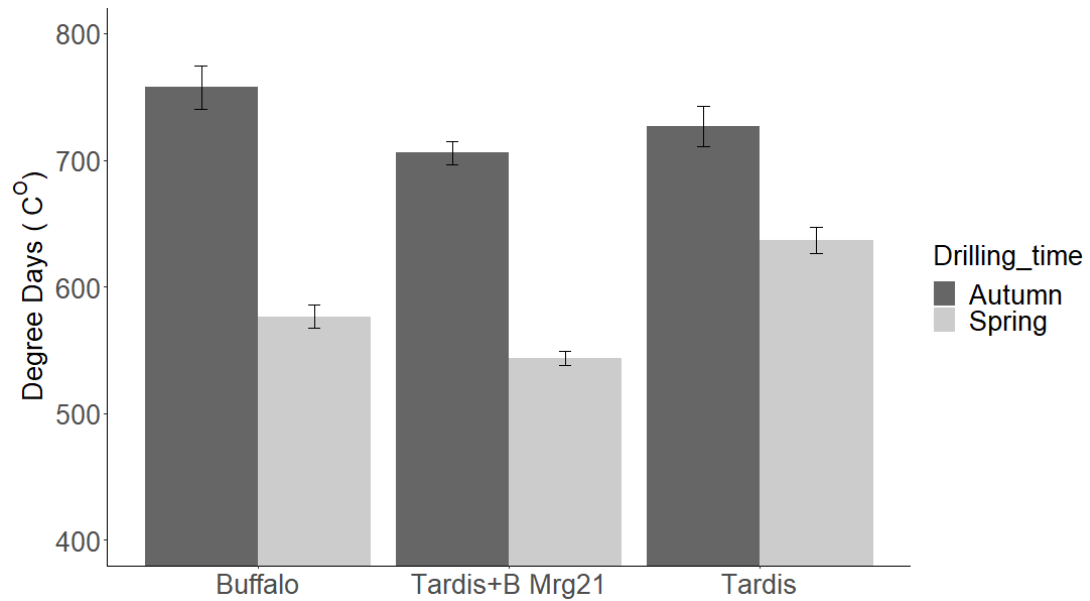


Figure 3.13: Degree days (5°C baseline) for Buffalo, Tardis+ B Mrg21. Results from four years of autumn and spring sown field experiments (2017-2020). Error bars represent the standard error of the mean.

Table 3.17: Contrast analysis comparing degree days and Julian days of the parent line Tardis with Tardis+B Mrg21. Results are reported in accumulated degree days to panicle emergence and Julian days to panicle emergence. Cohen's D is included as a measure of effect size.

Contrast	N	Degree days			Julian Days to panicle emergence		
		Estimate (°C) (difference between contrasted values)	P value	Cohen's D	Estimate (days) (difference between contrasted values)	P value	Cohen's D
Autumn: Tardis vs Tardis + B Mrg21	32	-20.9	<0.001	0.22	-1.84	<0.001	0.26
Spring: Tardis vs Tardis + B Mrg21	32	-94.46	<0.001	1.53	-7.44	<0.001	0.62

3.3.4.3. Mrg20

The Mrg20 QTL has a much lower impact on time to panicle emergence than Mrg04 or Mrg21 in either Buffalo or Tardis. Figure 3.14 and Figure 3.15 show Buffalo and Tardis contrasted against NIL with Mrg20 introgressed from the opposing parent sown in autumn and spring. The NIL lines act in almost exactly the same manner to the parent lines, not altering the time to panicle emergence based on degree days or Julian days in either autumn or spring. Table 3.18 and Table 3.19 show the precise figures by

which the NIL vary from their respective parents. It is only in the autumn sowing of the Tardis + B Mrg20 that a statistical difference is detected for degree days ($P=0.019$) and Julian days ($P=0.015$). The Buffalo Mrg20 introgression made the NIL later in autumn sowings. The Cohen's D value is low for both degree days and Julian days.

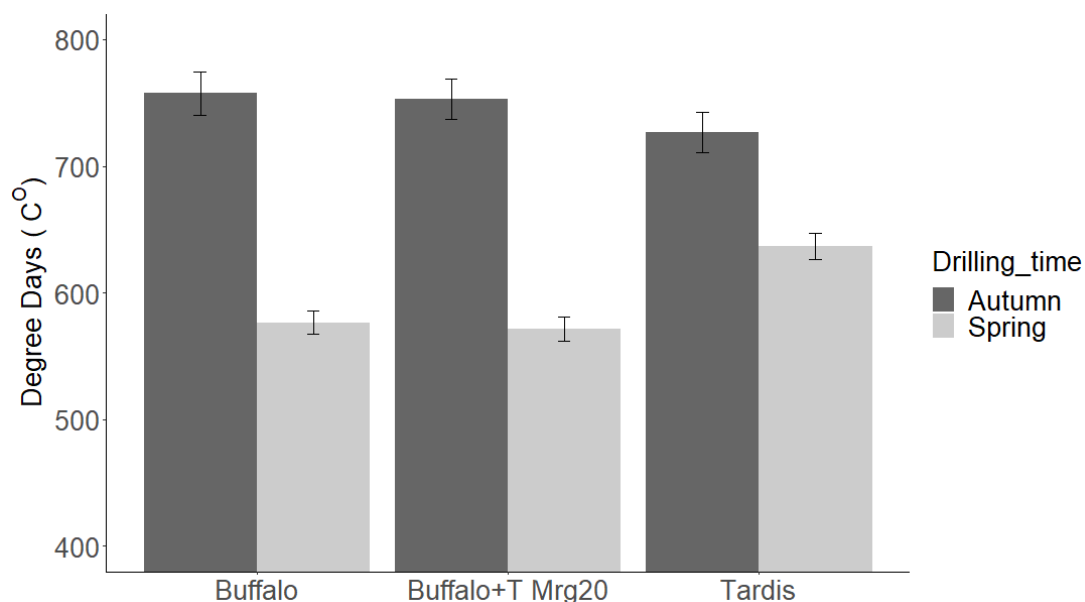


Figure 3.14: Degree days (5°C baseline) for Buffalo+ T Mrg20, Buffalo, and Tardis. Results from four years of autumn and spring sown field experiments (2017-2020). Error bars represent the standard error of the mean. Cohen's D is included as a measure of effect size and N is the number of samples.

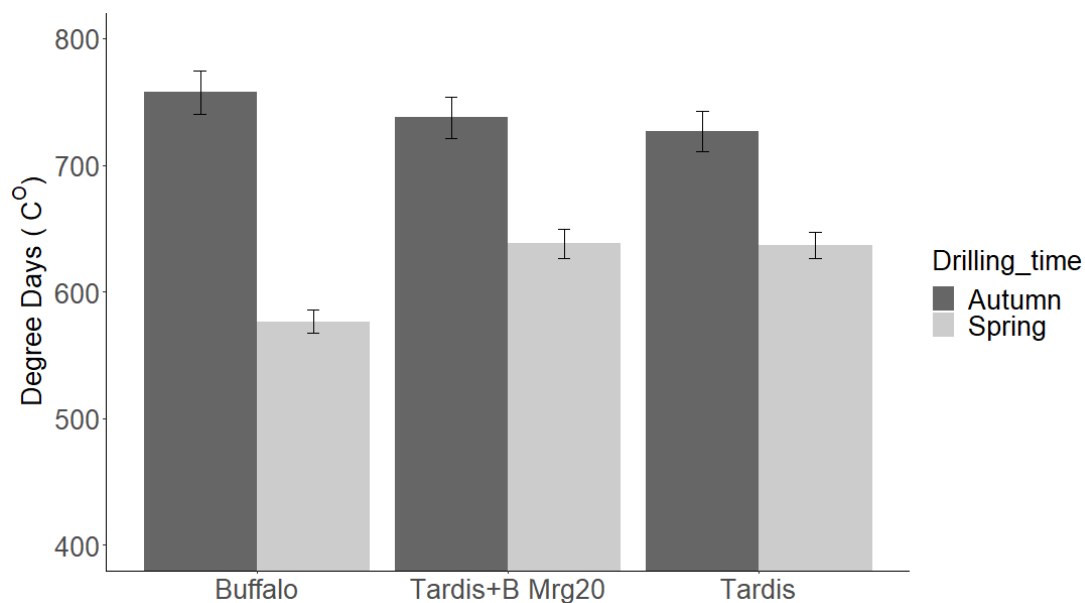


Figure 3.15: Degree days (5°C baseline) for Buffalo, Tardis + B Mrg20, and Tardis. Results from four years of autumn and spring sown field experiments (2017-2020). Error bars represent the standard error of the mean.

Table 3.18: Contrast analysis comparing degree days and Julian days of the parent line Buffalo to Buffalo + T Mrg20. Results are reported in accumulated degree days to panicle emergence and Julian days to panicle emergence.

Contrast	N	Degree days			Julian Days to panicle emergence		
		Estimate (°C) (difference between contrasted values)	P value	Cohen's D	Estimate (days) (difference between contrasted values)	P value	Cohen's D
Autumn: Tardis vs Tardis + B Mrg20	16	10.83	0.0188	0.12	0.94	0.0152	0.21
Spring: Tardis vs Tardis + B Mrg20	16	1.41	0.8390	0.02	0.06	0.9081	0.01

Table 3.19: Contrast analysis comparing degree days and Julian days of the parent line Tardis with Tardis + B Mrg20. Results are reported in accumulated degree days to panicle emergence and Julian days to panicle emergence. Cohen's D is included as a measure of effect size.

Contrast	N	Degree days			Julian Days to panicle emergence		
		Estimate (°C) (difference between contrasted values)	P value	Cohen's D	Estimate (days) (difference between contrasted values)	P value	Cohen's D
Autumn: Buffalo vs Buffalo + T Mrg20	16	-4.43	0.3343	0.05	-0.38	0.3291	0.09
Spring: Buffalo vs Buffalo + T Mrg20	16	-5.10	0.4619	0.1	-0.44	0.4196	0.04

3.3.4.4. Mrg11

The Mrg11 QTL did not have any significant effect ($P > 0.05$) on either the growing degree days to panicle emergence or Julian days to panicle emergence (Table 3.20). The numerical differences are small between Buffalo and Buffalo + T Mrg11 as can be seen in Figure 3.16.

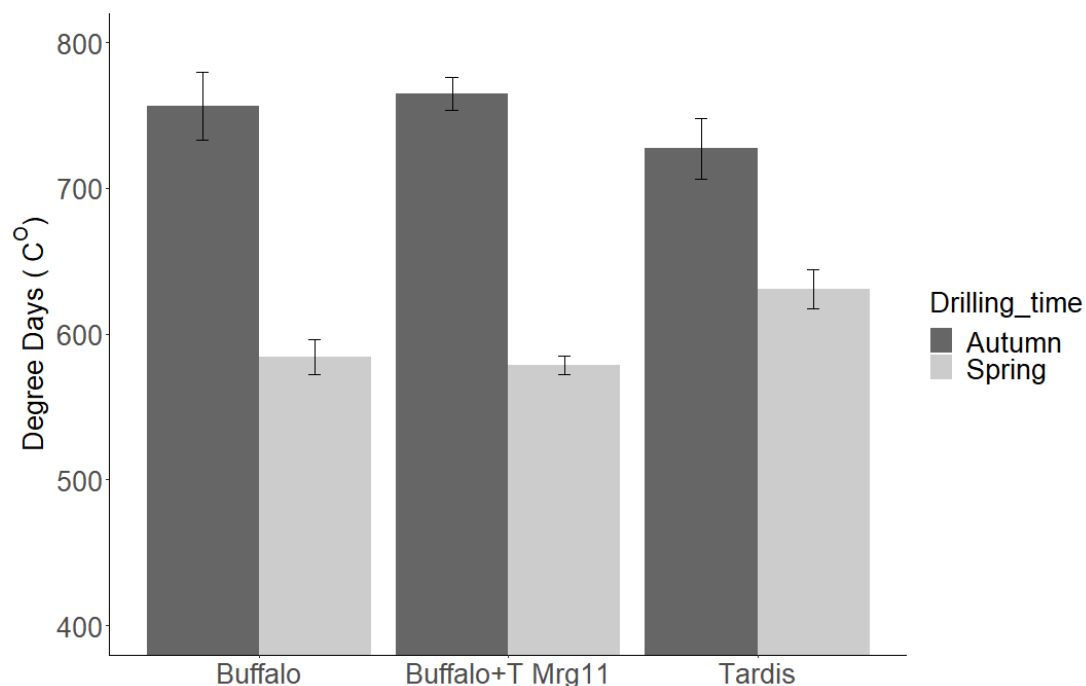


Figure 3.16: Degree days (5°C baseline for Buffalo, Buffalo + T Mrg11, and Tardis. Results from three years of autumn and spring sown field experiments (2018-2020). Error bars represent the standard error of the mean.

Table 3.20: Contrast analysis comparing degree days and Julian days of the parent line Buffalo to Buffalo + T Mrg11. Results are reported in accumulated degree days to panicle emergence and Julian days to panicle emergence. Cohen's D is included as a measure of effect size.

Contrast	N	Degree days			Julian Days to panicle emergence		
		Estimate (°C) (difference between contrasted values)	P value	Cohen's D	Estimate (days) (difference between contrasted values)	P value	Cohen's D
Autumn: Buffalo vs Buffalo + T Mrg11	48	8.65	0.7359	0.10	0.71	0.1535	0.21
Spring: Buffalo vs Buffalo + T Mrg11	48	-5.63	0.2679	0.12	-0.542	0.4942	0.07

3.4. Discussion

3.4.1. Pearson correlations

The Pearson correlation constants for comparisons across experiments were high for time to panicle emergence in degree days and plant height for both autumn and spring

sown experiments. The P values were all below 0.001 adding confidence that genotypes performed consistently across years within each sowing season. This also gives confidence that the different genotypes remained true throughout the four years of field experiments, without a high degree of crossing between genotypes. This consistency of phenotype between genotypes demonstrates that the traits of time to panicle emergence and plant height are heritable traits under genetic control.

3.4.2. *Height model*

For height, genotype explained 45.5% of the variation across all four years in autumn and spring sown experiments, year accounted for 26% of the variation and sowing time accounted for 11.4%. Most of the variation for time to panicle emergence was accounted for by sowing season, year and interactions between the two, however genotype accounted for 12.6% of the variation across all four years and sowing seasons. The interactions between year and genotype, sowing season and genotype, and year, sowing season and genotype contributed very little to the model in terms of variation accounted for. For both height and time to panicle emergence, the low impact of interaction terms involving year and genotype agrees with the strong correlations between genotypes from different years and further supports the assertion that both traits are under genetic control and are stable across different conditions introduced by different years.

Year introduced the most variation into the data likely as the weather in each growing season was different.

3.4.3. *Height Mrg04*

Mrg04 contains the dwarfing gene *Dw6* known to reduce the length of the upper three internodes (Milach *et al.*, 2002). Buffalo + T Mrg04 is significantly taller than the Buffalo parent by approximately 44 cm and 38 cm across autumn and spring sowing seasons respectively and is also significantly taller than the Tardis parent.

However, two NILs exist that carry the Tardis Mrg04 QTL in the Buffalo background. The 2012-125/1/27 was statistically shorter than 2012-139/6/25 by 25 cm on average across drilling seasons. The two NILs were identical except that 2012-125/1/27 has a deletion on Mrg18 and Tardis alleles at Mrg03 (Howarth, 2020. Pers Comm. (Dr C. Howarth is a Reader in plant breeding at Aberystwyth University)) either of which could impact on 2012-125/1/27's height, the NIL was still statistically taller than Tardis by 8 cm across drilling seasons.

3.4.4. *Panicle length and panicle extrusion*

As further described below, there was a significant relationship between panicle length and plant height. This in accordance with Yan *et al.* (2021) who found that plant height

was strongly linked to panicle length. The germplasm examined in this study had a range of heights however height was controlled genetically meaning that it is difficult to attribute the change in panicle length solely to height as genetic linkage or pleiotropy could be influencing the panicle length. The multiple linear model in which plant height accounted for 51% of the variation in panicle length also identified that the Mrg04 QTL origin of the NILs had a significant effect on panicle length and that the interaction between plant height and the Mrg04 QTL origin was significant. Yan *et al.* (2021) also saw a significant difference in panicle length depending on the presence of the *Dw6* gene. Germplasm with a Buffalo derived Mrg04 generally had longer panicles relative to their height than those with a Tardis derived Mrg04. The average difference between panicle lengths for genotypes grouped on the basis of their Mrg04 QTL was 0.5 cm, the measurements made on the plants were only recorded to an accuracy of 0.5 cm. Due to the large sample size generated by the multiple experiments across years statistically significant differences are found between genotypes differing for the other QTL even when those differences are smaller than 0.5 cm. However, when the other QTL were examined in the same manner by entering them into the model in the same position none accounted for such a high proportion of the variation.

The Buffalo parent mostly did not fully extrude whereas Tardis parent plants fully extruded, although there were instances of both either fully extruding or not fully extruding. Whether a plant did or did not fully extrude was related to height. The relationship with height was dependant on the parental origin of the QTL Mrg04: those NIL possessing the Tardis derived Mrg04 extruded further per unit of plant height than those possessing the Buffalo derived Mrg04. During research on the *Dw6* gene Yan *et al.* (2021) did not measure the degree to which panicle were extruded. The nature of the *Dw6* dwarfing gene located on the Mrg04 QTL is likely the driver for the incomplete panicle extrusion phenotype through the reduction of the length of the upper three internodes (Milach and Federizzi *et al.*, 2001); however, it is interesting to note that the panicle is in fact longer per unit of height of the plant when it possesses the *Dw6* gene.

3.4.5. Mrg04

3.4.5.1. Flowering time

Before year was taken into account by including it in the linear model, the Mrg04 QTL did not significantly change the degree days to panicle emergence when introgressed into the Buffalo background but the Buffalo +T Mrg04 panicles emerged ~30 degree days later. However, when the same model was run with year accounted for, the differences in spring and autumn drilled plots became significant. Plots were consistent in flowering time within each year for each genotype, the overall range ignoring year was considerably higher. Considering the scale on which the time to

panicle emergence was growing degree days and therefore accounted for air temperature, the variation within year must have come from other factors including drilling date, soil temperature, soil moisture, sunlight hours, disease and nutrient availability. Marshall *et al.* (2015) reported that the Mrg04 (then reported as LG17) flowering time QTL only expressed in autumn sown plants and not spring sown. Results in this report suggest that the QTL does express in spring sown plants. In the Tardis + B Mrg04 NIL the growing degree days to panicle emergence and Julian days were higher in the spring sown than the autumn sown plants.

Accumulated day degrees are a useful measure for the growth and development of plants. However, given that oats are long day plants and the day length/night length required for the genotypes studied in this work to switch to reproductive growth is unknown, and potentially altered by the presence of certain QTL controlling the requirement for vernalisation, exclusively using day degrees for autumn sown crops results in overly high accumulated degree days values as degree days are accumulated prior to the switch to reproductive growth. Days to panicle emergence as a measure also leads to high values for the winter sown plants compared to the spring sown. Ideally an earlier growth stage could be examined to record as closely as possible the change at the apex and the initiation of reproductive growth, stem extension (GS 30). The data available from this study is only the date of panicle emergence, sowing date and weather data. If the growth rate from reproductive growth initiation to panicle emergence is constant across all genotypes then days to panicle emergence or accumulated day degrees is adequate. Julian days remove days of growth in the months leading to the new year (October, November and December) all of which constitute vegetative growth for the autumn sown plots but adds between three and four months to the spring crop's Julian days to panicle emergence, during which the crop is not planted. All these differences are important as in days from drilling to panicle emergence and Julian days the differences in days between panicle emergence are the same as measured by days but those differences are smaller or larger relative to the growth time of the plants depending on whether that growth time has been measured in days from sowing to panicle emergence or Julian days.

3.4.5.2. Degree days and 2018

2018 was a hot summer and the spring crop was drilled late due to the wet weather in late winter/early spring leaving the field site too wet to travel on. Late sown spring plots reached panicle emergence later in the summer than in other years, as such the degree days calculated for the spring sown plots exceeded the autumn sown plots in the 2018 experiment for some genotypes. For example, the panicles of Tardis + B Mrg04 emerged late in spring compared to the parent Tardis, as such and in

combination with the late sowing of 2018 the spring sown plants were exposed to and accumulated greater degree days from the higher temperatures and longer days in late June and early July before panicles had emerged giving those NIL higher accumulated degree days in spring than in autumn.

Given that most oats are long day plants (Holland *et al.*, 2002) their flowering will likely have been triggered by shorter nights, it is unsurprising that there is not a great deal of difference in degree days or days from planting in terms of differentiating the NIL from one another. Neither parent line nor the subsequent NIL required a vernalisation period to flower.

3.4.6. *Mrg21*

3.4.6.1. *Flowering*

The presence of the Tardis *Mrg21* in the Buffalo background genome increased the growing degree days and Julian days to panicle emergence in autumn sown plots; 9.9 growing days degrees and 0.88 Julian days to panicle emergence respectively. These differences were detected as significant in this experiment even given the small relative difference (Cohen's $D = 0.21$). The estimated difference in autumn sown plants was close to one day, such a difference is useful in QTL stacking. The activity of *Mrg21* was much increased in spring sown plots increasing the degree days and Julian days to panicle emergence significantly by 94.5 growing degrees days and 7.3 Julian days to panicle emergence respectively, with a Cohen's D score of 0.75.

The Tardis derived *Mrg21* in the Buffalo background increased the days and degree days to panicle emergence of Buffalo + T *Mrg21* in spring sown plots, whereas Tardis + B *Mrg21* spring sown plants took significantly fewer degree days and Julian days; -94 and -7.44 respectively for the panicle to emerge. The effect size described as the Cohen's D score was 0.62, similar to that of the Tardis *Mrg21* in the Buffalo background. The *Mrg21* position has a strong influence on time to panicle emergence and therefore time to flowering. It is possible that the Tardis derived *Mrg21* increases the time to panicle emergence when the plant has not had a vernalisation period. The dependence on drilling time could be the result of vernalisation influencing the expression of genes within the *Mrg21* QTL.

3.4.6.2. *Height*

The estimated height difference between Buffalo and Buffalo + T *Mrg21* was 0.4 cm not constituting a significant difference in autumn. For spring sowing a larger difference was found (3.3 cm) this was significantly different even with a small Cohen's D value (0.13). Such a small difference on its own is likely not useful however that it is reliable enough to be detected makes it worth accounting for in QTL stacking.

For Tardis and Tardis + B Mrg21 the height difference was statistically different at 6.4 cm in autumn sown plants and 4.1 cm in the spring sown plants. These differences were statistically significant and as such could be used in QTL stacking for height control albeit with small effect sizes with Cohen's D values between 0.2 and 0.1 respectively.

3.4.7. *Mrg20*

3.4.7.1. *Height*

In terms of height Mrg20 did not have a significant effect in either spring or autumn sowings in the Tardis Mrg20 introgression into the Buffalo background. Only small differences in height were seen.

The difference between Tardis and Tardis + B Mrg20 in autumn sown plants as expressed as a Cohen's D value was 0.23 and the contrast between the two lines was statistically significant. The difference in spring sown plants was also significant although the Cohen's D value was smaller (0.16). Such height differences associated with QTL could be used to stack QTL to develop taller plants although again the magnitudes of the differences were small.

3.4.7.2. *Flowering*

In terms of time to panicle emergence the Mrg20 QTL had minimal impact in either introgressions examined. Buffalo + T Mrg20 was 4.4 growing degree days earlier than Buffalo in autumn plots and 5.1 growing degree days earlier in spring plots, neither of which were significant. The Tardis + B Mrg20 NIL was statistically significantly different in the autumn sowing, with a difference of ~10 degree days and almost one day later with the introgression of the Buffalo Mrg20 into the Tardis background. A shift of almost one day is significant agronomically especially if the QTL can be stacked with others to produce a later flowering plant.

3.4.8. *Mrg11*

The differences in flowering time were non-significant with small effect sizes for the Tardis Mrg11 introgressed into the Buffalo background. There was not a corresponding NIL available to observe the impact of the Buffalo Mrg11 introgressed into the Tardis background. The impact on height was negligible and not statistically significant. Mrg11's lack of impact on height and flowering time is consistent with Stančić (2016) findings.

3.4.9. *Conclusions*

Although oats are long day plants initiating flowering only after the night-time period falls below a critical length (Locatelli *et al.*, 2008; Holland *et al.*, 2002), there is variation between genotypes in their response to photoperiod including some day length

insensitive genotypes (Sampson and Burrows, 1972). Other factors such as vernalisation can influence flowering time (Sampson and Burrows, 1972). Flowering in wheat and barley can be accelerated by exposure to temperatures between 0°C and 10°C for approximately two weeks (Locatelli *et al.*, 2008). The response can be relative to the length of time the plant is exposed to the cold. The earliness of oats is important in adapting plants to different environments and maximising yields through making full use of the growing season. The Mrg21 QTL has been associated with the *Vrn1* gene (Zimmer *et al.*, 2021). In temperate cereals the *Vrn1* gene is induced through low temperatures (vernalisation period) and the resultant protein binds to the promotor region of the *Vrn2* gene reducing its expression. The *Vrn2* gene downregulates the *Vrn3* gene the upregulation of which promotes flowering in the presence of long days (Shrestha *et al.*, 2014; Brambilla *et al.*, 2017). The increase in the time to panicle emergence when the Tardis Mrg21 was introgressed into the Buffalo background in spring sown plots suggests that the lack of a vernalization period made the NIL less sensitive to the lengthening days of spring. Whereas the reduction in the time to panicle emergence of the Tardis + B Mrg21 spring sown plots compared to Tardis spring sown plots suggests that the introgression of the Buffalo Mrg21 reduced or removed the requirement for a vernalization period to promote flowering. The Buffalo parent reaches panicle emergence faster than Tardis in spring sown plots, potentially this is caused by Mrg21 containing *Vrn1* alleles in the Tardis parent that require a vernalisation period to be upregulated. Such upregulation of the *Vrn1* gene is not achieved in spring sowings.

Mrg20 has been associated with heading date and frost tolerance (Tumino *et al.*, 2016) and an ortholog of the *Vrn1* gene was mapped to the Mrg20 QTL (Klos *et al.*, cited Nava *et al.* 2012). However, in this work introgressing either Tardis or Buffalo Mrg20 QTL into the opposing parental background genomes had minimal impact of on the time to panicle emergence for spring or autumn sowing. Potentially for this locus very little variation exist between the two parents of the population examined within this study

This work supports the findings of Stančić (2016) that Mrg11 has no impact on either height or flowering time, although it was not possible to examine the Buffalo allele in the Tardis background.

This work has demonstrated a relationship between panicle length and plant height in oats and shown that the relationship is influenced by the Mrg04 QTL, a similar relationship was seen in wheat by Heidari *et al.* (2012); QTLs associated with plant height were also coincident with peduncle length.

4. Chapter 4: Examination of genetic basis for resistance or susceptibility of winter oats (*Avena sativa*) to *Fusarium langsethiae*

4.1. Introduction

It has been demonstrated in previous experimental work (Edwards, 2007a; Edwards, 2009; Edwards, 2015; and Edwards, 2017) that cultivar and therefore the genetics of the crop have an impact on the concentration of HT2+T2 in the grain of *F. langsethiae* infected crops. Furthermore, the difference between spring and autumn sowings in terms of HT2+T2 grain concentrations has been shown to be genetic rather than a result of the different sowing timings (Stančić, 2016). Very few studies have been published on the genetic basis of the resistance of oats to *F. langsethiae*. A great deal more research has been conducted on wheat and its resistance to Fusarium head blight (Hilton *et al.*, 1999; Draeger *et al.*, 2007; He *et al.*, 2015; and Gosman *et al.*, 2009). Varietal resistance to *Fusarium* in wheat is known to be quantitative: it is influenced by multiple quantitative traits each inferring onto the plant some small resistance or susceptibility to the pathogen (Parry *et al.*, 1995). A quantitative trait is one that shows a continuous variation and is encoded for by multiple genes (polygenic). The expression of quantitative traits can be influenced cumulatively, through epistatic interactions, by dominance and recessive relationships between alleles and through environmental effects.

In MAS, identifying molecular markers present in germplasm associated with traits of interest is a decision aid for selecting lines for crossing and continuation in breeding programmes. The marker can be observed at any stage in the plants' development and is not influenced by environmental conditions such as the presence or absence of a disease. For a pathogen such as *F. langsethiae* which is difficult to observe in the field, to have QTL already associated with resistance would enable those QTL to be consistently selected for in breeding programmes without the presence of the pathogen. QTL of varying effect size can also be stacked together to generate resistant plants. Plants with multiple QTL inferring resistance via different mechanisms are likely to remain resistant for longer as multiple quantitative traits apply a wider range of selection pressures for the pathogen to overcome. This differs from single gene resistance that can fail within a growing season should a new race of pathogen develop that can overcome it.

When using collections of genotypes with low variation in the traits of interest, observing and identifying differences can be difficult; Bjørnstad *et al.* (2017) suggested that in the case of *Fusarium* resistance, including very susceptible varieties made it easier to identify resistant traits. In the Buffalo Tardis mapping population, Buffalo is

the susceptible variety and its inclusion in the mapping population allows introgressed Tardis traits to be evaluated against a susceptible background. Buffalo is a dwarf oat with a mean straw length of 97 cm in official trials (HGCA, 2005) whereas Tardis is a conventional height oat with a mean straw length of 115cm (HGCA, 2013).

Stančić (2016) used a microsatellite annotated mapping population of recombinant inbred lines (RIL) derived from a Buffalo Tardis cross to conduct an association analysis examining *F. langsethiae* DNA and HT2+T2 concentration in the harvested oat grain. QTL for DNA and HT2+T2 were identified on the same linkage groups. QTL associated with *F. langsethiae* DNA and HT2+T2 frequently co-localised with height and flowering time. The linkage group Mrg04 on chromosome 18D contained markers associated with height, flowering time, *F. langsethiae* DNA and HT2+T2. The *Dw6* dwarfing gene has previously been mapped to this linkage group (Chaffin *et al.*, 2016). A further linkage group identified was associated with *F. langsethiae* DNA, HT2+T2 and flowering time but not height (Mrg20). Lastly a QTL was identified that was only associated with *F. langsethiae* DNA and HT2+T2 and not with either height or flowering time (Mrg11). This last QTL could allow for a breeding decision to be made to retain or gain some resistance to *F. langsethiae* without an associated change in flowering time or height.

This work aims to use an experimental field managed to have a high risk for *F. langsethiae* infection to screen near isogenic lines (NIL) as described in chapter 3, selected for their possession of alleles at QTL associated with height and earliness traits and for resistance/susceptibility to HT2+T2 accumulation in unprocessed grain. Results will further allow inspection of height and earliness as resistance traits themselves. Previous work on UK oats has shown dwarf varieties to accumulate higher concentrations of HT2+T2 (Edwards, 2007a; Edwards *et al.*, 2012b; Edwards, 2015). Such observations are not sufficient on their own to prove a link between height and susceptibility because of other morphological and molecular differences that coincide with shorter plants, due to genetic linkage or pleiotropy. Earliness of flowering time has previously been associated with resistance or susceptibility (Loskutov *et al.*, 2016; Hautsalo *et al.*, 2020) in oats to *Fusarium* species, but with conflicting results.

4.1.1.1. Objectives

To determine if height in itself influences the resistance of the plants to HT2+T2 accumulation in the harvested grain or if resistance occurs in the presence of QTL determining height due to linkage or pleiotropy.

To determine if the degree of panicle extrusion in itself influences the resistance of the plants to HT2+T2 accumulation in the harvested grain or if resistance occurs in the presence of QTL determining panicle extrusion due to linkage or pleiotropy.

To understand if earliness in itself influences the resistance of the plants to the accumulation of HT2+T2 accumulation in the grain or if resistance occurs in the presence of QTL determining earliness due to linkage or pleiotropy.

To understand the impact of introgressing QTL from either parent into the opposing parent on HT2+T2 concentration in the harvested oat grain under natural infection.

4.1.1.2. Null hypothesis

The HT2+T2 concentration in the harvested grain is not related to the height of the original crop.

The HT2+T2 concentration in the harvested grain is not related to the extent of panicle extrusion of the original plant

The HT2+T2 concentration in the harvested grain is not related to the earliness of the original plant

The introgression of Mrg04 between Buffalo into Tardis has no impact on the accumulation of HT2+T2 in the resultant NIL.

The introgression of Mrg20 between Buffalo into Tardis has no impact on the accumulation of HT2+T2 in the resultant NIL.

The introgression of Mrg21 between Buffalo into Tardis has no impact on the accumulation of HT2+T2 in the resultant NIL.

The introgression of Mrg11 between Buffalo into Tardis has no impact on the accumulation of HT2+T2 in the resultant NIL.

4.2. Methodology

4.2.1. Experimental Design and Environment

The same experimental plots from Chapter 3 were used for data collection for HT2+T2 quantification (Table 3.1). The site on which the experiments were conducted was maintained in an alternating wheat and oat rotation with only shallow non-inversion tillage from 2010. Straw was chopped and returned onto the field and the next crop was sown into the previous crop residue, meaning that as plants emerged, they were in contact with the previous crop residue, as can be seen in Figure 4.1 a. In the 2019 and 2020 experiments it was necessary to plough the field prior to drilling for weed control. In these two years straw from the previous wheat crop was collected and distributed back onto the plots once they were sown (Figure 4.1 b).

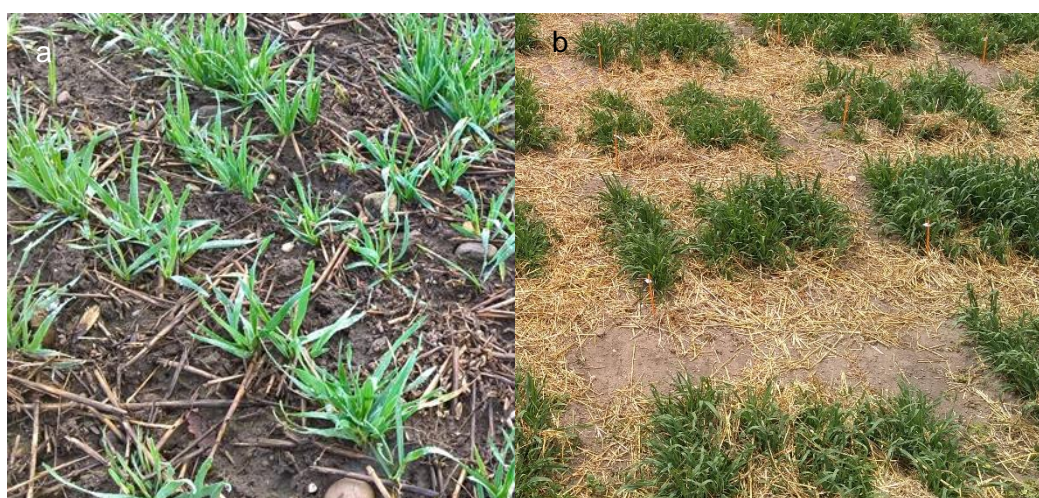


Figure 4.1: a Crop debris from the previous wheat crop visible amongst young oat plants. b Wheat straw distributed in between plants after sowing.

4.2.2. Harvest and Sampling

Plots were combined using a Winterstieger nursery master combine; the combine was allowed to thresh the plot sample entirely before moving to the next plot. Due to poor weather conditions at harvest in 2020 the spring sown plots were harvested by hand and threshed later after drying in cotton bags in a glass house for two weeks to below 12% moisture. A ~200 g sample of grain was milled using a ZM200 centrifugal laboratory mill (Retsch, Leeds, England) using a 1 mm sieve. Milled samples were used for HT2+T2 extraction and analysis as described in Chapter 2.

4.2.3. Statistical analysis

Multiple linear regressions were run to examine the impact of height, panicle extrusion, and three measures of time to panicle emergence. As panicle extrusion can be described as either partially extruded or fully extruded, a one-way ANOVA was used to compare those plots that were fully extruded to those that were only partially extruded. A boxplot was used to present the data.

Contrast analysis was used to contrast the parent and NIL with one another. The lsmeans package in R version 4.0.4 (R Core Team, 2020) was used to generate reference grids with which to apply the contrasts within simple linear models. The linear models within which contrasts were performed were run by year as the variation was variable across years. All data was Log10 transformed to achieve Gaussian distributions. Linear models were generated using the lm() function from which ANOVA tables were generated using the anova() function.

4.3. Results

4.3.1. Summary results for the field experiments

There were large differences between the years for the HT2+T2 concentrations in the harvested grain (Figure 4.2). In the multiple linear models detailed below the models accounted for 70-74% of the variance in HT2+T2 concentration with year being by far the strongest factor accounting for 51-60% of the total variance (73-82% of the explained variance). The season (autumn or spring) in which the NIL experiments were sown also had little impact on the average HT2+T2 concentration when averaged across all genotypes for each harvest year (Figure 4.2). In 2019 and 2020 the experiments were sown after ploughing, a simple ANOVA demonstrates the difference between these two years and 2017 and 2018 to be significant ($P < 0.001$). However, year and ploughing are confounded so it is not possible to determine which of these two factors is impacting HT2+T2 concentration.

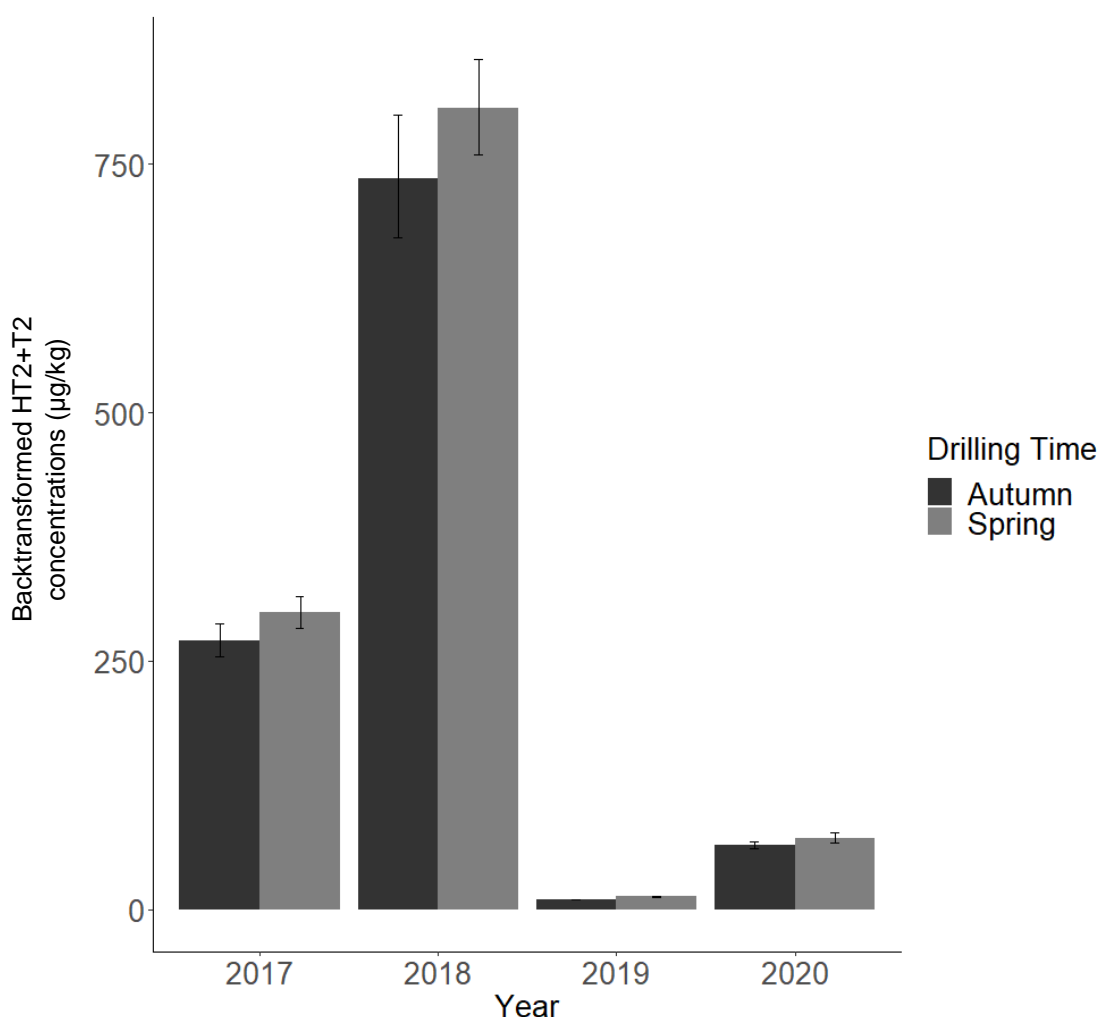


Figure 4.2: HT2+T2 average concentrations in the harvested oat grain from the NIL experiments for each sowing season in each harvest year. Error bars represent the standard error of the mean.

4.3.2. Plant height

Table 4.1 details the output of a multiple linear model examining HT2 +T2 and height along with year, and the parental origin of Mrg04. Figure 4.3 shows a scatter plot of log10 transformed HT2+T2 values against plant height. The shape of the data points represents the parental origin of the Mrg04 QTL and the colour represents the year. The four lines represent fitted values by year for plant height (cm) against the log10 transformed HT2+T2 concentrations. The model output from the multiple regression analysis shows that height was significant on its own, but only accounted for 6.1% of the variation in HT2+T2 concentration. Figure 4.3 shows that generally with increasing height, HT2+T2 concentrations decrease. The origin of the Mrg04 QTL accounted for 4.0% of the variation. The interaction terms in Table 4.1 are all significant: the Year * Mrg04 interaction accounts for the most variation (3.9%). In 2017 and 2018 plants possessing the Buffalo Mrg04 QTL had higher HT2+T2 concentrations with increasing height.

Table 4.1: Output from the plant height model showing the significance and the percentage variance accounted for by each factor in the model as well as their interactions.

Factor	DF	Sum of squares	Mean sq	F value	P	% Variation accounted for
Year	3	136.6	136.6	576.4	<0.001	54.6
Height	1	15.3	15.3	191.4	<0.001	6.1
Mrg04	1	10.1	10.1	126.3	<0.001	4.0
Height*Year	3	3.3	1.1	13.9	<0.001	1.3
Year*Mrg04	3	9.8	3.2	41.1	<0.001	3.9
Height*Mrg04	1	2.5	2.5	31.8	<0.001	1
Year*Height*Mrg04	3	2.5	0.8	10.3	<0.001	1
Residual	876	70	0.08			

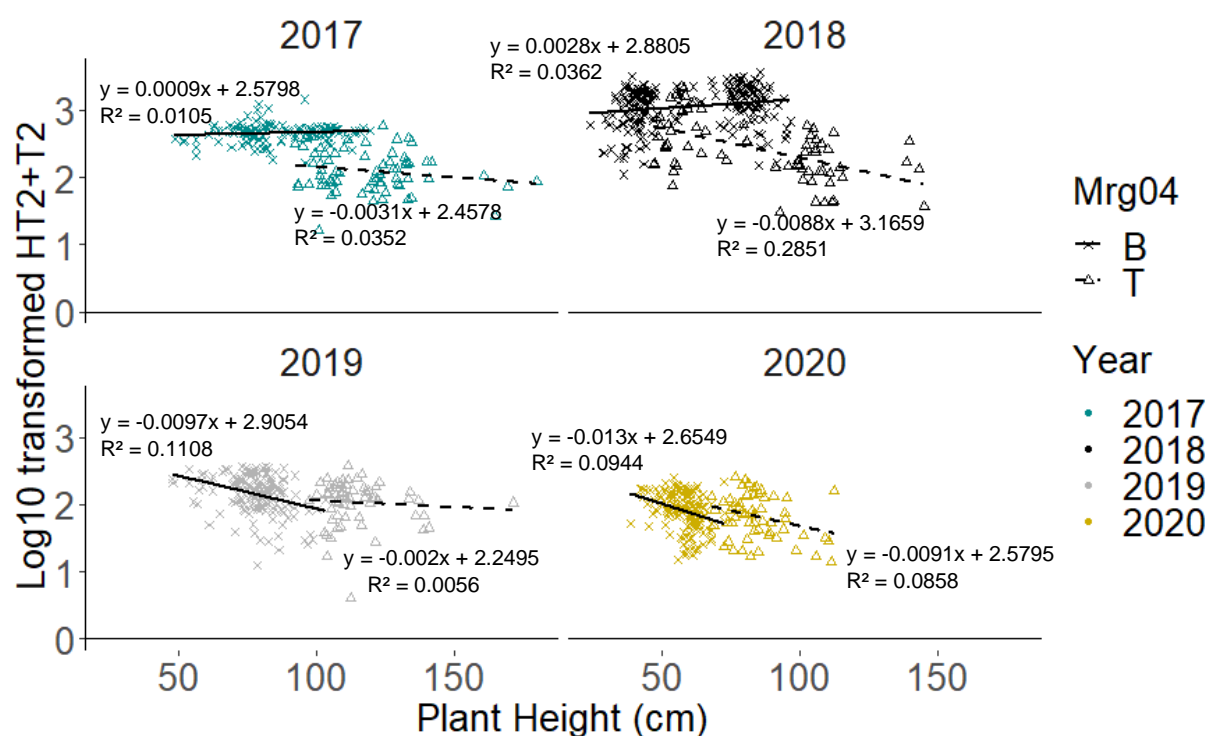


Figure 4.3: A graphical representation of the model presented in Table 4.1, plotting HT2+T2 concentration against plant height. The shape of the data points indicates the parental origin of the Mrg04 QTL, the colours indicate the different years described in the legend. Differently textured lines represent the fitted values according to year from the model described in Table 5.1.

4.3.3. Panicle Extrusion

Panicle extrusion was measured in 2018, 2019 and 2020: it is the distance between the flag leaf ligule and the first whorl of the tiller's panicle expressed as either a positive or negative value if the plant is fully extruded or partially extruded respectively. The concentration of HT2+T2 was modelled against the panicle extrusion value in addition

to year and the parental origin of Mrg04. In a comparative model to height, panicle extrusion accounted for approximately the same percentage variation as height (6.7%). The interaction between panicle extrusion and year was larger than between height and year (Table 4.1 and Table 4.2). Figure 4.4 shows a scatter graph of log₁₀ transformed HT₂+T₂ values against panicle extrusion. Generally, HT₂+T₂ concentrations are lower with increasing panicle extrusion. The parental origin of the Mrg04 QTL is represented in the graph by the shape of the data points and it should be noted that the plants with the Tardis alleles at the Mrg04 site are extruded to a greater degree as well as having lower HT₂+T₂ concentrations. Both the Mrg04 parental origin and the interaction of the parental origin of Mrg04 and panicle extrusion are significant but account for very little variation within the model (0.2% and 0.04% respectively). In Figure 4.4 it can be seen that the origin of the Mrg04 QTL causes the data points to form two distinct clusters.

Table 4.2: Output from multiple linear model based on panicle extrusion of the panicle showing the F value, statistical significance and percentage variance, accounted for by selected factors and interactions entered into the model.

Factor	DF	Sum of squares	Mean sq	F value	P value	% Variation accounted for
Year	2	136.6	68.3	793.6	<0.001	60.4
Panicle extrusion	1	15.1	15.1	175.9	<0.001	6.7
Mrg04 parental origin	1	0.4	0.4	4.1	0.04	0.2
Year*panicle extrusion	2	6.6	3.3	38.5	<0.001	2.9
Year*Mrg04 parental origin	2	5.3	2.6	30.6	<0.001	2.3
Panicle extrusion*Mrg04 parental origin	1	0.1	0.05	1.1	0.3	0.04
Year* Panicle extrusion*Mrg04 parental origin	2	3.5	1.7	20.3	<0.001	1.5
Residual	679	458.4	0.1			

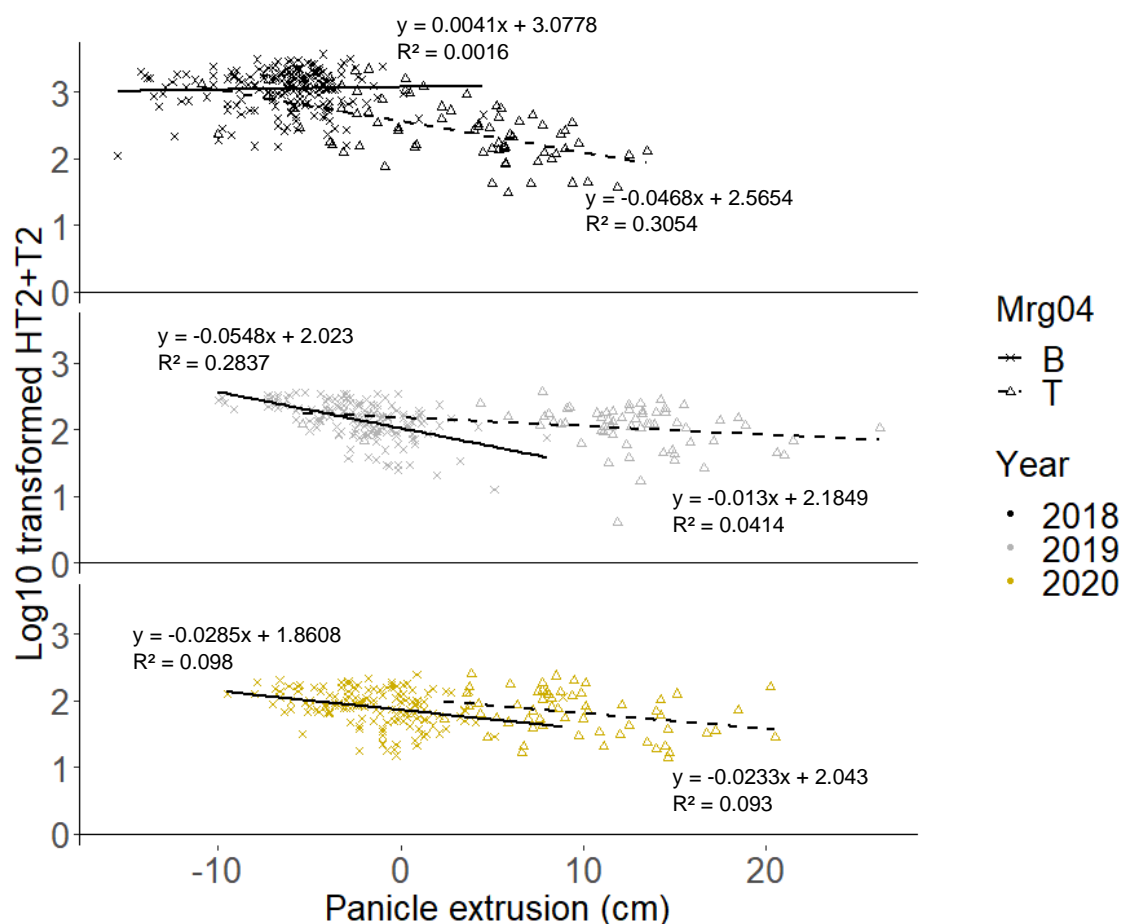


Figure 4.4: A graphical representation of the model presented in Table 4.2, plotting log10 transformed HT2+T2 concentration against panicle extrusion. The shape of the data points indicates the parental origin of the Mrg04 QTL, the colours indicate the different years described in the legend. Differently textured lines represent the fitted values according to year from the model described in Table 5.2.

Figure 4.5 is a boxplot comparing the data for all years for HT2 +T2 concentration in fully extruded plants to partially extruded plants. The back transformed arithmetic mean of the two groups is displayed on the figure: the partially extruded panicle plants accumulated 465 µg/kg more HT2+T2 than the fully extruded panicles. A one-way ANOVA using panicle fully extruded or partially extruded as the sole factor was significant ($P < 0.001$) and accounted for 15% of the variation.

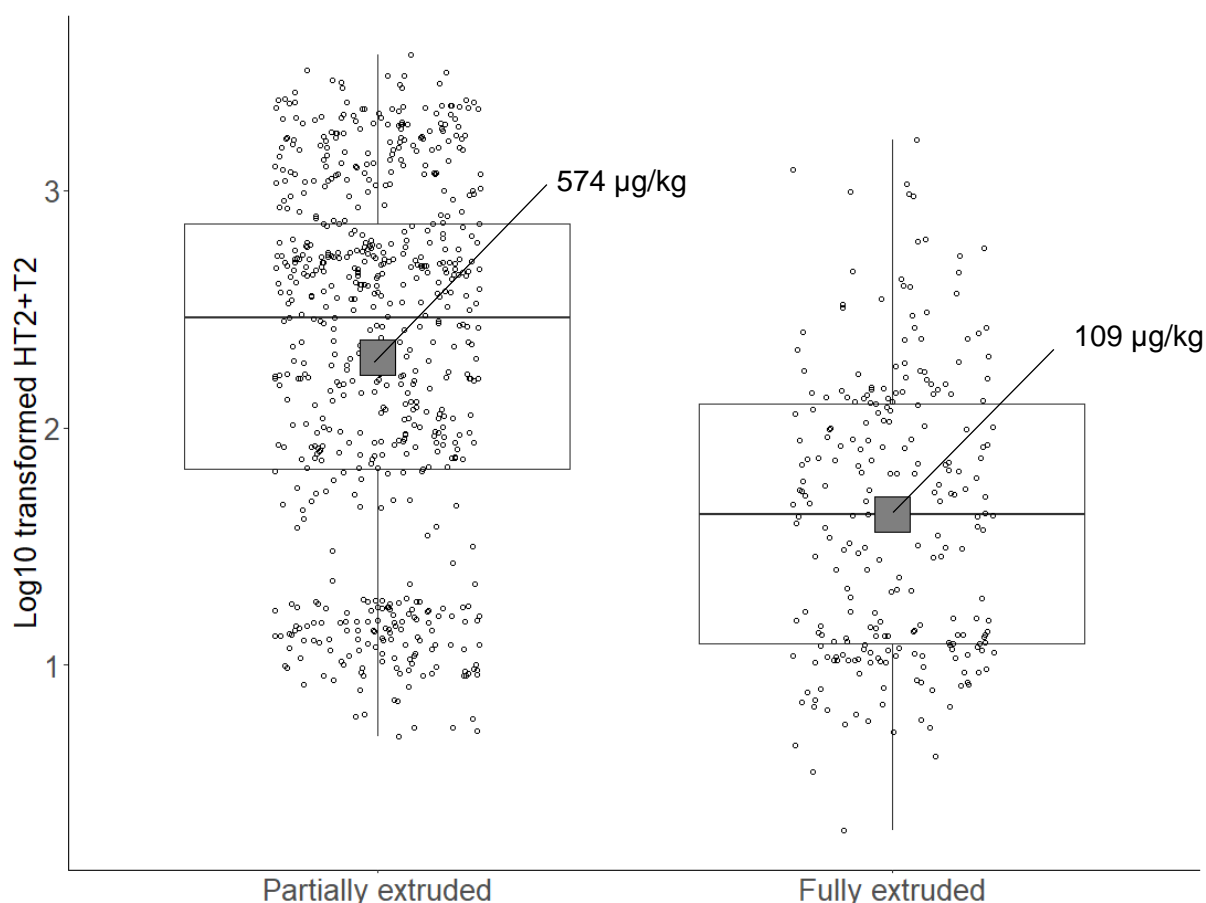


Figure 4.5: Boxplot comparing plants with fully extruded panicles against those with only partially extruded panicles. The y axis displays log₁₀ transformed HT₂+T₂ values, the mean values for each the fully extruded and partially extruded plant's are represented by the grey boxes and labelled with the back transformed HT₂+T₂ concentrations.

4.3.4. Earliness

Table 4.4, Table 4.6 and Table 4.8 display linear models of concentration of HT₂+T₂ and earliness measured by: days from sowing to panicle emergence, degree days from sowing to panicle emergence, and Julian day of panicle emergence, and using the parental origin of Mrg21 as a factor. All three measures of time were significant ($P < 0.001$). The parental origin of Mrg21 was significant in all three models but only accounted for 5.4%, 2.4%, and 4.1% of the variance for days from sowing to panicle emergence, day degrees and Julian day of emergence, respectively. The interaction between sowing season and the parental origin of Mrg21 accounted for 0.6%, 0.9%, and 0.3% of the variation for days from sowing to panicle emergence, day degrees and Julian day of emergence, respectively. Figure 4.6, Figure 4.8 and Figure 4.10 plot the log₁₀ transformed HT₂+T₂ concentrations plotted against days from sowing to panicle emergence, day degrees and Julian day of emergence, respectively for autumn sown plots. Figure 4.7, Figure 4.9 and Figure 4.11 plot the log₁₀ transformed HT₂+T₂ concentrations plotted against days from sowing to panicle emergence, day degrees and Julian day of emergence, respectively for spring sown plots Year is represented by

different colours of the data points and fitted lines are applied to the data by year; different shaped data points represent the parental origin of Mrg21.

Table 4.3, Table 4.5 and Table 4.7 display linear models of earliness measured by: days from sowing to panicle emergence, degree days from sowing to panicle emergence, and Julian day of panicle emergence, using the parental origin of Mrg04 as a factor. The origin of the Mrg04 QTL had a larger effect than that of the Mrg21 QTL accounting for 9.8%, 11.3% and 9.0% of the variation for days from sowing to panicle emergence, day degrees and Julian day of emergence respectively. The interaction between sowing season and Mrg04 was much lower than for Mrg21 at 1.7%, 0.3%, and NA respectively for days from sowing to panicle emergence, day degrees and Julian day of emergence, respectively. The effect of the origin of the Mrg04 QTL is therefore not so dependent on sowing season as Mrg21.

Table 4.3: Output from multiple linear model based on days from sowing to panicle emergence, year and the parental origin of Mrg04 showing the F value, P value and percentage variance accounted for by selected factors and interactions entered into the model. Percentage variation was not calculated for non-significant results.

	DF	Sum of squares	Mean sq	F value	P value	% Variation
DTPE	1	3.7	3.7	57.7	<0.001	1.5
Year	3	138.2	46.1	721.0	<0.001	54.9
Mrg04 parental origin	1	24.7	24.7	386.7	<0.001	9.8
Sowing season	1	0.03	0.03	0.4	0.5	NA
DTPE*Year	3	4.5	1.5	23.3	<0.001	1.8
DTPE*Mrg04 parental origin	1	1.0	1.0	16.4	<0.001	0.4
Year * Mrg04 parental origin	3	9.9	3.3	51.8	<0.001	3.9
DTPE * Sowing season	1	0.001	0.001	0.01	0.9	NA
Year * Sowing season	3	3.2	1.1	16.5	<0.001	1.3
Sowing season*Mrg04	1	4.4	4.4	68.7	<0.001	1.7
DTPE * Year * Mrg04	3	4.7	1.6	24.6	<0.001	1.9
DTPE * Year * Sowing season	3	1.6	0.5	8.5	<0.001	0.6
DTPE * Mrg04 * Sowing season	1	0.3	0.3	4.2	0.04	0.1
Year * Mrg04 * Sowing season	3	0.4	0.1	2.0	0.1	NA
DTPE * Year * Mrg04 * Sowing season	3	0.2	0.07	1.1	0.3	NA
Residual	860	54.9	0.06			

Table 4.4: Output from multiple linear model based on days from sowing to panicle emergence, year and the parental origin of Mrg21 showing the F value, P value and percentage variance accounted for by selected factors and interactions entered into the model. Percentage variation was not calculated for non-significant results.

	DF	Sum of squares	Mean sq	F value	P value	% Variation
DTPE	1	5.5	5.5	72.4	<0.001	2.1
Year	3	136.4	45.5	597.8	<0.001	54.2
Mrg21 parental origin	1	8.0	8.0	105.8	<0.001	5.4
Sowing season	1	4.1	4.1	54.2	<0.001	1.6
DTPE*Year	3	5.4	1.8	23.5	<0.001	2.1
DTPE*Mrg21	1	5.5	5.5	72.3	<0.001	2.2
Year * Mrg21	3	3.9	1.3	17.2	<0.001	1.6
DTPE * Sowing season	1	0.1	0.1	1.6	0.2	<0.1
Year * Sowing season	3	3.1	1.0	13.7	<0.001	1.2
Sowing season*Mrg21	1	1.6	1.6	20.4	<0.001	0.6
DTPE * Year * Mrg21	3	2.4	0.8	10.7	<0.001	1.0
DTPE * Year * Sowing season	3	9.0	3	39.4	<0.001	3.6
DTPE * Mrg21 * Sowing season	1	0.4	0.4	5.3	0.02	0.2
Year * Mrg21 * Sowing season	3	0.3	0.1	1.3	0.3	<0.1
DTPE * Year * Mrg21 * Sowing season	3	0.6	0.2	2.8	0.04	0.3
Residual	874	83.0	0.1			

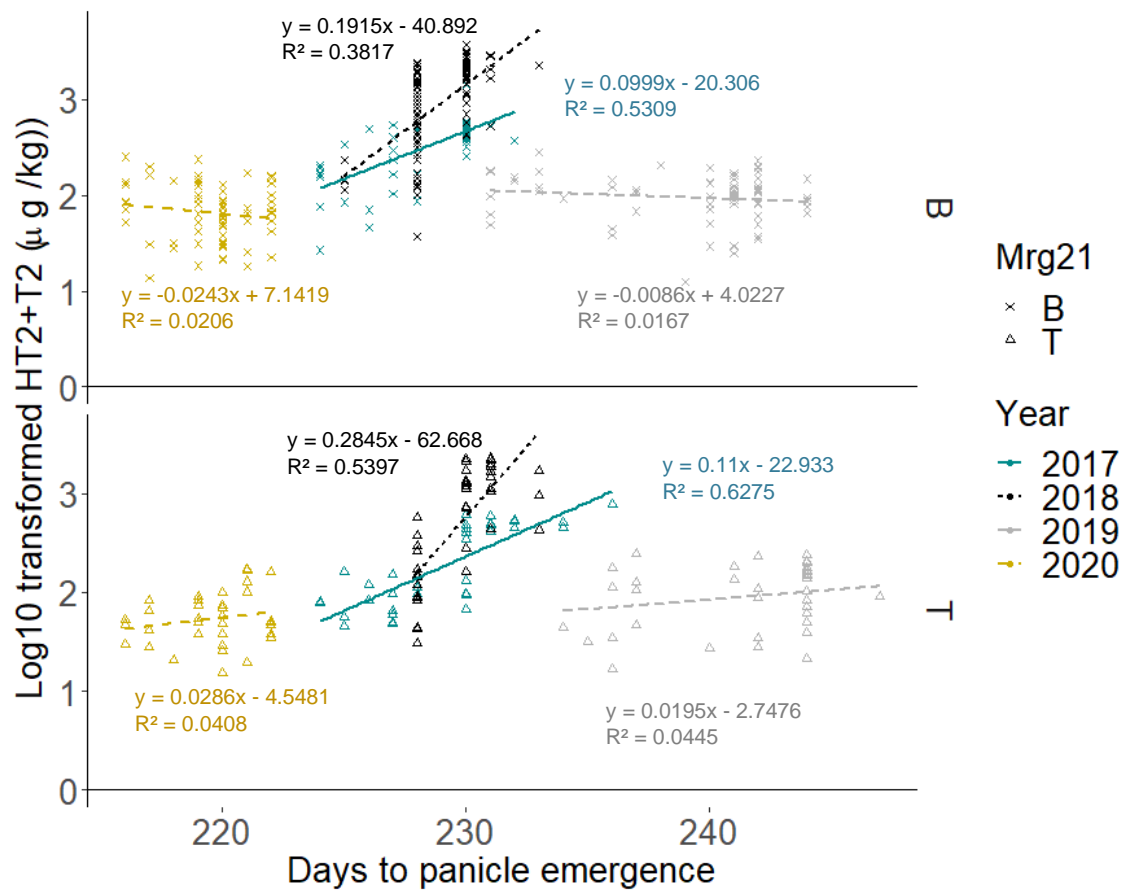


Figure 4.6: A graphical representation of the model presented in Table 4.4, plotting log10 transformed HT2+T2 concentration against days from sowing to panicle emergence of the autumn sown plots. The shape of the data points indicates the parental origin of the Mrg21 QTL, the colours indicate the different years described in the legend. Differently textured and coloured lines represent the fitted values according to year from the model described in Table 5.4.

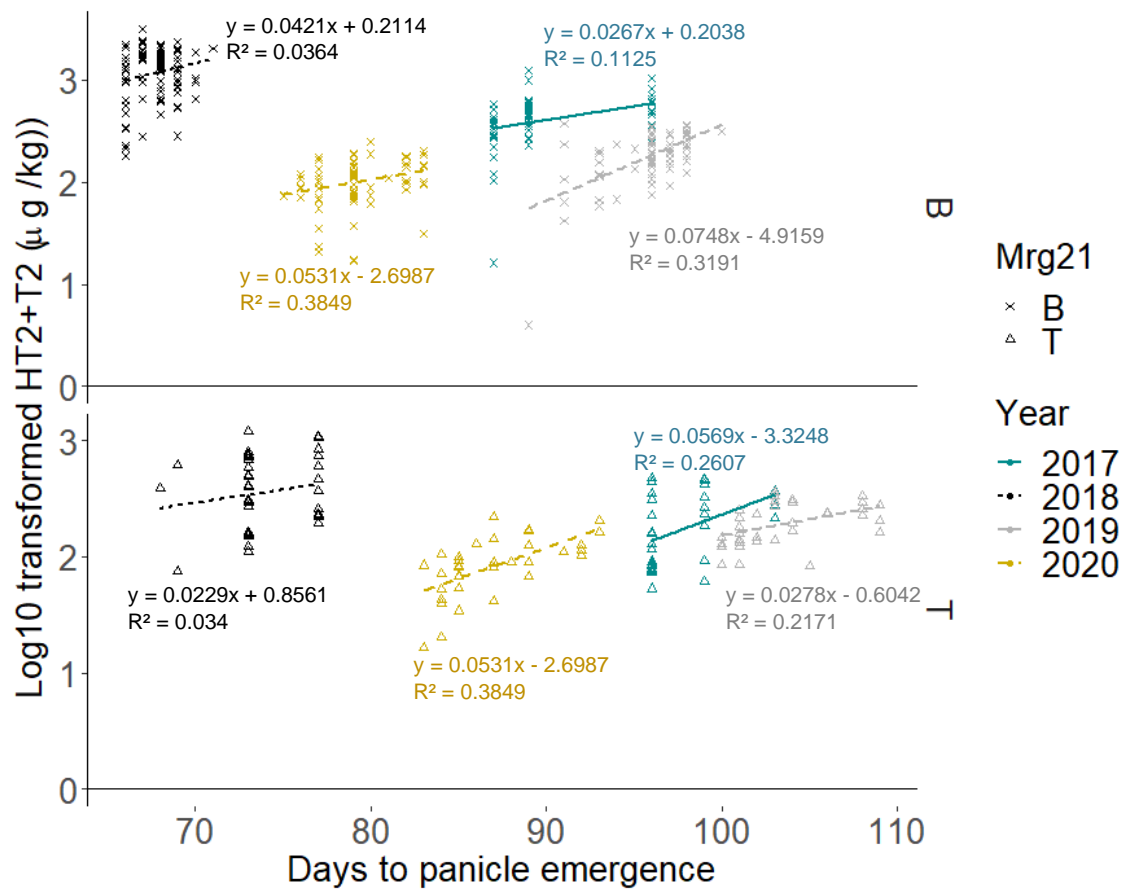


Figure 4.7: A graphical representation of the model presented in Table 4.4, plotting log₁₀ transformed HT₂+T₂ concentration against days from sowing to panicle emergence of spring sown plots. The shape of the data points indicates the parental origin of the Mrg21 QTL, the colours indicate the different years described in the legend. Differently textured and coloured lines represent the fitted values according to year from the model described in Table 5.4.

Table 4.5: Output from multiple linear model based on degree days from sowing to panicle emergence, year and the parental origin of the Mrg04 QTL showing the F value, statistical significance and percentage variance accounted for by selected factors and interactions entered into the model. Percentage variation was not calculated for non-significant results.

	DF	Sum of squares	Mean sq	F value	P value	% Variation
Degree days	1	4.0	4	53.0	<0.001	1.6
Year	3	138.2	46.1	616.2	<0.001	54.9
Mrg04 parental origin	1	28.5	28.5	381.6	<0.001	11.3
Sowing season	3	1.2	0.4	6.3	0.0003	0.13
Degree days*Year	3	1.0	0.3	4.6	0.003	0.5
Year * Mrg04	3	10.3	3.5	53.8	<0.001	4.1
Degree days * Mrg04	1	0.07	0.07	1.1	0.3	NA
Year * Sowing season	3	2.4	0.8	12.6	<0.001	1.0
Degree days * Sowing season	1	0.6	0.6	9.7	0.002	0.2
Mrg04*Sowing season	1	0.9	0.9	13.8	0.0002	0.3
Year*Degree days*Mrg04	3	5.5	1.8	28.6	<0.001	2.2
Degree days * Sowing season * Year	3	2.4	0.8	12.7	<0.001	1.0
Year * Mrg04 * sowing season	3	1.9	0.6	10.0	<0.001	0.8
Degree days * Mrg04 * Sowing season	1	0.2	0.2	3.5	0.06	NA
Year * Degree days * Mrg04 * sowing season	3	0.25	0.08	1.3	0.2	NA
Residual	874	65.3	0.08			

Table 4.6: Output from multiple linear model based on degree days from sowing to panicle emergence, year and the parental origin of Mrg21 showing the F value, statistical significance and percentage variance accounted for by selected factors and interactions entered into the model. Percentage variation was not calculated for non-significant results.

	DF	Sum of squares	Mean sq	F value	P value	% Variation
Degree days	1	4.0	4.0	43.3	<0.001	1.6
Year	3	138.2	46.1	504.2	<0.001	54.9
Mrg21 parental origin	1	6.0	6.0	65.3	<0.001	2.4
Sowing season	1	3	3	31.9	<0.001	1.2
Year*Degree days	3	3.3	1.1	12.0	<0.001	1.3
Year * Mrg21	3	9.4	3.1	34.3	<0.001	3.7
Degree days*Mrg21	1	1.4	1.4	17.6	<0.001	0.5
Year*Sowing season	3	1.8	0.6	7.8	<0.001	0.7
Degree days*Sowing season	1	2.3	2.3	29.9	<0.001	0.9
Mrg21*Sowing season	1	2.2	2.2	28.7	<0.001	0.9
Year*Degree days*Mrg21	3	1.8	0.6	7.6	<0.001	0.7
Degree days * Sowing season * Year	3	11.4	3.8	49.5	<0.001	4.5
Year*Mrg21*sowing season	3	0.06	0.02	0.25	<0.8	0
Degree days*Mrg21*Sowing season	1	0.5	0.5	6.1	0.013	0.2
Year*Degree days*Mrg21*sowing season	3	0.6	0.2	2.6	<0.05	0.2
Residual	860	66.1	0.1			

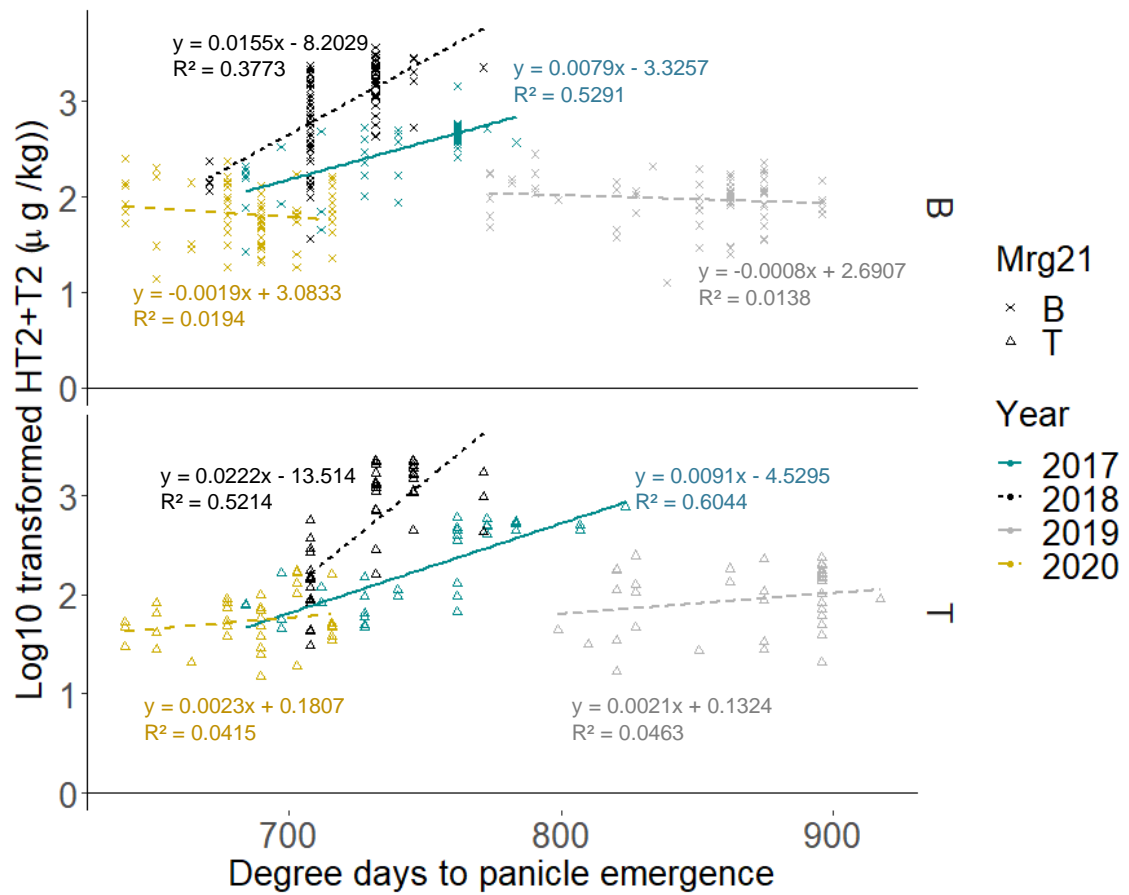


Figure 4.8: A graphical representation of the model presented in Table 4.6, plotting \log_{10} transformed HT2+T2 concentration against degree days from sowing to panicle emergence for autumn sown plots. The shape of the data points indicates the parental origin of the Mrg21 QTL, the colours indicate the different years described in the legend. Differently textured and coloured lines represent the fitted values from the model described in Table 5.6.

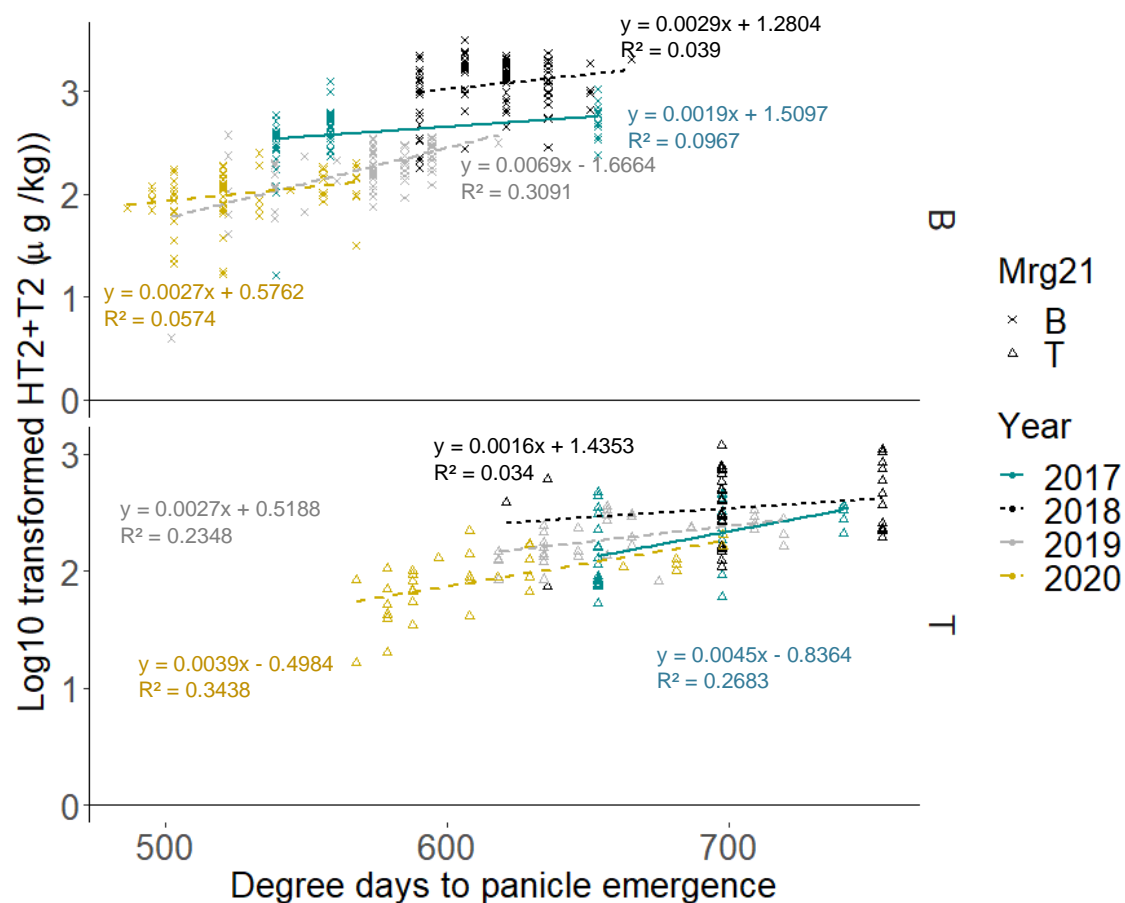


Figure 4.9: A graphical representation of the model presented in Table 4.6, plotting \log_{10} transformed HT2+T2 concentration against degree days from sowing to panicle emergence for spring sown plots. The shape of the data points indicates the parental origin of the Mrg21 QTL, the colours indicate the different years described in the legend. Differently textured and coloured lines represent the fitted values from the model described in Table 5.6.

Table 4.7: Output from multiple linear model based on Julian day of panicle emergence, year, and the parental origin of Mrg04 showing the F value, statistical significance and percentage variance accounted for by selected factors and interactions entered into the model. Percentage variation was not calculated for non-significant results.

	DF	Sum of squares	Mean sq	F value	P value	% Variation
Julian DTPE	1	4.0	4.0	62.2	<0.001	1.6
Year	3	138.2	46.1	721.0	<0.001	54.9
Mrg04 parental origin	1	22.6	22.6	353.1	<0.001	9.0
Sowing season	1	3.2	3.2	49.5	<0.001	1.3
Julian DTPE*Year	3	2.5	0.8	13.1	<0.001	1.0
Julian DTPE*Mrg04 parental origin	1	0.9	0.9	13.7	<0.001	0.3
Year * Mrg04 parental origin	3	11.4	3.8	59.3	<0.001	4.5
Julian DTPE * Sowing season	1	0	0	0	0.98	NA
Year * Sowing season	3	2.5	0.8	13.0	<0.001	1
Sowing season*Mrg04	1	0.05	0.05	0.8	0.4	NA
Julian DTPE * Year * Mrg04	3	8.5	2.8	44.2	<0.001	3.4
Julian DTPE * Year * Sowing season	3	1.9	0.6	10.1	<0.001	0.8
Julian DTPE * Mrg04 * Sowing season	1	0.3	0.3	4.2	0.04	0.1
Year * Mrg04 * Sowing season	3	0.7	0.2	3.9	<0.01	0.3
Julian DTPE * Year * Mrg04 * Sowing season	3	0.2	0.07	1.1	0.3	NA
Residual	860	54.9	0.06			

Table 4.8: Output from multiple linear model based on Julian day of panicle emergence, year, and the parental origin of Mrg21 showing the F value, statistical significance and percentage variance accounted for by selected factors and interactions entered into the model. Percentage variation was not calculated for non-significant results.

	DF	Sum of squares	Mean sq	F value	P value	% Variation
Julian DTPE	1	11.6	11.6	152.1	<0.001	4.6
Year	3	130.6	43.5	572.5	<0.001	51.9
Mrg21	1	10.4	10.4	173.1	<0.001	4.1
Sowing season	1	1.1	1.1	13.8	<0.001	0.4
Julian DTPE*Year	3	5.4	1.8	23.8	<0.001	2.2
Julian DTPE*Mrg21	1	2.5	2.5	33.0	<0.001	1.0
Year * Mrg21	3	4.0	1.3	17.6	<0.001	1.6
Julian DTPE*Sowing season	1	0.4	0.4	5.8	0.016	0.2
Year*Sowing season	3	4.8	1.6	21.2	<0.001	1.9
Sowing season*Mrg21	1	0.8	0.8	10.5	0.001	0.3
Julian DTPE*Year*Mrg21	3	4.5	1.5	19.8	<0.001	1.8
Julian DTPE * Sowing season * Year	3	8.9	3.0	39.2	<0.001	3.6
Julian DTPE*Mrg21*Sowing season	1	0.3	0.3	4.0	<0.05	0.1
Year*Mrg21*Sowing season	3	0.3	0.1	1.3	0.27	0.1
Julian DTPE*Year*Mrg21*sowing season	3	0.6	0.2	2.8	0.04	0.3
Residual	860	65.4	0.1			

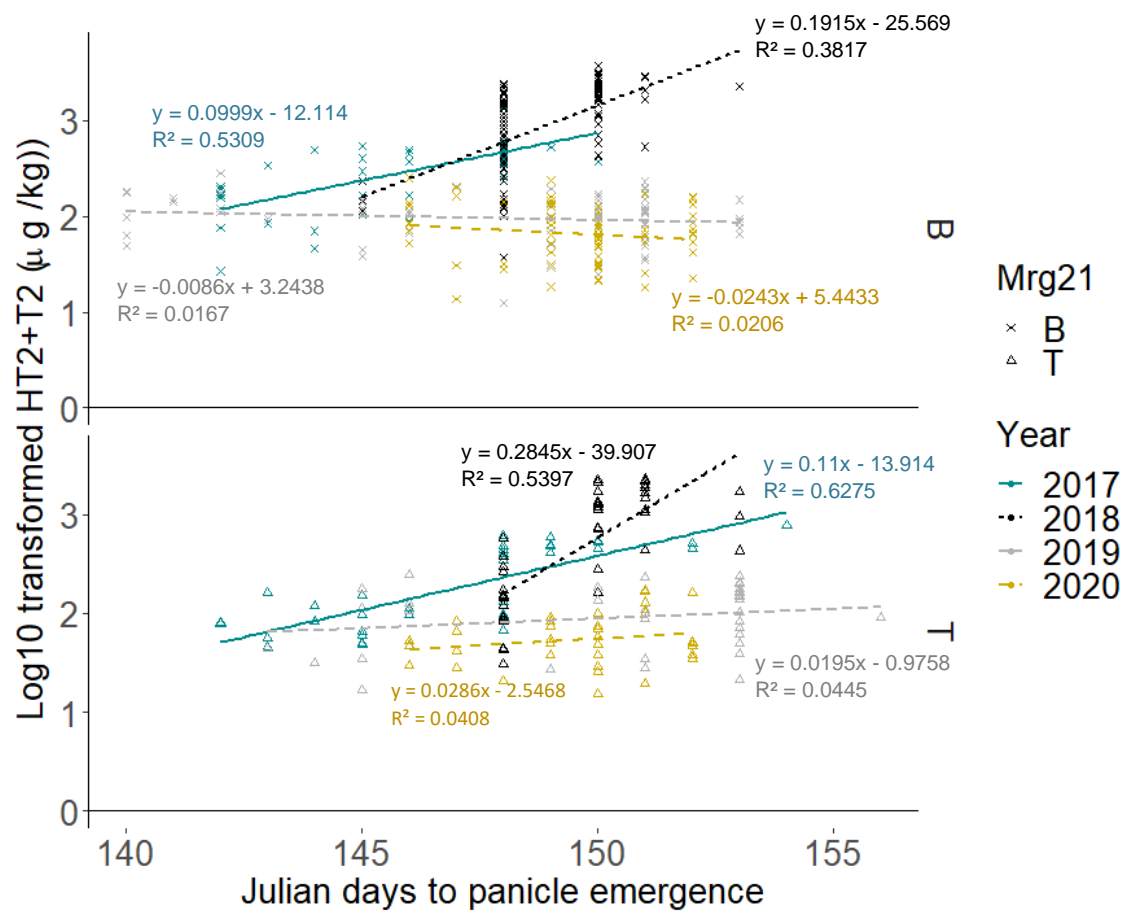


Figure 4.10: A graphical representation of the model presented in Table 5.8, plotting log₁₀ transformed HT₂+T₂ concentration against Julian day of panicle emergence for autumn sown plots. The shape of the data points indicates the parental origin of the Mrg21 QTL, the colours indicate the different years described in the legend. Differently textured and coloured lines represent the fitted values according to year from the model described in Table 5.8.

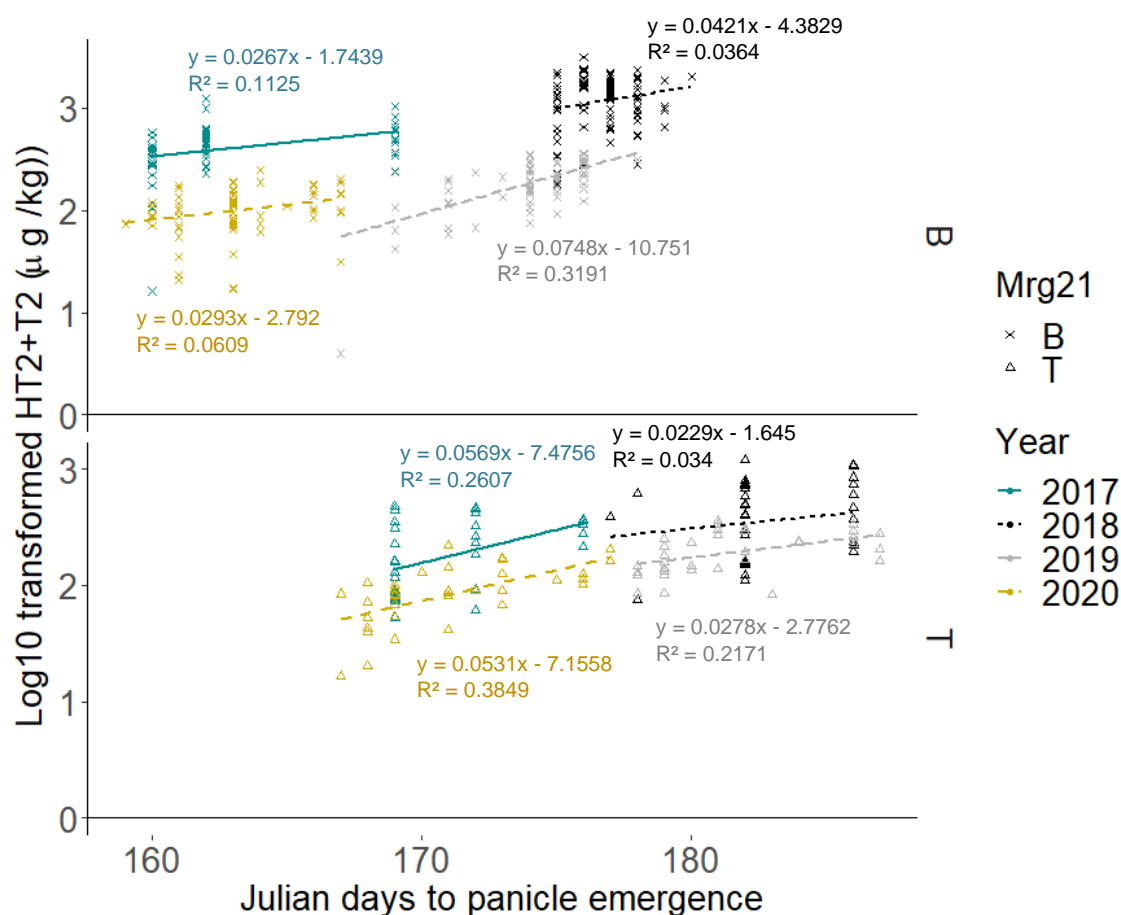


Figure 4.11: A graphical representation of the model presented in Table 5.8, plotting log10 transformed HT2+T2 concentration against Julian day of panicle emergence for spring sown plots. The shape of the data points indicates the parental origin of the Mrg21 QTL, the colours indicate the different years described in the legend. Differently textured and coloured lines represent the fitted values according to year from the model described in Table 5.8.

4.3.5. Mrg04

The results of contrasts performed between Buffalo and the Buffalo + T Mrg04 NIL are displayed below in Table 4.9 and Figure 4.12. The introgression of the Tardis Mrg04 QTL into the Buffalo background caused significant ($P < 0.002$) reductions in the HT2+T2 concentration in the harvested grain in all years and seasons except for autumn sown crops in 2019 and 2020 where the concentrations of HT2 +T2 were extremely low in all samples.

Table 4.9: Contrast analysis comparing average log transformed HT2+T2 concentrations of the parent line Buffalo with Buffalo + T Mrg04. Percentage differences were calculated from the differences between back transformed values.

Year	Contrast	Estimate (Log) (difference between contrasted values)	% Difference	DF	P value
2017	Autumn: Buffalo vs Buffalo + T Mrg04	-0.7	-78.1	75	<0.001
	Spring: Buffalo vs Buffalo + T Mrg04	-0.3	-53.6	75	0.002
2018	Autumn: Buffalo vs Buffalo + T Mrg04	-0.9	-88.5	101	<0.001
	Spring: Buffalo vs Buffalo + T Mrg04	-0.5	-70.5	100	0.0002
2019	Autumn: Buffalo vs Buffalo + T Mrg04	-0.04	-8.4	80	0.7
	Spring: Buffalo vs Buffalo + T Mrg04	-0.3	-44.8	81	0.001
2020	Autumn: Buffalo vs Buffalo + T Mrg04	0.1	31.0	77	0.4
	Spring: Buffalo vs Buffalo + T Mrg04	-0.6	-73.2	77	<0.001

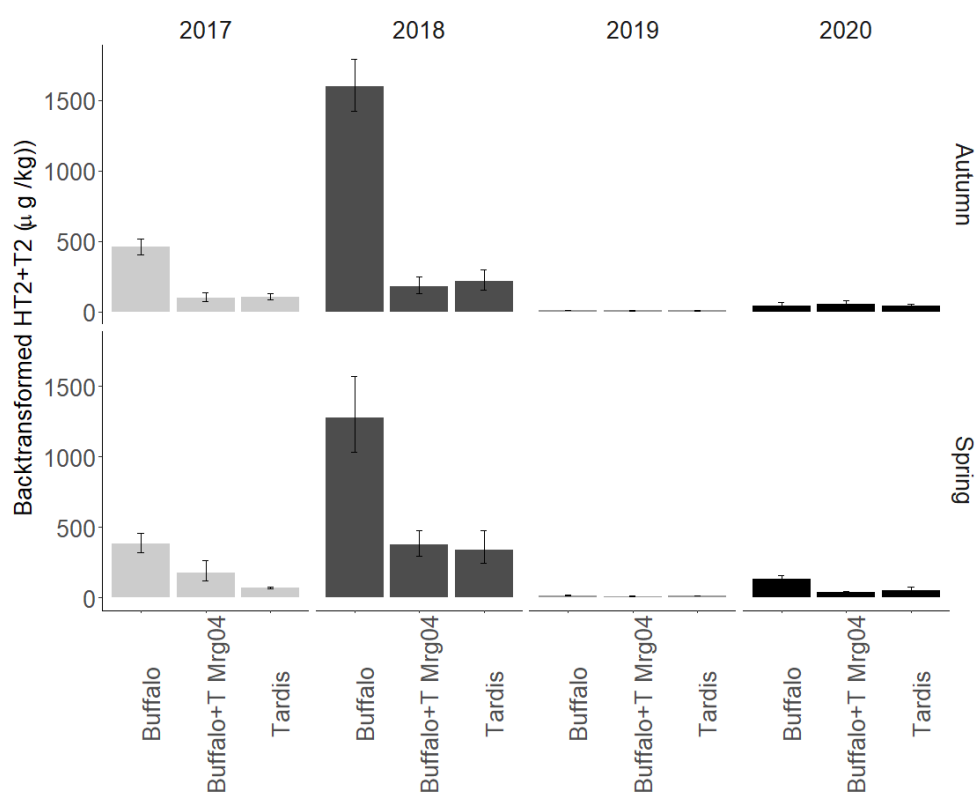


Figure 4.12: Back transformed concentrations of HT2+T2 from Buffalo + T Mrg04, Buffalo and Tardis sown in autumn and spring. Results from four years of autumn and spring sown field experiments (2017-2020). The error bars represent the back transformed standard error of the means.

The results of contrasts performed between Tardis and the Tardis + B Mrg04 NIL are displayed below in Table 4.10 and Figure 4.13. The introgression of the Buffalo Mrg04 QTL into the Tardis background caused significant ($P < 0.0004$) increases in the HT2+T2 concentration in the harvested grain in 2017, 2018, and 2020 autumn results and 2017 and 2020 spring results.

Table 4.10: Contrast analysis comparing average Log10 transformed HT2+T2 concentrations of the parent line Tardis with the NIL Tardis + B Mrg04. Percentage differences were calculated from the differences between back transformed values.

Year	Contrast	Estimate (Log) (difference between contrasted values)	% Difference	DF	P value
2017	Autumn: Tardis vs Tardis + B Mrg04	0.71	411.0	75	<0.001
	Spring: Tardis vs Tardis + B Mrg04	0.7	360.2	75	<0.001
2018	Autumn: Tardis vs Tardis + B Mrg04	0.8	535.7	101	<0.001
	Spring: Tardis vs Tardis + B Mrg04	0.1	29.4	100	0.4008
2019	Autumn: Tardis vs Tardis + B Mrg04	-0.003	-0.8	80	0.9683
	Spring: Tardis vs Tardis + B Mrg04	0.05	12.8	81	0.4815
2020	Autumn: Tardis vs Tardis + B Mrg04	0.3	123.4	77	0.0231
	Spring: Tardis vs Tardis + B Mrg04	0.4	178.3	77	<0.001

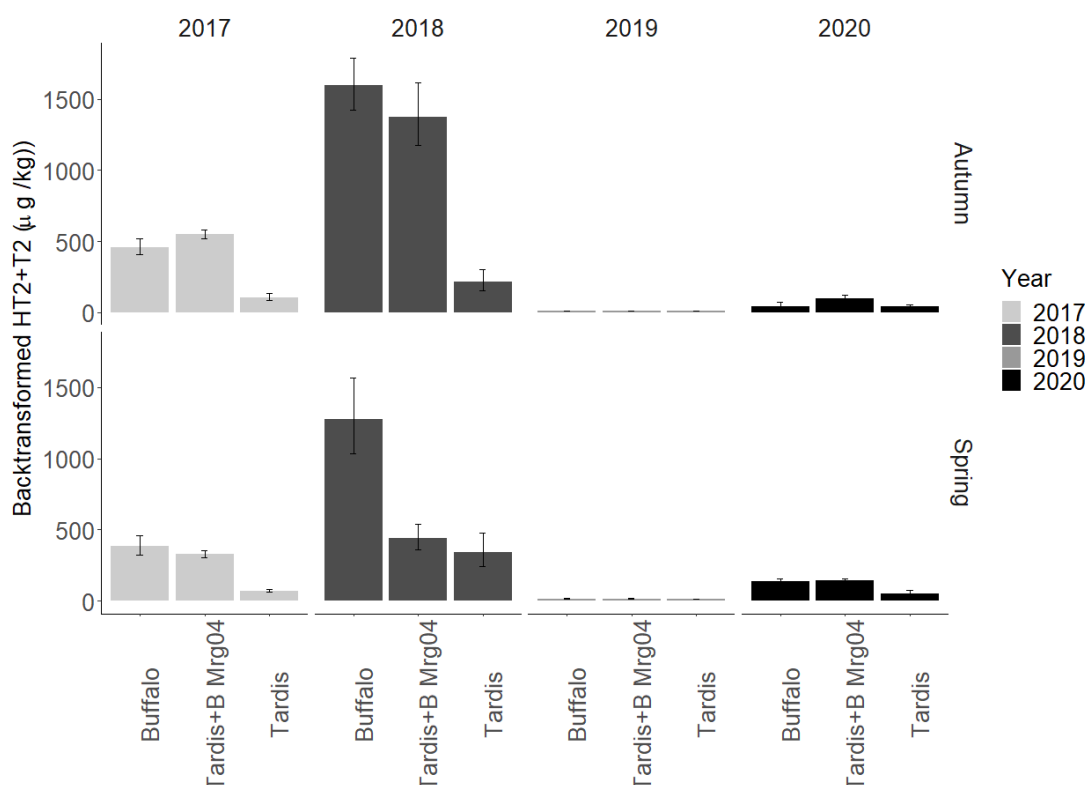


Figure 4.13: Back transformed concentrations of HT2+T2 from Tardis + B Mrg04, Buffalo and Tardis sown in autumn and spring. Results from four years of autumn and spring sown field experiments (2017-2020). The error bars represent the back transformed standard error of the means.

4.3.6. Mrg21

The results of contrasts performed between Buffalo and the Buffalo + T Mrg21 NIL are displayed below in Table 4.11 and Figure 4.14. The introgression of the Tardis Mrg21 QTL into the Buffalo background caused significant ($P < 0.001$) decreases in the HT2+T2 concentration in the harvested grain in 2018 and 2020 spring results.

Table 4.11: Contrast analysis comparing average Log transformed HT2+T2 concentrations of the parent line Buffalo with the NIL Buffalo + T Mrg21.

Year	Contrast	Estimate (Log10) (difference between contrasted values)	% Difference	DF	P value
2017	Autumn: Buffalo vs Buffalo + T Mrg21	-0.03	-7.6	75	0.7528
	Spring: Buffalo vs Buffalo + T Mrg21	0.01	3.4	75	0.9052
2018	Autumn: Buffalo vs Buffalo + T Mrg21	-0.2	-35.5	101	0.3142
	Spring: Buffalo vs Buffalo + T Mrg21	-0.7	-81.1	100	<0.001
2019	Autumn: Buffalo vs Buffalo + T Mrg21	-0.03	-5.6	80	0.7965
	Spring: Buffalo vs Buffalo + T Mrg21	-0.07	-14.8	81	0.4169
2020	Autumn: Buffalo vs Buffalo + T Mrg21	-0.1	-20.2	77	0.5756
	Spring: Buffalo vs Buffalo + T Mrg21	-0.3	-47.1	77	0.0503

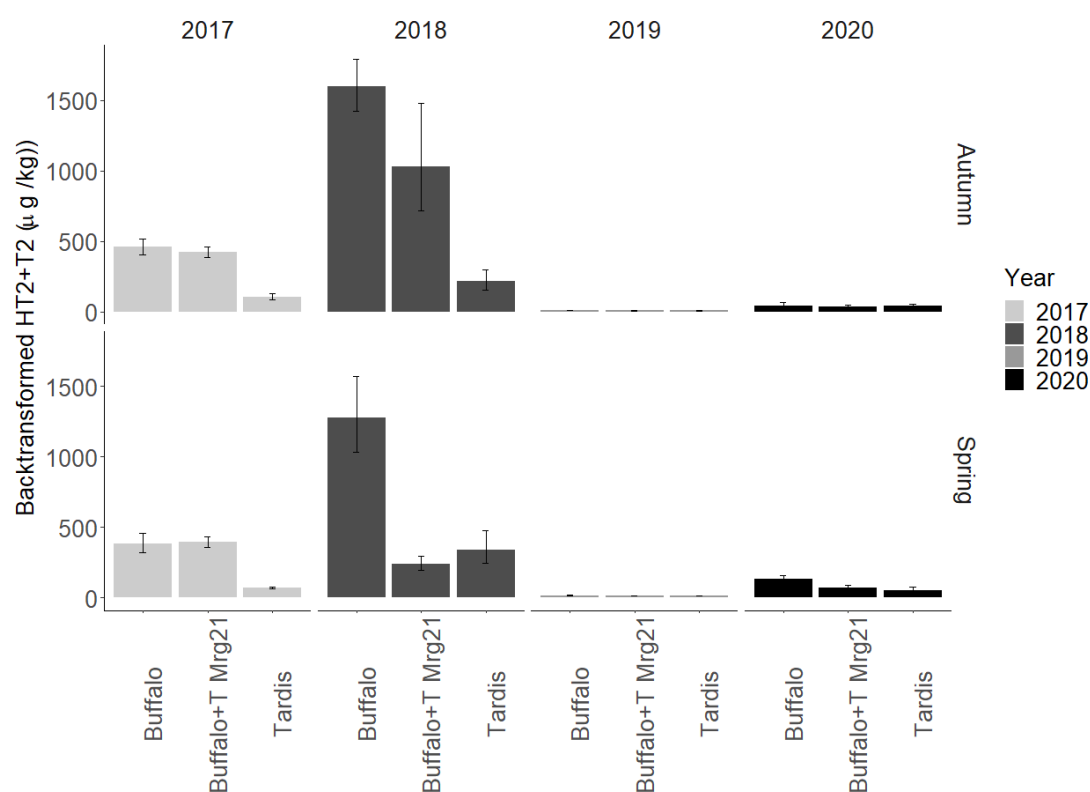


Figure 4.14: Back transformed HT2+T2 concentrations for Buffalo + T Mrg21, Buffalo and Tardis for all years and both sowing seasons. Error bars represent one standard error of the mean.

The results of contrasts performed between Tardis and the Tardis + B Mrg21 NIL are displayed below in Table 4.12 and Figure 4.15. The introgression of the Buffalo Mrg21 QTL into the Tardis background caused significant ($P < 0.02$) increases in the HT2+T2 concentration in the harvested grain in 2017, 2018, and 2020 spring results, as well as 2020 autumn.

Table 4.12: Contrast analysis comparing average Log transformed HT2+T2 concentrations of the parent line Tardis with the NIL Tardis + B Mrg21. Percentage differences were calculated from the differences between back transformed values.

Year	Contrast	Estimate (Log) (difference between contrasted values)	% Difference	DF	P value
2017	Autumn: Tardis vs Tardis + B Mrg21	0.1296	34.8	75	0.1736
	Spring: Tardis vs Tardis + B Mrg21	0.7	360.2	75	<0.001
2018	Autumn: Tardis vs Tardis + B Mrg21	-0.04	-9.3	101	0.7952
	Spring: Tardis vs Tardis + B Mrg21	0.6	297.4	100	<0.001
2019	Autumn: Tardis vs Tardis + B Mrg21	0.02	4.5	80	0.8209
	Spring: Tardis vs Tardis + B Mrg21	-0.04	-8.8	81	0.5870
2020	Autumn: Tardis vs Tardis + B Mrg21	0.5	228.0	77	0.0231
	Spring: Tardis vs Tardis + B Mrg21	0.4	135.5	77	0.0045

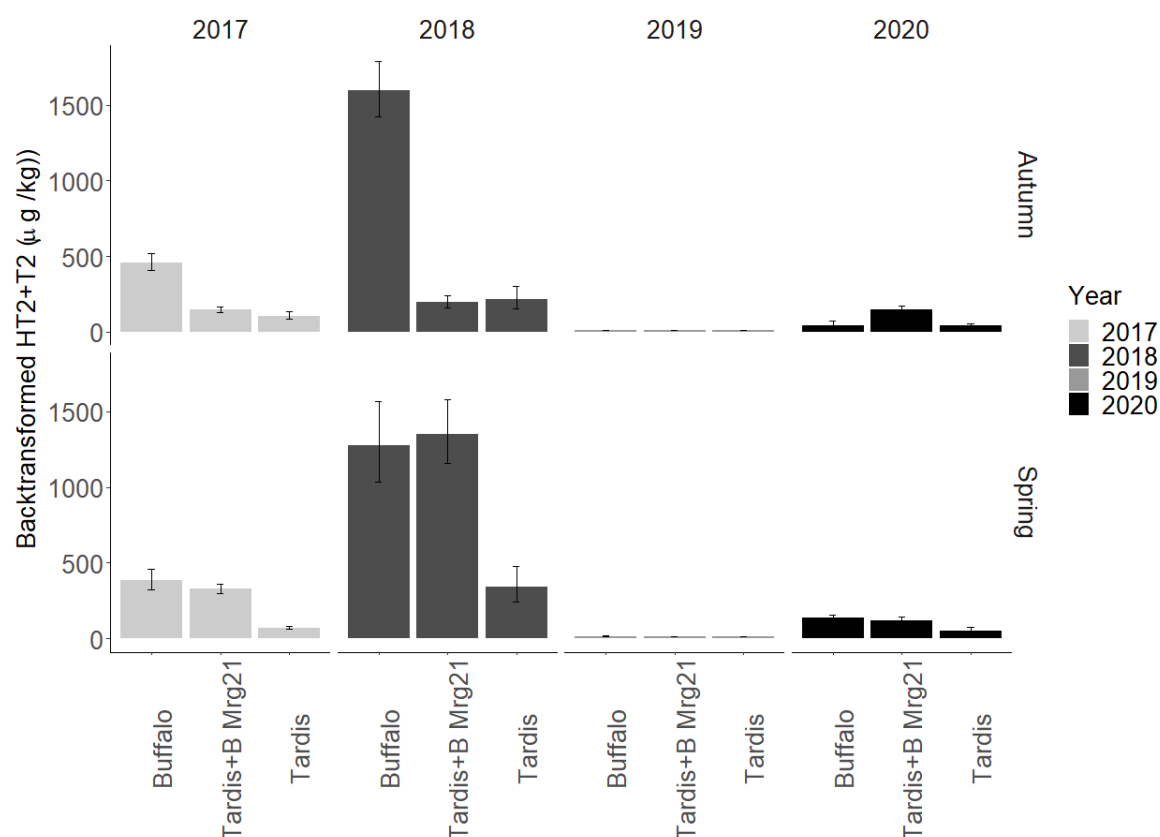


Figure 4.15: Back transformed HT2+T2 concentrations for Tardis + B Mrg21, Buffalo and Tardis for all years and both sowing seasons. Error bars represents one standard error of the mean.

4.3.7. Mrg20

The results of contrasts performed between Buffalo and the Buffalo + T Mrg20 NIL are displayed below in Table 4.13 and Figure 4.16. The introgression of the Tardis Mrg20 QTL into the Buffalo background did not have a significant ($P < 0.05$) impact on HT2+T2 concentration in any year or sowing season.

Table 4.13: Contrast analysis comparing average Log transformed HT2+T2 concentrations of the parent line Buffalo with the NIL Buffalo + T Mrg20. Percentage differences were calculated from the differences between back transformed values.

Year	Contrast	Estimate (Log) (difference between contrasted values)	% Difference	DF	P value
2017	Autumn: Buffalo vs Buffalo + T Mrg20	0.05	11.7	75	0.7
	Spring: Buffalo vs Buffalo + T Mrg20	0.07	17.3	75	0.6
2018	Autumn: Buffalo vs Buffalo + T Mrg20	-0.3	-46.7	101	0.1
	Spring: Buffalo vs Buffalo + T Mrg20	0.1	37.6	100	0.4
2019	Autumn: Buffalo vs Buffalo + T Mrg20	-0.1	-22.5	80	0.3
	Spring: Buffalo vs Buffalo + T Mrg20	0.09	-18.4	81	0.3
2020	Autumn: Buffalo vs Buffalo + T Mrg20	0.1	26.0	77	0.6
	Spring: Buffalo vs Buffalo + T Mrg20	-0.02	-5.4	77	0.9

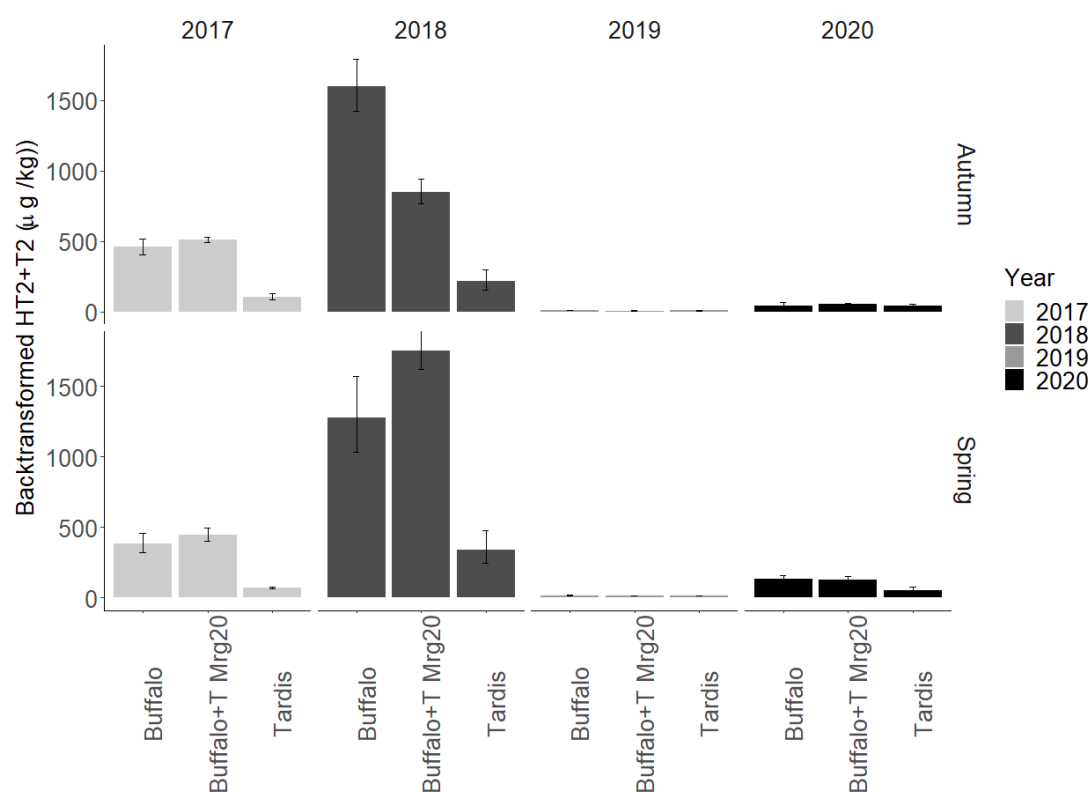


Figure 4.16: Back transformed concentrations of HT2+T2 from Buffalo + T Mrg20, Buffalo and Tardis sown in autumn and spring. Results from four years of autumn and spring sown field experiments (2017-2020). The error bars represent the back transformed standard error of the means.

The results of contrasts performed between Tardis and the Tardis + B Mrg20 NIL are displayed below in Table 4.14 and Figure 4.17. The introgression of the Buffalo Mrg20 QTL into the Tardis background significantly ($P=0.03$) increased HT2+T2 concentration in spring sown 2017 plots, but significantly ($P<0.02$) decreased HT2+T2 in autumn sown plots in 2018 and 2019.

Table 4.14: Contrast analysis comparing average Log transformed HT2+T2 concentrations of the parent line Tardis with the NIL Tardis + B Mrg20. The estimate is the difference between the logged values of the Parent and NIL. Percentage differences were calculated from the differences between back transformed values.

Year	Contrast	Estimate (Log) (difference between contrasted values)	% Difference	DF	P value
2017	Autumn: Tardis vs Tardis + B Mrg20	-0.1	-25.0	75	0.3
	Spring: Tardis vs Tardis + B Mrg20	0.3	82.0	75	0.03
2018	Autumn: Tardis vs Tardis + B Mrg20	-0.4	-63.2	101	0.02
	Spring: Tardis vs Tardis + B Mrg20	-0.1	-28.2	100	0.4
2019	Autumn: Tardis vs Tardis + B Mrg20	-0.3	-45.3	80	0.009
	Spring: Tardis vs Tardis + B Mrg20	-0.07	-14.4	81	0.4
2020	Autumn: Tardis vs Tardis + B Mrg20	-0.1	-20.6	77	0.6
	Spring: Tardis vs Tardis + B Mrg20	-0.2	-34.5	77	0.2

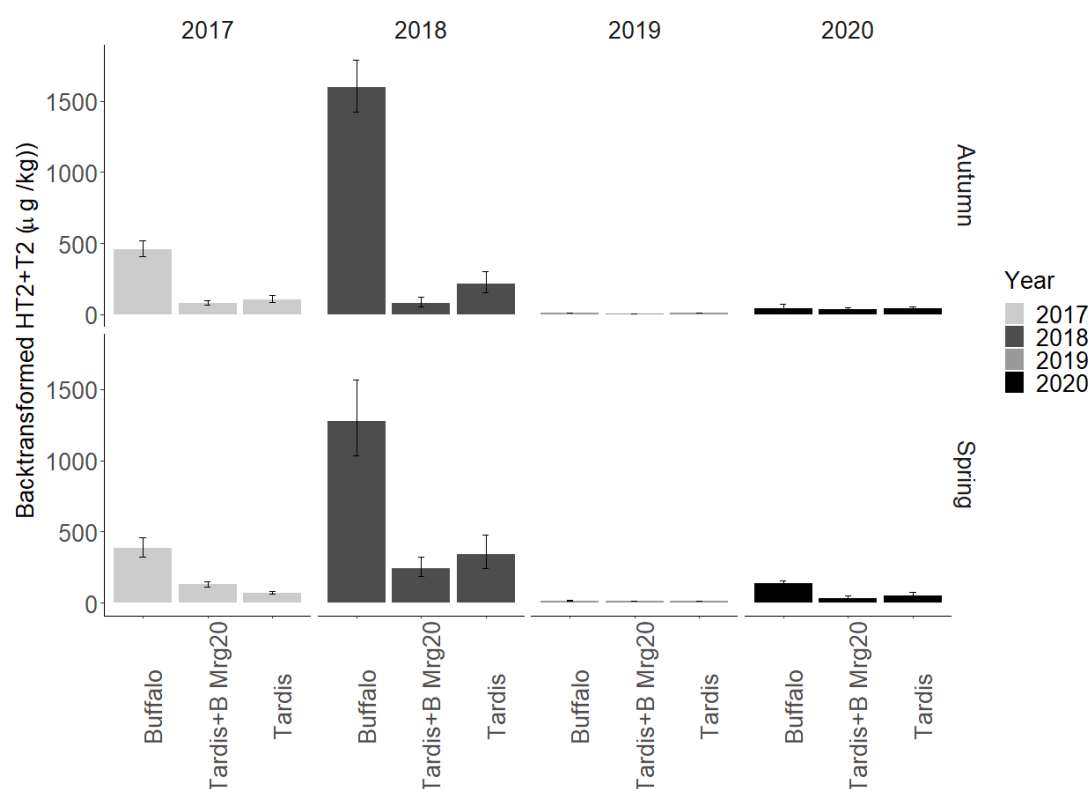


Figure 4.17: Back transformed concentrations of HT2+T2 from Tardis+B Mrg20, Buffalo and Tardis sown in autumn and spring. Results from four years of autumn and spring sown field experiments (2017-2020). The error bars represent the back transformed standard error of the means.

4.3.8. Mrg11

The results of contrasts performed between Buffalo and the Buffalo + T Mrg20 NIL are displayed below in Table 4.15 and Figure 4.18. The introgression of the Tardis Mrg11 QTL into the Buffalo background had no significant impact on the HT2+T2 concentrations in any year or sowing season.

Table 4.15: Contrast analysis comparing average Log transformed HT2+T2 concentrations of the parent line Buffalo with the NIL Buffalo + T Mrg11. The estimate is the difference between the logged values of the parent and NIL. Percentage differences were calculated from the differences between back transformed values.

Year	Contrast	Estimate (Log) (difference between contrasted values)	% Difference	DF	P value
2018	Autumn: Buffalo vs Buffalo + T Mrg11	0.1	40.1	101	0.3
	Spring: Buffalo vs Buffalo + T Mrg11	-0.03	-6.3	100	0.8
2019	Autumn: Buffalo vs Buffalo + T Mrg11	-0.003	-0.8	80	1.0
	Spring: Buffalo vs Buffalo + T Mrg11	-0.02	-4.6	81	0.8
2020	Autumn: Buffalo vs Buffalo + T Mrg11	0.3	86.3	77	0.053
	Spring: Buffalo vs Buffalo + T Mrg11	-0.02	-5.3	77	0.8

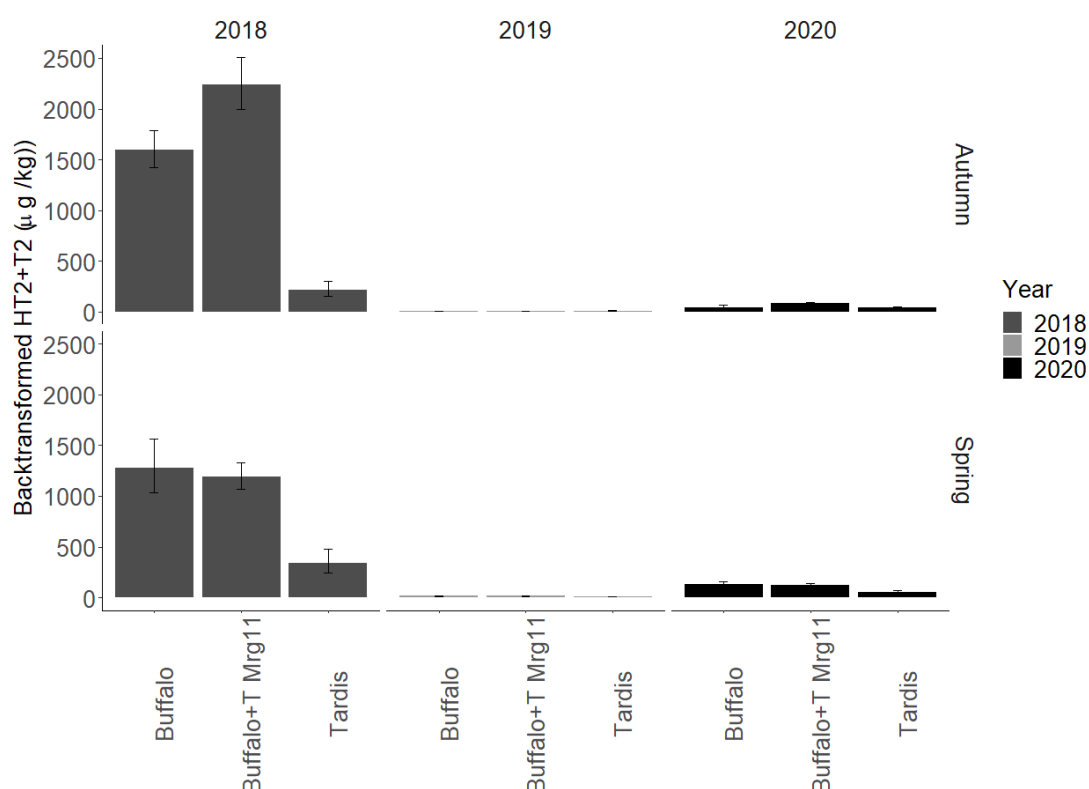


Figure 4.18: Back transformed concentrations of HT2+T2 from Buffalo + T Mrg11, Buffalo and Tardis sown in autumn and spring. Results from three years of autumn and spring sown field experiments (2018-2020). The error bars represent the back transformed standard error of the means.

Figure 4.6 through to Figure 4.18 highlight the high impact of year on the HT2+T2 concentrations; large percentage differences occurring in years with low HT2+T2 concentrations can still be considered modest increases in most cases.

4.4. Discussion

This chapter uses HT2+T2 concentrations in the harvested grain to measure resistance or susceptibility to *F. langsethiae*. Although this is not a direct measure of the degree to which the *F. langsethiae* has infected the plants the concentration of HT2+T2 is the only impact of *F. langsethiae* of commercial interest. Furthermore, a consistent relationship between HT2+T2 and *F. langsethiae* DNA concentrations has been demonstrated (Edwards *et al.*, 2012a). The resistance being measured could be either type I, type II, type III, or type V resistance described in section 1.8.1.

Eight experiments which involved growing the same genotypes in spring and autumn sowings were conducted in the work described in this chapter. Although those sowings were not randomised within the same experiments, spring and winter averages across the entire trials were comparatively very similar, suggesting that sowing date is not a predominant factor in *F. langsethiae* infection. This agrees with the findings of Stančić (2016) who examined six spring and six winter varieties of oat each sown in both spring and winter, in split plot designs. At both sowing times the winter varieties accumulated

higher HT2+T2 concentrations than the spring varieties. Stančić (2016) did not make a direct comparison of the varieties sown in different seasons. Opoku (2012) who examined both spring and winter oat varieties in identical agronomic conditions, with the exception of sowing date, showed winter varieties accumulated more HT2+T2 per unit DNA than spring varieties. It is difficult logistically to randomise sowing date which is likely why it is rarely done, however the work presented here suggests that sowing date does not have a large impact on the HT2+T2 concentration in harvested grains from naturally infected oat plants.

There was large year to year variation with year accounting for the highest proportion of the variation described by the linear models developed in this chapter (ca. 55% of total variance). The work described in this chapter was conducted over four years and infection was natural, encouraged through field management. The fact that high cereal intensity (specifically oats and wheat) and reduced tillage leaving crop debris on the field surface, contribute to high HT2+T2 concentration is supported by Schöneberg *et al.* (2018), Parikka *et al.* (2007), and Edwards (2017). The data recovered from 2019 was so low that the variation inherent in the pathogen and additionally introduced by the quantification of the mycotoxins likely masks any true differences in concentrations. The 2020 data was higher than 2019 and statistically significant differences ($P < 0.05$) were observed between genotypes. The data from 2017 and 2018 was sufficiently high to give confidence in its interpretation. The validity of the results is strengthened by the natural infection that the plants were exposed to. No isolates were recovered from the field for examination or testing of virulence. The high variation accounted for by year can be explained as year covers such a large number of potential factors, such as weather, seed quality, establishment of the crop, as well as presence and vigour of the pathogen. The fact that the field required ploughing prior to sowing in 2019 and 2020 may have attributed to the lower levels of HT2+T2 in these years.

4.4.1. Height

Height has been suggested as an evasion mechanism in wheat against FHB (Yan *et al.*, 2011; Mesterhazy, 1995), adding to the plants' type I resistance (resistance to initial infection). The same concept is supported for oats and *F. langsethiae* by evidence that stubble from previous cereal crops can be a source of inoculum (Kaukoranta *et al.*, 2019; Edwards, 2007; Edwards and Jennings, 2016; Edwards, 2017; Schöneberg *et al.*, 2019). From this stubble the spores must reach the panicle at the top of the plant. As yet no mechanism for the transport of *F. langsethiae* spores from the debris has been observed. Opoku *et al.* (2013) was able to detect *F. langsethiae* DNA in commercially grown oats at tillering, perhaps suggesting that spores are endemic in the crop throughout the season. *Fusarium langsethiae* DNA then proliferated after the

emergence of the panicle once the target site of the pathogen became available to those ever-present spores. Other researchers have questioned height as an evasion mechanism for cereals and *Fusarium* adding to type I resistance: Horsley *et al.* (2006) saw no correlation between height and infection with *F. graminearum* in barley.

Previously dwarf oat varieties have been identified as accumulating higher concentrations of HT2+T2 in their grain (Edwards, 2007a; Edwards, 2015). However, researchers have struggled to successfully correlate the plant height of oats with resistance to *Fusarium* using plant growth regulators (Stančić, 2016; Edwards, 2011; Edwards and Anderson, 2011; Edwards, 2017) or mapping populations of oat (He *et al.*, 2013; Stančić, 2016). Loskutov *et al.* (2017) and Bjørnstad *et al.* (2017) concluded that taller plants resistant to lodging were more resistant to *Fusarium* infection and mycotoxin concentration. However, in work based on various *Avena* species, Gagkaeva *et al.* (2018) found a negative relationship with certain tricothecene producing species of *Fusarium* and plant height: this relationship was not present when exclusively examining *F. poae* which is morphologically similar to *F. langsethiae*. Drawing conclusions on the resistance of plants to a pathogen from experiments examining differences in quantitative traits between different genotypes of plants risks erroneously concluding a causal mechanism between those quantitative traits and resistance. The basis of resistance in those instances could be pleiotropy or genetic linkage from closely located genes to those coding the traits being examined. The experiments in this chapter are subject to this same flaw.

In wheat, Draeger *et al.* (2007) found several instances in an Arina/Riband population where height QTL did not overlap with FHB QTL and concluded that height itself was not the causal factor in resistance and that the *Rht-D1b* allele was linked to genes inferring susceptibility to FHB rather than the allele itself conferring susceptibility. Gosman *et al.* (2009) also suggested that for wheat it was possible to infer type II resistance in wheat to FHB using the *Rht-B1b* allele even though the crop would be shorter. Using a mapping population of Clho 4196 (FHB resistant two row barley) and Foster (susceptible six row barley) Horsley *et al.* (2006) were unable to disentangle QTL from height and *F. graminearum* resistance but noted that there were many tall accessions in their population that were susceptible to *F. graminearum* infection, leading to the conclusion that linkage or pleiotropy were at play.

In the work described in this chapter, height and panicle extrusion were seen to have negative relationships to HT2+T2 concentration in the harvested grains with increasing height or panicle extrusion leading to lower HT2+T2 concentration. Variation in height was largely achieved with the presence or absence of the *Dw6* dwarfing gene within the Mrg04 QTL which also introduces other traits associated with the extrusion of the

panicle, the length and number of grains in the panicle and the panicle emergence date. The *Dw6* gene works by shortening the upper internodes which often has the effect of preventing the panicle from fully extruding. It is possible that spikes that survive to form grain still within the flag leaf sheath are in an environment more conducive to high mycotoxin production: analysis of fully extruded and partially extruded plants demonstrated the increase in HT2+T2 concentration in partially extruded panicles. However, height and panicle extrusion are related traits with height explaining almost 50% of the variation in the level of panicle extrusion (chapter 4) and the parental origin of the allele at the Mrg04 QTL accounting for almost 20%. Therefore, it is difficult to place height and panicle extrusion in the same model, however when placed in equivalent models both are highly significant ($P < 0.001$), and account for similar proportions of the variation in the respective models (6.1% – 6.7%). The interaction term between year and height was less than that of year and panicle extrusion; the influence of panicle extrusion varies to a greater degree than that of height by year. In higher infection years panicle extrusion had a greater impact on the HT2+T2 concentration in the grain. It was, however, difficult to differentiate between the effect of panicle extrusion and the influence of the Mrg04 QTL as of the 671 partially extruded plots included in the analysis, only 97 possessed the Tardis derived Mrg04 QTL, the remainder possessing the Buffalo derived Mrg04 containing the *Dw6* dwarfing gene.

Height is also linked to longer panicles (as shown in chapter 4) potentially with higher type II resistance. However, there was no significant relationship between panicle size and HT2+T2 concentration within the 2018 data set (results not shown). It has been speculated that longer branches on oat panicles will increase type II resistance to *Fusarium* (Bjørnstad and Skinnnes, 2008). However, using artificial inoculation, Divon *et al.* (2019) did not observe any instances of hyphal growth out of the spikelet towards the branch. There is as yet no evidence the pathogen moves to any degree through the branches of the panicles.

A relationship between plant height and HT2+T2 infection could be a result of the infection influencing the plant height. Mousavi (2016) investigated whether infection with *F. langsethiae* or *F. graminearum* had an influence on the length of the oat panicle or the length between the flag leaf ligule and the top of the panicle. Across three varieties (Odal, Vinger, Belinda) and four inoculation timings and methods, no consistent differences were seen between inoculated and uninoculated plants. Equally, conditions that lead to taller plants may be less conducive to *F. langsethiae* infection: once year is placed in the model ahead of height the impact of height is reduced. Although still highly significant, the percentage of variance accounted for is

reduced. The change in height between years is accompanied by a change in HT2+T2 concentration but the relationship may not be causal.

Stančić (2016) also investigated height as a contributing factor using a mapping population of RILs derived from a cross between Buffalo and Tardis cultivars. The RILs were selected by Stančić on the basis of their heights to deliver a wide range of heights. Experiments were conducted over three years in the same field but at different sites within that field at Harper Adams University. Natural infection varied across the three years with the 2012/13 season having the highest level of infection. Stančić (2016) reported a highly significant regression between height and accumulated HT2+T2 mycotoxins as well as *F. langsethiae* DNA using linear regression with groups (year was the grouping factor). In every instance when the data was plotted there were two distinct clusters of data points on the plot which Stančić attributed to height, however no further investigation was made of the genetic composition of those RILs and its potential impact on HT2+T2 concentration. The two distinct groups could have represented genotypes possessing either the Buffalo derived Mrg04 QTL (carrying the *Dw6* dwarfing gene) or the Tardis Mrg04. Placing the Mrg04 QTL within the model in the current work accounted for some of the genetic component and height. Year was the most important factor followed by the origin of the Mrg04 QTL; height, although significant, did not contribute greatly to the resistance of the NIL when Mrg04 was already considered. The other QTL examined within this chapter were entered into the model in the place of Mrg04 but Mrg04 remained the most influential. The high number of samples within the analysis led to a high degree of freedom in the residual allowing almost any factor entered into the model to be significant, but not necessarily biologically significant in terms of its impact on HT2+T2 concentration.

4.4.2. Days to panicle emergence

The linear regressions frequently found almost all factors and interactions to be significant due to the high degrees of freedom of the residuals leading to high F values. As in the model run to examine the impact of height on HT2+T2 concentrations in oats, the most important factor was year.

Running a multiple linear model using year, drilling time, sowing season, a select QTL group and either degree days, days from sowing, or Julian day of panicle emergence gives marginally different results. Each time to panicle emergence metric is measuring a different parameter: degree days to panicle emergence, or accumulated degree days, is the sum of the average temperature measured in degrees over a five-degree threshold from sowing to panicle emergence. Days from sowing to panicle emergence is the sum of the days from sowing to panicle emergence measured in days. Because

the sowing date varies from year to year, days to panicle emergence is only a measure of the age of the plant. The Julian day of panicle emergence specifies the number of days from the beginning of the year to panicle emergence and as such the value is independent of sowing date and instead describes the date the panicle emerged. All three measurements of earliness were significant ($P < 0.001$) and accounted for similar percentages of variation (1.5% - 4.6%).

The days from sowing to panicle emergence model shows a positive relationship between panicle emergence and HT2+T2 concentration, with later emerging panicles coinciding with higher HT2+T2 concentrations in all years, except autumn sown plants with Buffalo Mrg21 parentage in 2019 and 2020 where relationships were negative although R squared values were low. When using degree days the relationship for autumn sown plots is positive in all the years except for 2019 and 2020 where the relationship is negative. For spring sown the relationship between degree days and HT2+T2 concentration is positive in all years for all parental origins of Mrg21. Furthermore, when using Julian days, the relationship is positive in all years for both sowing seasons. In all cases the panicle emergence date accounts for a lower proportion of the variation and the gradients of the lines representing their relationships to HT2+T2 concentration vary depending on the severity of infection for each year. Bjørnstad *et al.* (2017) found negative correlations between days to flowering and FHB (DON producing) scores in an analysis of 424 spring oat lines grown in Norway. However, Hautsalo *et al.* (2020) found later maturing varieties of oat to have higher concentrations of DON when investigating *F. graminearum* (spore suspension inoculated) and *F. culmorum* (grain spawn inoculated) field experiments. In such work, evasion of the pathogen by the plant is less possible given the inoculum is introduced at conducive times. There is evidence that inoculum is endemic within the environment (Opoku *et al.*, 2013), if it were present throughout the growth season its presence would certainly coincide with the plant's susceptible growth stage. Whether or not a susceptible growth stage coincides with environmental conditions conducive to *F. langsethiae* infection or high levels of inoculum could dictate the level of infection in any given crop. In such a situation, using earliness as a trait in oats to combat *F. langsethiae* infection would be unsuccessful. The strong effect of year supports weather conditions at the susceptible growth stage being the driving mechanism behind infection. There is evidence from artificial inoculation work (Divon *et al.*, 2012; Divon, 2019; Drakulic *et al.*, 2016; and Opoku, 2012) that anthesis is the most susceptible growth stage or at least that the growth stage at which inoculum is introduced is important in terms of the level of infection achieved. As such investigation into environmental conditions at anthesis may be informative, whether or not such conditions occur at all in a season could influence the impact of earliness on

HT2+T2 concentration. The interaction terms of all three measures of time and year were significant, indicating that the relationship between time to panicle emergence and HT2+T2 concentration was not consistent. Parry *et al.* (1995) cited Love and Seitz (1987) concluding that there was evidence of resistance independent of maturity factors in wheat to FHB. The conclusion was based on different cultivars maturing at different times and finding that susceptibility was independent of maturity factors as cultivars with similar heading dates differed in the degree of FHB infection.

The time of day at which hexaploid oats flower has been recorded as early afternoon (~3pm) (Misonoo, 1936; Nishiyama, 1970) and the flowering time of diploid oats *A. strigosa* much later at between 9-10pm (Nishiyama, 1970). In the present work wild oat samples collected in the field frequently had undetectable or very low HT2+T2 concentrations, but in glasshouse inoculations wild oat samples proved to be as susceptible to *F. langsethiae* as domestic oats. Potentially the wild oats were employing an evasion mechanism by flowering late in the day when *F. langsethiae* spores were not present. Herrmann *et al.* (2020) did not find a clear relationship between open flowering and *Fusarium* susceptibility in oats. The mechanism and timing of *F. langsethiae* spore dispersal are not well understood, and further understanding would help to clarify whether such an evasion mechanism is possible. The time of day at which the oats flower is likely under genetic control: potentially the effect on HT2+T2 concentration that is seen from flowering time is as a result of linkage or pleiotropy between genetic loci determining flowering time and the duration and time of day the plants flower. It has also been demonstrated that retention of anthers and the associated pollen are important in assisting infection of the floret (Divon *et al.*, 2019; Buerstmayr and Buerstmayr, 2015). However, it is possible that the QTL coding for earliness also carries genes influencing resistance to *F. langsethiae* through different mechanisms.

4.4.3. Contrasts

For the Buffalo + T Mrg04 NIL the contrasts against Buffalo were significant ($P \leq 0.0021$) in every year and sowing season, with the exception of autumn 2019 and 2020 (the lowest HT2+T2 accumulating years). The contrasts remained significant irrespective of sowing season: the magnitudes of the difference were between 44.8% and 88.5% less HT2+T2 in the Buffalo +T Mrg04 NIL than Buffalo. Potentially this difference could be attributed to height or panicle extrusion, although the impact of both within the multiple linear models was small. The Buffalo + T Mrg04 genotypes differ in panicle emergence date as well as potentially carrying other genetic drag from the introgressed QTL.

The Tardis + B Mrg04 NIL grew very short compared to the Tardis parent and was late to initiate panicle emergence; the panicle never fully emerged in any year or sowing season. The HT2+T2 concentration of the Tardis + B Mrg04 NIL was often far higher than the Tardis parent. For example, in autumn sown 2018 the Tardis + B Mrg04 NIL had an HT2+T2 concentration 535.7% higher than Tardis. The concentrations of HT2+T2 were more similar to Buffalo than Tardis (the large impact this QTL had on the plant phenotype has already been seen in chapter 4). In the spring sown 2018 plots, however, the HT2+T2 concentration remained similar to the Tardis concentration and the contrast between the two was not significant ($P=0.4$). The Tardis + B Mrg04 genotypes were much later to undergo panicle emergence than any other genotype in the experiment in both spring and autumn sowings.

The Mrg21 QTL had a significant effect on the time to panicle emergence as demonstrated earlier in chapter 4: the effect was larger when sown in spring, bringing forward panicle emergence in the Tardis + B Mrg21 NIL by 7.4 days compared to Tardis and causing the Buffalo + T Mrg21 to be 7.3 days later compared to Buffalo.

The contrast between Tardis + B Mrg21 and Tardis in terms of HT2+T2 concentration was significant in the 2017, 2018 and 2020 spring sowing as well as the 2020 autumn sowing. Height was only increased by 6.3% in autumn and 4.9 % in spring with the introgression of the Buffalo derived Mrg21 into Tardis. Such small differences in height are not likely to have caused the relatively large (360.2 %, 297.4 %, 228.0 % and 135.5 % in spring 2017, 2018, 2020 and autumn 2020 respectively) increases seen in HT2+T2 concentration of Tardis + B Mrg21 compared to Tardis. The introduction of the Buffalo allele within the Mrg21 QTL made the Tardis plants more susceptible, potentially as a result of bringing forward the panicle emergence date. Introducing the Tardis allele at Mrg21 QTL into the Buffalo background had a less consistent effect on the HT2+T2 concentrations: in spring sown 2018 plots (the year with the highest infection levels) Buffalo + T Mrg21 constituted an 80% reduction in HT2+T2. These plants had also reached panicle emergence 7.3 days later than Buffalo.

The expectation was for plants possessing different alleles at the Mrg21 QTL position to react differently when sown in spring or autumn; as such the interaction between the sowing season, and the QTL in the model should be significant and account for a proportion of the variation. This was the case for Mrg21 and Mrg04, however the percentage of variation accounted for by the interaction term of Mrg21 was consistently higher than that of Mrg04. Mrg04 had a higher impact on the HT2+T2 concentration than Mrg21 in terms of the percentage variation accounted for, typically between two to three times greater. In chapter 4 the effect of sowing season on the Mrg21 QTL was seen; it caused Buffalo plants with the Tardis Mrg21 to become later, but to a greater

degree in spring sowings, and Tardis plants with the Buffalo Mrg21 introgression to become earlier, more so in spring sowings. In the contrast analysis, introgressing the Buffalo + T Mrg21 lead to significantly lower HT2+T2 concentrations in 2018 spring and 2020 spring sowings. Tardis + B Mrg21 had significantly higher HT2+T2 concentrations in 2017, 2018, and 2020 spring sowing and 2020 autumn sowing. These contrasts would seemingly contradict the linear models examining measures of time to panicle emergence that described time to panicle emergence as accounting for a low proportion of the HT2+T2 variation.

In this study NIL with the Buffalo derived Mrg20 introgressed into the Tardis background did not have a consistent impact on the HT2+T2 concentration in the harvested grain. A significant ($P=0.035$) increase in HT2+T2 concentration as compared to the Tardis parent was seen in spring sown plots in 2017, but significant decreases ($P<0.023$) was observed in autumn sown plots in 2018 and 2019. All other contrasts for the remaining years and sowing seasons were non-significant reductions compared to the parent Tardis. In the opposing NIL where Tardis Mrg20 was introgressed into the Buffalo background no significant ($P>0.05$) differences were seen. Bjørnstad *et al.* (2017) identifies Mrg20/19A as having had a significant impact on FHB symptoms in one year of data collection and only when days to flowering were incorporated into their model as a covariate.

4.4.4. Across flowering time and height

The heights across the NIL grown were consistent in autumn and spring sown lines showing a range of heights; the spring sown lines showed high and consistent variation in earliness, but the autumn sown lines had comparatively low variation in earliness. The low variation in autumn earliness might be why the regression of HT2+T2 concentration against days to panicle emergence was not significant and why height was a more influential factor in autumn sowings.

4.4.5. Mrg011

Stancic (2016) identified a QTL designated Mrg011 in the Buffalo Tardis RIL mapping population that was associated with *F. langsethiae* DNA and HT2+T2 concentration in the grain. Four separate NILs (composed of the Tardis derived Mrg11 in the Buffalo background) were grown in 2018, 2019 and 2020, sown in autumn and spring. There were no significant ($P<0.05$) differences between the NIL and the Buffalo parent line in any year or sowing season. On two occasions there were large percentage differences between Buffalo and the NIL showing an increase with the presence of the Tardis QTL, both in autumn sowings.

4.5. Conclusions

The impact of any of the QTL seem to not always be consistent across years or sowing seasons and given the large differences in years seen in the examined data set, longer term studies using multiple sites would be advantageous to observe trends over a larger data set. Evidence and analysis reported here suggests that height as a trait that infers resistance has a small but significant impact.

The impact of Mrg21 when introgressed from one parent line to the other is evidence for an effect of panicle emergence date influencing the HT2+T2 concentration in the grain harvested from those plots. However, it is not supported by a wider examination of time to panicle emergence across the whole populations and all years.

The Mrg04 and Mrg21 QTL demonstrate an impact on resistance or susceptibility to HT2+T2 accumulation in the grain. The mechanism through which it is achieved for either QTL is not clear; although some impact of height and panicle extrusion is likely for Mrg04, it may well not be the whole story. For Mrg21, its influence on earliness is apparent: that such influence is seen more in spring sowings where those same NIL also differ more from their respective parents in terms of their HT2+T2 concentrations, is suggestive of earliness being the causative mechanism for resistance. However, that is contradicted by separate analysis showing the lack of impact earliness has across the entire collection on HT2+T2 concentrations and its inconsistency across years.

The Mrg20 QTL had a small impact on HT2+T2 concentration in autumn sown crops when the Buffalo Mrg20 was introgressed into the Tardis line (Tardis + B Mrg20), resulting in a plant with lower HT2+T2 concentrations than either parent in autumn sowings. Autumn is the typical timing for these winter oat lines.

The Mrg11 QTL had no detectable impact on the HT2+T2 concentrations of plants in this set of experiments.

5. Chapter 5: Correlating weather conditions relative to panicle emergence with HT2+T2 concentration in harvested grain

5.1. Introduction

Using weather variables to build prediction models for *Fusarium* disease epidemics has been done in wheat previously (Obst A *et al.*, 2000; Wolf *et al.*, 2005), similarly contamination risk assessments are available for the more commercially important *F. graminearum* and *F. culmorum* in wheat which cause FHB and the associated DON and ZON. The AHDB offer an online resource within the UK for assessing risk of mycotoxin contamination that uses previous crop, cultivation, cultivar, rainfall at flowering, rainfall prior to harvest, T3 fungicide application (at head fully emerged) and region within the UK as risk factors to develop an overall risk score (AHDB, Not dated). That particular risk score is used on grain passports but several of those factors can be used as decision aids for whether or not to apply a fungicide such as Prothioconazole at or just before flowering to protect against FHB.

Similar risk factors have been highlighted by researchers on *F. langsethiae* (previous crop, cultivation/debris management, cultivar) (Hofgaard *et al.*, 2016a; Edwards, 2017; Schöneberg *et al.*, 2018). Rain at flowering remains a large risk factor for FHB on wheat (Parry *et al.*, 1995; Trail *et al.*, 2001) but its effect on the activity of *F. langsethiae* is less clear; outdoor artificial inoculation utilising misting irrigation at flowering, for instance, has unreliable results (Imathiu, 2008; Schöneberg *et al.*, 2019). In earlier work, Edwards and Jennings (2016) looked at rainfall during predicted panicle emergence of oat crops in the UK from the 2014 harvest and found a weak positive, but significant ($P=0.025$) correlation between rainfall and HT2+T2 concentration ($r^2 = 0.35$). There is, however, no remedial action that a grower can currently undertake, such as applying a fungicide (Edwards and Anderson, 2011), were a high risk to be identified.

Edwards (2017) found a negative correlation between harvest rainfall and HT2+T2 concentration in harvested oats from samples taken between 2002 and 2008. The regression used a weighted average favouring rainfall in July in addition to August rainfall and achieved a significant relationship ($P=0.008$) which accounted for 74% of the variation in HT2+T2 concentrations.

Window-pane analysis is the method of examining relationships between an independent variable over a discrete period of time (the window-pane) with the dependant variable, for each independent variable reported in a data set. Summarised values of the independent variable over discrete time frames (window-panes) are then

correlated against the dependant variable; multiple correlations of different window-pane sizes and time frames can be conducted to establish the optimum window-pane.

A window-pane analysis with respect to weather is one that summarises environmental variables such as daily temperature and rainfall over discrete time frames and then correlates those summarised values with the dependent variable of interest, in this case the HT2+T2 concentration in the harvested oat grain. With respect to understanding the epidemiology of a plant pathogen the objective of a window-pane analysis of weather data is to examine multiple crops, each with unique weather preceding and following potentially important growth stages, be that through different crop locations or crops arriving at growth stages at different times at the same location. Then those weather variables for the window-panes can be correlated to the infection of the crop.

Work has previously been conducted using window-pane analysis of weather variables on FHB. Kriss *et al.* (2010) used data collected from Ohio, Indiana, Kansas and North Dakota over several decades. Their analysis was based on an ordinal score of FHB severity for each season relative to the previous seasons, the scale was 0 to 9 and reflected disease levels and yield losses. The window-panes initially examined ranged from the sowing of the crops to maturity (280 days) to 10 days, but the highest correlations were found for windows of between 10 and 30 days. The best correlations were between infection and moisture-related variables such as RH and daily total rainfall for windows approximately 60 days prior to maturity, described by the authors as surrounding anthesis. The specific *Fusarium* species were not identified for each year and will likely have been a mix with the predominant species being *F. graminearum*.

Several studies have attempted to associate weather conditions such as humidity, rainfall and temperature with HT2+T2 concentration in commercially grown oat crops. Xu *et al.* (2014) used 300 samples from UK oats with agronomic data and environmental data to identify conditions at key periods within the growing season. The data in Xu *et al.* (2014) study did not have growth stages of the oats regularly recorded, so the key growth stages of interest had to be predicted. Panicle emergence was predicted as occurring in mid to late May. However, there would likely be a wide range of growth stages ranging from booting, panicle emergence and the beginning of flowering depending on sowing date, latitude, and variety, during the window assigned to panicle emergence. The findings indicated that wet weather in early to mid-May, and warm and dry weather from that point on, correlated with high HT2 + T2 concentrations in oats. Hjelkrem *et al.* (2018) estimated phenological windows in 188 fields of oats in Norway, along with weather variables recorded at weather stations

within 20 km of the farm addresses, which were then used to correlate weather variables with HT2+T2 concentration in the harvested grain. The study found that in the lead up to flowering (booting) cool (<12°C) or moderate (10-20°C) temperatures coupled with humid conditions correlated with higher HT2+T2 concentrations. High temperature and high humidity were seen to be negatively correlated to HT2+T2 concentration. Conditions during flowering were not found to correlate to HT2+T2 concentrations, but high humidity and high temperatures during the early milk stage (GS70-75) were found to correlate to higher HT2+T2 concentrations at harvest. The analysis also identified that high temperatures and low humidity could negatively impact the concentration of HT2+T2 if they occurred during dough development. Kaukoranta *et al.* (2019) also examined the relationship between weather and growth stage in terms of HT2+T2 concentration in 804 spring oat crops in Norway, estimating the date of mid-anthesis (GS65). They determined that warm weather from four weeks preceding mid anthesis up until harvest, and humid conditions in the two weeks leading up to mid anthesis, were the most important climatic factors in terms of *F. langsethiae* infection.

Some of the above studies report conflicting results; Kaukoranta *et al.* (2019) identified anthesis as a key growth stage whereas Hjelkrem *et al.* (2018) did not identify anthesis itself as important rather the growth stages surrounding it. Both Xu *et al.* (2014) and Kaukoranta *et al.* (2019) found that warm dry conditions after flowering through until harvest led to higher HT2+T2 concentrations, but Hjelkrem *et al.* (2018) stated the opposite, instead suggesting that such conditions reduced HT2+T2 concentrations when they occurred during dough development (GS80-90).

Rain in early to mid-May could be transporting microconidia from the ground to the panicle through rain splash (Paul *et al.*, 2004). Rain splash has been demonstrated to be capable of carrying spores as high as 100 cm within a cereal canopy (Jenkinson and Parry, 1994). The angle of travel could also provide dispersal upwards into the downward facing glumes and florets.

5.2. Method

This experiment makes use of the NIL samples and their recorded panicle emergence dates detailed in Chapter 4. The HT2+T2 results for each experiment were averaged across reps and +1 log transformed to generate one value per genotype per year per sowing season. Only genotypes that appeared in the data a minimum of three times and only genotypes from the NIL population were used in the analysis.

Hourly maximum and minimum air temperature and daily relative humidity and rainfall data was compiled from the Harper Adams weather station located approximately 1 km

from the experimental site. Degree hours for the pathogen's growth were calculated. Previous laboratory work has reported (Medina and Magan, 2010) that the optimum temperature for the growth of *F. langsethiae in vitro* is 25°C, however neither site frequently recorded temperatures above 25°C, so 20°C was used for the calculation of degree hours. Similar work reported that the optimum temperature for HT2+T2 production was 15°C (Kokkonen *et al.*, 2010). Overall, the degree hours were divided into four groups: <15°C (L15DH), ≥15°C (G15DH), <20°C (L20DH) and ≥20°C (G20DH).

Window-pane size was chosen as one through to 30 days, beginning at panicle emergence for each individual genotype/year/sowing season, based on previous work of the same nature (Xu *et al.*, 2014). Panicle emergence was the only growth stage recorded. A window-pane either preceded panicle emergence or followed it, the days over which a window pane existed was unique for each genotype as the it was dictated by that genotypes panicle emergence date.

Average values for each environmental variable for each window-pane length were calculated using the `cummean()` function in R version 4.0.4 (R Core Team, 2020) and used to plot against the average HT2+T2 concentrations for each genotype. Pearson correlation coefficients and associated P values were taken from those plots. The analysis is presented as a plot of the Pearson correlation coefficients for each window length against average HT2+T2 concentration for each environmental variable. Computational work was conducted by Xiangming Xu (NIAB EMR).

5.3. Results

In the four years where the NIL were observed, the duration of flowering time varied between year and sowing season. The intensity of plots recorded as having reached panicle emergence in each year is detailed in Figure 5.1. In 2018 the difference in days between the autumn sowing undergoing panicle emergence and the spring sowing starting panicle emergence was approximately 20 days. Autumn sown plots had narrower periods over which plots underwent panicle emergence, showing the NIL were more similar in terms of growth stage.

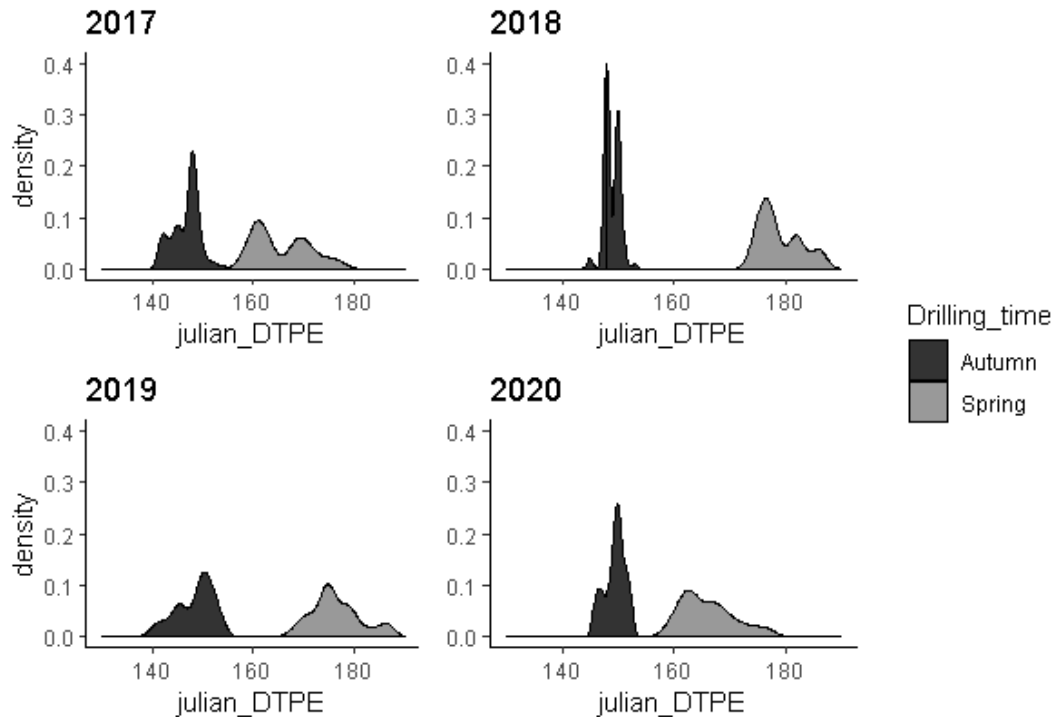


Figure 5.1: Density plots describing the variation in the durations of panicle emergence for each year in spring and winter from 2017 to 2020. Only genotypes that appeared in every year are included. The x axis uses Julian days to panicle emergence, measured in days.

When looking at the correlation coefficients for both average air temperature and degree hours above 20 and 15 degrees post panicle emergence with HT2+T2 in Figure 5.2 and Figure 5.3, they increase up to window lengths of seven days ($r = 0.53$, $r = 0.60$, $r = 0.45$ respectively) and then remain relatively consistent but increasing up until window lengths as long as 30 days ($r = 0.57$, $r = 0.63$, $r = 0.60$ respectively). All correlations for temperature, and degree hours above 20 and 15 degrees, post panicle emergence, were significant ($P < 0.0004$). For pre-emergence of the panicle, degree hours $> 20^\circ\text{C}$ was more strongly correlated to HT2+T2 accumulation than temperature alone or for degree hours over 15 degrees, largely plateauing by seven days. Pre-emergence temperature reached its highest correlation coefficient values between the 27 and 30 day length window-panes of $r = 0.46$. Degree hours $> 20^\circ\text{C}$ reached $r = 0.73$ for 22 day length windows-panes pre panicle emergence and remained above $r = 0.70$ thereafter.

Average rainfall did not correlate strongly for any window length pre-emergence of the panicle, with a maximum correlation coefficient of $r = -0.24$ for a two day window-pane. Post emergence rainfall negatively correlated with HT2+T2 concentration increasing to $r = -0.70$ by 30-day length window-panes.

The correlation between average relative humidity and T2+HT2 for post panicle emergence starts positive for short window-panes immediately after panicle emergence

reaching a maximum of $r = 0.20$ for three-day long window panes, but for longer window-panes increasingly became negative, $r = -0.62$ for 30 day window-pane lengths. The strongest correlation post panicle emergence was for a window-pane 30 days long. Pre-panicle emergence relative humidity had a weak positive correlation for the shortest window-panes but increased with increasing window-pane length to reach $r = 2.5$ at 20 day window pane lengths.

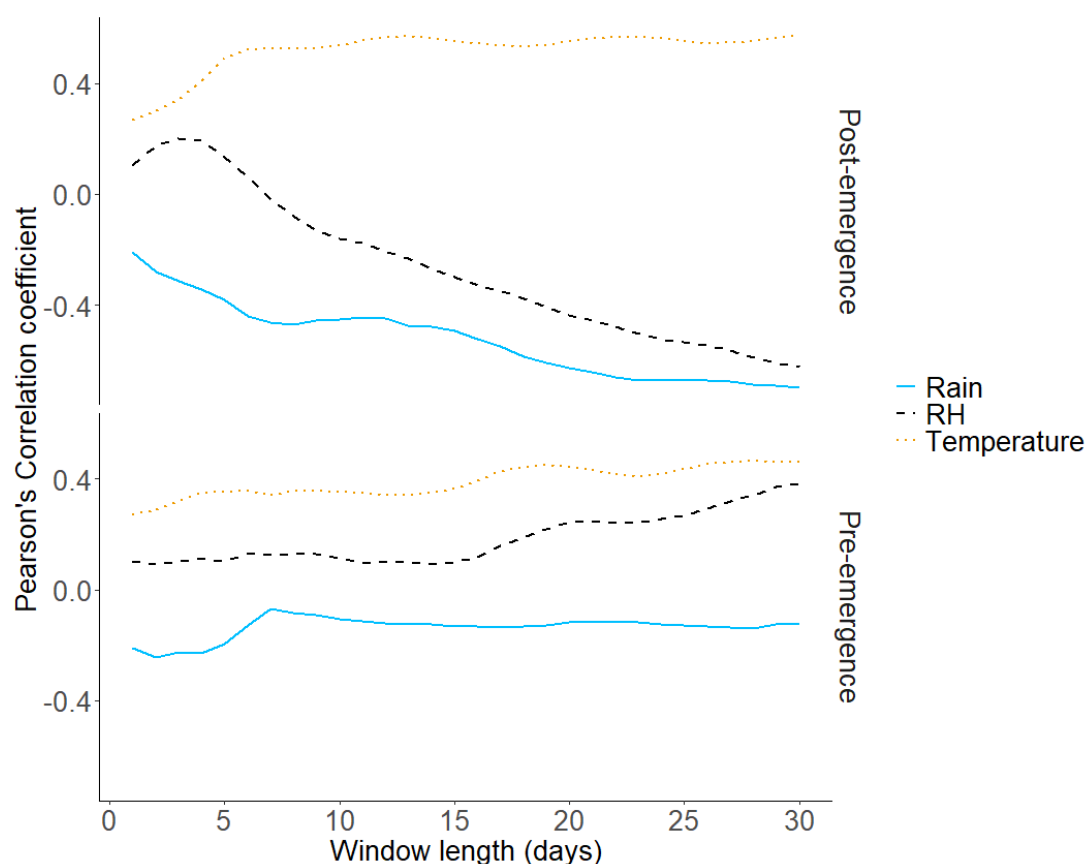


Figure 5.2: Pearson correlation coefficients plotted for average rainfall, average relative humidity, and average air temperature against each window-pane length for pre- and post-panicle emergence.

Growing degree hours accumulated above 20 and 15 degrees were positively correlated with HT2+T2 concentration and growing degree days below 15 and 20 degrees were correlated negatively (Figure 5.3).

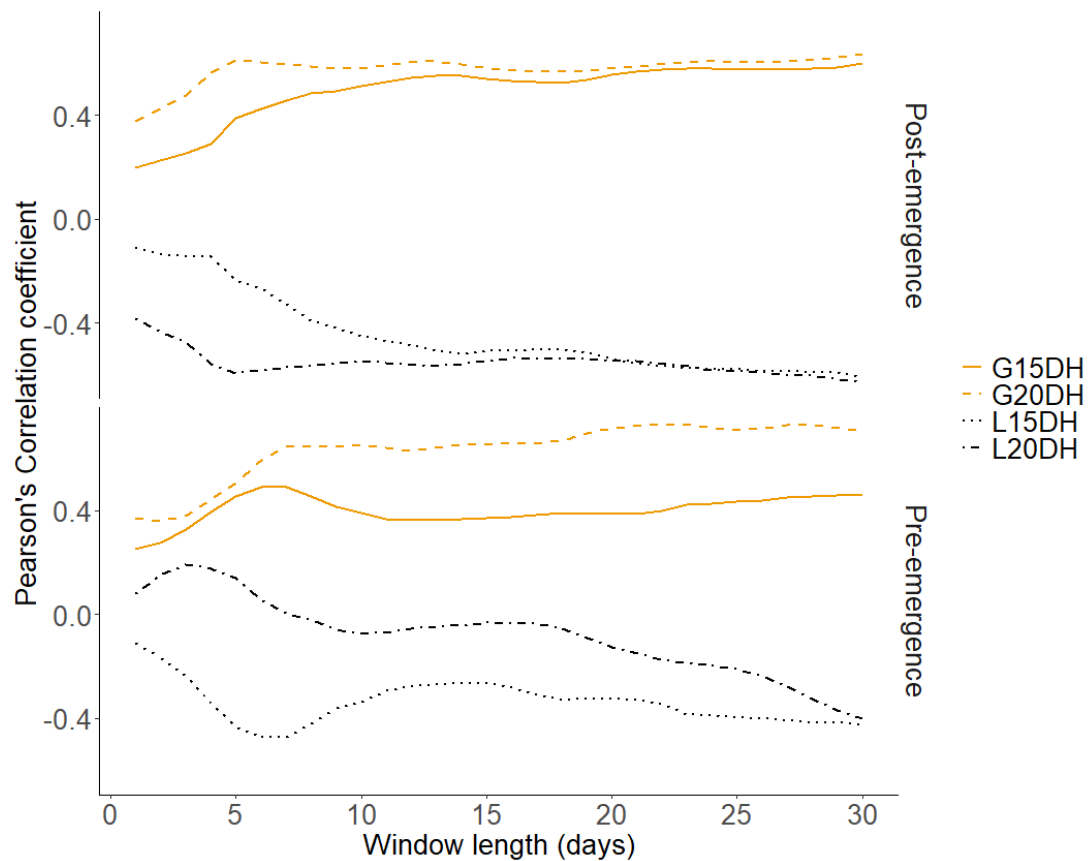


Figure 5.3: Pearson correlation coefficients for growing degree hours categories: $<15^{\circ}\text{C}$ (L15DH), $\geq 15^{\circ}\text{C}$ (G15DH), $<20^{\circ}\text{C}$ (L20DH) and $\geq 20^{\circ}\text{C}$ (G20DH) with HT_2+T_2 average concentrations plotted against each window-pane length for pre- and post-panicle emergence.

When the analysis is looked at by year, clear relationships become harder to identify (Figure 5.4 and Figure 5.5): the negative correlation of rainfall in post panicle emergence is weaker in most years, or only occurs for certain window lengths, but is very strong in 2019 up until 29 days after which it weakens again.

In 2018 temperature post panicle emergence had correlation coefficients close to zero for all lengths of window-pane pre and post emergence of the panicle. This was reflected in the growing degree hours correlations. Whereas 2019 and 2020 were more consistent in having positive correlations post panicle emergence for temperature. Pre-panicle emergence temperature was inconsistent across years and for either >20 degree hours or >15 degree hours, only 2019 showed a positive correlation. The remaining years showed very weak correlations.

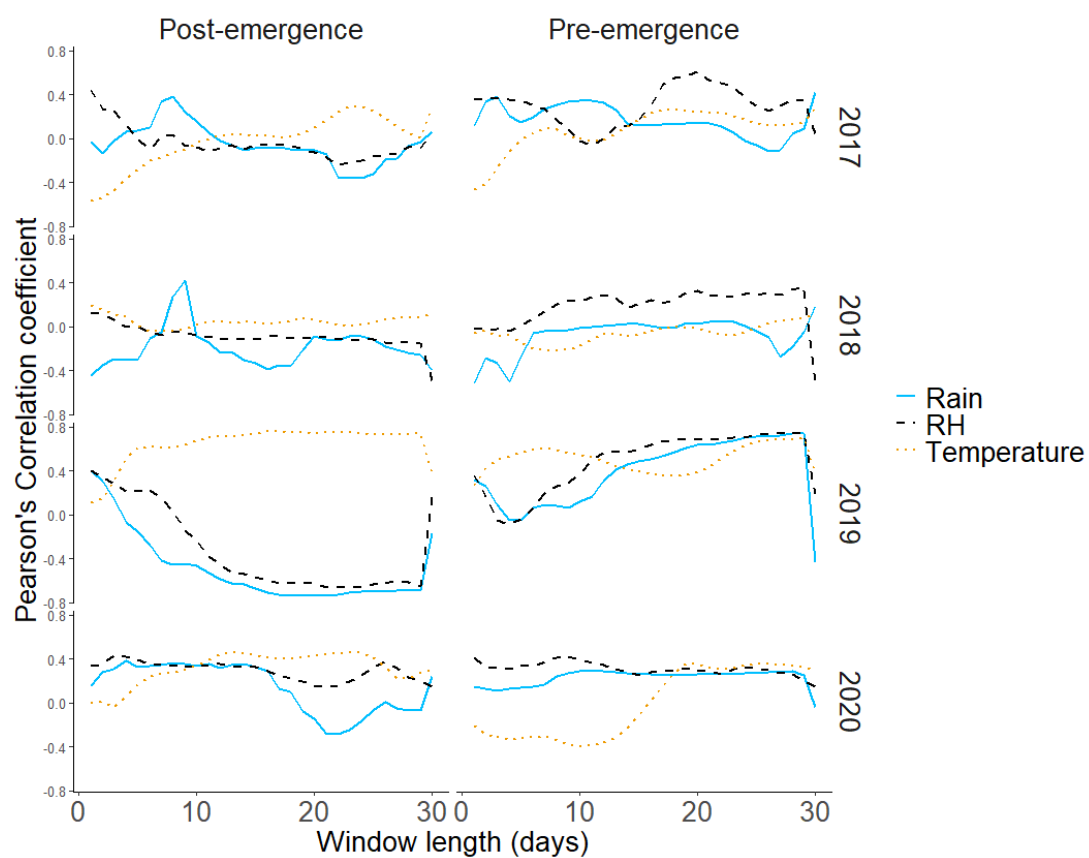


Figure 5.4: Pearson correlation coefficients plotted for rain, relative humidity, and temperature against each window-pane length for pre- and post-panicle emergence. Different panels represent the individual years in which the plots were grown as labelled on the right-hand side of the figure.

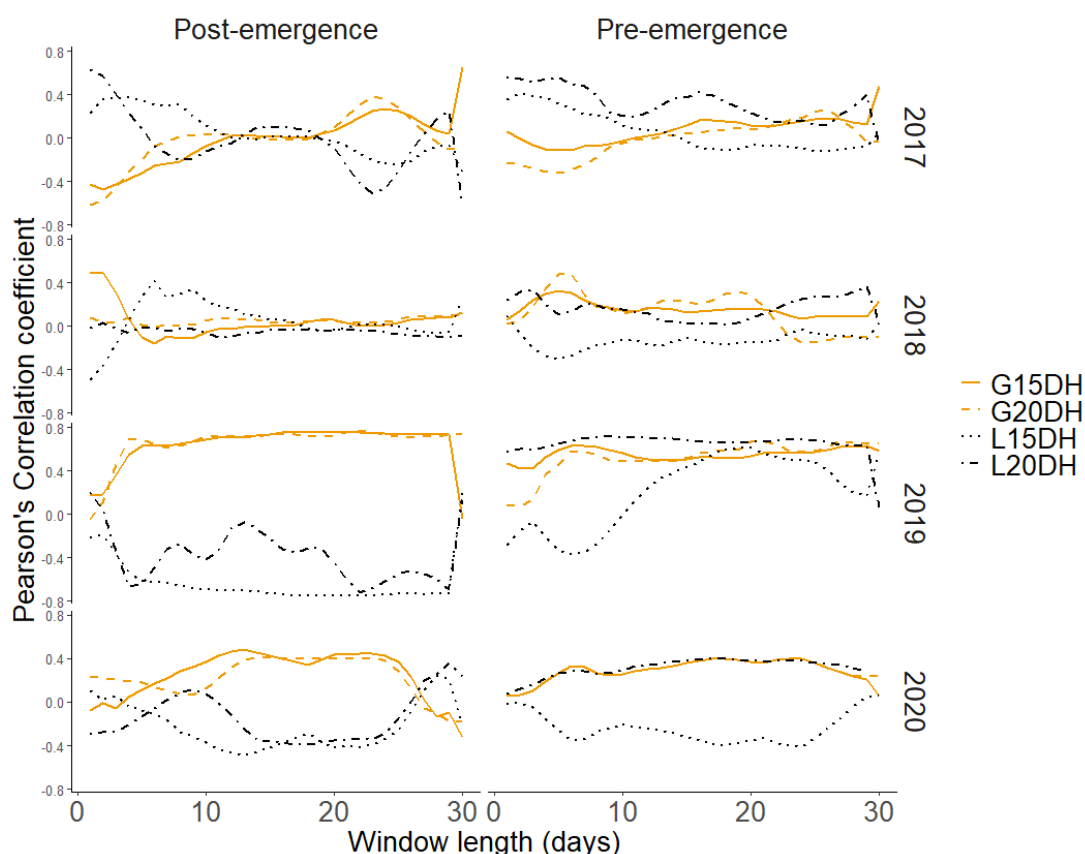


Figure 5.5: Pearson correlation coefficients plotted for the growing degree hours categories: $<15^{\circ}\text{C}$ (L15DH), $\geq 15^{\circ}\text{C}$ (G15DH), $<20^{\circ}\text{C}$ (L20DH) and $\geq 20^{\circ}\text{C}$ (G20DH) plotted against each window-pane length for pre- and post-panicle emergence. Different panels represent the individual years in which the plots were grown as labelled on the right-hand side of the figure

5.4. Discussion

The strong negative correlation between rainfall and HT2+T2 concentration by the 30 day length window-pane post panicle emergence presented in this work from the across all years analysis and the positive correlation of temperature post panicle emergence for window-panes up to 30 days agrees with the findings of Xu *et al.* (2014) in that dry warm weather after anthesis is correlated to higher HT2+T2 concentrations. Bjørnstad and Skinnes (2008) state that *F. langsethiae* is more common in dry years in Norwegian and Finnish oats, while a wet year is more likely to have *F. culmorum* infection. For pre-emergence of the panicle degree hours $> 20^{\circ}\text{C}$ was more strongly correlated to HT2+T2 accumulation than temperature, which supports the findings of Medina and Megan (2010) that higher temperatures approaching 25°C are supportive of *F. langsethiae* growth.

Xu *et al.*, 2014 also concluded that warm wet weather in early to mid-May correlated strongly with higher HT2+T2 concentrations prior to anthesis. To compare that finding to this work is difficult as Xu *et al.* (2014) used calendar months rather than specific growth stages and the spring sown NIL plots emerged as late as July in 2018 but generally about 20 days later than the autumn sown plots. However, very low

correlations for rainfall were found prior to panicle emergence, although for relative humidity, correlations were stronger for window-panes prior to panicle emergence of lengths greater than 16 days, after which correlations achieve significance ($P < 0.02$). Eventually at 30 day length window-panes achieve a correlation coefficient of $r = 0.38$ ($P < 0.001$).

Kaukoranta *et al.* (2019) and Hjelkrem *et al.* (2018) found that humid conditions in the two weeks prior to mid anthesis were important to high infection. The study presented here did not find strong correlations between higher relative humidity values in the two weeks prior to panicle emergence; a positive significant ($P < 0.02$) correlation existed for window-panes between 17 and 30 days but never exceeded $r = 0.38$. Kaukoranta *et al.* (2019) also concluded that warm conditions in the four weeks leading up to mid anthesis were related to higher *F. langsethiae* infection, a finding which is supported by the current work where the degree hours $> 20^{\circ}\text{C}$ had a strong positive correlation for window-panes between three to four weeks prior to panicle emergence.

Hjelkrem *et al.* (2018) also analysed later growth stages not examined in the presented analysis. Milk development (GS70-79) and dough development (GS80-89) was also analysed; it was seen that high humidity and high temperatures during milk development was associated to higher HT2+T2 concentration but that during dough development high temperature and low rainfall were associated with lower HT2+T2 concentrations. It has been demonstrated that *F. langsethiae* can grow on dry ripe oat grain and continue to produce HT2+T2 (Mylona and Magan, 2011), as is also the case for *F. graminearum* and DON in wheat (Odenbach, K. J. 2009)

Panicle emergence has been used as a proxy for anthesis in this work due to the difficulty in identifying the time of anthesis in oats. As such it is difficult to compare with confidence studies that use different but chronologically close growth stages such as anthesis compared to panicle emergence, as is the case with Kaukoranta *et al.* (2019) and Hjelkrem *et al.* (2018).

Hjelkrem *et al.* (2018) did not include sites with HT2+T2 below the limit of detection for fear of those sites not having inoculum present. Variation between year and site in previous work has potentially been influenced by the presence of inoculum. The presence of *Fusarium* species can be influenced by the crop species, level of decomposition of crop residue, and the soil biota (Edwards, 2017; Hofgaard *et al.*, 2016a). In the present study, the close proximity and uniform management of the plots coupled with HT2+T2 having been detected in all years, means that there is high confidence that inoculum was available to all plots in all years. The final two years (2019 and 2020) had been ploughed prior to sowing and then had spring wheat straw

from the other side of the field applied to the soil surface prior to plant emergence and these years had lower HT2+T2 concentrations than the first two.

The time period over which panicles emerged across the four years varies, likely due to the weather, specifically temperature. A short panicle emergence time frame such as that of the autumn sown 2018 plot produced window-panes covering very similar time frames for each genotype and therefore less variation to correlate against the HT2+T2 concentration. However, the differences in the spring and autumn sown plots provides a greater range of conditions through wider time frames over which plants can undergo panicle emergence and so adds strength to the analysis.

Previous studies of a similar nature (Hjelkrem *et al.*, 2018; Kaukoranta *et al.*, 2019) have often reported and interpreted previous research associating growth stages and weather conditions by use of singular growth stage descriptions for any one moment in time. However, growth stages often occur concurrently; head emergence and flowering can occur simultaneously and flowering in oats can take sufficiently long that earlier spikelets are arguably in early milk.

Although this analysis can be viewed alongside previous similar work, it does not provide conclusive answers to the conditions that could predict a *F. Langsethiae* epidemic. The failure for better consensus between the four studies (Xu *et al.*, 2014; Hjelkrem *et al.*, 2018; Kaukoranta *et al.*, 2019 and the present) could be attributed to different techniques, different pathogen populations in the regions within which they were conducted (Hjelkrem *et al.*, 2018 and Kaukoranta *et al.*, 2019 were conducted in Scandinavia), and all studies having inadequate sample sizes combined with being conducted over too few years. In the present study there is little similarity between each year when they are examined on their own, however as was seen in chapter 5 the average concentrations of HT2+T2 varied a great deal from year to year, as was seen in Stančić (2016). Studies do not agree on all aspects of the conditions that lead to higher HT2+T2 concentrations. Constants that do emerge are that the pathogen prefers warmer conditions and that rainfall post-anthesis leads to lower HT2+T2 concentrations.

6. Chapter 6: Spatial distribution

6.1. Introduction

One important question with regards to oat resistance to *F. langsethiae* is whether the fungus grows through the pedicels of the panicle. Stančić (2016) recorded higher mycotoxin concentrations of the entire panicles compared to the harvested grain, and Opoku (2012) also recorded high concentrations of HT2+T2 in panicle structures. Brown (2015) has shown that within wheat, *F. graminearum* moves from one spikelet down the peduncle into the rachis and up into other spikelets by hyphal growth. For the same to be true in oats, the hyphae would need to grow much further to reach the rachis. Langevin *et al.* (2004) compared six cereal crops in terms of their Type II resistance by using point inoculations of *F. graminearum* on single spikelets and found that in the oat accessions, the infection never spread beyond the first floret and concluded that *F. graminearum* infection is unlikely to move from one spikelet to another within the oat panicle. However, it has been speculated that longer branches on oat panicles will increase Type II resistance to *Fusarium* (Bjørnstad and Skinnies, 2008). Loskutov *et al.* (2016) using principle component analysis of genotypes from four species of oat, suggested that an increase in panicle length along with lateness, a decrease in plant height, resistance to lodging and resistance to other plant diseases, was detrimental to *Fusarium* resistance in oats. The *Fusarium* species was not defined, only that the pathogen should produce DON or T2 and be observed on PDA (Loskutov *et al.*, 2016). Loskutov also found through the same analysis that plants with equilateral (branches on all sides) rather than unilateral panicle shapes (branches only occurring on one side of the panicle) were less likely to be susceptible to *Fusarium* infection.

To date the distribution of *Fusarium* species within cereal fields has had limited research undertaken upon it. Investigations have been made into the distribution and make up of FHB causing pathogens on wheat (Schlang *et al.*, 2008; Xu *et al.*, 2008; Oerke *et al.*, 2010; Müller *et al.*, 2011). Frequently the distribution of FHB causing species has been seen to be random and sampling points independent of one another (Schlang *et al.*, 2008; Xu *et al.*, 2008; Oerke *et al.*, 2010). Such results are indicative of inoculum being dispersed by wind-blown spores (Xu *et al.*, 2008). All such research has indicated the wide range of infection incidence and mycotoxin concentrations within fields of wheat. Müller *et al.* (2011) was able to consistently show a difference in hilltop sites as compared to sites in depressions in terms of their DON and ZON concentrations. It was hypothesized that those differences were induced by moisture conditions being more favourable to *Fusarium* species in the depressions. No work has been published to date on the spatial distribution of HT2+T2 within a crop of oats.

Two studies were conducted to identify the spatial distribution of *F. langsethiae* on an oat crop. Firstly, at the level of individual panicles and secondly at the field level with samples taken from a grid. In some years it was possible to return to the same grid points two years later to identify whether any pattern persisted across non-consecutive years.

6.2. Methods

6.2.1. Panicle dissection

Two genotypes were selected from the 2018 harvest sown in autumn 2017 that represented two extremes within the NIL population. The first was the Tardis + B Mrg04 (the shortest variety in the population) and the other was Buffalo + T Mrg04 (the tallest NIL). Panicle size (defined as the distance from the lowest whorl to the top of the plant) was measured in all plots grown at Harper Adams University after 2017. The two NIL chosen also had the smallest and largest panicles respectively. In 2018 grain of the Tardis + B Mrg04 had an average concentration across replicates of 1486 µg/kg, the value for the plot from which the panicle was sampled was 1269 µg/kg. In the same year, grain of the Buffalo + T Mrg04 had an average concentration of 172 µg/kg and the plot from which the plant was sampled had a concentration of 168 µg/kg.

Each of the four panicles were mapped, each whorl was labelled and every branch from that whorl was measured in length. The distance to each branching point of each branch was measured so that a scale drawing could be made of each panicle and the distance between spikes calculated. Each spikelet (including glumes) was placed in an Eppendorf tube and labelled with its position on the panicle.

DNA extraction was carried out on each entire spikelet in accordance with the methodology laid out in Edwards *et al.* (2012a) and described in Chapter 2. The weight of each individual spikelet was measured and used to calculate the total *F. langsethiae* DNA present in each spikelet. Scale drawing were produced to visualise the distribution of infected spikelets across the panicles. Once infected spikelets had been identified and the concentration of *F. langsethiae* measured, the distance (in branch length) between each infected spikelet and every other spikelet within the same whorl was calculated along with the difference in their respective *F. langsethiae* DNA concentrations. It was assumed that the pathogen would not move between whorls via the main culm. Distance and the difference in *F. langsethiae* DNA concentration were plotted and the correlation coefficient calculated.

6.2.1. Single grain DNA extraction

Single spikelets stored in labelled 2 ml Eppendorf tubes were milled within the same Eppendorf tubes with a single 6.5 mm diameter ceramic bead for 30 seconds using a

3M RotoMix (Sicherung, Germany); 0.8 ml of CTAB was added to each sample in the same tube and shaken for one minute. The CTAB suspension was incubated for one hour at 65°C and then spun at 6000 G for 10 minutes.

As much of the supernatant as possible was pipetted out from the tubes into 1.5 ml Eppendorf tubes and 0.2 ml of 5 M potassium acetate was added before the sample was vortexed and frozen at -20 °C for a minimum of one hour. Once thawed to room temperature 0.7 ml of chloroform was added and mixed for one minute by gentle inversion, then spun at 6000 G for a further 10 minutes.

The aqueous layer was then collected into fresh 2 ml Eppendorf tubes and 0.8 ml of 100% isopropanol added. The mix was shaken for one minute and incubated for one hour at room temperature before being spun at 6000 G for a further 10 minutes.

The supernatant was discarded, and the resultant pellet was washed with 1 ml of 44 % isopropanol for 45 minutes before being spun again. The pellet was then dried overnight. The pellet was resuspended in 0.2 ml of TE buffer (10 mM Tris–HCl, 1 mM EDTA, pH 8.0) and incubated at 65 °C for one hour, vortexed and spun down at 6000 G for 10 minutes.

A Nanodrop spectrophotometer was used to quantify the concentration of the DNA in each sample, which were subsequently diluted to a fixed concentration of 20 ng/μl. The dilutions for each sample were recorded to calculate the total quantities of DNA in the spikes. DNA concentration in the diluted samples were measured to confirm their concentrations after dilution. Undiluted extracted samples were archived at -20°C. A master mix was prepared using Eva green qPCR mix; 20 μl per sample was analysed as described in Table 6.1.

Table 6.1: The composition of the master mix used in the single grain DNA quantification.

EVA green	water	F primer	R primer	sample	Total
5 μl	14.9 μl	0.05 μl	0.05 μl	0	20 μl

The prepared 20 ng/μl samples were added to the qPCR master mix described in Table 2.2 on ice and amplified using a Bio-Rad CFX96 T (UK) with 40 cycles: the annealing temperature was 62°C for all cycles. The cycles started with denaturation at 95°C for 15 seconds then annealing for 10 seconds and extension for 30 seconds at 75°C and 82°C for a further 10 seconds.

For standards 10^0 - 10^{-5} dilutions were used in duplicate of a *F. langsethiae* DNA standard. The 10^0 standard was 2.5 ng/μl, a negative control of SDW was also included.

6.2.2. Grid

In 2016-2020 oat samples were taken at harvest from the experimental field Black Britch in which a single variety of oats had been sown (Table 6.2). In 2016, 2018 and 2020, samples were collected from the same side of the field which that year had grown oats. These samples were collected as a grid that covered the entire field; each intersection of the grid was sampled, and the intersections were all 20 m apart from one another. In 2018 and 2020 each GPS location was recorded so that those positions were the same in both years. In 2017 and 2019, on the other side of the field, a much smaller grid was used: the total area examined was 20 x 20 m and within it 36 points were sampled on 4 m intersections. For the 2017 and 2019 years all the positions were recorded using the GPS so that for those two years the intersections of the grid sampled were the same.

Table 6.2: Details for grid dimensions, variety and whether or not GPS locations were stored for each year.

Year	Variety	Grid size	GPS positioned
2016	Gerald	20m	No
2017	Mascani	4m	Yes
2018	Mascani	20m	Yes
2019	Mascani	4m	Yes
2020	Balado	20m	Yes

At each intersection, panicles of all oats were sampled within a 60 cm radius of the marked intersection. Panicles were then threshed and milled before being analysed by ELISA for their HT2+T2 concentration as detailed in Chapter 2.

6.3. Statistical analysis

The DNA values for individual spikelets were broken down into whorls and analysed using the Kruskal-Wallis test to ascertain whether a difference in infection was present between whorls. A parametric test was not possible as transformation on a data set with such a high proportion of zeros failed to achieve a Gaussian distribution. The Wilcoxon rank sum test was used to compare whorls with one another once the Kruskal-Wallis test showed a significant difference ($P < 0.05$).

The Mantel test is a method of evaluating the correlation coefficient between two sets of distances or differences derived from two matrices, for significance. First the

correlation coefficient of the two matrices is calculated by correlating the distances or differences between each matrix's respective positions with one another. Then that correlation coefficient is compared to correlation coefficients generated by randomly permutating one matrix and correlating it to the other. The P value is the proportion of the correlation coefficients derived from the permutations that have a higher correlation coefficient than the original (Zar, 2007).

The results were analysed using the Mantel test and half the maximum number of possible unique permutations were used in the `nrepet` argument. The `mantel.rtest` function from the `ade4` package was used.

6.4. Results

6.4.1. *Panicle dissection*

The mapped panicle of Buffalo + T Mrg04 is displayed in Figure 6.1. Only three spikelets had detectable *F. langsethiae* DNA: these are coloured red and orange. The panicle contained 139 spikelets in total, organised into eight whorls. The red coloured spikelet in whorl 1 had an *F. langsethiae* DNA concentration 12.9 pg/ng; the yellow-coloured spikelet in whorl 2 had 0.01 pg/ng; and the yellow spikelet in whorl 3 had 0.02 pg/ng. A photograph of the panicle is shown in Figure 6.2: the panicle was originally unilateral, although the diagram in Figure 6.1 shows it as equilateral.

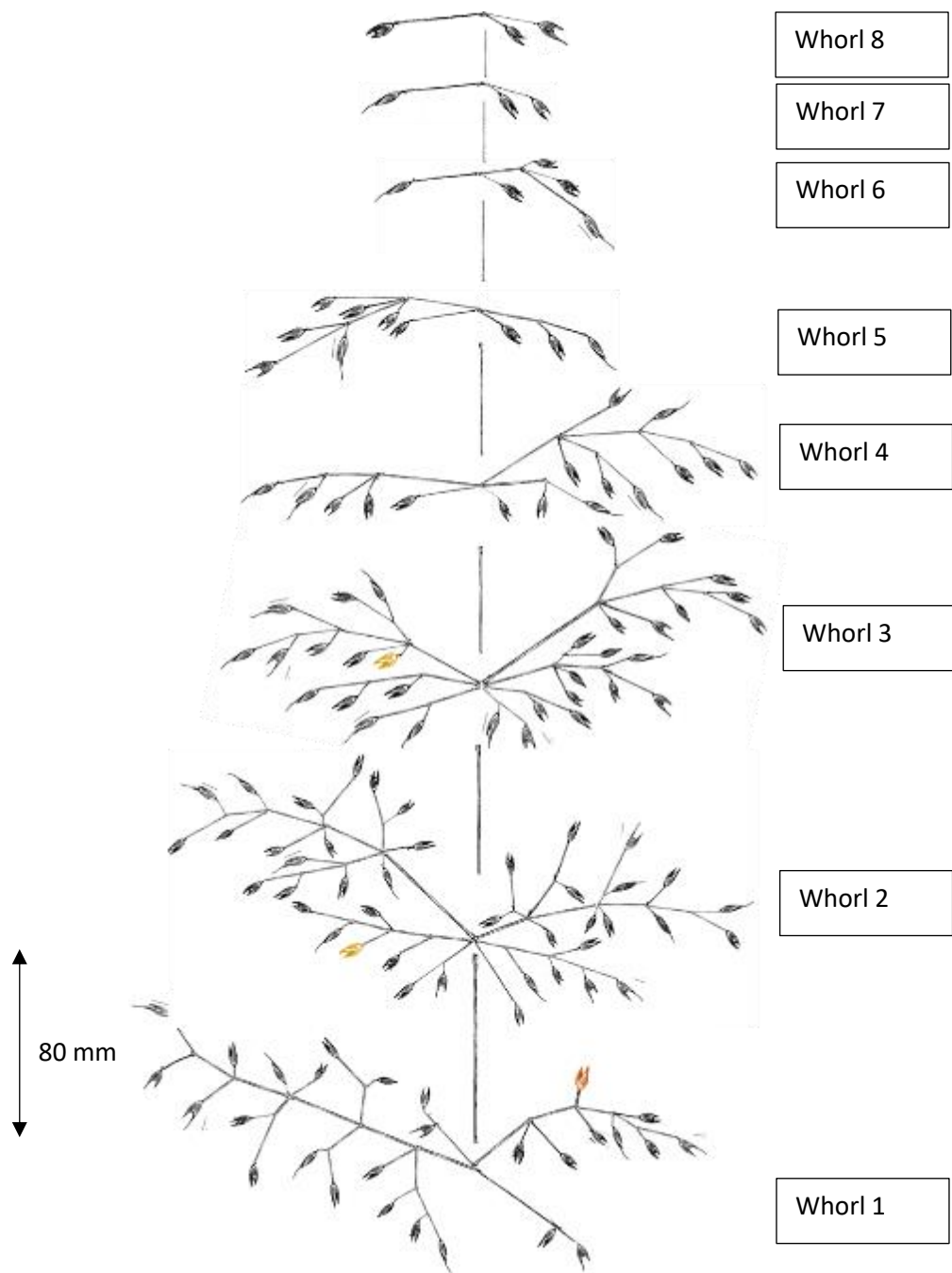


*Figure 6.1: Mapped panicle of Buffalo + T Mrg04. Red spikelets showed detectable *F. langsethiae* DNA at 5 pg/ng or above; yellow spikelets showed detectable *F. langsethiae* DNA at 4.9 pg/ng and below; and black spikelets had no detectable *F. langsethiae* DNA. The panicle has been drawn so that no branches overlap for clarity, the original panicle was not orientated as depicted but instead as shown in Figure 7.2. A scale is present in the bottom left of the diagram. Whorls were counted from the bottom up and are labelled on the right of the panicle.*

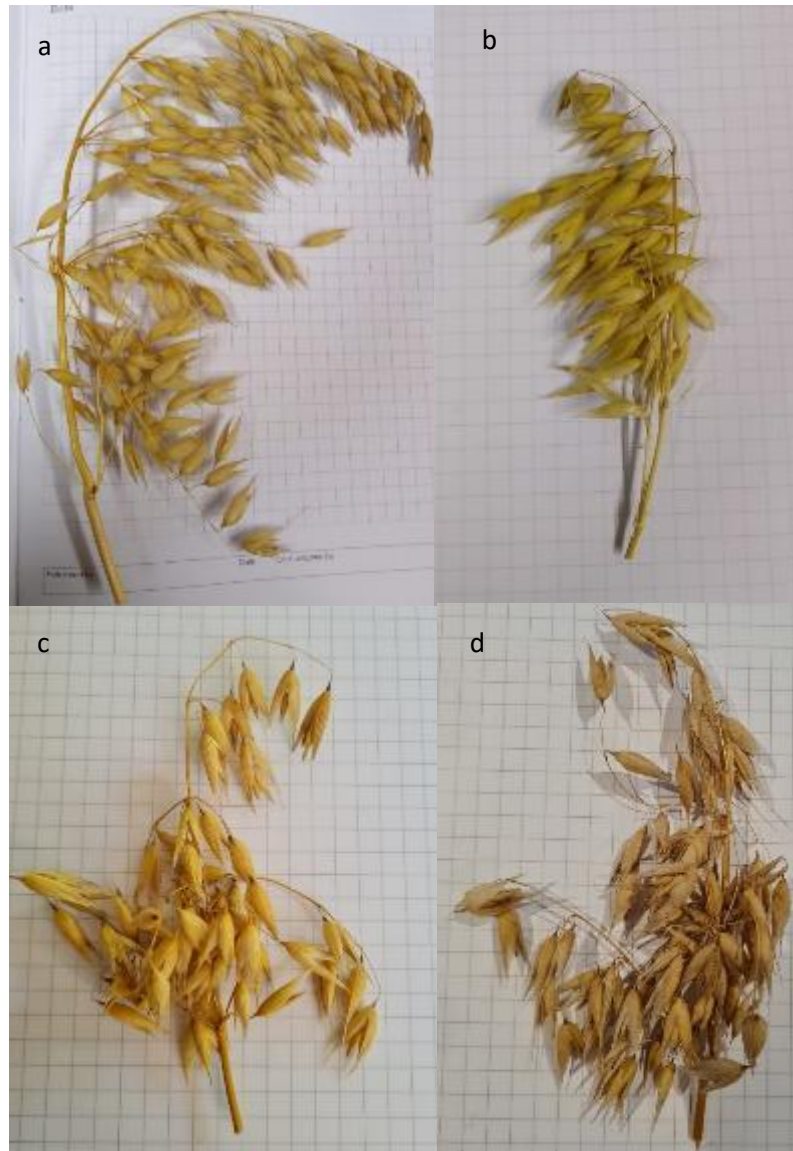


Figure 6.2: **a:** Buffalo + T Mrg04 panicle before it was mapped and dissected (plant 1). **b:** Tardis + B Mrg04 panicle before it was dissected (plant 2). **c:** Tardis + B Mrg04 panicle before it was dissected (plant 3). **d:** Tardis + B Mrg04 panicle before it was dissected (plant 4). Panicles were selected from a larger sample of panicles collected on the day of harvest.

The mapped panicle of Tardis + B Mrg04 (plant 2) is displayed in Figure 6.3b: 18 spikelets had detectable *F. langsethiae* DNA (coloured red and yellow). Originally 47 spikelets were present on the panicle; 44 of these were analysed and presented in Figure 6.3. A photograph of the panicle is shown in Figure 6.2: the panicle was originally unilateral, although the diagram in Figure 6.3 shows it as equilateral.

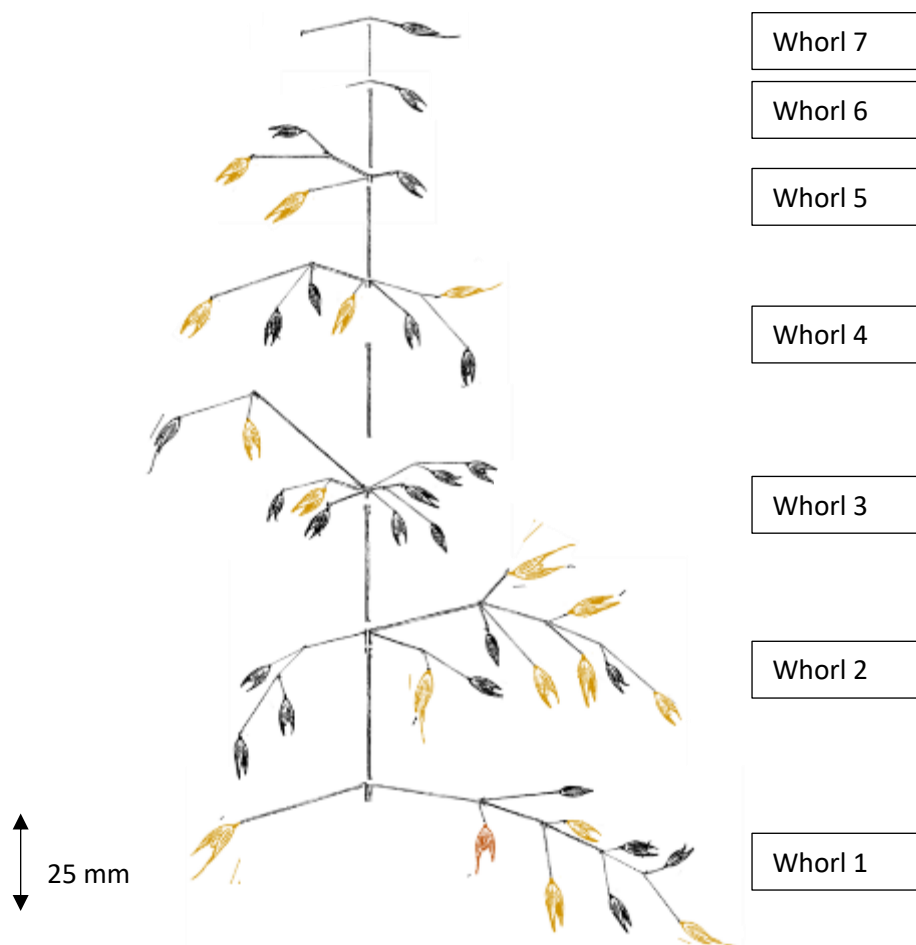


Figure 6.3: Mapped panicle of Tardis + B Mrg04 (plant 2). Red spikelets showed detectable *F. langsethiae* DNA at 5 pg/ng or above; yellow spikelets showed detectable *F. langsethiae* DNA at 4.9 pg/ng and below; and black spikelets had not detectable *F. langsethiae* DNA. The panicle has been drawn so that no branches overlap for clarity, the original panicle was not orientated as depicted but instead as shown in Figure 7.2 b. A scale is present in the bottom left of the diagram. Whorls were counted from the bottom up and are labelled on the right of the diagram.

The mapped panicle of Tardis + B Mrg04 (plant 3) is displayed in Figure 6.4: 32 spikelets had detectable *F. langsethiae* DNA (coloured red and yellow). Sixty four spikelets were present and analysed and presented in Figure 6.4. A photograph of the panicle is shown in Figure 6.2c, the panicle was originally equilateral.

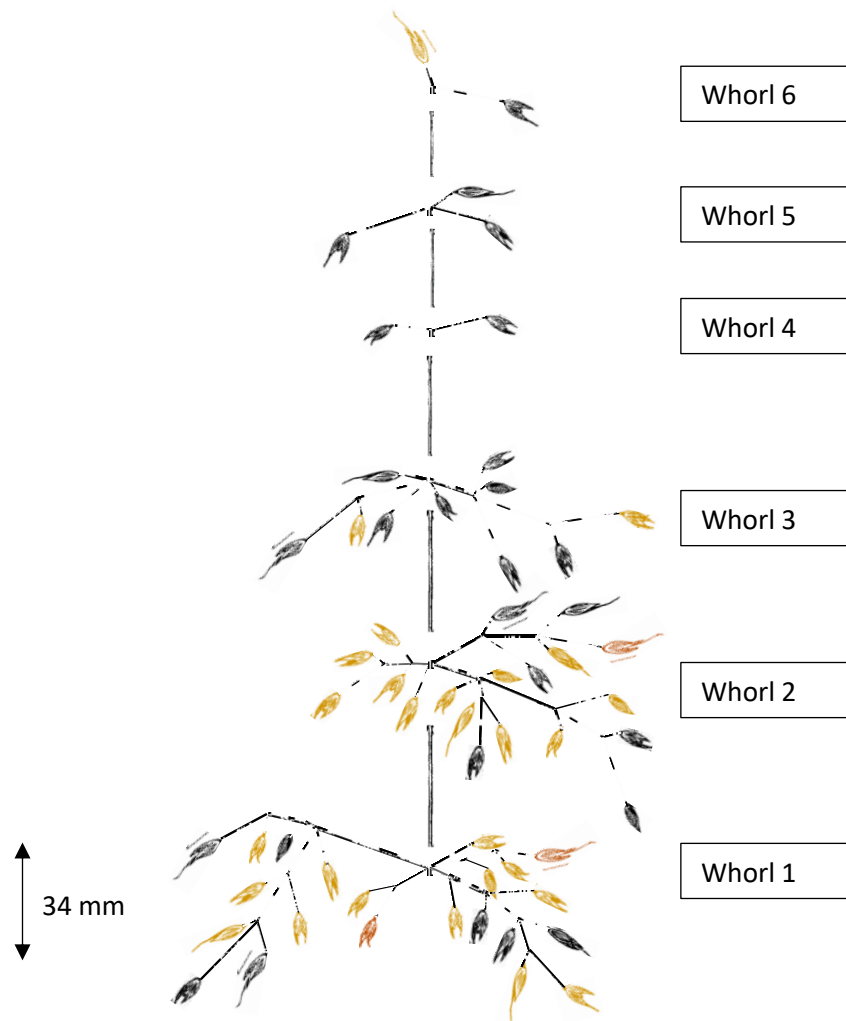


Figure 6.4: Mapped panicle of *Tardis + B Mrg04* (plant 3). Red spikelets showed detectable *F. langsethiae* DNA at 5 pg/ng or above; yellow spikelets showed detectable *F. langsethiae* DNA at 4.9 pg/ng and below; and black spikelets had no detectable *F. langsethiae* DNA. The panicle has been drawn so that no branches overlap for clarity; the original panicle was not orientated as depicted but instead as shown in Figure 7.2 c. A scale is present in the bottom left of the diagram. Whorls were counted from the bottom up and are labelled on the right of the panicle.

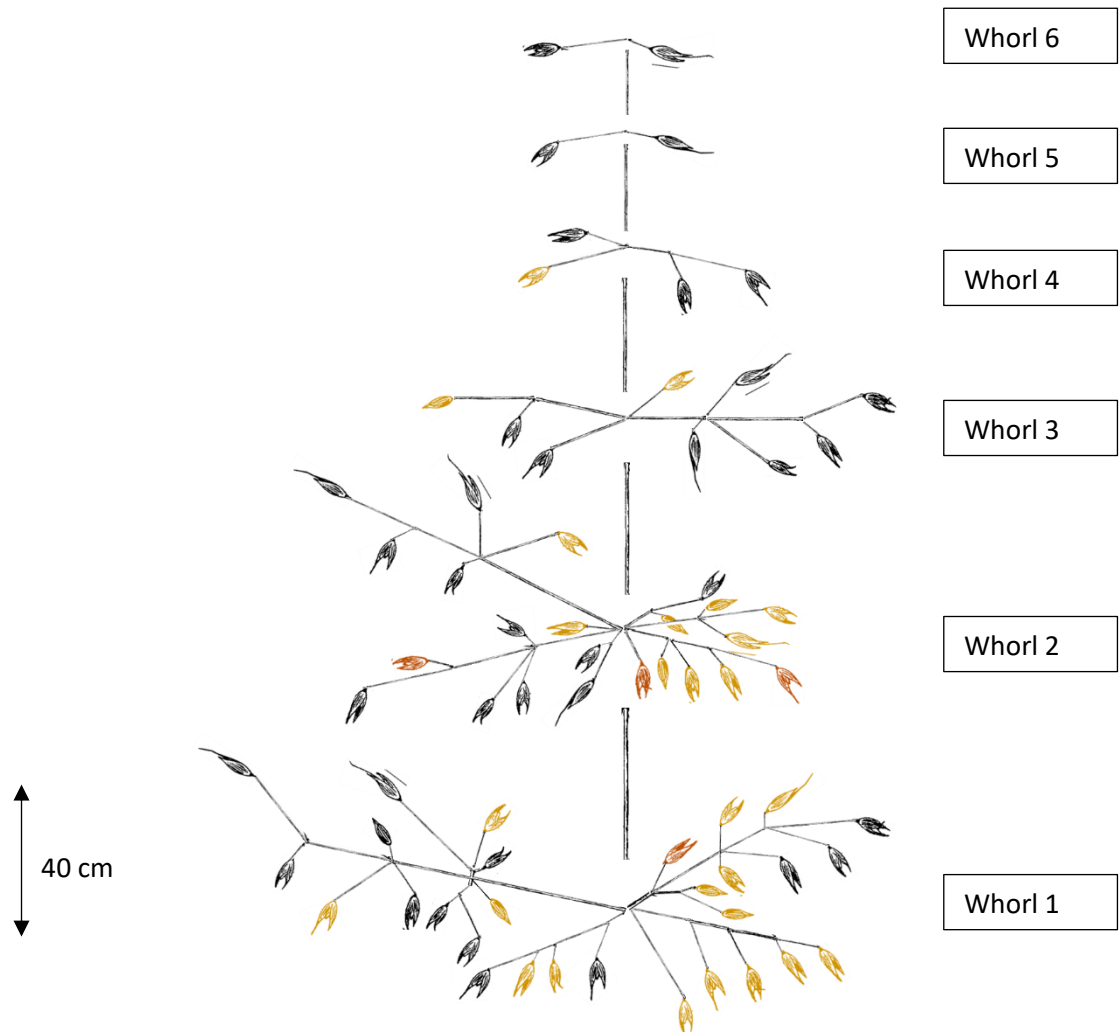


Figure 6.5: Mapped panicle of Tardis + B Mrg04 (plant 4). Red spikelets showed detectable *F. langsethiae* DNA at 5 pg/ng or above; yellow spikelets showed detectable *F. langsethiae* DNA at 4.9 pg/ng and below; and black spikelets had no detectable *F. langsethiae* DNA. The panicle has been drawn so that no branches overlap for clarity; the original panicle was not orientated as depicted but instead as shown in Figure 7.2 d. A scale is present in the bottom left of the diagram. Whorls were counted from the bottom up and are labelled on the right of the panicle.

For panicles 2, 3 and 4, Figure 6.6 shows the plot of the distance between each infected spikelet and all other spikelets within the same whorl plotted against the difference in *F. langsethiae* DNA concentration of the respective spikelet pairs. The Pearson's correlation coefficient for all three panicles together was 0.048 and was not statistically significant ($P = 0.11$). The Pearson's correlation coefficient for plant 2, 3 and 4 distances between spikelets and the difference between *F. langsethiae* DNA concentration in those spikelets were -0.096, 0.093 and 0.008 respectively; the P values were 0.3, 0.06 and 0.9 respectively. Figure 6.6 shows the scatter plot of the differences between individual spikelets in terms of *F. langsethiae* DNA concentration (pg/ng) against their respective branch distances from one another for plant 2, 3, and 4. Too few of plant 1's spikelets were infected to include.

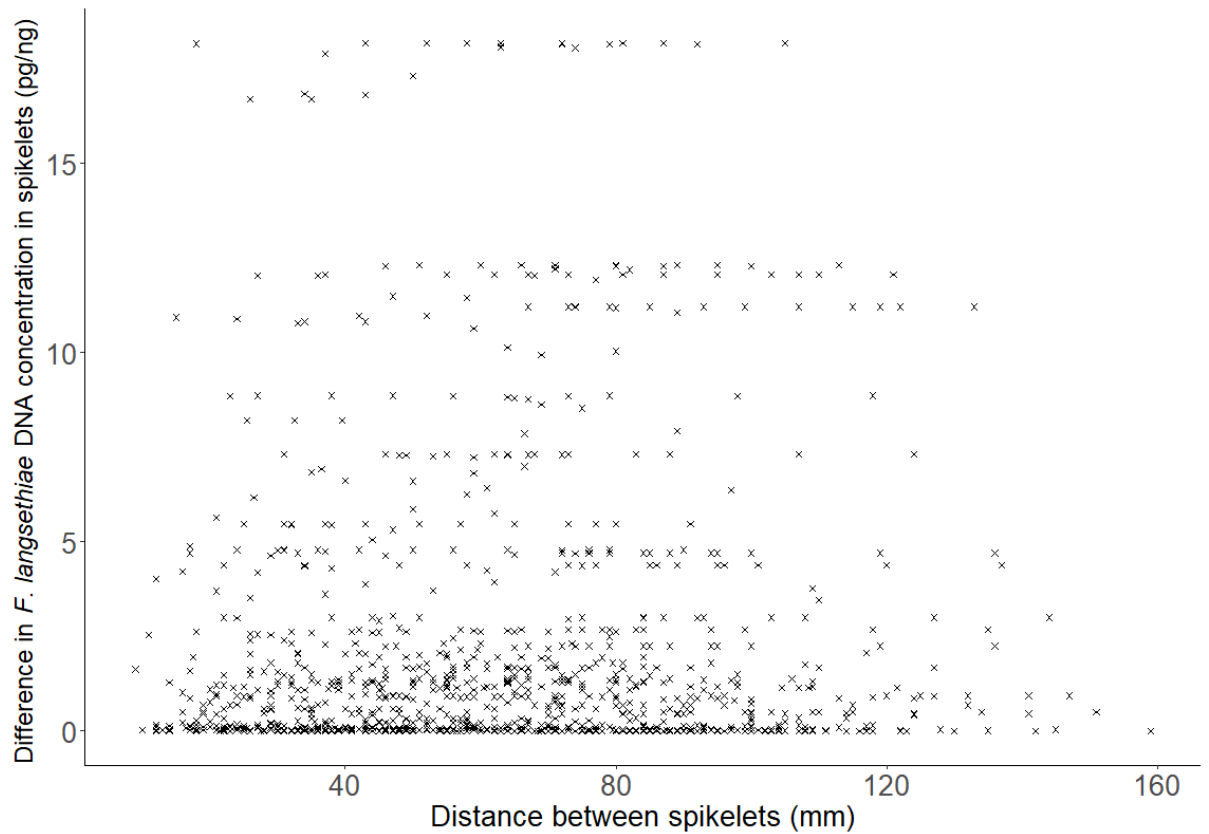


Figure 6.6: Scatter plot showing the difference between individual spikelets from plants 2 and 3 and 4 in terms of *F. langsethiae* DNA concentration (pg/ng) against their respective branch distances from one another (mm).

Figure 6.7 is a boxplot showing the *F. langsethiae* DNA concentration by whorl for the panicles of plant 2, 3 and 4; the mean values are displayed on the figure above the larger grey square for each whorl. The Kruskal-Wallis test failed to detect any significant differences between whorls for the plant 2 and 4 data set. However, for plant 3 the Kruskal Wallis test returned a P value of 0.044 indicating that the whorls of plant 3 differ in their respective *F. langsethiae* DNA concentrations. A pair wise Wilcoxon rank test was not able to identify which whorls differed significantly ($P < 0.05$).

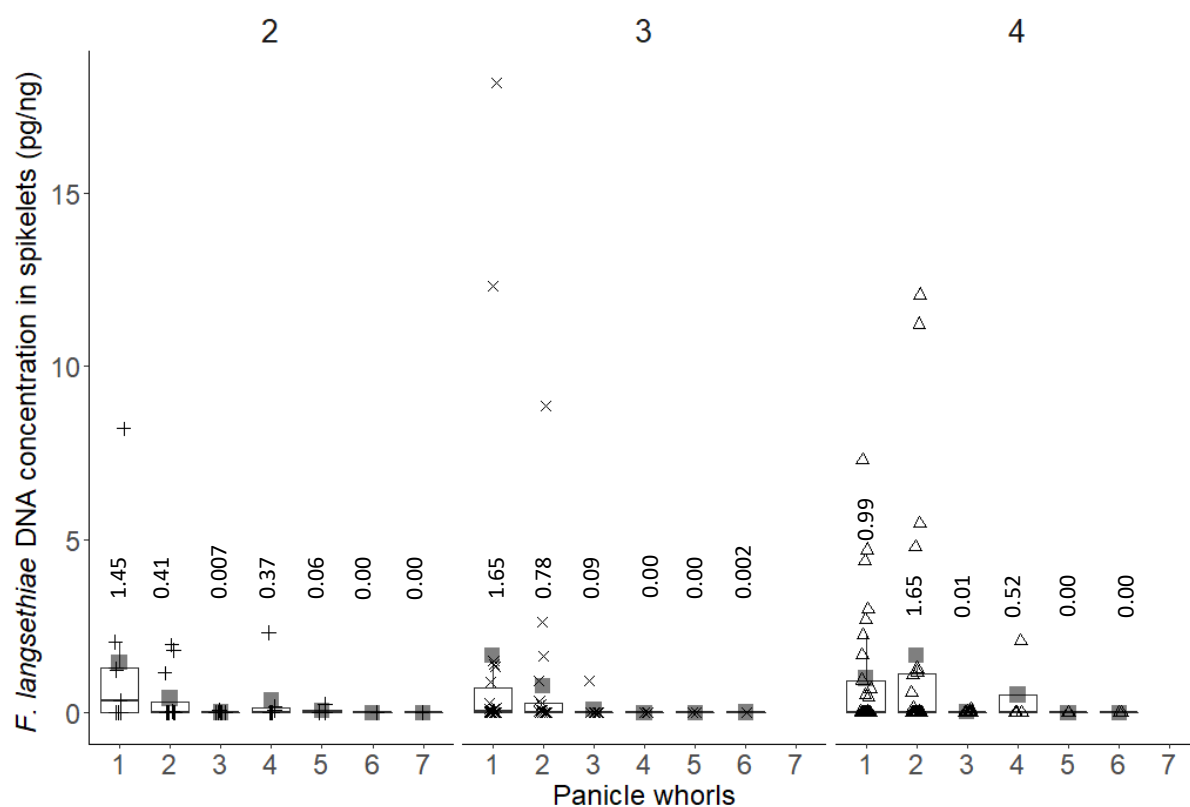


Figure 6.7: Boxplot of *F. langsethiae* DNA of spikelets by whorl for Tardis + B Mrg04 (plants 2, 3 and 4). The +, x, and Δ symbols represent DNA concentrations for individual spikelets, grey squares represent the mean of whorl, values of which in pg/ng are labelled directly above each boxplot.

The distribution of *F. langsethiae* DNA concentrations in each of the three Tardis +B Mrg04 panicles were very similar. Figure 6.8 is a frequency plot of DNA concentrations by plants and shows how skewed the concentration values are. The majority of values are less than 0.5 pg/ng for all spikelets.

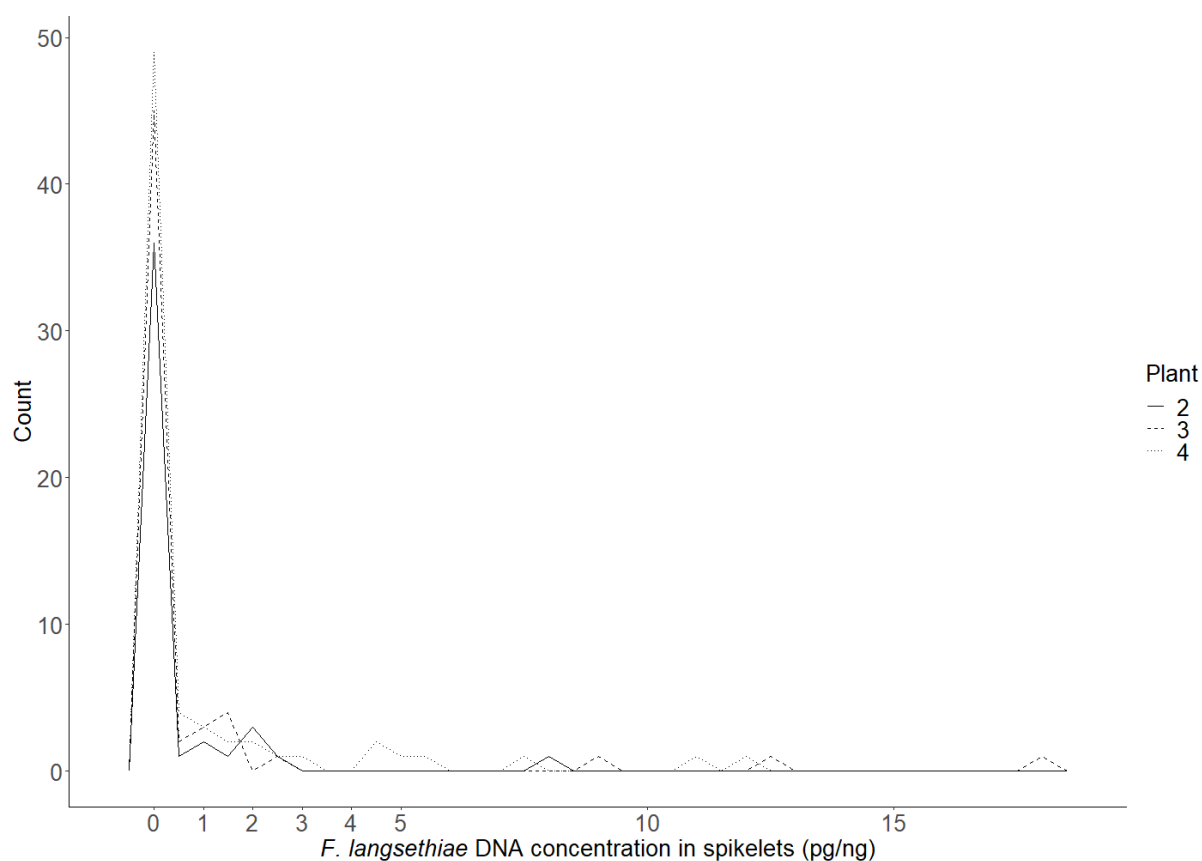


Figure 6.8: Density plot of *F. langsethiae* DNA concentration (pg/ng) of individual spikelets from three Tardis + B Mrg04 (plant 2, 3, and 4) panicles.

6.4.2. Small Grids

Figure 6.9 and Figure 6.10 show the HT2+T2 concentrations ($\mu\text{g/kg}$) within the 20 x 20 m square sampled in 2017 and 2019 respectively. The values for each location are displayed on the figure; the raster is conditionally formatted to reflect the magnitudes of the HT2+T2 concentrations linearly.

The Mantel test indicates that the relationship between the distance between locations and the difference in location values for HT2+T2 concentration were not significantly different in either 2017 ($P = 0.971$) or 2019 ($P = 0.133$). Values of HT2+T2 concentration are randomly distributed across the grid. For the 2019 data set four values on the grid are recorded as 51 $\mu\text{g/kg}$. These samples were lost during processing and the assigned 51 $\mu\text{g/kg}$ represents the average of the data set.

The Mantel test was used to compare the differences between concentrations of HT2+T2 at each location within each grid across the two years (2017 and 2019). The test returned a P value of 0.78, indicating that there was not a significant relationship between the locations from the two years. The concentrations by position did not remain relative to one another between the two years.

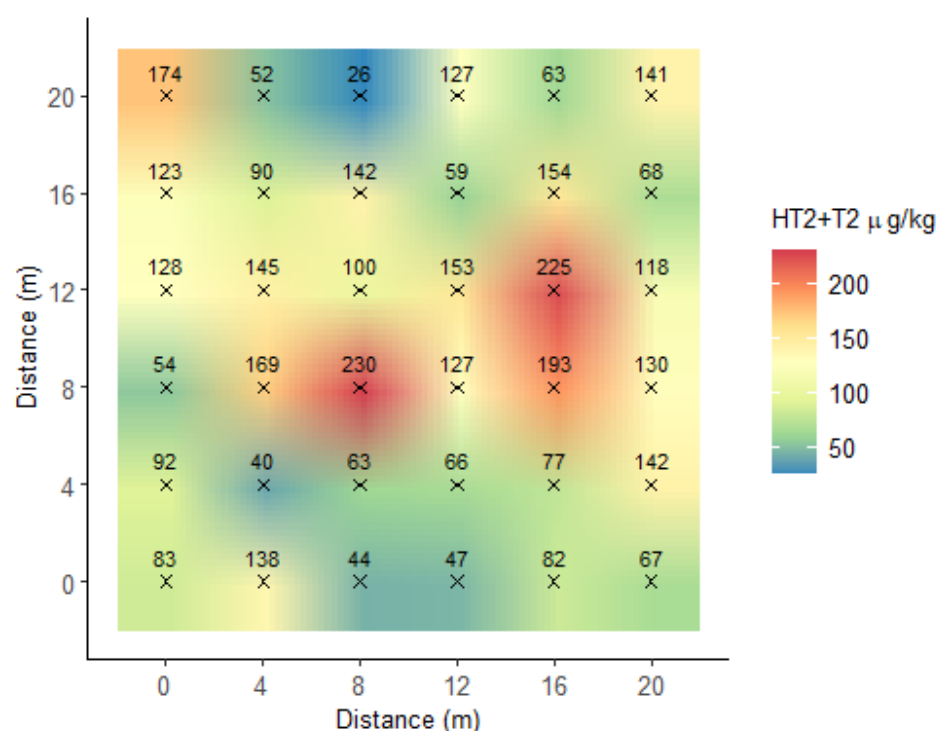


Figure 6.9: A heat map of the HT2+T2 concentrations of grain samples taken in 2017 from the experimental field. Colours on the chart represent linear interpolations of the HT2+T2 concentrations of each sampled location and can be interpreted using the scale in the legend. The relative position of each location is marked by a black x, labelled with the HT2+T2 value for each location.

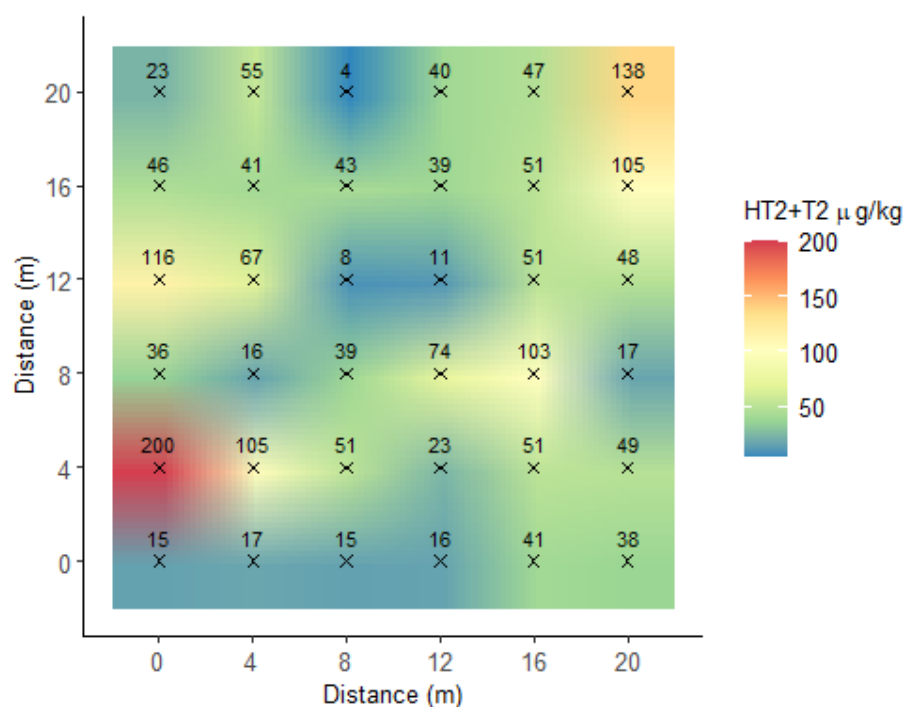


Figure 6.10: A heat map of the HT2+T2 concentrations of grain samples taken in 2019 from the experimental field. Colours on the chart represent linear interpolations of the HT2+T2 concentrations of each sampled location and can be interpreted using the scale in the legend. The relative position of each location is marked by a black x, labelled with the HT2+T2 value for each location.

6.4.3. *Large Grids*

Figure 6.10 shows the HT2+T2 concentrations ($\mu\text{g/kg}$) within an 80 x 180 m area sampled in 2016. The values for each point are displayed on the figure. The raster is conditionally formatted to reflect the magnitudes of the HT2+T2 concentrations linearly. A high concentration is apparent at the top centre left of the grid which exceeds any other concentration present in the rest of the field. The Mantel test indicates that the correlation between the distance between locations and the difference in location values for HT2+T2 concentration (0.127) was significant ($P = 0.024$). Removing the high value at the top of the grid marginally reduces the quality of the correlation but still leads to a significant correlation. The correlation is therefore caused by other clusters of values that increase in their difference from one another with increasing distance from one another. No GPS data was recorded for 2016 and as such it was not possible to compare 2016 with subsequent years.

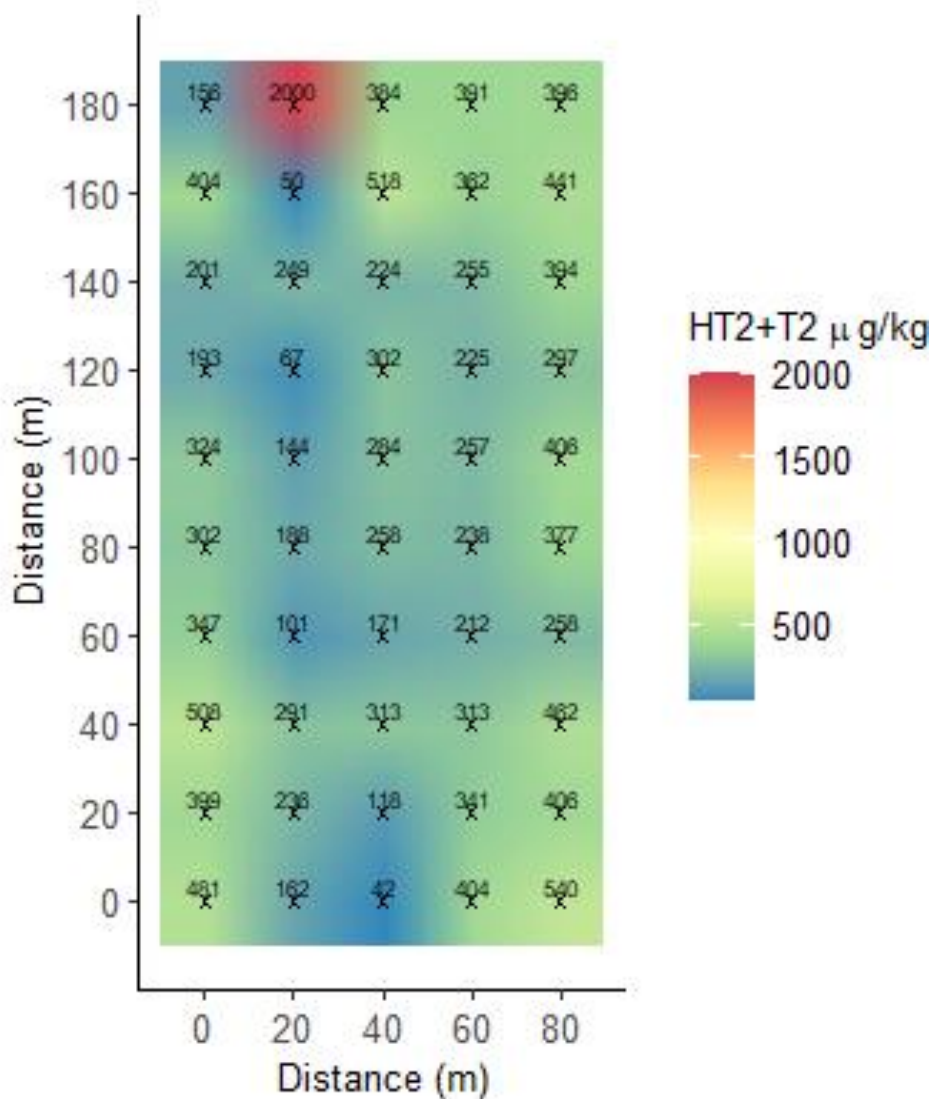


Figure 6.11: A heat map of the HT2+T2 concentrations of grain samples taken in 2016 from the experimental field. Colours on the chart represent linear interpolations of the HT2+T2 concentrations of each sampled location and can be interpreted using the scale in the legend. The relative position of each location is marked by a black x, labelled with the HT2+T2 value for each location.

Figure 6.12 and Figure 6.13 show the HT2+T2 concentrations ($\mu\text{g/kg}$) within the 80 x 80 m square sampled in 2018 and 2020 respectively. The values for each location are displayed on the figure. The raster is conditionally formatted to reflect the magnitudes of the HT2+T2 concentrations linearly.

The Mantel test indicates that the relationship between the distance between locations and the difference in location values for HT2+T2 concentration were not significantly different in 2018 ($P = 0.908$). However, in 2020 the correlation was found to have a significant ($P = 0.003$) correlation. Looking at Figure 6.13, the highest values are in the centre and the bottom left of the grid with far lower values on the right and the top left. This grouping of similar concentrations of HT2+T2 has led to the higher correlation

than seen in previous grids. Five values on the grid are recorded as 295 $\mu\text{g/kg}$. These samples were lost during processing and the assigned 295 $\mu\text{g/kg}$ represents the average of the data set.

The Mantel test was used to compare the differences between concentrations of HT2+T2 at each location within each grid across the two years (2018 and 2020). The test returned a P value of 0.38, indicating that there was not a significant relationship between the differences between locations from the two years. The concentrations by position did not remain relative to one another between the two years.

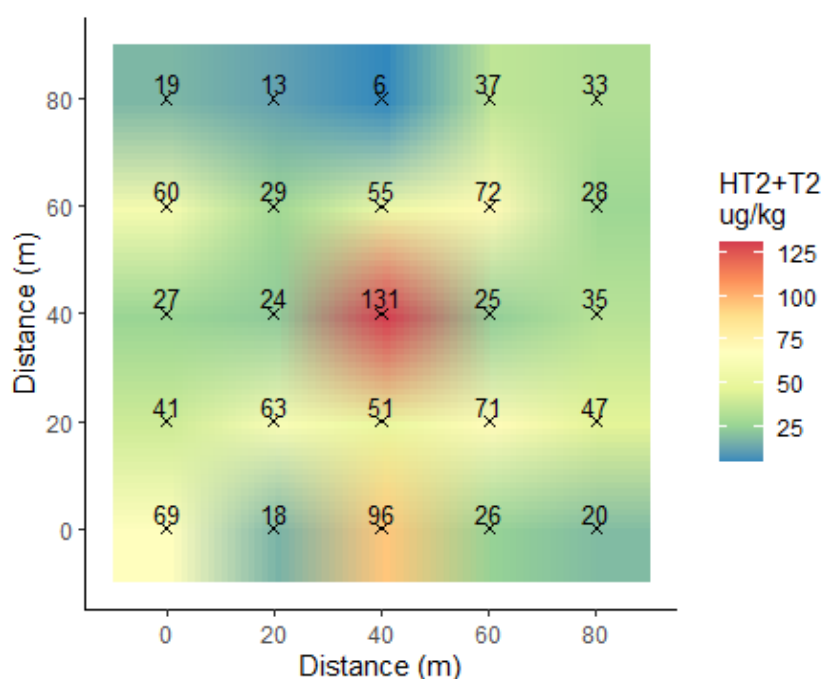


Figure 6.12: A heat map of the HT2+T2 concentrations of grain samples taken in 2018 from the experimental field. Colours on the chart represent linear interpolations of the HT2+T2 concentrations of each sampled location and can be interpreted using the scale in the legend. The relative position of each location is marked by a black x, labelled with the HT2+T2 value for each location.

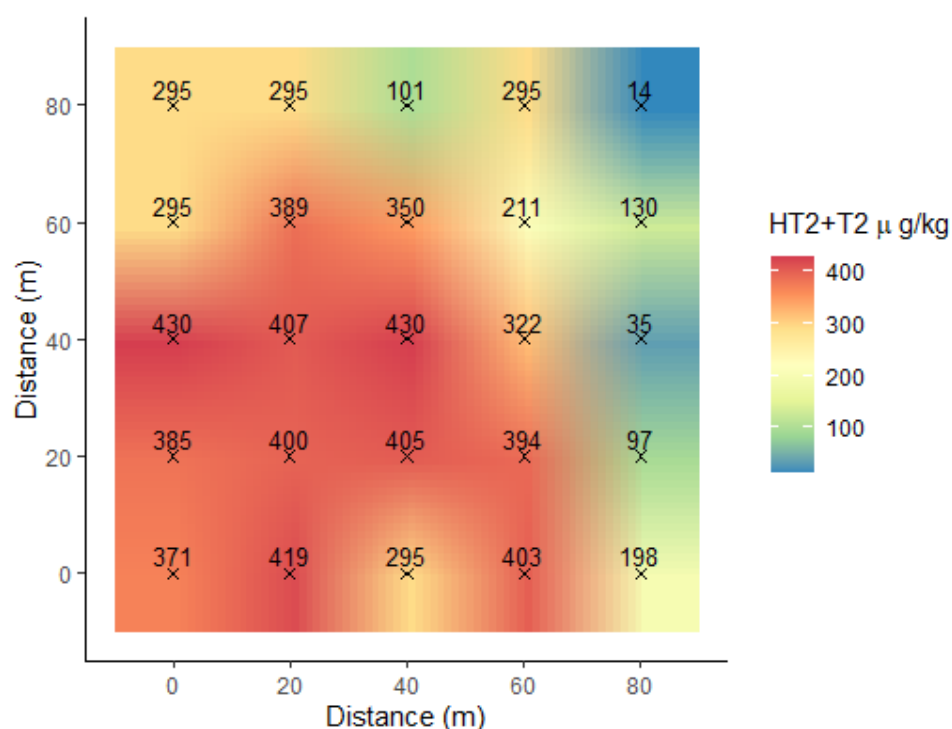


Figure 6.13: A heat map of the HT2+T2 concentrations of grain samples taken in 2020 from the experimental field. Colours on the chart represent linear interpolations of the HT2+T2 concentrations of each sampled location and can be interpreted using the scale in the legend. The relative position of each location is marked by a black x, labelled with the HT2+T2 value for each location

6.5. Discussion

6.5.1. Distribution within a panicle

Estimating the proportion of infected *F. langsethiae* kernels by surface sterilising and incubating on a growth medium is problematic as shown by Edwards *et al.* (2012a). In a sample of 122 oat grains all were shown to contain *F. langsethiae* DNA by real time PCR, whereas only 8% of grain from the same sample were able to grow *F. langsethiae* on PDA (Edwards *et al.*, 2012a).

As a result of this finding, this chapter used molecular techniques to examine the proportion of grains infected with *F. langsethiae*.

Previous work (Stančić, 2016; Imathiu, 2008) and work presented earlier in Chapter 3 showed high concentrations of HT2+T2 in entire panicles. The single spikelet extraction of DNA included the glumes. No evidence has been published to suggest that the pathogen progresses from the spikelet into the peduncle. Divon *et al.* (2019) specifically noted that they never observed such a progression in microscopy studies of the infection of oats with *F. langsethiae*. The higher HT2+T2 concentrations seen in whole panicles is potentially derived from the glumes of the spikelets which have been seen to be some of the first infected parts of the plant (Divon *et al.*, 2019). Tekle *et al.* (2012) observed in *F. graminearum* infection of oats that within spikelet spread of

infection occurred by close contact of florets rather than hyphal growth through the rachilla.

Examination of the Buffalo + T Mrg04 panicle, a tall plant with a low infection of *F. langsethiae*, shows the infected spikelets are on different whorls. In this low infection scenario, it seems that there is no evidence of spikelet to spikelet movement or a locus of infection of the pathogen, a conclusion which agrees with Divon *et al.* (2019).

Edwards *et al.* (2012a) used a real time PCR-assay to quantify the *F. langsethiae* DNA concentration in 122 oat grains from one field sample. The concentration of *F. langsethiae* DNA ranged between 0.0002 pg/ng and 13.85 pg/ng, with a mean of 0.54 pg/ng from a bulk sample with 8399 µg/kg HT2+T2. The highest concentration of *F. langsethiae* DNA across all three panicles from Tardis + B Mrg04 was 18.2 pg/ng, and the lowest value (excluding 0) was 0.0005 pg/ng, similar to the single grain extractions undertaken by Edwards *et al.* (2012). The distribution of DNA concentrations was skewed with most spikelets having DNA concentrations between 0 and 0.5 pg/ng. Opoku (2012) found that the “rest” of the head, constituting the rachis, rachis branches and glumes, had five times the *F. langsethiae* DNA in winter oats and 17 times the concentration in spring oats than the grain including the husk. In this work entire spikelets were analysed including the glumes, the peduncle connecting primary and secondary spikes and the husks. Divon *et al.* (2019) did not observe any growth of *F. langsethiae* into the rachis of the oat in their microscopy study, but it was seen that *F. langsethiae* initially germinated on the glumes of the oat plants potentially leading to high concentrations of *F. langsethiae* DNA and HT2+T2 on the glumes of the plants.

The distance between the spikelets and the difference in their *F. langsethiae* DNA concentrations did not significantly ($P>0.05$) correlate with one another in any of the three Tardis + B Mrg04 panicles when examined within whorls. In plant 2, the correlation was negative but for plants 3 and 4 it was positive. The concentration of *F. langsethiae* DNA seems independent within each spikelet, supporting the theory that each spikelet is infected independently. Bjørnstad and Skinnnes (2008) speculated that oats may have an inherent resistance to *Fusarium* species due to their panicle structure. However, as the infection has never been observed to move out of the initially infected spikelet (Divon *et al.*, 2019) then the length of branches and the panicle structure potentially has no direct impact on resistance. Likely the infection does not move through the pedicels or branches as described by Brown *et al.* (2010) for *F. graminearum* in wheat. Tekle *et al.* (2012) observed that *F. graminearum* moved between florets of oats within spikelets through physical contact rather than through the rachis. Through point inoculation of *F. graminearum* onto four oat cultivars, Langevin *et al.* (2004) observed no spread to adjacent spikelets. The evidence presented in this

work supports infection being retained within the originally infected spikelets. Dissecting more panicles from the same harvest and across different genotypes to perform the same analysis would strengthen the conclusion that *F. langsethiae* infection does not travel through the peduncle and latterly the branches. While this experiment only measured *F. langsethiae* DNA, Edwards *et al.* (2012) quantified *F. langsethiae* DNA and HT2+T2 from the same individual grains and achieved a correlation of 0.77, indicating that *F. langsethiae* DNA and HT2+T2 occur in the same locations and that their respective concentrations are relative to one another. Furthermore, Meng-Reiterer *et al.* (2016) found that neither HT2 nor T2 were mobile within the oat plant and that the mycotoxins had to be metabolised to facilitate partial movement around the plant. Therefore, the absence of *F. langsethiae* DNA from spikelets can be regarded as strong evidence that HT2+T2 would not be found in detectable quantities either.

Oats flower from the top of the panicle down (Misonoo 1936; Doehlert *et al.*, 2002). If flowering time is an important resistance mechanism in terms of coincidence of inoculum and flowering florets, then differences in *F. langsethiae* DNA concentration between whorls that have flowered at different times might be expected. In this work it was possible to prove statistical difference in whorls in plant 3 in terms of their *F. langsethiae* DNA concentration, but not to define between which whorls those differences were significant. With so few panicles to assess in this preliminary study it is difficult to draw robust conclusions, for which more panicles with high natural infections should be assessed. The higher whorls contain far fewer spikelets to examine and given the relatively low proportion of spikelets infected across the panicle, there will frequently be no infected spikelets in the top whorls.

6.5.2. *Distribution within a field*

In all 4 years of study, considerable variation in T2 +HT2 was found across the field. The 2016 grid (20 m intervals, 80 m x 180 m) showed a significant relationship between the distance between locations with the difference in value of each location, leading to the conclusion that similar concentrations are more likely to be located close to one another. No such significant relationship was seen in either of the smaller scale grids sampled in 2017 and 2019. A significant relationship between distance and the difference in concentration was seen in the 2020 (4 m interval, 20 m x 20 m) grid. Significant correlations could be evidence of infection loci within the field, points of high infection or initial points of infection from which surrounding crop becomes infected, as is the case in other pathogenic fungi such as *Puccinia striiformis*. Schlang *et al.* (2008) performed a similar study on two sites of wheat, samples were collected in a grid pattern spaced 25 m from one another and DON concentration was measured at each

point, no relationship was detected between the distance of sampled positions and their respective DON concentrations. Xu *et al* (2008) used quadrat sampling to measure within field variability of *F. avenaceum*, *F. culmorum*, *F. graminearum*, *F. poae*, *M. majus*, and *M. nivale*, in chaff and grain samples. The distance between quadrants was not measured however the researchers concluded that the presence or absence of FHB pathogens within quadrates were independent of one another. The evidence presented here does not support such independence for *F. langsethiae*.

In the two instances where it was possible to compare grids across years with one another using the Mantel test, no relationships were found between the two.

Therefore, there is no evidence that location at the scale examined within this work influences infection in subsequent years. The examples used in the work described here sampled the same points after a year break in which wheat was grown. It has been demonstrated that wheat can become infected by *F. langsethiae* (Opoku *et al.*, 2013; Drakulic *et al.*, 2016b; Divon *et al.*, 2019). However, the infection of wheat leads to lower *F. langsethiae* DNA and HT2+T2 (Opoku *et al.*, 2013; Divon *et al.*, 2019) than in oats, suggesting that the interim year of wheat could have interrupted the accumulation of inoculum in relevant locations. Location at a larger scale has effectively been associated with *F. langsethiae* infection (Edwards, 2017) by demonstrating that cereal intensity was influential on the level of infection as measured by HT2+T2 concentration in the grain.

As sampling at the locations was not replicated there is no estimate of the variation for each location's value. It would be difficult to replicate as the location from which each sample is taken is important, however given that the ELISA has relatively large error associated with it perhaps three 5 g sub-samples should have been taken from each sample to give a measure of the variation due to sub-sampling and analysis. Year to year variation is very high as described in Chapter 5, and variety of oats has a large impact also, in this work the year with the lowest concentrations of HT+T2 was 2020 when Balado was grown which has been shown to be a consistently high accumulator of HT2+T2 (Edwards, 2015).

The grid areas examined through sampling displayed a higher degree of heterogeneity, in most instances samples points were independent of one another, much the same as reported by Xu *et al.* (2008). The maximum difference between two adjacent samples taken in 2016 based on 20 m spacing was 40-fold, no other year at 20 m spacing produced such a difference. When sampling grids were based on 4 m spacings the maximum difference was just over 13-fold, Xu *et al.* (2008) found differences between sampled quadrats of 880 fold within the sample field although the distance between quadrats was not reported. Using 25 m spacings Schlang *et al.* (2008) reported an

approximate range equalling a 45-fold difference in DON concentration in wheat sampled in a similar grid system to the work reported here.

No other parameters were measured within the grid areas with which to associate with the HT2+T2. Müller *et al.* (2011) was able to statistically differentiate hilltop sites from depressions by DON and ZON concentration of wheat. Sites were selected on the basis of different topography to influence soil moisture as well as relative humidity. The experimental field used in this study (Black Britch) is relatively flat with uniform soil type so these factors are unlikely to have contributed to the heterogeneity reported here. Similar work, quantifying HT2+T2 in oats in fields with more variable topography could help explain why some locations in the field have such high levels of heterogeneity.

This is the first study to identify the spatial heterogeneity in HT2 and T2 at the level of oat panicles and at the field scale.

7. Chapter 7: General Discussion

This PhD sought to quantify the impact on *F. langsethiae* resistance or susceptibility of specific QTL which were previously identified (Stančić, 2016). Edwards *et al.* (2012a) demonstrated that the concentration of HT2+T2 in oat grain was strongly correlated to the level of *F. langsethiae* DNA. Therefore, the large differences seen in the HT2+T2 concentrations in this study are likely an accurate reflection of the differences in *F. langsethiae* infection driven by variation in weather and inoculum availability.

Chapter 4 demonstrated that introducing alleles by introgressing QTL from different genotypes could influence the resistance or susceptibility of the resultant plant to *F. langsethiae*. The introgression of the Mrg04 QTL from the Tardis genotype into the Buffalo background genome caused the resultant plant to accumulate lower concentrations of HT2+T2 with an overall average reduction across all experiments of 48%. The reduction in HT2+T2 concentration in the Buffalo+T Mrg21 NIL in spring sown plots (average reduction of 35%) combined with the reduced time (7.6 days) to panicle emergence suggests that earlier flowering in the year is a resistance mechanism. This is supported by analysis in Chapter 5 using the Julian day on which panicles emerged, showing that panicles emerging later in the year led to harvested grains with higher HT2+T2 concentrations. Models examining days, and degree days from sowing were less consistent and both indicated that later flowering led to lower HT2+T2 concentration but they were more influenced by sowing date and temperatures through the year.

The Mrg11 QTL had no detectable impact on HT2+T2 concentration in the harvested grain despite having been identified in a previous gene wide association study (Stančić, 2016) as inferring resistance to *F. langsethiae*. The Mrg20 QTL had a sporadic impact on the HT2+T2 concentration of grain, having a significant impact only in some years and significantly increasing HT2+T2 concentration in the spring sown 2017 plots. The HT2+T2 concentration did, however, reduce when the Buffalo derived Mrg20 was introgressed into the Tardis background in autumn sown plots for all years (average reductions of 39%) and significantly in two years. The impact on the panicle emergence date of the Buffalo derived Mrg20 on the Tardis + B Mrg20, was to reduce the days to panicle emergence by one day in autumn sown plots. Such a small difference is unlikely to have had a large effect on the level of infection by *F. langsethiae*, possibly some other aspect of flowering not measured in this work was also influenced by Mrg20 or any of the QTL examined in this study. Gilsinger *et al.* (2005) associated four molecular markers with both reduced FHB incidence and narrow flower opening in wheat.

The purpose of artificial inoculation is to provide a sufficient level of uniform infection with which to differentiate control methods including resistant genotypes, biological or chemical controls. The inoculation must also sufficiently simulate the natural epidemiology such that control measures that are successful against the artificial method are also successful against natural infections.

The degree to which panicles are extruded in the glasshouse seems to impact the concentration of HT2+T2 in the milled panicles with more extruded panicles accumulating higher concentrations. However, in the field under natural infection, the fully extruded plants (which are typically taller) have lower HT2+T2 concentrations. This potentially explains how the rankings of cultivars from glasshouse inoculated experiments do not match those from the field where natural infection could be taking place concurrently with any inoculation attempt.

The NIL glasshouse experiment was unable to statistically differentiate the different NIL from one another in terms of their HT2+T2 concentrations after inoculation. To numerically compare the NIL, their ranking in terms of HT2+T2 accumulation was the opposite to what was seen in the field experiments. In field experiments the naturally infected Buffalo and the Buffalo NIL (2012-125/1/26) were broadly equivalent and contained statistically higher concentrations of HT2+T2 than Buffalo + T Mrg04 in the 2017 and 2018 field experiments. A similar relationship was seen by Aamot, (2017) where the Norwegian oat varieties Odal, Belindar and Vingar were ranked as shown in Table 7.1.

Table 7.1: Cultivar ranking from field to glasshouse experiments conducted in Norway (Adapted from Aamot, 2017).

Environment	Ranking highest to lowest HT2+T2 concentration
Glass house inoculation	Belinda > Odal > Vingar
Field infection	Odal > Belinda > Vingar

Hautsalo *et al.* (2020) suggested that glasshouse inoculated experiments should only be used in conjunction with field experiments, as passive evasion mechanisms such as height and earliness are bypassed by applying spores directly to the most susceptible plant part at the most susceptible timing. It was also possible to artificially inoculate wild oat (*Avena strigosa*) in the glasshouse, but samples collected from the field rarely had detectable HT2+T2 (data not shown). Potentially the very early flowering of the wild oats and their tall height was leading to high evasion.

In terms of developing disease nurseries, current methodologies are not reliable or when reported do not include uninoculated controls (Schöneberg *et al.*, 2019; Isidro-

Sánchez *et al.*, 2020). Potentially the most reliable method identified so far is to develop a high-risk field as was done for this work, by using a rotation of a susceptible oat variety and wheat, with crop debris being left on the surface. Such a method takes a number of years and will develop high grass weed populations which are difficult to control and it still not as reliable as artificial inoculation for other *Fusarium* species.

It was seen in the 2019 inoculation experiment that irrigated plants were taller than non-irrigated plants. Xu *et al.* (2014) associated dry summers with higher HT2+T2 concentration in oats. Some of the correlation between height and a reduction in HT2+T2 could be associated with oats growing less tall in conditions conducive to high HT2+T2 infection. When genotypes are looked at within the same year and location, as in this study, such an effect will be minimised.

Given that it is difficult to grow two plots of the same variety of oat adjacent to one another where one plot has a high level of infection and the other a low level of infection, it is difficult to say with confidence that there is no yield penalty from *F. langsethiae* infection. Børnstad and Skinnes (2008) suggest that *Fusarium* infection of oats could cause yield loss as a result of aborted spikelets early in grain development. Glasshouse experiments conducted in this study showed high levels of “blind” spikelets in inoculated plants. The difference in their frequency was not assessed between inoculated treatments and uninoculated controls and the conditions within the plastic bags could also have led to greater spikelet abortion.

Smaller grains have been shown to have higher concentrations of HT2+T2 (Brodal, 2020), potentially due to a higher proportion of the mass constituting the husk. Removal of the husk reduces the HT2+T2 during the milling process (Scudamore *et al.*, 2007; Scudamore, *et al.*, 2009) by up to 95%. Most work conducted on varietal resistance (Edwards, 2016; Edwards, 2007b) in the UK has been on uncleaned field samples which will have included some blinds. Growers will seek to remove blinds by using appropriate combine-harvester settings to discard lighter blinds; some, however, will still remain.

The age and condition of isolates used in the inoculation experiments could have a bearing on the level of infection they achieve. The highest level of infection was in the earliest glasshouse experiment; however, the isolates were propagated from the same culture kept at 5°C for the duration. Potential isolates are selected for inoculation experiments on the basis of their ability to grow well *in vitro* rather than infect plants. The virulence of isolates is a continuous variable (Aamot, 2017). Different authors have used varying numbers of isolates in inoculation experiments: Divon *et al.*, (2012)

used three isolates whereas Imathiu (2008) used 11 isolates and achieved a maximum HT2+T2 concentration of 1301 µg/kg.

There is evidence that the glumes of the panicle are the first point of infection (Divon *et al.*, 2019) and as such high concentrations from glasshouse studies in this thesis could be attributed to high initial colonisation of the glumes of plants. The mass of grains from each individual plant in glass house experiments recorded in Chapter 3 were very low compared to what one would expect in field grown plants. There was also a high proportion of blind grains (those containing no developed groat), further reducing the mass of harvestable material. As a result, entire panicles were harvested and analysed although disproportionately high HT2+T2 concentrations could have been recorded as the proportion of glumes to grain was higher than one would expect in field grown and harvested plots. Such an imbalance could be one explanation as to why glasshouse methods of artificial inoculation work so poorly in field conditions. Potentially introducing such highly concentrated spore suspensions caused spikelet abortion and led to high infestation of the remaining panicle material. Certainly, in the first inoculation attempt on Gerald oats visible mycelial growth was observed on the outside of the glumes after a 14-day bagging period.

Reliable artificial inoculation of other *Fusarium* species is possible in outdoor grown plants. However, outdoor field inoculations in this work were not successful. As yet reliable artificial inoculation of *F. langsethiae* in outdoor oats has not been effectively demonstrated. Evidence to date on the initial infection mechanism of *F. langsethiae* in oats (Divon *et al.*, 2019) has shown that it is similar to that of *F. graminearum* in oats (Tekle *et al.*, 2012) and that the presence of pollen is an important growth stimulant for the pathogen. Although the results of glasshouse inoculation work in this study suggest that anthesis is the most susceptible growth stage of oats to *F. langsethiae*, experimental work to date does not support the use of current glasshouse inoculation methods for differentiating varietal resistances.

Previous work on understanding the conditions that lead to high natural infection have generally concluded that anthesis is the likely timing for infection (Opoku *et al.*, 2013; Divon *et al.*, 2012; Mousavi, 2016; Divon *et al.*, 2019; Schöneberg *et al.*, 2019); that some level of free water is required when the inoculum is introduced; and that after the point of infection, warm dry weather favours *F. langsethiae* (Xu *et al.*, 2014) over other pathogenic *Fusarium* species that otherwise would compete strongly with *F. langsethiae*. Cereal intensity and especially the frequency of oats in the previous cropping history is important (Edwards, 2017), leading to suggestions that crop debris is the source of inoculum (Edwards, 2017; Hofgaard *et al.*, 2016a). The field used in this work had been kept in an alternating wheat and oat rotation for over six years with

only shallow (less than 15 cm depth) cultivations. The HT2+T2 concentrations were relatively high in 2017 and 2018 after which the field had to be ploughed for wild oat control. The HT2+T2 concentrations post ploughing were much reduced. Although such evidence is only anecdotal, it supports the theory that the previous crop debris acts as a source of inoculum.

The results from the naturally infected NIL experiments should carry more weight than previous work conducted on varietal resistance in glasshouses due to the natural infection that took place.

The spatial grid analysis demonstrates that there can be uneven distribution of infection severity across the field. The aim of artificial inoculation is not only to increase the likelihood of high infection but also increase the homogeneity of infection across the trial area. Artificial inoculation has been used for research in one gene wide association study (Isidro-Sánchez *et al.*, 2020) searching for resistance in oat genotypes to *F. langsethiae* but the impact of the inoculation was difficult to gauge as no uninoculated results were presented.

The statistical models used in Chapter 4 to describe the impact of height and time to panicle emergence indicate that neither trait had a high impact on the accumulated HT2+T2 and that year was the most important factor, highlighting the unpredictability of the pathogen. Differences in the cultivation and debris management of the field could also have contributed to differences between years.

Panicle extrusion and height were correlated to one another; they were both seen to be significant in models examining HT2+T2 concentration. It was not possible to differentiate which of these traits influenced the susceptibility of the oat plant to *F. langsethiae* or by what mechanism.

In Chapter 3 it was shown that genotypes possessing the Buffalo derived Mrg04 QTL containing the *Dw6* dwarfing gene were more often partially extruded. Combined with the negative correlation between panicle extrusion and HT2+T2 and the higher levels of infection in the lower part of the dissected panicles, it could be surmised that partial panicle extrusion leads to increased susceptibility to HT2+T2 accumulation from *F. langsethiae* infection. The increased *F. langsethiae* infection in the lower part of panicles could on inspection of more samples fail to continue or could be a product of the specific flowering time of each spikelet, with the lower spikelets flowering last. The relationship previously observed between panicle extrusion and HT2+T2 concentration could instead be being caused by the height of the plants (a characteristic which correlates with the degree of panicle extrusion).

The large variation in HT2+T2 concentration between years could be partly attributed to the presence of *F. langsethiae* inoculum in the field. After the experimental field was ploughed and the original crop debris buried, wheat straw from the same field was applied again. The loss of the original crop debris could have reduced the amount of inoculum available to the 2019 and 2020 plots.

Although conducted with low replication, the work examining individual grain infection supports previously made statements that oats have a high type II resistance (Tekle *et al.*, 2012), potentially to such a high degree that no growth of *F. langsethiae* ever spreads further than the initially infected spikelet

The panicle dissections did not record which spikelets remained within the flag leaf sheath and which had extruded, although the Tardis + B Mrg04 NIL characteristically failed to fully extrude in all years and sowing seasons. That panicles in the lower parts of the panicle showed a higher level of infection could be used as evidence that unextruded spikelets are more susceptible to *F. langsethiae* infection. Panicle extrusion was negatively correlated to HT2+T2 concentration (Chapter 4) accounting for 6.7% of the variation. In an equivalent model using an extra year of data height accounted for 6.1% of the variation.

Although the window-pane analysis used panicle emergence (GS51) as the key growth stage for infection, the best results from the glasshouse artificial inoculation work came from inoculation at panicle fully emerged (GS59). Some genotypes never achieved a fully emerged panicle but it would have been possible to record an estimated proportion of the panicle emerged from the flag leaf boot and use the first day 50% of plots achieved the highest proportion of emerged panicles as a pseudo fully emerged panicle growth stage. The fully emerged panicle is the growth stage closest to anthesis which is easily observed within the field.

7.1. Conclusions

- Impact of QTL
 - The introgression of Mrg04 QTL had the largest and most consistent effect on HT2+T2 concentration of the QTL studied.
 - Introgression of the Tardis (more resistant) Mrg04 QTL into the Buffalo (susceptible) background results in a taller earlier plant in both spring and autumn sowing that is more resistant to the accumulation HT2+T2.
 - The introgression of the Buffalo (susceptible) Mrg04 QTL into the Tardis (more resistant) background results in a shorter later plant in both spring and autumn sowing that that accumulates higher HT2+T2 concentrations.

- The introgression of the Tardis Mrg21 QTL into the Buffalo background reduced HT2+T2 concentrations in spring sowings and created a later flowering plant. The opposite was true for the introgression of the Buffalo Mrg21 into the Tardis background, an earlier flowering plant was generated that often accumulated higher HT2+T2 concentrations
- The introgression of the buffalo derived Mrg20 QTL into the Tardis background genome lead to a plant only marginally later than the Tardis parent but with a reduction in HT2+T2 concentration in autumn sown plots.
- Introgressions of the Tardis Mrg11 had no impact on the concentration of HT2+T2, height or earliness.
- This work has provided further evidence that warmer dryer summers are conducive to higher *F. langsethiae* infection.
- The field scale distribution of *F. langsethiae* in oats is similar to that of *F. graminearum* in wheat in that it does not spread from foci and is heterogeneous.
- The distribution of *F. langsethiae* within the panicle is random and not related to the proximity of infected spikelets to one another.
- The discrete manner in which the *F. langsethiae* DNA is distributed across spikelets in the panicle is further evidence that the pathogen and associated mycotoxins are not mobile across the panicle.

7.2. Future work

Further grid work should be undertaken in a similarly conditioned field as used in this thesis but selected on the basis of distinct areas in terms of microclimates. Such further work could usefully record soil moisture, relative humidity at panicle height, wind speed and associate those parameters with disease severity.

Further dissection of naturally infected panicles would help to reinforce the findings of this work, specifically using panicles that were partially extruded. Recording which spikelets were below the flag leaf ligule could be informative as to whether remaining within the boot increases susceptibility to *F. langsethiae* infection.

Recording more morphological traits such as the time of day at which florets open, the degree to which they open and the extrusion of anthers in the field, although time consuming and impractical by hand, would allow such traits to be associated to molecular markers and would allow relationships with *F. langsethiae* infection to be examined.

The Buffalo and Tardis cultivars used to develop the NIL used in this work were not originally selected for their respective susceptibilities to *F. langsethiae*, as such they do

not represent the most and least resistant phenotypes available from the UK germplasm. A mapping population utilising a very susceptible cultivar such as Balado and the most resistant so far observed Maestro (Edwards, 2015).

Developing further mapping populations to include the other dwarfing genes present in oats such as *Dw7* and *Dw8*. The role of panicle extrusion in HT2+T2 concentration could be examined more closely through the use of *Dw7* as genotypes carrying this gene extrude their panicles to a greater degree than those carrying the *Dw6* gene.

There is as yet no reliable method for artificial inoculation and the similarity of current methodologies to the natural epidemiology is unknown. Further work examining naturally infected oats could potentially inform future work in artificial inoculation.

References

- Aamot H (2017) SafeOats RT 2: Investigate potential resistance to *F. langsethiae* in selected oat varieties. SafeOats project progress meeting, NIBIO, Norway. November 2017
- Abdelhalim, M., Brurberg, M. B., Hofgaard, I. S., Rognli, O. A. and Tronsmo, A. M. 2020. Pathogenicity, host specificity and genetic diversity in Norwegian isolates of *Microdochium nivale* and *Microdochium majus*. *European Journal of Plant Pathology*, 156 (3), pp. 885-895.
- Abramson, D., Clear, R. and Smith, D. 1993. Tricothecene production by *Fusarium spp.* isolated from Manitoba grain. *Canadian Journal of Plant Pathology*, 15 (3), pp. 147-152.
- Adams, G. C. and Hart, L. P. 1989. The role of deoxynivalenol and 15-acetyldeoxynivalenol in pathogenesis by *Gibberella zeae*, as elucidated through protoplast fusions between toxigenic and nontoxigenic strains. *Phytopathology*, 79 (4), pp. 404-408.
- AHDB. Not dated. *Risk Assessment for Fusarium Mycotoxins in Wheat*. [Online].
AHDB. Available from: <https://ahdb.org.uk/mycotoxins> [Accessed on 26 September 2021].
- AHDB. January 2021. *Nutrient Management Guide (RB209)*
- Bagga, P. 2008. Fusarium head blight (FHB) of wheat: Role of host resistance, wheat aphids, insecticide and strobilurin fungicide in disease control in Punjab, India. *Cereal Research Communications*, 36 (Supplement 6), pp. 667-670.
- Bekele, W. A., Wight, C. P., Chao, S., Howarth, C. J. and Tinker, N. A. 2018. Haplotype-based genotyping-by-sequencing in oat genome research. *Plant Biotechnology Journal*, 16 (8), pp. 1452-1463.
- Bjørnstad, Å., He, X., Tekle, S., Klos, K., Huang, Y., Tinker, N. A., Dong, Y. and Skinnes, H. 2017. Genetic variation and associations involving fusarium head blight and deoxynivalenol accumulation in cultivated oat (*Avena sativa* L.). *Plant Breeding*, 136 (5), pp. 620-636.
- Bjørnstad, Å. and Skinnes, H. 2008. Resistance to fusarium infection in oats (*Avena sativa* L.). *Cereal Research Communications*, 36 (Supplement-6), pp. 57-62.

- Bolley, H. L. 1913. Wheat: Soil troubles and seed deterioration, causes of soil sickness in wheat lands, possible methods of control, cropping methods with wheat. North Dakota Agricultural College, Government Agricultural Experiment Station for North Dakota.
- Borojevic, K. and Borojevic, K. 2005. The transfer and history of “reduced height genes” (*rht*) in wheat from Japan to Europe. *Journal of Heredity*, 96 (4), pp. 455-459.
- Brambilla, V., Gomez-Ariza, J., Cerise, M. and Fornara, F. 2017. The importance of being on time: Regulatory networks controlling photoperiodic flowering in cereals. *Frontiers in Plant Science*, 8 pp. 665.
- Brodal, G., Aamot, H. U., Almvik, M. and Hofgaard, I. S. 2020. Removal of small kernels reduces the content of *Fusarium* mycotoxins in oat grain. *Toxins*, 12 (5), pp. 346.
- Brown, C. 1980. Oat. *Hybridization of Crop Plants*, pp. 427-441.
- Brown, J. K. 2015. Durable resistance of crops to disease: A darwinian perspective. *Annual Review of Phytopathology*, 53 pp. 513-539.
- Brown, N. A., Urban, M., Van de Meene, Allison ML and Hammond-Kosack, K. E. 2010. The infection biology of *Fusarium graminearum*: Defining the pathways of spikelet to spikelet colonisation in wheat ears. *Fungal Biology*, 114 (7), pp. 555-571.
- Brown, P., McKenzie, R. and Mikaelsen, K. 1980. Agronomic, genetic, and cytologic evaluation of a vigorous new semidwarf oat 1. *Crop Science*, 20 (3), pp. 303-306.
- Buerstmayr, H., Steiner, B., Lemmens, M. and Ruckenbauer, P. 2000. Resistance to fusarium head blight in winter wheat: Heritability and trait associations. *Crop Science*, 40 (4), pp. 1012-1018.
- Buerstmayr, M. and Buerstmayr, H. 2015. Comparative mapping of quantitative trait loci for fusarium head blight resistance and anther retention in the winter wheat population Capo × Arina. *Theoretical and Applied Genetics*, 128 (8), pp. 1519-1530.
- Canales, F. J., Montilla-Bascón, G., Bekele, W., Howarth, C., Langdon, T., Risipail, N., Tinker, N. A. and Prats, E. 2021. Population genomics of Mediterranean oat (*A. sativa*) reveals high genetic diversity and three loci for heading date. *Theoretical and Applied Genetics*, 134 (7), pp. 2063-2077.

Casañas, F., Simó, J., Casals, J. and Prohens, J. 2017. Toward an evolved concept of landrace. *Frontiers in Plant Science*, 8 pp. 145.

Chaffin, A. S., Huang, Y., Smith, S., Bekele, W. A., Babiker, E., Gnanesh, B. N., Foresman, B. J., Blanchard, S. G., Jay, J. J. and Reid, R. W. 2016. A consensus map in cultivated hexaploid oat reveals conserved grass synteny with substantial subgenome rearrangement. *The Plant Genome*, 9 (2), pp. plantgenome2015.10.0102.

Chouard, P. 1960. Vernalization and its relations to dormancy. *Annual Review of Plant Physiology*, 11 (1), pp. 191-238.

Clarke, S. 2015. Opportunities and Challenges of Oat Agronomy. *ADAS Oats 2020 Conference*. Coventry.

Cockram, J., Jones, H., Leigh, F. J., O'Sullivan, D., Powell, W., Laurie, D. A. and Greenland, A. J. 2007. Control of flowering time in temperate cereals: Genes, domestication, and sustainable productivity. *Journal of Experimental Botany*, 58 (6), pp. 1231-1244.

Commission Regulation (EC) No 1881/2006 of 19 December 2006 setting maximum levels for certain contaminants in foodstuffs. [Online]. Official Journal of the European Union L 364/5. Available from: <https://eur-lex.europa.eu/LexUriServ/LexUriServ.do?uri=OJ:L:2006:364:0005:0024:EN:PDF> [Accessed 26 September 2021].

De Boevre, M., Landschoot, S., Audenaert, K., Maene, P., Di Mavungu, D., Eeckhout, M., Haesaert, G. and De Saeger, S. 2014. Occurrence and within field variability of *Fusarium* mycotoxins and their masked forms in maize crops in Belgium. *World Mycotoxin Journal*, 7 (1), pp. 91-102.

De Wolf, E., Madden, L. and Lipps, P. 2003. Risk assessment models for wheat fusarium head blight epidemics based on within-season weather data. *Phytopathology*, 93 (4), pp. 428-435.

De Zutter, N., Audenaert, K., Ameye, M., De Boevre, M., De Saeger, S., Haesaert, G. and Smagghe, G. 2016. The plant response induced in wheat ears by a combined attack of *Sitobion avenae* aphids and *Fusarium graminearum* boosts fungal infection and deoxynivalenol production. *Molecular Plant Pathology*, 18 (1), pp. 98-109.

Dedeurwaerder, G., Ghysselinckx, J., Hellin, P., Janssen, F., Duvivier, M. and Legrève, A. 2014. Detection of *Fusarium langsethiae* on wheat in Belgium. *European Journal of Plant Pathology*, 139 (3), pp. 453-455.

Desjardins, A. E., Hohn, T. M. and McCormick, S. P. 1993. Trichothecene biosynthesis in *Fusarium* species: Chemistry, genetics, and significance. *Microbiological Reviews*, 57 (3), pp. 595-604.

Dickson, J. G. 1923. Influence of soil temperature and moisture on the development of the seedling-blight of wheat and corn caused by *Gibberella saubinetii*. *Jour. Agr. Res.*, 23 pp. 837-870.

Divon, H. H., Bøe, L., Tveit, M. M. N. and Klemsdal, S. S. 2019. Infection pathways and penetration modes of *Fusarium langsethiae*. *European Journal of Plant Pathology*, 154 (2), pp. 259-271.

Divon, H. H., Razzaghian, J., Udnes-Aamot, H. and Klemsdal, S. S. 2012. *Fusarium langsethiae* (torp and nirenberg), investigation of alternative infection routes in oats. *European Journal of Plant Pathology*, 132 (1), pp. 147-161.

Doehlert, D. C., McMullen, M. S. and Riveland, N. R. 2002. Sources of variation in oat kernel size. *Cereal Chemistry*, 79 (4), pp. 528-534.

Doohan, F., Weston, G., Rezanoor, H., Parry, D. and Nicholson, P. 1999. Development and use of a reverse transcription-PCR assay to study expression of Tri5 by *Fusarium* species in vitro and in planta. *Applied and Environmental Microbiology*, 65 (9), pp. 3850-3854.

Draeger, R., Gosman, N., Steed, A., Chandler, E., Thomsett, M., Schondelmaier, J., Buerstmayr, H., Lemmens, M., Schmolke, M. and Mesterhazy, A. 2007. Identification of QTLs for resistance to *Fusarium* head blight, DON accumulation and associated traits in the winter wheat variety Arina. *Theoretical and Applied Genetics*, 115 (5), pp. 617-625.

Drakulic, J., Bruce, T. and Ray, R. 2016. Direct and host-mediated interactions between *Fusarium* pathogens and herbivorous arthropods in cereals. *Plant Pathology*, 66(1), pp.3-13.

Drakulic, J., Kahar, M. H., Ajigboye, O., Bruce, T. and Ray, R. V. 2016. Contrasting roles of deoxynivalenol and nivalenol in host-mediated interactions between *Fusarium graminearum* and *Sitobion avenae*. *Toxins*, 8 (12), pp. 353.

Drakulic, J., Ajigboye, O., Swarup, R., Bruce, T. and Ray, R. V. 2016. Aphid infestation increases *Fusarium langsethiae* and T-2 and HT-2 mycotoxins in wheat. *Applied and Environmental Microbiology*, 82 (22), pp. 6548-6556.

Drakulic, J., Caulfield, J., Woodcock, C., Jones, S. P., Linforth, R., Bruce, T. J. and Ray, R. V. 2015. Sharing a host plant (wheat [*Triticum aestivum*]) increases the fitness of *Fusarium graminearum* and the severity of fusarium head blight but reduces the fitness of grain aphids (*Sitobion avenae*). *Applied and Environmental Microbiology*, 81 (10), pp. 3492-3501.

Edwards, S. G. 2004. Influence of agricultural practices on *Fusarium* infection of cereals and subsequent contamination of grain by trichothecene mycotoxins. *Toxicology Letters*, 153 (1), pp. 29-35.

Edwards, S. 2007a. *Investigation of Fusarium mycotoxins in UK barley and oat production*. Home-Grown Cereals Authority.

Edwards, S. 2007b. *Investigation of fusarium mycotoxins in UK wheat production*. Home-Grown Cereals Authority.

Edwards, S. G. 2009. *Fusarium* mycotoxin content of UK organic and conventional oats. *Food Additives and Contaminants*, 26 (7), pp. 1063-1069.

Edwards, S. G. and Godley, N. P. 2010. Reduction of fusarium head blight and deoxynivalenol in wheat with early fungicide applications of prothioconazole. *Food Additives and Contaminants*, 27 (5), pp. 629-635.

Edwards, S. and Anderson, E. 2011. Impact of agronomy on HT-2 and T-2 toxin content of oats. *Plant Breeding and Seed Science*, 63 pp. 49-57.

Edwards, S. G., Imathiu, S. M., Ray, R. V., Back, M. and Hare, M. C. 2012a. Molecular studies to identify the fusarium species responsible for HT-2 and T-2 mycotoxins in UK oats. *International Journal of Food Microbiology*, 156 (2), pp. 168-175.

Edwards, S. 2012b. Improving risk assessment to minimise *Fusarium* mycotoxins in harvested oats and malting barley. HGCA.

Edwards, S. G. 2015. *Fusarium* mycotoxins in UK oat varieties - monitoring in preparation for legislation. London: AHDB Cereals and Oilseeds.

Edwards, S. G. 2017. Impact of agronomic and climatic factors on the mycotoxin content of harvested oats in the United Kingdom. *Food Additives & Contaminants: Part A*, 34 (12), pp. 2230-2241.

Edwards, S. G. and Jennings, P. 2018. Impact of agronomic factors on fusarium mycotoxins in harvested wheat. *Food Additives & Contaminants: Part A*, 35 (12), pp. 2443-2454.

EFSA Panel on Contaminants in the Food Chain (CONTAM), Knutsen, H., Barregård, L., Bignami, M., Brüschweiler, B., Ceccatelli, S., Cottrill, B., Dinovi, M., Edler, L. and Grasl-Kraupp, B. 2017. Appropriateness to set a group health based guidance value for T2 and HT 2 toxin and its modified forms. *EFSA Journal*, 15 (1), pp. e04655.

EFSA. 2018. Scientific Opinion on the substantiation of a health claim related to oat beta-glucan and lowering blood cholesterol and reduced risk of (coronary) heart disease pursuant to Article 14 of Regulation (EC) No 1924/2006. *EFSA Journal*, 2010 8(12):1885

Esvelt Klos, K., Huang, Y. F., Bekele, W. A., Obert, D. E., Babiker, E., Beattie, A. D., Bjornstad, A., Bonman, J. M., Carson, M. L., Chao, S., Gnanesh, B. N., Griffiths, I., Harrison, S. A., Howarth, C. J., Hu, G., Ibrahim, A., Islamovic, E., Jackson, E. W., Jannink, J. L., Kolb, F. L., McMullen, M. S., Mitchell Fetch, J., Murphy, J. P., Ohm, H. W., Rines, H. W., Rossnagel, B. G., Schlueter, J. A., Sorrells, M. E., Wight, C. P., Yan, W. and Tinker, N. A. 2016. Population genomics related to adaptation in elite oat germplasm. *The Plant Genome*, 9 (2), pp. 10.3835/plantgenome2015.10.0103.

European Commission. 2021. *DG AGRI – Cereals – Gross production by All Crops (1000 Tonnes) for All Member States*. [Online]. European Commission. Available from: <https://agridata.ec.europa.eu/extensions/DashboardCereals/CerealsProduction.html> [Accessed 26 September 2021].

Farnham, M., Stuthman, D. and Pomeranke, G. 1990. Inheritance of and selection for panicle exertion in semidwarf oat. *Crop Science*, 30 (2), pp. 328-334.

Ferruz, E., Atanasova-Pénichon, V., Bonnin-Verdal, M., Marchegay, G., Pinson-Gadais, L., Ducos, C., Lorán, S., Ariño, A., Barreau, C. and Richard-Forget, F. 2016. Effects of phenolic acids on the growth and production of T-2 and HT-2 toxins by *Fusarium langsethiae* and *F. sporotrichioides*. *Molecules*, 21 (4), pp. 449.

Gagkaeva, T., Gavrilova, O., Yli-Mattila, T. and Loskutov, I. 2011. Evaluation of oat germplasm for resistance to fusarium head blight. *Plant Breeding and Seed Science*, 64 pp. 15-22.

Gagkaeva, T. Y., Gavrilova, O., Orina, A., Blinova, E. and Loskutov, I. 2018. Diversity of *Avena* species by morphological traits and resistance to fusarium head blight. *Russian Journal of Genetics: Applied Research*, 8 (1), pp. 44-51.

Gale, M. D. and Marshall, G. A. 1975. The nature and genetic control of gibberellin insensitivity in dwarf wheat grain. *Heredity*, 35 (1), pp. 55-65.

Gilsinger, J., Kong, L., Shen, X. and Ohm, H. 2005. DNA markers associated with low fusarium head blight incidence and narrow flower opening in wheat. *Theoretical and Applied Genetics*, 110 (7), pp. 1218-1225.

Glynn, N. C., Hare, M. C. and Edwards, S. G. 2008. Fungicide seed treatment efficacy against *Microdochium nivale* and *M. majus* in vitro and in vivo. *Pest Management Science: Formerly Pesticide Science*, 64 (8), pp. 793-799.

Gosman, N., Steed, A., Hollins, T., Bayles, R., Jennings, P. and Nicholson, P. 2009. Semi-dwarfing *rht-B1* and *rht-D1* loci of wheat differ significantly in their influence on resistance to fusarium head blight. *Theoretical and Applied Genetics*, 118 (4), pp. 695-702.

Häggblom, P. and Nordkvist, E. 2015. Deoxynivalenol, zearalenone, and *Fusarium graminearum* contamination of cereal straw; field distribution; and sampling of big bales. *Mycotoxin Research*, 31 (2), pp. 101-107.

Haidukowski, M., Visconti, A., Perrone, G., Vanadia, S., Pancaldi, D., Covarelli, L., Balestrazzi, R. and Pascale, M. 2012. Effect of prothioconazole-based fungicides on fusarium head blight, grain yield and deoxynivalenol accumulation in wheat under field conditions. *Phytopathologia Mediterranea*, pp. 236-246.

Hanson, L.E, and A.L Hill. 2004. *Fusarium* Species Causing Fusarium Yellows of Sugarbeet. *Journal of the American Society of Sugar Beet Technologists*, v. 41,.4 pp. 163-178.

Hanson, L. 2006. Fusarium yellowing of sugar beet caused by *Fusarium graminearum* from Minnesota and Wyoming. *Plant Disease*, 90 (5), pp. 686-686.

Hardy, M. Y., Tye-Din, J. A., Stewart, J. A., Schmitz, F., Dudek, N. L., Hanchapola, I., Purcell, A. W. and Anderson, R. P. 2015. Ingestion of oats and barley in patients with celiac disease mobilizes cross-reactive T cells activated by avenin peptides and immuno-dominant hordein peptides. *Journal of Autoimmunity*, 56 pp. 56-65.

Hare, M.C., 1997. Epidemiology and chemical control of Fusarium seedling blight of winter wheat (*Triticum aestivum* L.). Open University (United Kingdom).

Harlan, J. R. and de Wet, J. M. 1971. Toward a rational classification of cultivated plants. *Taxon*, 20 (4), pp. 509-517.

Hessor, L. 2006. *The Man Who Fed the World*. Texas: Durban House Publishing Company, Inc.

HCGA. 2005. *HGCA Recommended List Winter Oats 2005/06*

HCGA. 2013. *HGCA Recommended Lists 2013/14 for cereals and oilseeds*.

Hautsalo, J., Jalli, M., Manninen, O. and Veteläinen, M. 2018. Evaluation of resistance to *Fusarium graminearum* in oats. *Euphytica*, 214 (8), pp. 1-18.

Hautsalo, J., Jauhiainen, L., Hannukkala, A., Manninen, O., Veteläinen, M., Pietilä, L., Peltoniemi, K. and Jalli, M. 2020. Resistance to fusarium head blight in oats based on analyses of multiple field and greenhouse studies. *European Journal of Plant Pathology*, 158 (1), pp. 15-33.

He, X., Skinnies, H., Oliver, R. E., Jackson, E. W. and Bjørnstad, Å. 2013. Linkage mapping and identification of QTL affecting deoxynivalenol (DON) content (*Fusarium* resistance) in oats (*Avena sativa* L.). *Theoretical and Applied Genetics*, 126 (10), pp. 2655-2670.

He, X., Osman, M., Helm, J., Capettini, F. and Singh, P. K. 2015. Evaluation of canadian barley breeding lines for fusarium head blight resistance. *Canadian Journal of Plant Science*, 95 (5), pp. 923-929.

Heidari, B., Saeidi, G., SAYED, T. B. and Suenaga, K. 2012. QTLs involved in plant height, peduncle length and heading date of wheat (*Triticum aestivum* L.). *Journal of Agricultural Science and Technology*, 14 (5), pp. 1093-1104.

- Herrmann, M. H., Hautsalo, J., Georgieva, P., Bund, A., Winter, M. and Beuch, S. 2020. Relationship between genetic variability of flowering traits and *Fusarium* mycotoxin contamination in oats. *Crop Science*, 60 (2), pp. 852-862.
- Hilton, A., Jenkinson, P., Hollins, T. and Parry, D. 1999. Relationship between cultivar height and severity of fusarium ear blight in wheat. *Plant Pathology*, 48 (2), pp. 202-208.
- Hjelkrem, A. R., Aamot, H. U., Brodal, G., Strand, E. C., Torp, T., Edwards, S. G., Dill-Macky, R. and Hofgaard, I. S. 2018. HT-2 and T-2 toxins in Norwegian oat grains related to weather conditions at different growth stages. *European Journal of Plant Pathology*, 151 (2), pp. 501-514.
- Hofgaard, I. S., Seehusen, T., Aamot, H. U., Riley, H., Razzaghian, J., Le, V. H., Hjelkrem, A. G., Dill-Macky, R. and Brodal, G. 2016a. Inoculum potential of *Fusarium* spp. relates to tillage and straw management in Norwegian fields of spring oats. *Frontiers in Microbiology*, 7 pp. 556.
- Hofgaard, I., Aamot, H., Torp, T., Jestoi, M., Lattanzio, V., Klemsdal, S., Waalwijk, C., Van der Lee, T. and Brodal, G. 2016b. Associations between *Fusarium* species and mycotoxins in oats and spring wheat from farmers' fields in Norway over a six-year period. *World Mycotoxin Journal*, 9 (3), pp. 365-378.
- Holland, J., Portyanko, V., Hoffman, D. and Lee, M. 2002. Genomic regions controlling vernalization and photoperiod responses in oat. *Theoretical and Applied Genetics*, 105 (1), pp. 113-126.
- Horsley, R., Steffenson, B., Schmierer, D., Maier, C., Kudrna, D., Urrea, C., Schwarz, P., Franckowiak, J., Green, M. and Zhang, B. 2006. Identification of QTLs associated with fusarium head blight resistance in barley accession Clho 4196, *Crop Sci.* 46, pp. 145-156.
- Huang, Y., Poland, J. A., Wight, C. P., Jackson, E. W. and Tinker, N. A. 2014. Using genotyping-by-sequencing (GBS) for genomic discovery in cultivated oat. *PloS One*, 9 (7), pp. e102448.
- Imathiu, S. M. 2008. *Fusarium langsethiae* infection and mycotoxin production in oats. Newport, UK, Harper Adams University College, PhD Thesis,

- Imathiu, S. M., Ray, R. V., Back, M., Hare, M. C. and Edwards, S. G. 2009. *Fusarium langsethiae* pathogenicity and aggressiveness towards oats and wheat in wounded and unwounded in vitro detached leaf assays. *European Journal of Plant Pathology*, 124 (1), pp. 117-126.
- Imathiu, S. M., Hare, M. C., Ray, R. V., Back, M. and Edwards, S. G. 2010. Evaluation of pathogenicity and aggressiveness of *Fusarium langsethiae* on oat and wheat seedlings relative to known seedling blight pathogens. *European Journal of Plant Pathology*, 126 (2), pp. 203-216.
- Imathiu, S. M., Ray, R. V., Back, M. I., Hare, M. C. and Edwards, S. G. 2013. A survey investigating the infection of *Fusarium langsethiae* and production of HT-2 and T-2 mycotoxins in UK oat fields. *Journal of Phytopathology*, 161 (7-8), pp. 553-561.
- Imathiu, S., Edwards, S., Ray, R. and Back, M. 2014. Artificial inoculum and inoculation techniques commonly used in the investigation of fusarium head blight in cereals. *Acta Phytopathologica Et Entomologica Hungarica*, 49 (2), pp. 129-139.
- Infantino, A., Pucci, N., Conca, G. and Santori, A. 2007. First report of *Fusarium langsethiae* on durum wheat kernels in Italy. *Plant Disease*, 91 (10), pp. 1362-1362.
- Isidro-Sánchez, J., D'Arcy Cusack, K., Verheecke-Vaessen, C., Kahla, A., Bekele, W., Doohan, F., Magan, N. and Medina, A. 2020. Genome-wide association mapping of *Fusarium langsethiae* infection and mycotoxin accumulation in oat (*Avena sativa* L.). *The Plant Genome*, 13 (2), pp. e20023.
- Jansen, C., von Wettstein, D., Schafer, W., Kogel, K. H., Felk, A. and Maier, F. J. 2005. Infection patterns in barley and wheat spikes inoculated with wild-type and trichodiene synthase gene disrupted *Fusarium graminearum*. *Proceedings of the National Academy of Sciences of the United States of America*, 102 (46), pp. 16892-16897.
- Jellen, E., Gill, B. and Cox, T. 1994. Genomic in situ hybridization differentiates between A/D-and C-genome chromatin and detects intergenomic translocations in polyploid oat species (genus *Avena*). *Genome*, 37 (4), pp. 613-618.
- Jenkinson, P. and Parry, D. 1994. Splash dispersal of conidia of *Fusarium culmorum* and *Fusarium avenaceum*. *Mycological Research*, 98 (5), pp. 506-510.
- Joffe, A. Z. 1960. The mycoflora of overwintered cereals and its toxicity. *Bulletin of the Research Council of Israel. Section D. Botany*, 9 (3), pp. 101-106.

- Jones, J. D. and Dangl, J. L. 2006. The plant immune system. *Nature*, 444 (7117), pp. 323-329.
- Kaukoranta, T., Hietaniemi, V., Rämö, S., Koivisto, T. and Parikka, P. 2019. Contrasting responses of T-2, HT-2 and DON mycotoxins and *Fusarium* species in oat to climate, weather, tillage and cereal intensity. *European Journal of Plant Pathology*, pp. 1-18.
- Kemp, G., Pretorius, Z. and Wingfield, M. 1996. Fusarium glume spot of wheat: A newly recorded mite-associated disease in south Africa. *Plant Disease (USA)*,
- Kimura, M., Tokai, T., O'Donnell, K., Ward, T. J., Fujimura, M., Hamamoto, H., Shibata, T. and Yamaguchi, I. 2003. The trichothecene biosynthesis gene cluster of *Fusarium graminearum* F15 contains a limited number of essential pathway genes and expressed non-essential genes. *FEBS Letters*, 539 (1-3), pp. 105-110.
- Kimura, M., Tokai, T., Takahashi-Ando, N., Ohsato, S. and Fujimura, M. 2007. Molecular and genetic studies of fusarium trichothecene biosynthesis: Pathways, genes, and evolution. *Bioscience, Biotechnology, and Biochemistry*, pp. 0707310525-0707310525.
- Kokkonen, M., Ojala, L., Parikka, P. and Jestoi, M. 2010. Mycotoxin production of selected *Fusarium* species at different culture conditions. *International Journal of Food Microbiology*, 143 (1-2), pp. 17-25.
- Kriss, A., Paul, P. and Madden, L. 2010. Relationship between yearly fluctuations in fusarium head blight intensity and environmental variables: A window-pane analysis. *Phytopathology*, 100 (8), pp. 784-797.
- Kriss, A., Paul, P. and Madden, L. 2012. Characterizing heterogeneity of disease incidence in a spatial hierarchy: A case study from a decade of observations of fusarium head blight of wheat. *Phytopathology*, 102 (9), pp. 867-877.
- Kubo, K., Kawada, N. and Fujita, M. 2013a. Evaluation of fusarium head blight resistance in wheat and the development of a new variety by integrating type I and II resistance. *Japan Agricultural Research Quarterly: JARQ*, 47 (1), pp. 9-19.
- Kubo, K., Fujita, M., Kawada, N., Nakajima, T., Nakamura, K., Maejima, H., Ushiyama, T., Hatta, K. and Matsunaka, H. 2013b. Minor differences in anther extrusion affect

resistance to fusarium head blight in wheat. *Journal of Phytopathology*, 161 (5), pp. 308-314.

Lacey, J., Bateman, G. and Mirocha, C. 1999. Effects of infection time and moisture on development of ear blight and deoxynivalenol production by *Fusarium spp.* in wheat. *Annals of Applied Biology*, 134 (3), pp. 277-283.

Landry, B., Comeau, A., Minvielle, F. and St-Pierre, C. 1984. Genetic analysis of resistance to barley yellow dwarf virus in hybrids between *Avena sativa* 'Lamar' and Virus-Resistant lines of *Avena sterilis* 1. *Crop Science*, 24 (2), pp. 337-340.

Langevin, F., Eudes, F. and Comeau, A. 2004. Effect of trichothecenes produced by *Fusarium graminearum* during fusarium head blight development in six cereal species. *European Journal of Plant Pathology*, 110 (7), pp. 735-746.

Lattanzio, V. M., Visconti, A., Haidukowski, M. and Pascale, M. 2012. Identification and characterization of new *Fusarium* masked mycotoxins, T2 and HT2 glycosyl derivatives, in naturally contaminated wheat and oats by liquid chromatography–high-resolution mass spectrometry. *Journal of Mass Spectrometry*, 47 (4), pp. 466-475.

Lemmens, M., Scholz, U., Berthiller, F., Dall'Asta, C., Koutnik, A., Schuhmacher, R., Adam, G., Buerstmayr, H., Mesterházy, Á. and Krska, R. 2005. The ability to detoxify the mycotoxin deoxynivalenol colocalizes with a major quantitative trait locus for fusarium head blight resistance in wheat. *Molecular Plant-Microbe Interactions*, 18 (12), pp. 1318-1324.

Lewandowski, S. and Bushnell, W. 2001. Development of *Fusarium graminearum* on floret surfaces of field grown barley. *2001 national fusarium head blight forum proceedings*. pp 128. Li, Y., Wang, Z., Beier, R. C., Shen, J., Smet, D. D., De Saeger, S. and Zhang, S. 2011. T-2 toxin, a trichothecene mycotoxin: Review of toxicity, metabolism, and analytical methods. *Journal of Agricultural and Food Chemistry*, 59 (8), pp. 3441-3453.

Locatelli, A., Federizzi, L., Milach, S. and McElroy, A. 2008. Flowering time in oat: Genotype characterization for photoperiod and vernalization response. *Field Crops Research*, 106 (3), pp. 242-247.

Logrieco, A., Bottalico, A., Mulé, G., Moretti, A. and Perrone, G. 2003. Epidemiology of toxigenic fungi and their associated mycotoxins for some Mediterranean crops. *European Journal of Plant Pathology*, 109 (7), pp. 645-667.

- Loskutov, I., Blinova, E., Gavrilova, O. and Gagkaeva, T. Y. 2017. The valuable characteristics and resistance to *Fusarium* disease of oat genotypes. *Russian Journal of Genetics: Applied Research*, 7 (3), pp. 290-298.
- Loskutov, I., Blinova, E., Gavrilova, O. and Gagkaeva, T. Y. 2016. The valuable characteristics of oats genotypes and resistance to *Fusarium* disease. *Vavilov J.Genet.Breed*, 20 (3), pp. 286.
- Lukanowski, A., Lenc, L. and Sadowski, C. 2008. First report on the occurrence of *Fusarium langsethiae* isolated from wheat kernels in Poland. *Plant Disease*, 92 (3), pp. 488-488.
- Lysøe, E., Frandsen, R. J., Divon, H. H., Terzi, V., Orrù, L., Lamontanara, A., Kolseth, A., Nielsen, K. F. and Thrane, U. 2016. Draft genome sequence and chemical profiling of *Fusarium langsethiae*, an emerging producer of type A trichothecenes. *International Journal of Food Microbiology*, 221 pp. 29-36.
- Magan, N., Medina, A. and Aldred, D. 2011. Possible climate-change effects on mycotoxin contamination of food crops pre-and postharvest. *Plant Pathology*, 60 (1), pp. 150-163.
- Mariotti Lippi, M., Foggi, B., Aranguren, B., Ronchitelli, A. and Revedin, A. 2015. Multistep food plant processing at grotta paglicci (southern Italy) around 32,600 cal B.P. *Proceedings of the National Academy of Sciences of the United States of America*, 112 (39), pp. 12075-12080.
- Marshall, A., Cowan, S., Edwards, S., Griffiths, I., Howarth, C., Langdon, T. and White, E. 2013. Crops that feed the world 9. oats-a cereal crop for human and livestock feed with industrial applications. *Food Security*, 5 (1), pp. 13-33.
- Marshall, A., Cowan, S., Griffiths, I., Moorby, J., Howarth, C., Langdon, T., Stewart, D., Edwards, S., Fradgley, N. and Clarke, S. 2015. *Project Report No. 543, Harnessing new technologies for sustainable oat production and utilization*. AHDB Cereals & Oilseeds.
- Martinez-Villaluenga, C. and Penas, E. 2017. Health benefits of oat: Current evidence and molecular mechanisms. *Current Opinion in Food Science*, 14 pp. 26-31.
- Mateo, E. M., Valle-Algarra, F. M., Mateo, R., Jimenez, M. and Magan, N. 2011. Effect of fenpropimorph, prochloraz and tebuconazole on growth and production of T-2 and

HT-2 toxins by *Fusarium langsethiae* in oat-based medium. *International Journal of Food Microbiology*, 151 (3), pp. 289-298.

McDonald, T., Brown, D., Keller, N. P. and Hammond, T. M. 2005. RNA silencing of mycotoxin production in aspergillus and *Fusarium* species. *Molecular Plant-Microbe Interactions*, 18 (6), pp. 539-545.

Medina, A. and Magan, N. 2010. Comparisons of water activity and temperature impacts on growth of *Fusarium langsethiae* strains from northern Europe on oat-based media. *International Journal of Food Microbiology*, 142 (3), pp. 365-369.

Medina, A. and Magan, N. 2011. Temperature and water activity effects on production of T-2 and HT-2 by *Fusarium langsethiae* strains from North European countries. *Food Microbiology*, 28 (3), pp. 392-398.

Meek, I. B., Peplow, A. W., Ake Jr, C., Phillips, T. and Beremand, M. N. 2003. *Tri1* encodes the cytochrome P450 monooxygenase for C-8 hydroxylation during trichothecene biosynthesis in *Fusarium sporotrichioides* and resides upstream of another new tri gene. *Applied and Environmental Microbiology*, 69 (3), pp. 1607-1613.

Mellers, G., Mackay, I., Cowan, S., Griffiths, I., Martinez-Martin, P., Poland, J. A., Bekele, W., Tinker, N. A., Bentley, A. R. and Howarth, C. J. 2020. Implementing within-cross genomic prediction to reduce oat breeding costs. *The Plant Genome*, 13 (1), pp. e20004.

Meng-Reiterer, J., Bueschl, C., Rechthaler, J., Berthiller, F., Lemmens, M. and Schuhmacher, R. 2016. Metabolism of HT-2 toxin and T-2 toxin in oats. *Toxins*, 8 (12), pp. 364.

Mesterhazy, A. 1995. Types and components of resistance to fusarium head blight of wheat. *Plant Breeding*, 114 (5), pp. 377-386.

Meydani, M. 2009. Potential health benefits of avenanthramides of oats. *Nutrition Reviews*, 67 (12), pp. 731-735.

Miedaner, T. 1997. Breeding wheat and rye for resistance to fusarium diseases. *Plant Breeding*, 116 (3), pp. 201-220.

Milach, S., Rines, H., Phillips, R., Stuthman, D. and Morikawa, T. 1998. Inheritance of a new dwarfing gene in oat. *Crop Science*, 38 (2), pp. 356-360.

- Milach, S. and Federizzi, L. 2001. Dwarfing genes in plant improvement. *Advances in Agronomy*, 73, pp 35-63.
- Milach, S., Rines, H. and Phillips, R. 2002. Plant height components and gibberellic acid response of oat dwarf lines. *Crop Science*, 42 (4), pp. 1147-1154.
- Miller, J. D., Young, J. C. and Trenholm, H. L. 1983. *Fusarium* toxins in field corn. I. time course of fungal growth and production of deoxynivalenol and other mycotoxins. *Canadian Journal of Botany*, 61 (12), pp. 3080-3087.
- Miller, J. D. and Young, J. C. 1985. Deoxynivalenol in an experimental *Fusarium graminearum* infection of wheat. *Canadian Journal of Plant Pathology*, 7 (2), pp. 132-134.
- Misonoo, G. 1936. Ecological and physiological studies on the blooming of oat flowers. *Journal of the Faculty of Agriculture, Hokkaido Imperial University*, 37 (4), pp. 211-337.
- Molnar, S. J., Chapados, J. T., Satheeskumar, S., Wight, C. P., Bancroft, B., Orr, W., Luckert, D. E. and Kibite, S. 2012. Comparative mapping of the oat *Dw6/dw6* dwarfing locus using NILs and association with vacuolar proton ATPase subunit H. *Theoretical and Applied Genetics*, 124 (6), pp. 1115-1125.
- Montilla-Bascón, G., Sánchez-Martín, J., Risipail, N., Rubiales, D., Mur, L., Langdon, T., Griffiths, I., Howarth, C. and Prats, E. 2013. Genetic diversity and population structure among oat cultivars and landraces. *Plant Molecular Biology Reporter*, 31 (6), pp. 1305-1314.
- Montilla-Bascón, G., Risipail, N., Sánchez-Martín, J., Rubiales, D., Mur, L. A., Langdon, T., Howarth, C. J. and Prats, E. 2015. Genome-wide association study for crown rust (*Puccinia coronata* f. sp. *Avenae*) and powdery mildew (*Blumeria graminis* f. sp. *Avenae*) resistance in an oat (*Avena sativa*) collection of commercial varieties and landraces. *Frontiers in Plant Science*, 6, p.103.
- Mousavi, S. H. 2016. Identifying Inoculation Methods for Screening of Resistance to *Fusarium langsethiae* in Selected Oat Varieties, *Master's thesis, Norwegian University of Life Sciences, Ås*.
- Müller, M. E. H., Koszinski, S., Brenning, A., Verch, G., Korn, U. and Sommer, M. 2011. Within-field variation of mycotoxin contamination of winter wheat is related to indicators of soil moisture. *Plant and Soil*, 342 (1), pp. 289-300.

Munkvold, G. P. 2003. Epidemiology of fusarium diseases and their mycotoxins in maize ears. In: Anonymous ed. *Epidemiology of Mycotoxin Producing Fungi*. Springer. pp. 705-713

Mylona, K. and Magan, N. 2011. *Fusarium langsethiae*: Storage environment influences dry matter losses and T2 and HT-2 toxin contamination of oats. *Journal of Stored Products Research*, 47 (4), pp. 321-327.

Nathanail, A. V., Varga, E., Meng-Reiterer, J., Bueschl, C., Michlmayr, H., Malachova, A., Fruhmann, P., Jestoi, M., Peltonen, K. and Adam, G. 2015. Metabolism of the *Fusarium* mycotoxins T-2 toxin and HT-2 toxin in wheat. *Journal of Agricultural and Food Chemistry*, 63 (35), pp. 7862-7872.

Nava, I. C., Wight, C. P., Pacheco, M. T., Federizzi, L. C. and Tinker, N. A. 2012. Tagging and mapping candidate loci for vernalization and flower initiation in hexaploid oat. *Molecular Breeding*, 30 (3), pp. 1295-1312.

Nishiyama, I. 1970. Four types of flowering time in *Avena*. *The Japanese Journal of Genetics*, 45 (5), pp. 399-409.

Obst, A., Lepschy, J., Beck, R., Bauer, G. and Bechtel, A. 2000. The risk of toxins by *Fusarium graminearum* in wheat—interactions between weather and agronomic factors. *Mycotoxin Research*, 16 (1), pp. 16-20.

Odenbach, K. J. 2009. Epidemiology and Variability of Disease and Deoxynivalenol in *Fusarium* Head Blight of Wheat in Ohio, *Doctoral dissertation, The Ohio State University*.

O'Donoghue, L., Sorrells, M., Tanksley, S., Autrique, E., Deynze, A. V., Kianian, S., Phillips, R., Wu, B., Rines, H. and Rayapati, P. 1995. A molecular linkage map of cultivated oat. *Genome*, 38 (2), pp. 368-380.

Oerke, E., Meier, A., Dehne, H., Sulyok, M., Krska, R. and Steiner, U. 2010. Spatial variability of fusarium head blight pathogens and associated mycotoxins in wheat crops. *Plant Pathology*, 59 (4), pp. 671-682.

Opoku, N., Back, M. and Edwards, S. 2011. Aggressiveness of *Fusarium langsethiae* isolates towards wheat, barley and oats in an in vitro leaf assay. *Plant Breeding and Seed Science*, 64 pp. 55-63.

- Opoku, N., Back, M. and Edwards, S. 2013. Development of *Fusarium langsethiae* in commercial cereal production. *European Journal of Plant Pathology*, 136 (1), pp. 159-170.
- Osborne, L. E. and Stein, J. M. 2007. Epidemiology of fusarium head blight on small-grain cereals. *International Journal of Food Microbiology*, 119 (1), pp. 103-108.
- Parikka, P., Hietaniemi, V., Rämö, S. and Jalli, H. 2007. *Fusarium workshop: Fusarium diseases in cereals—potential impact from sustainable cropping systems*
- Parry, D., Jenkinson, P. and McLeod, L. 1995. Fusarium ear blight (scab) in small grain cereals—a review. *Plant Pathology*, 44 (2), pp. 207-238.
- Paul, P., El-Allaf, S., Lipps, P. and Madden, L. 2004. Rain splash dispersal of *Gibberella zeae* within wheat canopies in Ohio. *Phytopathology*, 94 (12), pp. 1342-1349.
- Pepsico. 2021. GrainGenes, A database for Triticeae and Avena, ***Avena sativa*** – OT3098 v2, PepsiCo. [Online]. USDA. Available from <https://wheat.pw.usda.gov/jb?data=ggds/oat-ot3098v2-pepsico>
- Pettersson, H., Borjesson, T., Persson, L., Lerenius, C., Berg, G. and Gustafsson, G. 2008. T-2 and HT-2 toxins in oats grown in northern Europe. *Cereal Research Communications*, 36 (Suppl B), pp. 591-592.
- Plăcintă, D., Murariu, D. and Herrmann, M. 2015. Incidence of *Fusarium* mycotoxins on different oat cultivars under natural and artificial infection conditions. *Romanian Agricultural Research*, (32), pp. 63-68.
- Pritsch, C., Muehlbauer, G. J., Bushnell, W. R., Somers, D. A. and Vance, C. P. 2000. Fungal development and induction of defense response genes during early infection of wheat spikes by *Fusarium graminearum*. *Molecular Plant-Microbe Interactions*, 13 (2), pp. 159-169.
- Proctor, R. H., Hohn, T. M. and McCormick, S. P. 1995. Reduced virulence of *Gibberella zeae* caused by disruption of a trichthecine toxin biosynthetic gene. *MPMI-Molecular Plant Microbe Interactions*, 8 (4), pp. 593-601.
- Pugh, G. W., Johann, H. and Dickson, J. 1933. Factors affecting infection of wheat heads by *Gibberella saubinetii*. *Journal of Agricultural Research*, 46 (9).

- R Core Team (2020). *R: A language and environment for statistical computing*. R Foundation for Statistical Computing, Vienna, Austria. Available here: <https://www.R-project.org/>. [Accessed 25 September 2018]
- Rafai, P., Tuboly, S., Bata, A., Tilly, P., Vanyi, A., Papp, Z., Jakab, L. and Tury, E. 1995. Effect of various levels of T-2 toxin in the immune system of growing pigs. *The Veterinary Record*, 136 (20), pp. 511-514.
- Rajala, A. and Peltonen-Sainio, P. 2011. Pollination dynamics, grain weight and grain cell number within the inflorescence and spikelet in oat and wheat. *Agricultural Sciences*, 2 (03), pp. 283.
- Rines H.W., Molnar S.J., Tinker N.A., Phillips R.L. (2006) Oat. In: Kole C. (eds) *Cereals and Millets. Genome Mapping and Molecular Breeding in Plants*, vol 1. Springer, Berlin, Heidelberg. https://doi.org/10.1007/978-3-540-34389-9_5
- Rukmini, C., Prasad, J. and Rao, K. 1980. Effects of feeding T-2 toxin to rats and monkeys. *Food and Cosmetics Toxicology*, 18 (3), pp. 267-269.
- Salas, B., Steffenson, B., Casper, H., Tacke, B., Prom, L., Fetch Jr, T. and Schwarz, P. 1999. *Fusarium* species pathogenic to barley and their associated mycotoxins. *Plant Disease*, 83 (7), pp. 667-674.
- Sampson, D. and Burrows, V. 1972. Influence of photoperiod, short-day vernalization, and cold vernalization on days to heading in *Avena* species and cultivars. *Canadian Journal of Plant Science*, 52 (4), pp. 471-482.
- Sanz, M., Jellen, E., Loarce, Y., Irigoyen, M., Ferrer, E. and Fominaya, A. 2010. A new chromosome nomenclature system for oat (*Avena sativa* L. and *A. byzantina* C. koch) based on FISH analysis of monosomic lines. *Theoretical and Applied Genetics*, 121 (8), pp. 1541-1552.
- Schlang, N., Steiner, U., Dehne, H., Murakami, J., Duveiller, E. and Oerke, E. 2008. Spatial distribution of fusarium head blight pathogens and associated mycotoxins in wheat fields. *Cereal Research Communications*, 36 (Supplement-6), pp. 573-577.
- Schmidt, H., Adler, A., Holst-Jensen, A., Klemsdal, S., Logrieco, A., Mach, R., Nirenberg, H., Thrane, U., Torp, M. and Vogel, R. 2004. An integrated taxonomic study of *Fusarium langsethiae*, *Fusarium poae* and *Fusarium sporotrichioides* based on the

use of composite datasets. *International Journal of Food Microbiology*, 95 (3), pp. 341-349.

Schöneberg, T., Jenny, E., Wettstein, F. E., Bucheli, T. D., Mascher, F., Bertossa, M., Musa, T., Seifert, K., Gräfenhan, T. and Keller, B. 2018. Occurrence of *Fusarium* species and mycotoxins in swiss oats—Impact of cropping factors. *European Journal of Agronomy*, 92 pp. 123-132.

Schöneberg, T., Kibler, K., Wettstein, F., Bucheli, T., Forrer, H., Musa, T., Mascher, F., Bertossa, M., Keller, B. and Vogelgsang, S. 2019. Influence of temperature, humidity duration and growth stage on the infection and mycotoxin production by *Fusarium langsethiae* and *Fusarium poae* in oats. *Plant Pathology*, 68 (1), pp. 173-184.

Schuhmacher-Wolz, U., Heine, K. and Schneider, K. 2010. Report on toxicity data on trichothecene mycotoxins HT-2 and T-2 toxins. *EFSA Supporting Publications*, 7 (7), pp. 65E.

Scudamore, K., Baillie, H., Patel, S. and Edwards, S. G. 2007. Occurrence and fate of *Fusarium* mycotoxins during commercial processing of oats in the UK. *Food Additives and Contaminants*, 24 (12), pp. 1374-1385.

Scudamore, K., Patel, S. and Edwards, S. 2009. HT-2 toxin and T-2 toxin in commercial cereal processing in the United Kingdom, 2004-2007. *World Mycotoxin Journal*, 2 (3), pp. 357-365.

Shrestha, R., Gómez-Ariza, J., Brambilla, V. and Fornara, F. 2014. Molecular control of seasonal flowering in rice, *Arabidopsis* and temperate cereals. *Annals of Botany*, 114 (7), pp. 1445-1458.

Simpson, D., Rezanoor, H., Parry, D. and Nicholson, P. 2000. Evidence for differential host preference in *Microdochium nivale* var. *majus* and *Microdochium nivale* var. *nivale*. *Plant Pathology*, 49 (2), pp. 261-268.

Skinnes, H., Semagn, K., Tarkegne, Y., Marøy, A. and Bjørnstad, Å. 2010. The inheritance of anther extrusion in hexaploid wheat and its relationship to fusarium head blight resistance and deoxynivalenol content. *Plant Breeding*, 129 (2), pp. 149-155.

Snijders, C. H. and Krechting, C. 1992. Inhibition of deoxynivalenol translocation and fungal colonization in fusarium head blight resistant wheat. *Canadian Journal of Botany*, 70 (8), pp. 1570-1576.

Spanic, V., Lemmens, M., Drezner, G. and Mesterházy, Á. 2013. Variability in components of fusarium head blight resistance among wheat genotypes. *Cereal Research Communications*, 41 (3), pp. 420-430.

Stančić. T., 2016. *Identification of Fusarium Resistance Traits in UK Oat Varieties*, Newport: Harper Adams University.

Steffenson, B., Horsley, R., Schmierer, D., Maier, C., Kudrna, D., Urrea, C., Schwarz, P., Franckowiak, J., Green, M. and Zhang, B. 2006. Identification of QTLs associated with fusarium head blight resistance in barley accession Clho 4196. *Crop Science*. [Online]. Available here: <https://conservancy.umn.edu/handle/11299/188605> [Accessed 15 December 2019]. Stenglein, S. 2009. *Fusarium poae*: A pathogen that needs more attention. *Journal of Plant Pathology*, pp. 25-36.

Strange, R. and Smith, H. 1971. A fungal growth stimulant in anthers which predisposes wheat to attack by *Fusarium graminearum*. *Physiological Plant Pathology*, 1 (2), pp. 141-150.

Strange, R. and Smith, H. 1978. Specificity of choline and betaine as stimulants of *Fusarium graminearum*. *Transactions of the British Mycological Society*, 70 (2), pp. 187-192.

Sturz, A. and Johnston, H. 1983. Early colonization of the ears of wheat and barley by *Fusarium poae*. *Canadian Journal of Plant Pathology*, 5 (2), pp. 107-110.

Sundheim, L., Brodal, G., Hofgaard, I. S. and Rafoss, T. 2013. Temporal variation of mycotoxin producing fungi in Norwegian cereals. *Microorganisms*, 1 (1), pp. 188-198.

Tekle, S., Dill-Macky, R., Skinnnes, H., Tronsmo, A. M. and Bjørnstad, Å. 2012. Infection process of *Fusarium graminearum* in oats (*Avena sativa* L.). *European Journal of Plant Pathology*, 132 (3), pp. 431-442.

Tekle, S., Skinnnes, H. and Bjørnstad, Å. 2013. The germination problem of oat seed lots affected by fusarium head blight. *European Journal of Plant Pathology*, 135 (1), pp. 147-158.

Tekle, S., Lillemo, M., Skinnnes, H., Reitan, L., Buraas, T. and Bjørnstad, Å. 2018. Screening of oat accessions for fusarium head blight resistance using Spawn-Inoculated field experiments. *Crop Science*, 58 (1), pp. 143-151.

- Thrane, U., Adler, A., Clasen, P., Galvano, F., Langseth, W., Lew, H., Logrieco, A., Nielsen, K. F. and Ritieni, A. 2004. Diversity in metabolite production by *Fusarium langsethiae*, *Fusarium poae*, and *Fusarium sporotrichioides*. *International Journal of Food Microbiology*, 95 (3), pp. 257-266.
- Tinker, N. A., Kilian, A., Wight, C. P., Heller-Uszynska, K., Wenzl, P., Rines, H. W., Bjørnstad, Å., Howarth, C. J., Jannink, J. and Anderson, J. M. 2009. New DArT markers for oat provide enhanced map coverage and global germplasm characterization. *BMC Genomics*, 10 (1), pp. 1-22.
- Torp, M. and Langseth, W. 1999. Production of T-2 toxin by a *Fusarium* resembling *Fusarium poae*. *Mycopathologia*, 147 (2), pp. 89-96.
- Torp, M. and Adler, A. 2004. The European *Sporotrichiella* project: A polyphasic approach to the biology of a new fusarium species. *International Journal of Food Microbiology*, 95 (3), pp. 241-245.
- Torp, M. and Nirenberg, H. I. 2004. *Fusarium langsethiae* sp. nov. on cereals in Europe. *International Journal of Food Microbiology*, 95 (3), pp. 247-256.
- Tottman, D., Makepeace, R. and Broad, H. 1979. An explanation of the decimal code for the growth stages of cereals, with illustrations. *Annals of Applied Biology*, 93 (2), pp. 221-234.
- Trail, F., Xu, H., Loranger, R. and Gadoury, D. 2002. Physiological and environmental aspects of ascospore discharge in *Gibberella zeae* (anamorph *Fusarium graminearum*). *Mycologia*, 94 (2), pp. 181-189.
- Trevaskis, B., Hemming, M. N., Dennis, E. S. and Peacock, W. J. 2007. The molecular basis of vernalization-induced flowering in cereals. *Trends in Plant Science*, 12 (8), pp. 352-357.
- Tumino, G., Voorrips, R. E., Rizza, F., Badeck, F. W., Morcia, C., Ghizzoni, R., Germeier, C. U., Paulo, M., Terzi, V. and Smulders, M. J. 2016. Population structure and genome-wide association analysis for frost tolerance in oat using continuous SNP array signal intensity ratios. *Theoretical and Applied Genetics*, 129 (9), pp. 1711-1724.
- Van der Fels-Klerx, H. and Stratakou, I. 2010. T-2 toxin and HT-2 toxin in grain and grain-based commodities in Europe: Occurrence, factors affecting occurrence, co-occurrence and toxicological effects. *World Mycotoxin Journal*, 3 (4), pp. 349-367.

- Walker, A., Auclair, C., Gredt, M. and Leroux, P. 2009. First occurrence of resistance to strobilurin fungicides in *Microdochium nivale* and *Microdochium majus* from French naturally infected wheat grains. *Pest Management Science: Formerly Pesticide Science*, 65 (8), pp. 906-915.
- Walter, S., Nicholson, P. and Doohan, F. M. 2010. Action and reaction of host and pathogen during fusarium head blight disease. *New Phytologist*, 185 (1), pp. 54-66.
- Wanjiru, W. M., Zhensheng, K. and Buchenauer, H. 2002. Importance of cell wall degrading enzymes produced by *Fusarium graminearum* during infection of wheat heads. *European Journal of Plant Pathology*, 108 (8), pp. 803-810.
- World Health Organisation (WHO), *Mycotoxins*. 2018. [Online]. Available here: <https://www.who.int/news-room/fact-sheets/detail/mycotoxins> [Accessed 26 September 2021].
- Xu, X., Parry, D., Nicholson, P., Thomsett, M., Simpson, D., Edwards, S., Cooke, B., Doohan, F., Monaghan, S. and Moretti, A. 2008. Within-field variability of fusarium head blight pathogens and their associated mycotoxins. *European Journal of Plant Pathology*, 120 (1), pp. 21-34.
- Xu, X. and Nicholson, P. 2009. Community ecology of fungal pathogens causing wheat head blight. *Annual Review of Phytopathology*, 47 pp. 83-103.
- Xu, X., Madden, L. V. and Edwards, S. G. 2014. Modeling the effects of environmental conditions on HT2 and T2 toxin accumulation in field oat grains. *Phytopathology*, 104 (1), pp. 57-66.
- Yagen, B. and Joffe, A. Z. 1976. Screening of toxic isolates of *Fusarium poae* and *Fusarium sporotrichioides* involved in causing alimentary toxic aleukia. *Applied and Environmental Microbiology*, 32 (3), pp. 423-427.
- Yan, W., Li, H., Cai, S., Ma, H., Rebetzke, G. and Liu, C. 2011. Effects of plant height on type I and type II resistance to fusarium head blight in wheat. *Plant Pathology*, 60 (3), pp. 506-512.
- Yan, H., Yu, K., Xu, Y., Zhou, P., Zhao, J., Li, Y., Liu, X., Ren, C. and Peng, Y. 2021. Position validation of the dwarfing gene *Dw6* in oat (*Avena sativa* L.) and its correlated effects on agronomic traits. *Frontiers in Plant Science*, 12

Zadoks, J. C., Chang, T. T. and Konzak, C. F. 1974. A decimal code for the growth stages of cereals. *Weed Research*, 14 (6), pp. 415-421.

Zar, J. 2007. *Biostatistical Analysis*. United States: Prentice-Hall, Inc.

Zhao, J., Tang, X., Wight, C. P., Tinker, N. A., Jiang, Y., Yan, H., Ma, J., Lan, X., Wei, Y. and Ren, C. 2018. Genetic mapping and a new PCR-based marker linked to a dwarfing gene in oat (*Avena sativa* L.). *Genome*, 61 (7), pp. 497-503.

Zhou, X., Jellen, E. and Murphy, J. P. 1999. Progenitor germplasm of domesticated hexaploid oat. *Crop Science*, 39 (4), pp. 1208-1214.

Zimmer, C. M., Oliveira, G., Arruda, K. M. A., Pacheco, M. T. and Federizzi, L. C. 2021. Genome-wide association mapping for heading date in oats under subtropical environments. *Scientia Agricola*, 79, (3). [Online]. Available here: [Zimmer2022-GWAS_heading_date.pdf](#) [Accessed 26 September 2021].

1. Appendix 1

Table A1 1 :Selection of the main NIL grown as part of the NIL population examined. Genotype refers to the original unique breeders code, the background column details from which parent the majority of the plants genome comes from, Mrg columns detail the source of the QTL Mrg11, 20, 21 and 04, and the NIL name column details the generic name given to each NIL to describe their genomic composition.

Genotype	Background	Mrg04	Mrg20	Mrg21	Mrg04	NIL name	Number of Years present
2012-121/7/16	B	B	B	B	B	Buffalo	2
2012-124/23/8	B	B	B	B	B	Buffalo	4
2012-125/1/26	B	B	B	B	B	Buffalo	4
2012-131/4/23	B	B	B	B	B	Buffalo	2
2012-131/4/47	B	B	B	B	B	Buffalo	4
2012-131/4/5	B	B	B	B	B	Buffalo	4
2012-139/6/2	B	B	B	B	B	Buffalo	3
2013-212ACnI/16	B	B	B	B	B	Buffalo	4
2013-213ACnVII/15	B	B	B	B	B	Buffalo	2
2013-214ACnII/3	B	B	B	B	B	Buffalo	1
2013-214ACnX/31	B	B	B	B	B	Buffalo	4
Buffalo	B	B	B	B	B	Buffalo	4
2012-125/1/27	B	B	B	B	T	Buffalo_T_Mrg04	4
2012-139/6/25	B	B	B	B	T	Buffalo_T_Mrg04	4
2012-131/4/29/3	B	T	B	B	B	Buffalo_T_Mrg11	3
2012-131/4/29/7	B	T	B	B	B	Buffalo_T_Mrg11	3
2012-131/4/4/2	B	T	B	B	B	Buffalo_T_Mrg11	3
2012-131/4/4/7	B	T	B	B	B	Buffalo_T_Mrg11	3
2012-132/6/38	B	B	T	B	B	Buffalo_T_Mrg20	3
2013-212ACnI/23	B	B	T	B	B	Buffalo_T_Mrg20	4
2013-212ACnVII/11	B	B	T	B	B	Buffalo_T_Mrg20	1
2012-124/23/19	B	B	B	T	B	Buffalo_T_Mrg21	3
2013-213ACnIII/13	B	B	B	T	B	Buffalo_T_Mrg21	1
2013-214ACnX/21	B	B	B	T	B	Buffalo_T_Mrg21	4
2013-214ACnX/4	B	B	B	T	B	Buffalo_T_Mrg21	4
2013-214ACnX/41	B	B	B	T	B	Buffalo_T_Mrg21	4
2012-127/7/16	T	T	T	T	T	Tardis	2
2012-134/1/11	T	T	T	T	T	Tardis	4
Tardis	T	T	T	T	T	Tardis	4
2012-137/5/1	T	T	T	T	B	Tardis_B_Mrg04	4
2012-137/5/5	T	T	T	T	B	Tardis_B_Mrg04	4
2012-130/5/2	T	T	B	T	T	Tardis_B_Mrg20	1
2012-130/5/5	T	T	B	T	T	Tardis_B_Mrg20	4
2012-134/1/13	T	T	T	B	T	Tardis_B_Mrg21	3
2012-134/1/35	T	T	T	B	T	Tardis_B_Mrg21	4
2012-134/1/36	T	T	T	B	T	Tardis_B_Mrg21	4

2. Appendix 2

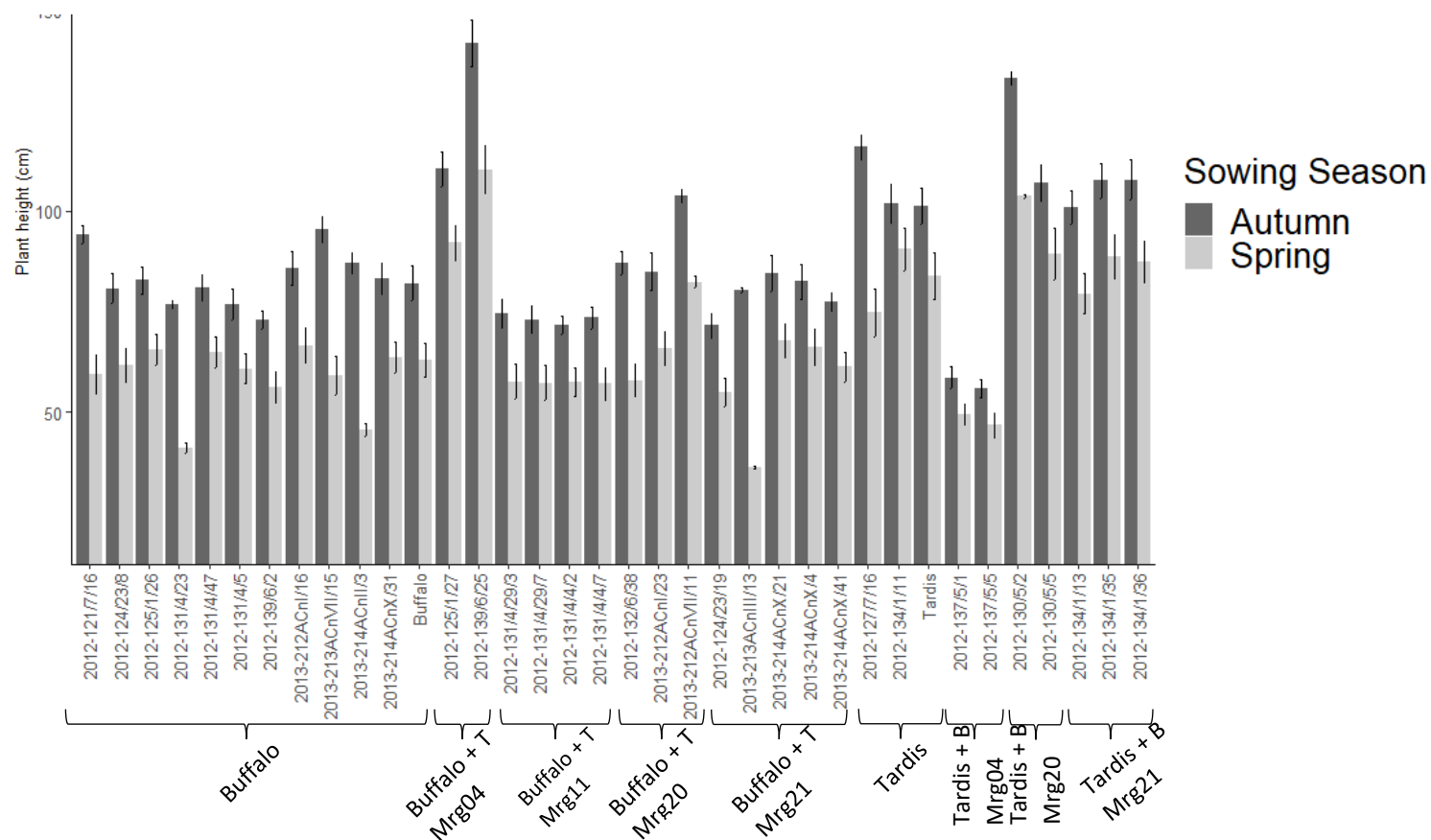


Figure A2.1 Bar chart showing the autumn and spring plant height for all field grown genotypes in 2017, 2018, 2019, and 2020. Breeder's names according to table A1 are displayed on the x axis with the NIL name below. Error bars represent the standard error of the mean.

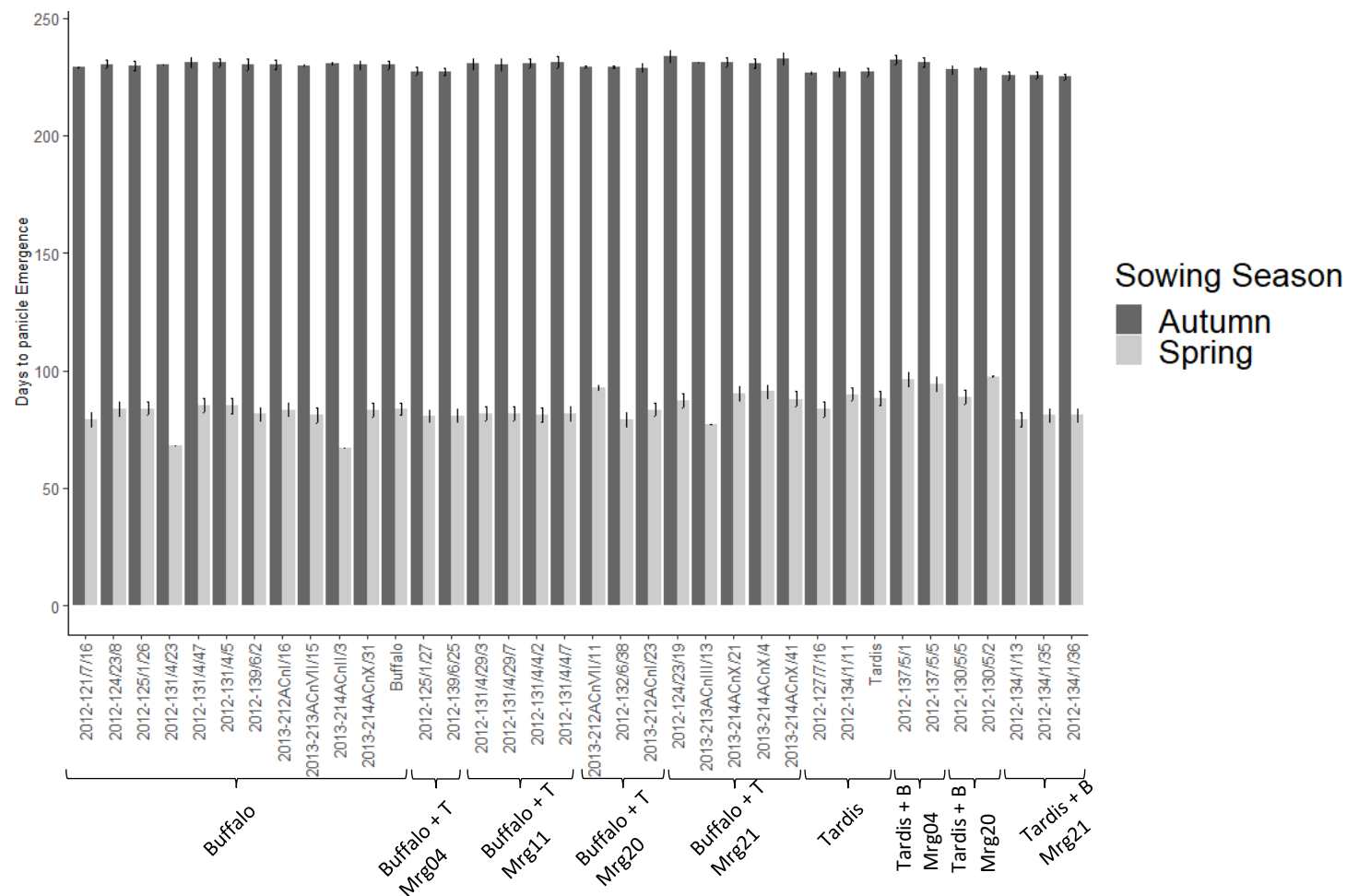


Figure A2.2: Bar chart showing the autumn and spring days to panicle emergence for all field grown genotypes in 2017, 2018, 2019, and 2020. Breeder's names according to table A1 are displayed on the x axis with the NIL name below. Error bars represent the standard error of the mean.

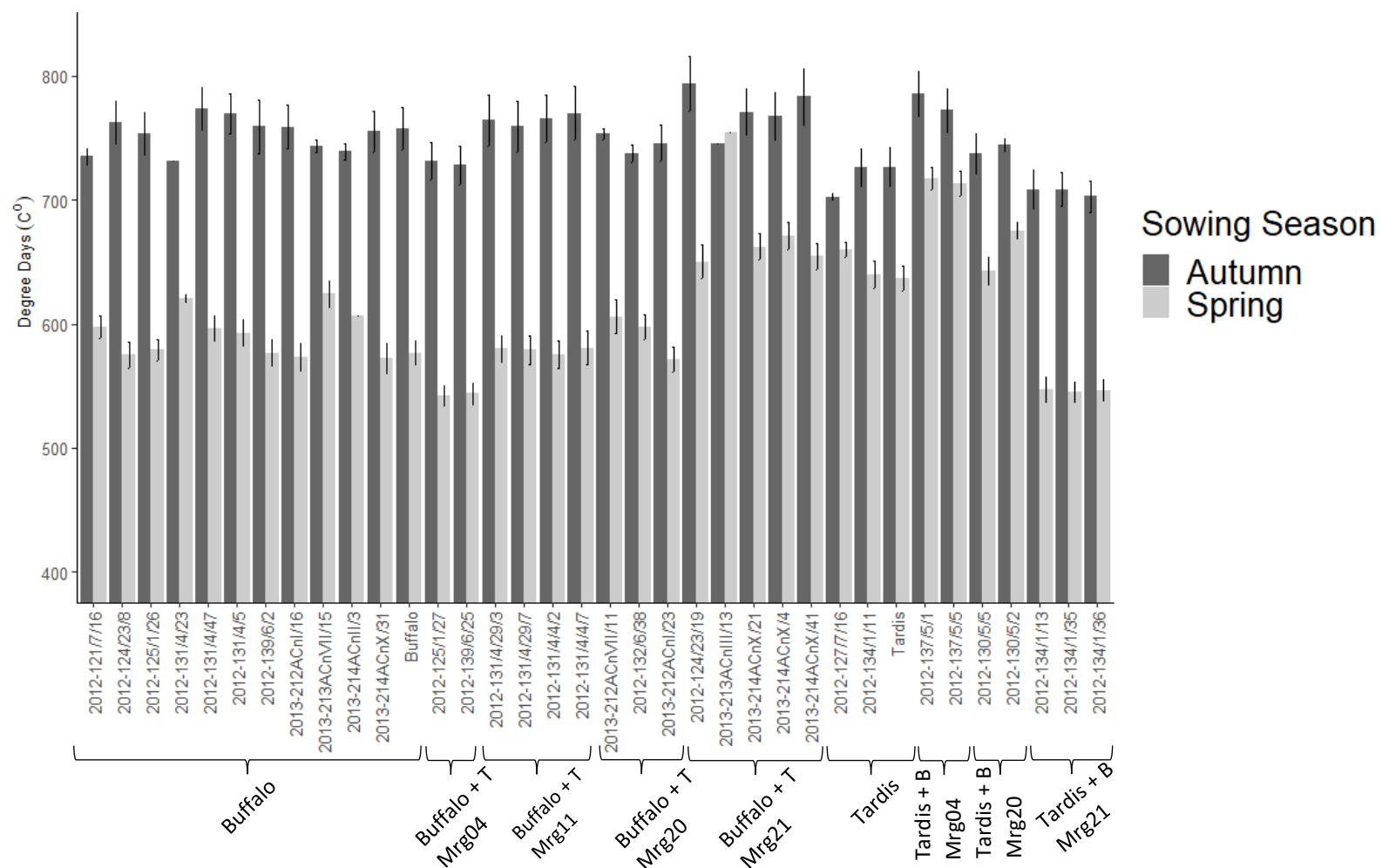


Figure A2.3: Bar chart showing the autumn and spring degree days for all field grown genotypes in 2017, 2018, 2019, and 2020. Breeder's names according to table A1 are displayed on the x axis with the NIL name below. Error bars represent the standard error of the mean.

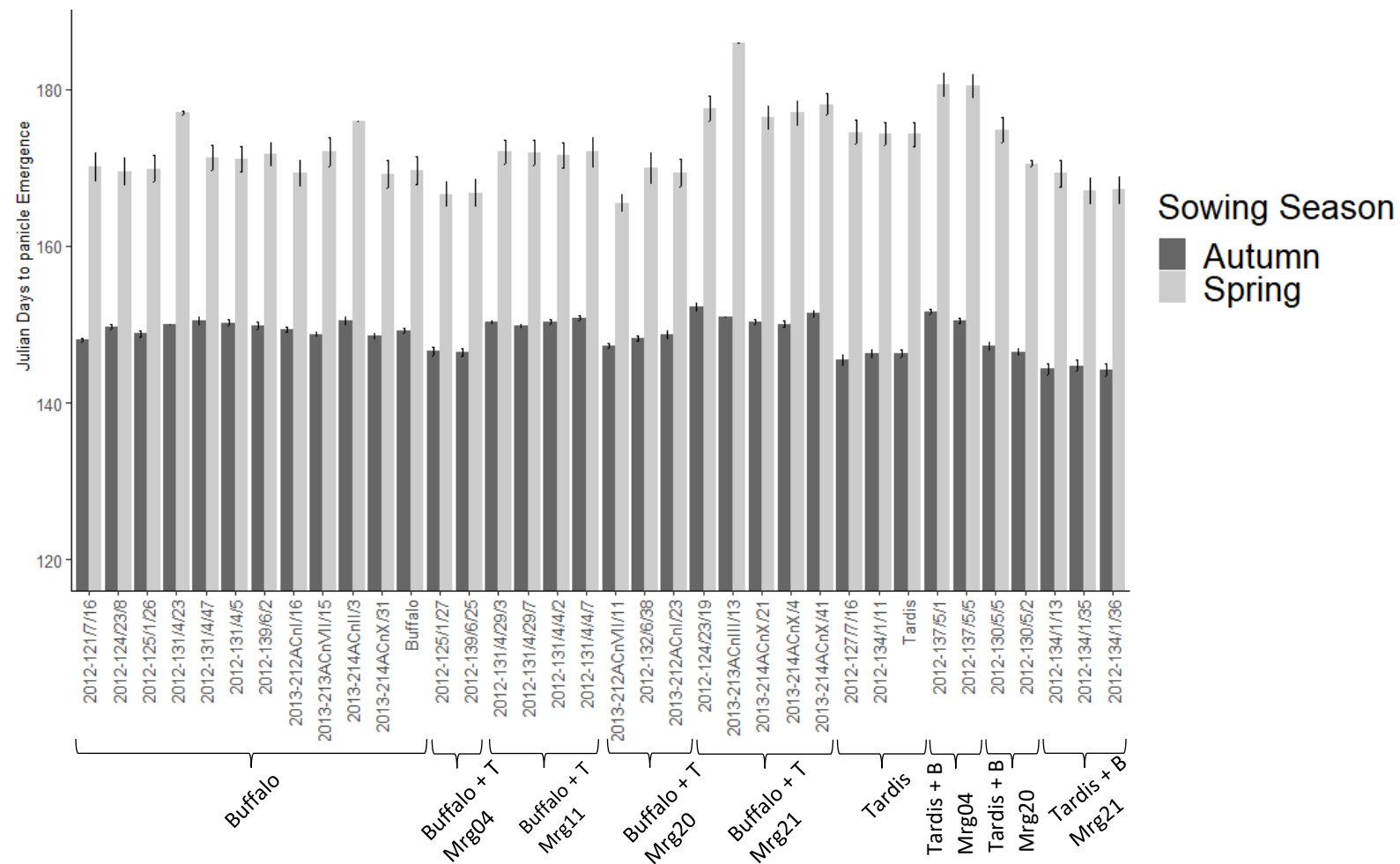


Figure A2.4: Bar chart showing the autumn and spring Julian days to panicle emergence for all field grown genotypes in 2017, 2018, 2019, and 2020. Breeder's names according to table A1 are displayed on the x axis with the NIL name below. Error bars represent the standard error of the mean.

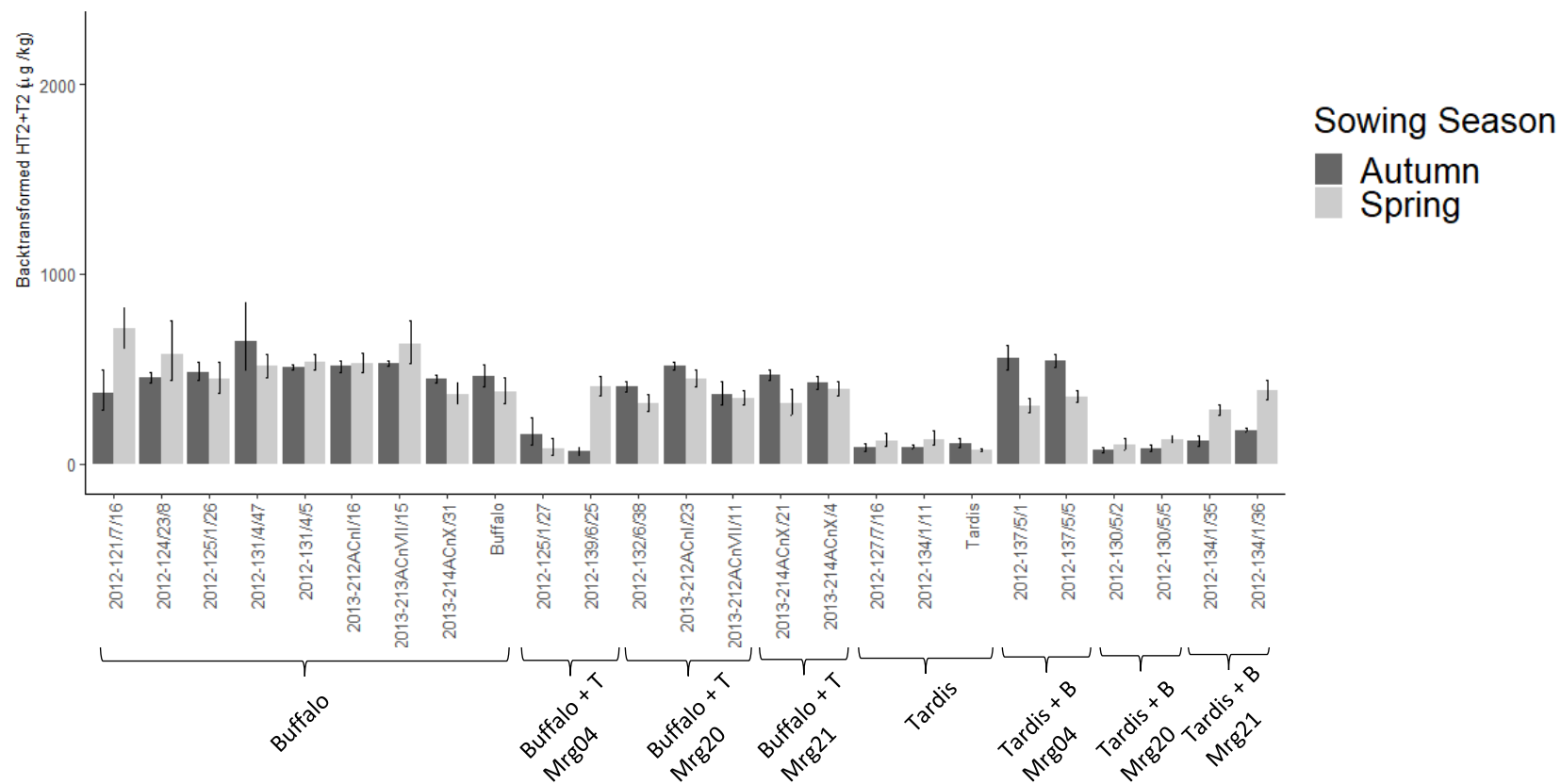


Figure A2.5: Bar chart showing the autumn and spring backtransformed HT2+T2 concentrations for all field grown genotypes in 2017. Breeder's names according to table A1 are displayed on the x axis with the NIL name below. Error bars represent the standard error of the mean.

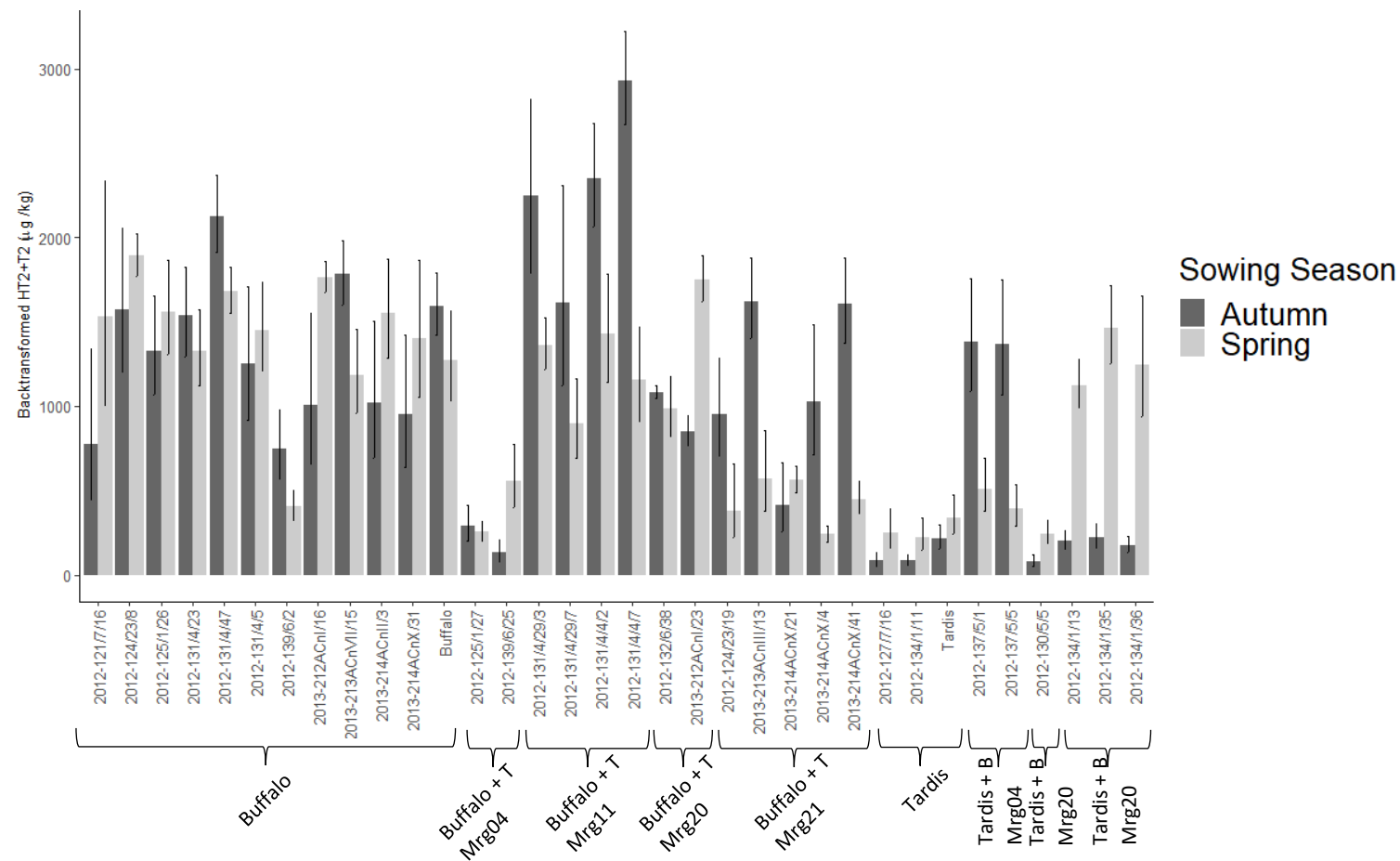


Figure A2.6: Bar chart showing the autumn and spring backtransformed HT2+T2 concentrations for all field grown genotypes in 2018. Breeder's names according to table A1 are displayed on the x axis with the NIL name below. Error bars represent the standard error of the mean.

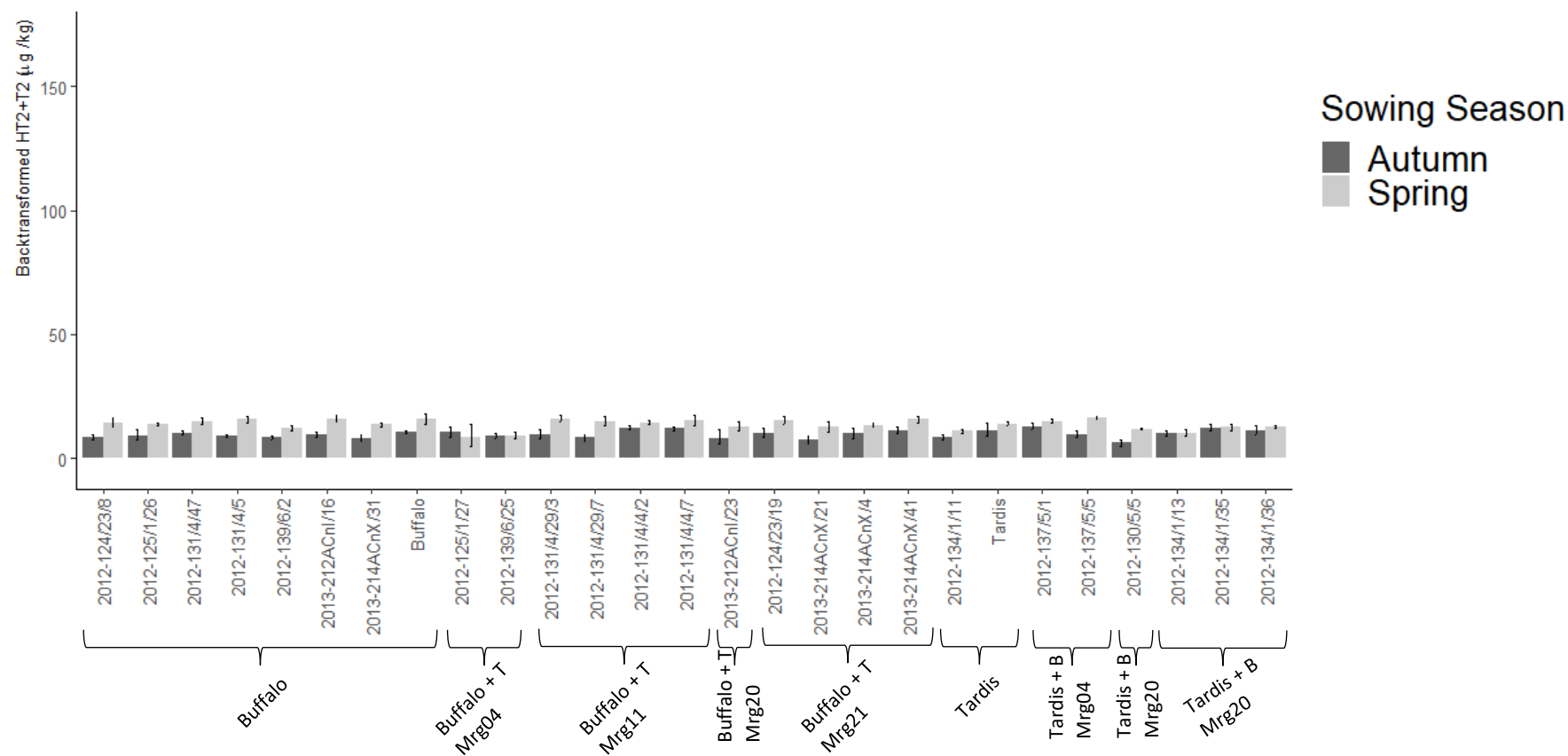


Figure A2.7: Bar chart showing the autumn and spring backtransformed HT2+T2 concentrations for all field grown genotypes in 2019. Breeder's names according to table A1 are displayed on the x axis with the NIL name below. Error bars represent the standard error of the mean.

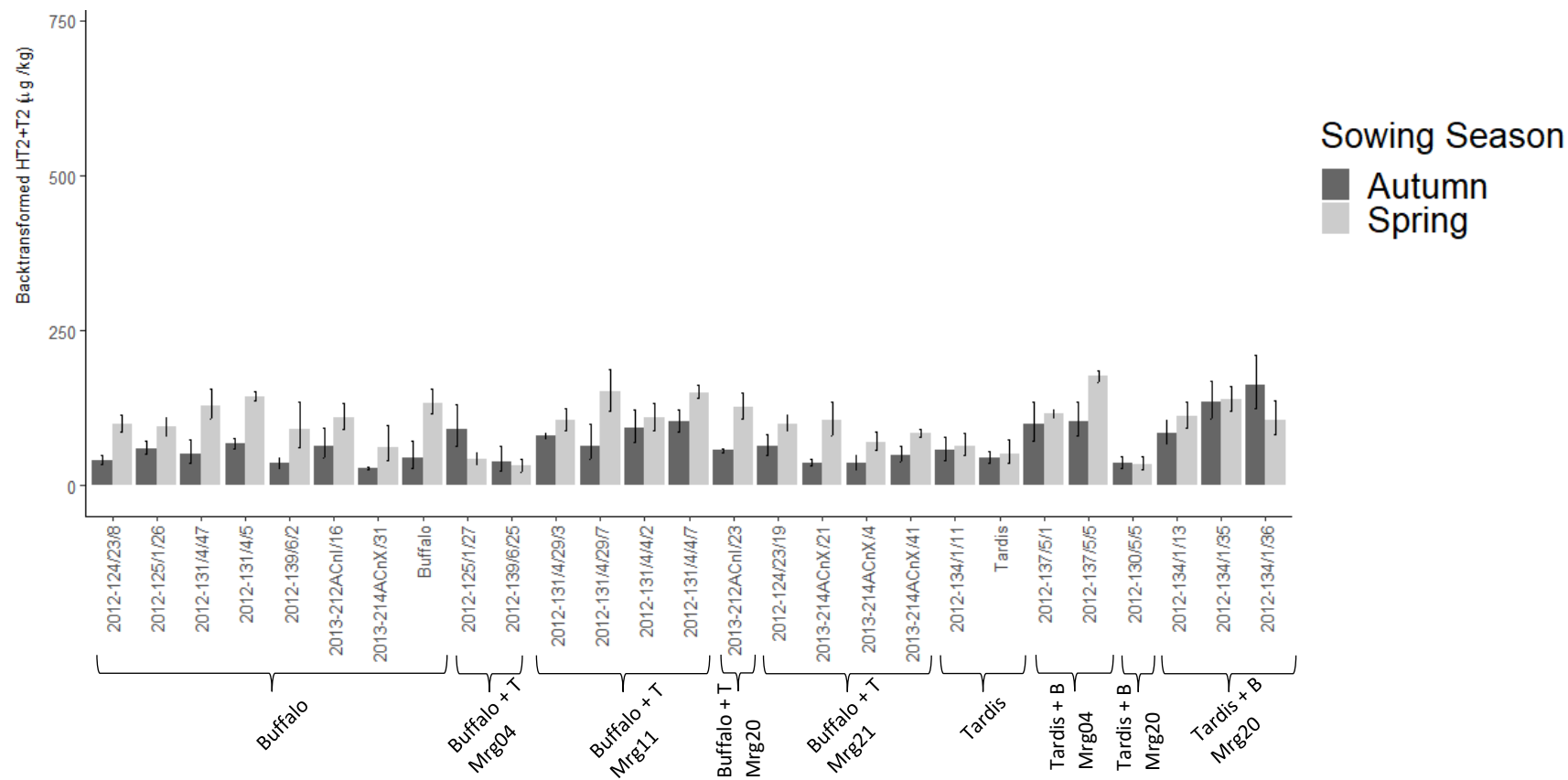


Figure A2.8: Bar chart showing the autumn and spring backtransformed HT2+T2 concentrations for all field grown genotypes in 2020. Breeder's names according to table A1 are displayed on the x axis with the NIL name below. Error bars represent the standard error of the mean.

3. Appendix 3

Table A3.1: Mean LOD scores from experiments conducted by Stancic (2016) relating traits to marker positions identifying QTL.

Year	Trait	QTL	Chromosome	Left Marker (name)	LOD
2013/2014	Log_Mean Flang /total DNA	Mrg11	7C	AME102	2.28
2012/2013	Log_Mean Flang/total DNA	Mrg11	7C	AME102	2.86
2012/2013	Mean Flang/total DNA (pg/ng)	Mrg11	7C	AME102	2.5
2013/2014	Log_Mean HT2/T2	Mrg11	7C	avgbs_21	2.49
2012/2013	Log_Mean HT2/T2	Mrg11	7C	TR293	3.96
2011/2012	Flowering	Mrg21	4D	AME152.1	7.82
2012/2013	Dwarf or Tall	Mrg04	6D	avgbs_42	12.99
2013/2014	Dwarf or Tall	Mrg04	6D	avgbs_42	13.38
2011/2012	Dwarf or Tall	Mrg04	6D	avgbs_42	13.95
2011/2012	Dwarf or Tall	Mrg04	6D	ASTB.384	22.11
2012/2013	Dwarf or Tall	Mrg04	6D	ASTB.384	23.06
2013/2014	Dwarf or Tall	Mrg04	6D	ASTB.384	23.63
2012/2013	Dwarf or Tall	Mrg04	6D	o793199	23.84
2013/2014	Dwarf or Tall	Mrg04	6D	o793199	25.52
2011/2012	Dwarf or Tall	Mrg04	6D	o793199	27.54
2012/2013	Dwarf or Tall	Mrg04	6D	m27/049.6	66.99
2013/2014	Dwarf or Tall	Mrg04	6D	m27/049.6	68.94
2011/2012	Dwarf or Tall	Mrg04	6D	m27/049.6	90.04
2013/2014	Log_Mean Flang /total DNA	Mrg04	6D	avgbs_42	2.12
2013/2014	Log_Mean Flang /total DNA	Mrg04	6D	o15157	4.19

2013/2014	Log_Mean Flang /total DNA	Mrg04	6D	avgbs_21	11.56
2012/2013	Log_Mean Flang/total DNA	Mrg04	6D	o793199	4.46
2012/2013	Log_Mean Flang/total DNA	Mrg04	6D	TR345	12.88
2013/2014	Mean Flang /total DNA	Mrg04	6D	o15157	5.09
2013/2014	Mean Flang /total DNA	Mrg04	6D	ASTB.384	5.26
2013/2014	Mean Flang /total DNA	Mrg04	6D	avgbs_21	9.85
2012/2013	Mean Flang/total DNA (pg/ng)	Mrg04	6D	o793199	2.73
2012/2013	Mean Flang/total DNA (pg/ng)	Mrg04	6D	TR345	7.66
2013/2014	Flowering	Mrg04	6D	o793199	5.11
2011/2012	Flowering	Mrg04	6D	o793199	8.46
2013/2014	Flowering	Mrg04	6D	ASTB.384	8.72
2012/2013	Flowering	Mrg04	6D	o793199	11.15
2011/2012	Flowering	Mrg04	6D	ASTB.384	11.19
2012/2013	Flowering	Mrg04	6D	ASTB.384	13.59
2013/2014	Flowering	Mrg04	6D	m27/049.6	15.41
2012/2013	Flowering	Mrg04	6D	m27/049.6	25.86
2011/2012	Flowering	Mrg04	6D	m27/049.6	27.7
2012/2013	Height (cm)	Mrg04	6D	avgbs_42	12.21
2011/2012	Height (cm)	Mrg04	6D	ASTB.384	17.13
2011/2012	Height (cm)	Mrg04	6D	o793199	17.65
2013/2014	Height (cm)	Mrg04	6D	ASTB.384	19.81
2013/2014	Height (cm)	Mrg04	6D	o793199	21.26
2012/2013	Height (cm)	Mrg04	6D	o793199	21.38
2012/2013	Height (cm)	Mrg04	6D	ASTB.384	22.38

2013/2014	Height (cm)	Mrg04	6D	m27/049.6	43.94
2011/2012	Height (cm)	Mrg04	6D	m27/049.6	59.57
2012/2013	Height (cm)	Mrg04	6D	m27/049.6	65.66
2013/2014	Log_Mean HT2/T2	Mrg04	6D	o15157	5.09
2012/2013	Log_Mean HT2/T2	Mrg04	6D	o793199	5.64
2013/2014	Log_Mean HT2/T2	Mrg04	6D	ASTB.384	7.44
2013/2014	Log_Mean HT2/T2	Mrg04	6D	TR345	8.58
2012/2013	Log_Mean HT2/T2	Mrg04	6D	m27/049.	11.56
2013/2014	Log_Mean HT2/T2	Mrg04	6D	avgbs_21	12.09
2012/2013	Mean HT2/T2	Mrg04	6D	o793199	4.61
2013/2014	Mean HT2/T2	Mrg04	6D	o15157	4.77
2013/2014	Mean HT2/T2	Mrg04	6D	TR345	7.95
2012/2013	Mean HT2/T2	Mrg04	6D	m27/049.	9.43
2013/2014	Mean HT2/T2	Mrg04	6D	avgbs_21	10.75
2013/2014	Log_Mean Flang /total DNA	Mrg20	4A	o16528	3.27
2013/2014	Mean Flang /total DNA	Mrg20	4A	avgbs_90	2.27
2012/2013	Flowering	Mrg20	4A	o16528	2.97
2011/2012	Flowering	Mrg20	4A	o16528	4.26
2011/2012	Height (cm)	Mrg20	4A	o16528	2.37
2013/2014	Height (cm)	Mrg20	4A	o16528	2.4
2011/2012	Mean height	Mrg20	4A	avgbs_90	2.43
2011/2012	Mean height	Mrg20	4A	m28/000.	2.89
2013/2014	Log_Mean HT2/T2	Mrg20	4A	avgbs_90	2.16

4. Appendix 4

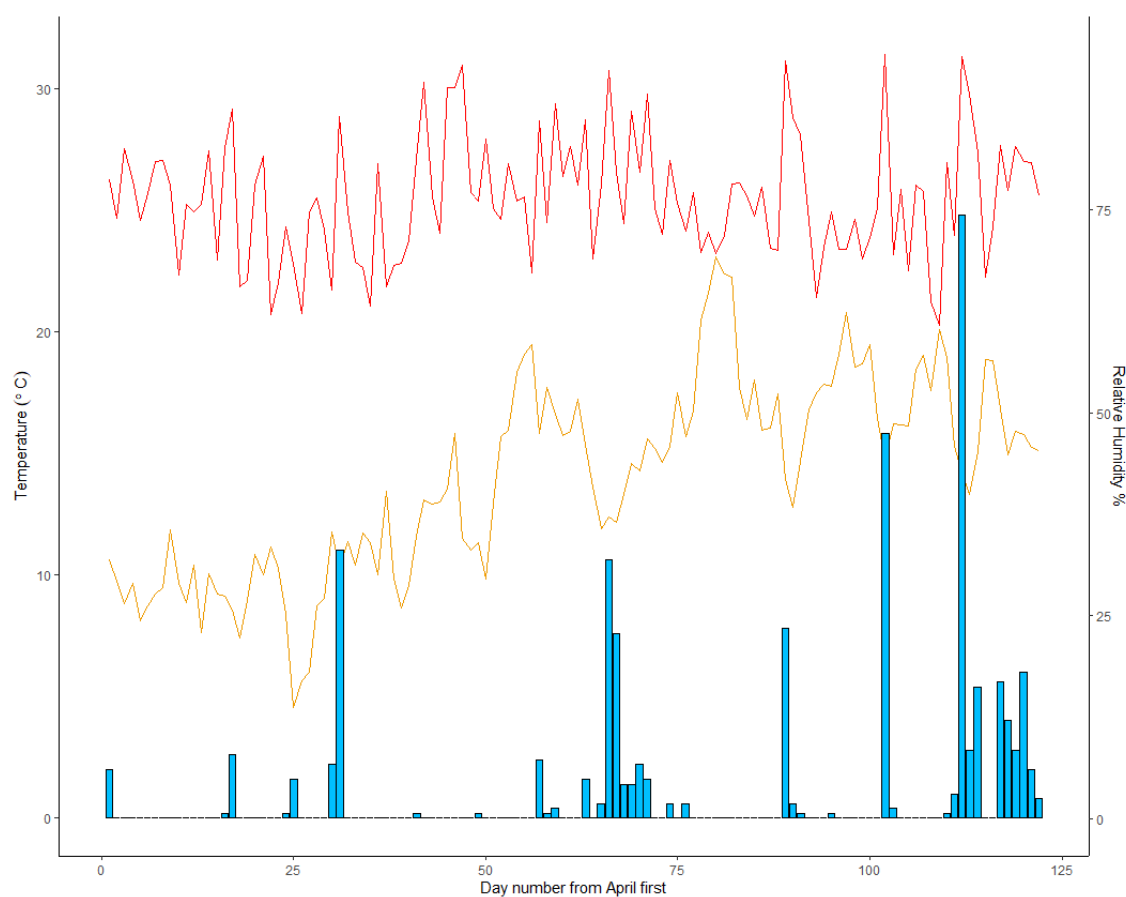


Figure A4.1: Weather data for the Harper Adams weather station from the 1st April 2017 to the beginning of August 2017. Graph details the total daily rainfall in blue (ml) the temperature in yellow (°C, primary y axis) and the relative humidity in red (% , secondary y axis).

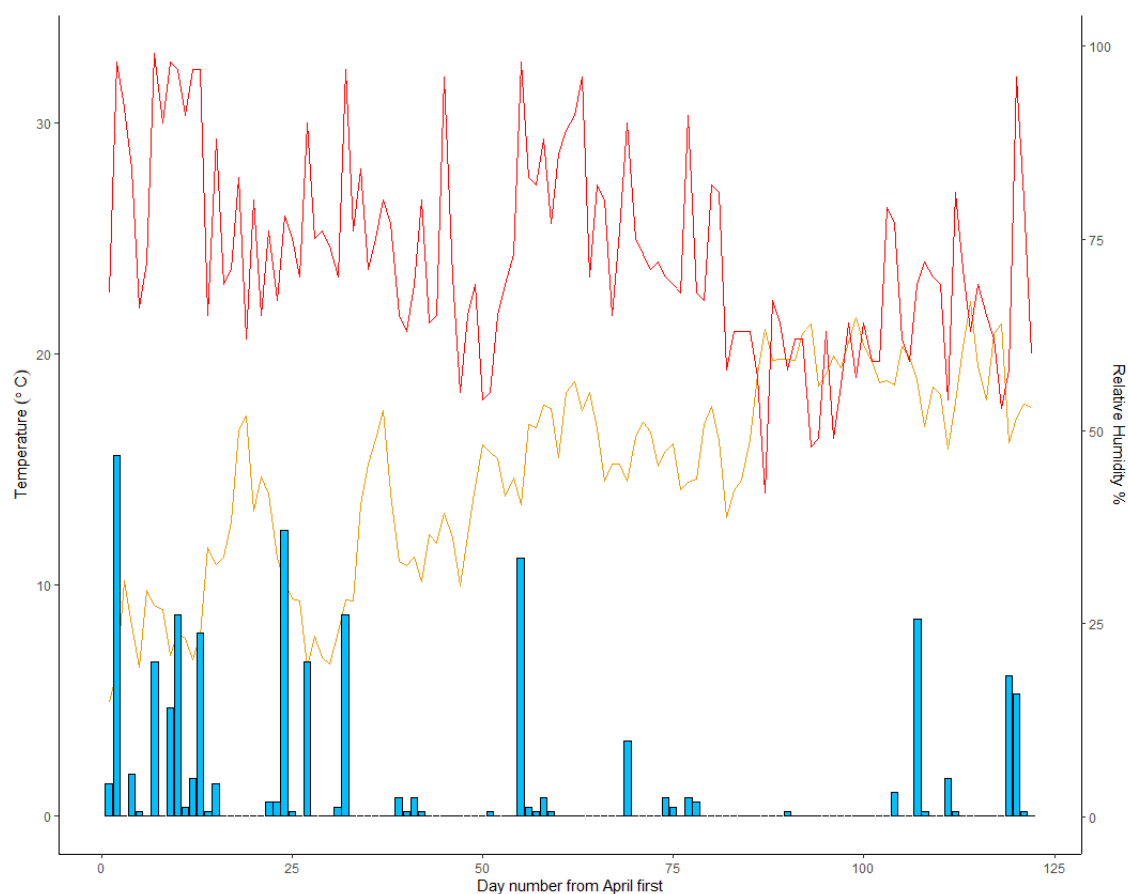


Figure A4.2: Weather data for the Harper Adams weather station from the 1st April 2018 to the beginning of August 2018. Graph details the total daily rainfall in blue (ml) the temperature in yellow (°C, primary y axis) and the relative humidity in red (% , secondary y axis).

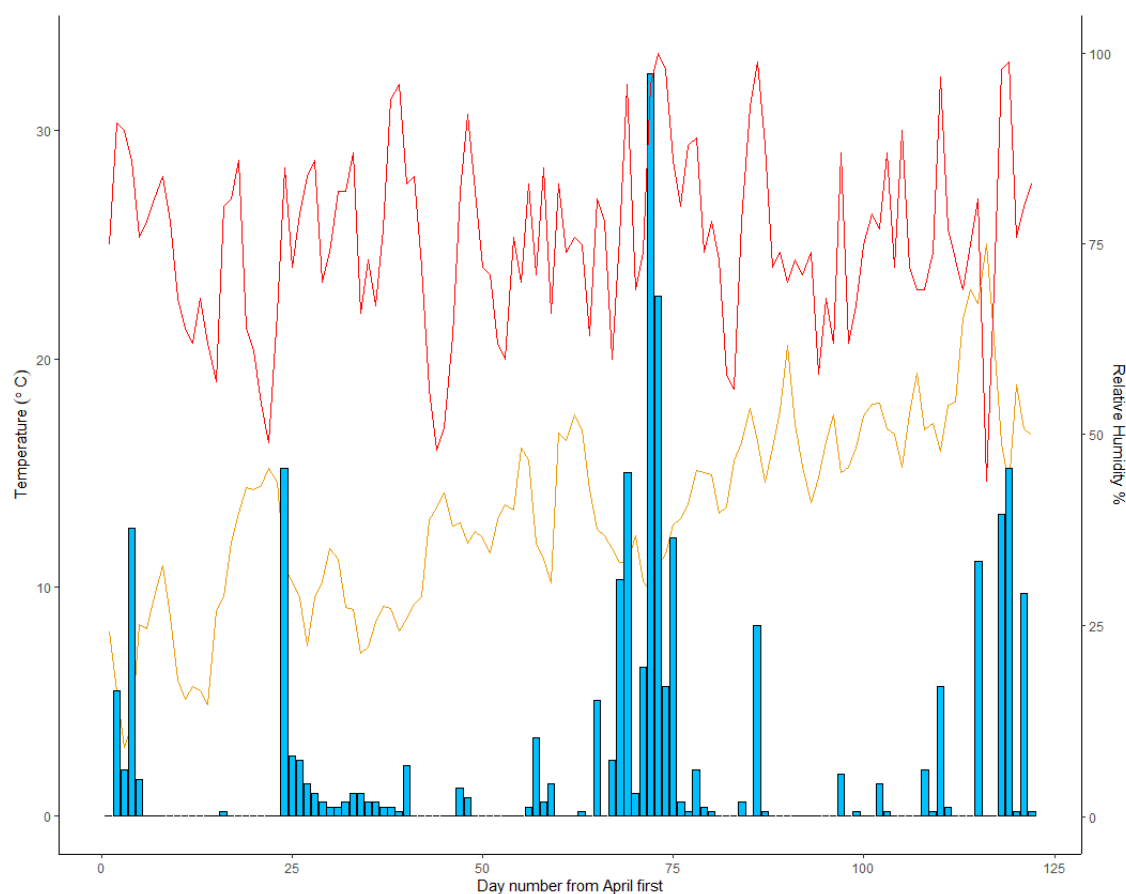


Figure A4.3: Weather data for the Harper Adams weather station from the 1st April 2019 to the beginning of August 2019. Graph details the total daily rainfall in blue (ml) the temperature in yellow (°C, primary y axis) and the relative humidity in red (% , secondary y axis).

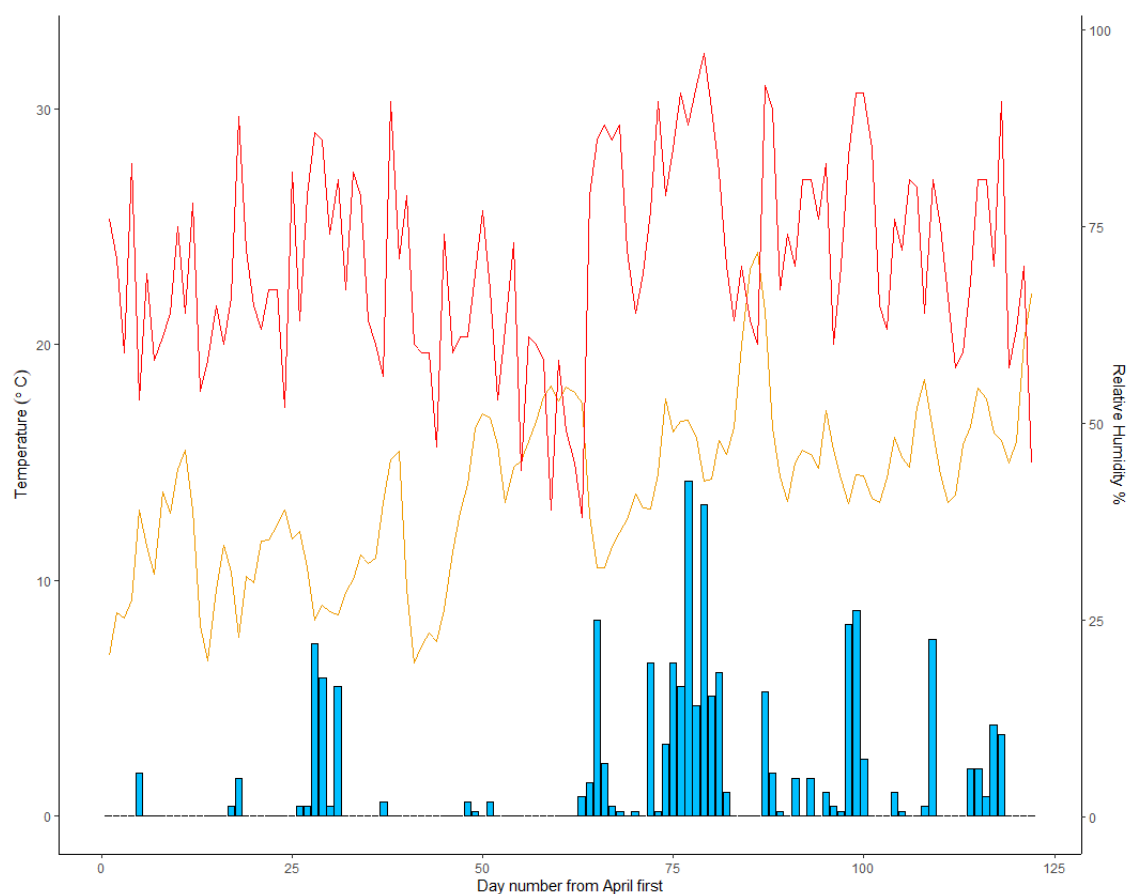


Figure A4.4: Weather data for the Harper Adams weather station from the 1st April 2020 to the beginning of August 2020. Graph details the total daily rainfall in blue (ml) the temperature in yellow (°C, primary y axis) and the relative humidity in red (% , secondary y axis).

5. Appendix 5

Table A5.1: Fungicide programme applied each year across the NIL experiments for autumn and spring sown experiments. Growth stages are described using according to Zadoks et al. (1974). Variations in rate were made according to disease pressure, no crown rust was seen in the field across all four seasons and as such no sprays were made to specifically tackle it.

Year	Growth stage	Product	Rate (L/ha)	Active ingredients
2017	GS31	Siltra Xpro	0.6	Bixafen + Prothioconazole
2017	GS31	Talius	0.15	Proquinazid
2017	GS39	Siltra Xpro	0.6	Bixafen + Prothioconazole
2017	GS39	Cyflamid	0.35	cyflufenamid
2018	GS31	Siltra Xpro	0.4	Bixafen + Prothioconazole
2018	GS31	Talius	0.15	Proquinazid
2018	GS39	Siltra Xpro	0.4	Bixafen + Prothioconazole
2018	GS39	Cyflamid	0.25	cyflufenamid
2019	GS31	Siltra Xpro	0.6	Bixafen + Prothioconazole
2019	GS31	Talius	0.15	Proquinazid
2019	GS39	Siltra Xpro	0.6	Bixafen + Prothioconazole
2019	GS39	Cyflamid	0.25	cyflufenamid
2020	GS31	Siltra Xpro	0.6	Bixafen + Prothioconazole
2020	GS31	Talius	0.15	Proquinazid
2020	GS39	Siltra Xpro	0.6	Bixafen + Prothioconazole
2020	GS39	Cyflamid	0.25	cyflufenamid